

City Research Online

City St George's, University of London

Citation: Toy, N. (1976). Local free & forced convection heat transfer from the human body. (Unpublished Doctoral thesis, The City University)

This is the accepted version of the paper.

This version of the publication may differ from the final published version. To cite this item please consult the publisher's version.

Permanent repository link: https://openaccess.city.ac.uk/id/eprint/38087/

Copyright and Reuse: Copyright and Moral Rights remain with the author(s) and/or copyright holders. Copies of full items can be used for personal research or study, educational, or not-for-profit purposes without prior permission or charge, unless otherwise indicated, provided that the authors, title and full bibliographic details are credited, a hyperlink and/or URL is given for the original metadata page and the content is not changed in any way. For full details of reuse please refer to City Research Online policy.

City Research Online: http://openaccess.city.ac.uk/ publications@citystgeorges.ac.uk

Local Free and Forced Convection Heat Transfer from the Human Body

by Norman Toy

A thesis submitted for the Degree of Doctor of Philosophy

Department of Aeronautics,

The City University, London.

November 1976

Dedicated to my dear wife [redacted], my daughter [redacted] and son [redacted], without their help this work would never have been completed.

Acknowledgements

The work in this thesis was carried out during the period 1970 to 1973 in the Department of Aeronautics, City University, London, and in the Department of Human Physiology, National Institute for Medical Research. I wish to acknowledge the help given to me by the Heads of these two Departments, [redacted], during the course of this study.

I am indebted to Professor R.N. Cox who acted as my supervisor throughout the postgraduate course.

Many thanks to [redacted] who read through the rough drafts of this thesis.

I am also very grateful for the assistance given to me by [redacted] (Laboratory for Aerobiology, Clinical Research Centre, Harrow) during the course of this study, and to [redacted], who as Experimental Officer in the Department of Aeronautics assisted with much of the technical work that was required.

Finally, I am most thankful to all the 'human guinea-pigs' from whom much of the heat transfer studies were taken. Without their kind assistance, this work would never have materialised. My thanks to:-

[redacted].

Contents

1. Introduction.

2. Convection heat loss from the human body.

2.1 Free convection heat loss from the human body.

2.2 Forced convection heat loss from the human body.

2.2.1 Convective heat loss from a standing subject.

2.2.2 Convective heat loss from a reclining subject.

2.2.3 Convective heat loss from a supine subject.

2.3 Discussion.

3. Convection heat loss from flat plates and cylinders.

3.1 Dimensional analysis for free convection.

3.1.1 Laminar free convection flow from a vertical flat plate.

3.1.2 Laminar free convection flow from cylinders.

3.2 Application of laminar free convection heat transfer theory to the human form.

3.2.1 Dimensions used in the mathematical model and assumptions used in computation.

3.2.2 Free convection heat loss for the standing case.

3.2.3 Free convection heat loss from the horizontal model.

3.3 Dimensional analysis for forced convection.

3.3.1 Forward stagnation point heat transfer from a heated cylinder in forced convection.

3.3.2 Local heat transfer distribution around a heated cylinder in forced convection.

3.3.3 Effect of freestream turbulence on the heat transfer from a cylinder.

3.3.4 Effect of flow direction.

3.4 Effect of radius of curvature on the heat transfer.

3.4.1 Laminar free convection.

3.4.2 Laminar forced convection.

4. Methods for measuring the local convective heat loss from warm bodies.

4.1 Selection of instrument.

4.2 Heat flow disc.

4.2.1 The calibration of the heat flow disc.

4.3 Experimental apparatus for testing the heat flow disc in free and forced convection.

4.3.1 Free convection test for the heat flow disc.

4.3.2 Forced convection test for the heat flow disc.

4.4 Concluding remarks on the heat flow disc.

4.5 The method of plug-type calorimetry.

4.5.1 Limitations to the use of the plug-type calorimeter.

4.6 The concept of a surface plate calorimeter.

4.6.1 Plate perfectly insulated from a heated body.

4.6.2 Plate imperfectly insulated from a heated body.

4.7 Design and construction of a surface plate calorimeter.

4.7.1 Selection of plate material.

4.7.2 Selection of electric heater.

4.7.3 Selection of thermosensor.

4.7.4 Selection of insulator.

4.8 Description of the completed surface plate calorimeter.

4.8.1 Method of use.

4.8.2 Radiation correction.

4.8.3 Conduction correction.

5. Experimental test for the surface plate calorimeter.

5.1 Free convection test.

5.1.1 Free convection test on a vertical heated cylinder.

5.1.2 Free convection test on a horizontal heated cylinder.

5.2 Forced convection test.

5.2.1 Stagnation point heat transfer from a vertical heated cylinder.

5.2.2 Heat transfer distribution around a vertical cylinder.

6. Preliminary tests for the calorimeter on the human body.

6.1 Subjective tests as to the comfort of the calorimeter on skin.

6.2 Combined convection and radiation heat loss measurements from the human body.

6.3 Observations to determine whether the calorimeter affects the local skin temperature.

6.4 Convective heat transfer test.

6.5 Summary.

7. Free convective heat transfer from the human body.

7.1 Free convection heat loss from the leg.

7.1.1 Convective heat loss from a vertical leg.

7.1.2 Convective heat loss from a horizontal leg.

7.2 Convective heat loss from the head.

7.2.1 Heat transfer distribution around the head.

7.2.2 Total heat loss from the face of a standing subject.

7.2.3 Heat loss from the head of a horizontal subject.

8. Forced convection heat transfer from the human body.

8.1 Heat transfer distribution around the leg.

8.1.1 Forward stagnation point heat transfer from the leg.

8.2 Convection heat loss from the human head.

8.2.1 Heat transfer distribution along the median plane of the head.

8.2.2 Forward stagnation point heat transfer from the face.

9. Applications of this heat transfer measuring technique.

9.1 Convective heat loss from the hand immersed in different gaseous environments.

9.2 Convective heat loss from the thigh of an athlete.

9.2.1 Experimental set-up.

9.3 Heat loss through clothing.

9.3.1 Heat loss through clothing from a cylinder.

9.3.2 Heat loss through clothing from a human subject.

10. Concluding remarks.

Appendix (A) Glossary of Physiological terms.

Appendix (B) Effect of cylinder height on the overall convective heat loss.

Appendix (C) Calibration of the hot-wire anemometer.

Appendix (D) Wind tunnel blockage correction.

References.

SUMMARY

The local free and forced convection heat loss from the human body has been investigated.

The convective heat loss from a cylindrical model of the human form in the standing and supine posture has been evaluated using boundary layer theory.

A surface plate calorimeter has been developed for measuring the local convective heat loss from a heated body. It is shown that this instrument can measure the heat loss from a heated cylinder in free and forced convection to within 10% of other known data.

The calorimeter is small (12 x 8 x 0.20 mm^3) and causes no discomfort when attached to a human subject, and does not inhibit movement.

The local convection heat loss from the leg and head of a human subject in free and forced convection has been measured. From these measurements it is shown that:- (a) the overall convective heat loss for these regions may be evaluated; (b) the heat transfer pattern around these areas is similar to the thermal boundary layer that exists around heated cylinders; (c) it is important to consider the local radius of curvature of the leg and head when measuring convection heat loss.

The calorimeter has been used in the following three fields of study:-

(1) Measurements have been taken in Helium and Nitrogen rich environments and the results show that about twice as much heat is lost by convection from the hand of a subject immersed in a Helium filled chamber compared to Nitrogen filled one.

(2) Measurements that have been taken from the thigh of an athlete running on a treadmill in a wind shows that more heat is lost from the thigh than can be accounted for by simply considering the thigh stationary in a wind; the reason for this difference is discussed in relation to the changes in the effective wind velocity due to the movement of the thighs.

(3) The heat loss through clothing assemblies from cylinders and a human subject have been measured. It is shown that the calorimeter may be used to evaluate the insulation value of a garment.

NOTATION (other than that specifically defined in the text)

Q	Overall heat loss.
M	Metabolic rate.
E	Evaporation heat loss.
S	Heat storage.
T_s	Local skin temperature.
T_w	Cylinder wall temperature.
T_∞	Ambient temperature of the surrounding air.
A_b	Body area.
$\bar{h}_c$	Overall convective heat transfer coefficient.
h_c	Local " " " "
X	Vertical height along cylinder wall.
Y	Horizontal distance from cylinder wall.
D,d	Diameter of cylinder.
r	Radius of curvature.
U_∞	Freestream velocity.
C_p	Specific heat of air.
k	Thermal conductivity of air.
ρ	Density of air.
μ	Dynamic viscosity of air.
ν	Kinematic " " " $(= \mu/\rho)$
g	Acceleration due to gravity.
β	Coefficient of thermal expansion $(= 1/T_\infty)$.
Nu	Nusselt number $(= h_c X/k)$.
Pr	Prandtl number $(= C_p \mu/k)$.
Gr	Grashof number $(= g\beta X^3 (T_w - T_\infty)/\nu^2)$.
Re	Reynolds number $(= U_\infty X/\nu)$.
σ	Stefan - Boltzmann radiation constant.
ϵ_o	Emissivity of the surroundings.
ϵ_1	Emissivity of the body surface.
q/A	Heat flux.

ε Freestream turbulence.

u' Velocity component in the x-direction.

v' " " " " y-direction.

w' " " " " z-direction.

k_p Thermal conductivity of plush.

i Electric current.

R Electrical resistance of the calorimeter.

A_c Area of the calorimeter.

I Insulation value for:-

a	Air,	Subscripts
c	Cotton,	
ag	Air gap,	
sv	String vest,	
s	Shirt,	
L	Laboratory overcoat.	

1. INTRODUCTION

When a warm body is immersed in a cool fluid whose coefficient of thermal expansion is positive, the fluid layer adjacent to the body surface is heated by conduction, and, in a gravitational field becomes less dense and rises due to the effect of buoyancy forces, to be replaced by cooler, heavier fluid. In the case of the human body, a natural convective boundary layer is generated by the temperature difference that occurs between the skin surface and the surrounding air.

In 1967, Lewis (1) visualised this boundary layer (the human micro-environment) by means of a schlieren technique (Lewis et al, 2). Following these initial observations, work on the interaction of this micro-environment and its effect on the human body has been expanded to include such topics as:-

(a) the simulation and investigation of the thermal boundary layers using a heated plastic manikin, Foster (3);

(b) the entrainment and dispersal of small particles, the size of micro-organisms and skin scales, within the boundary layer, Clark (4);

(c) the design and construction of a clean-air room using natural convection as a ventilating system, Clark et al, (5), (clean air rooms are required in a variety of medical and industrial applications);

(d) the measurement of the local free and forced convection heat transfer from the human body, Toy & Cox (6).

In temperate still air* conditions (average ambient temperature $T_a = 20^{\circ}C$, skin temperature $T_s = 33^{\circ}C$) the approximate proportions of

---

* The term 'still air' is used in this context to mean that there are no air currents present other than those generated by the natural convective boundary layer surrounding the human body.

the total heat lost by an unclothed human body to the environment are, 25% by evaporation and conduction, 25% by convection (in this case 'free convection'), and 50% by radiation. If the body is subjected to a wind or draught, a greater proportion of the total heat lost is transferred by convection. This mode of transfer is termed 'forced convection'.

The measurement of the convective heat loss from the human body has, to-date, mainly been investigated by the method of Partitional Calorimetry (Appendix A), that is, by measuring the quantity of heat lost via the other heat transfer modes and subtracting their sum from the total heat produced,

$$Q_{conv} = Q_{produced} - \left\{ Q_{evap} + Q_{rad} + Q_{cond} \right\} \quad \ldots (1)$$

Many physiologists (refs 9 → 31) have measured the overall convective heat transfer coefficient $\bar{h}_c$ from a human subject in either a standing, reclining, or lying horizontal posture, for either free or forced convection conditions, and have given a range of values for these conditions, section 2. Due to their different experimental set-ups the poor agreement between their results cannot easily be explained, but one probable contributory reason is that the thermal boundary layer around the body and its heat transfer characteristics markedly change with both body posture and air flow condition. In order to interpret these very different values of the convective heat losses, and in turn, to lead to an improved understanding of the man-environment interaction, some understanding is required of how the convective flows change with such variables as posture, wind, temperature, and clothing, and how, by altering the convective flow pattern, the local, and hence the total, convective heat transfer rate changes. This understanding may be achieved by first studying the convective boundary layer for a variety of conditions from physical models, and for

this reason, a discussion of the convective heat loss characteristics from heated vertical and horizontal cylinders is included in section 3. However, generalisations about the convective boundary layer around heated cylinders and the human body are insufficient for a detailed heat transfer analysis to be made. To make such an analysis requires either knowledge of the heat given up by the body to the surrounding environment by the convection process alone, or knowledge of the temperature profiles within the boundary layer over the entire body surface. An alternative and simpler approach to this problem would be to employ a number of instruments located at different positions each capable of providing a local heat transfer measurement; from these results the total convective heat loss could then be determined. This second approach poses the problem of finding or designing a suitable instrument to measure the local heat transfer. The instrument should ideally be small and capable of being attached easily either to a human body or to a physical model. The design and development of such an instrument (termed a surface plate calorimeter, Clark, Cox, & Toy (7) forms part of the work described in this thesis.

A number of these surface plate calorimeters were produced and a series of investigations of the local convective heat loss from a human body in different body postures and air flow conditions were made.

The human body has been represented with some success, by a cylinder (Plummer (8), Buttner (9)), or a series of cylinders (Clark (4)), for the purpose of predicting the convective heat exchange to the environment. When making this analogy between the body and a cylinder it is necessary to know if similar convective flow patterns are developed in both cases, and whether the same laws which govern convection heat transfer from heated cylinders are appropriate for use on the human body. To this end a comparison has been made between

the local free convection heat loss from vertical and horizontal heated cylinders and similar measurements taken from the leg and the head of a human subject in the standing and lying postures. Measurements of the local forced convection heat transfer coefficients from the leg and the head of a sitting subject, subjected to varying air velocities, are also presented and discussed.

By integrating the local convective heat losses over the region of interest, the overall convective heat loss from that area may be determined. This has been performed for the head of a subject in the standing and lying postures and the results are presented and compared with values calculated for a cylinder whose dimensions are similar to those of the head.

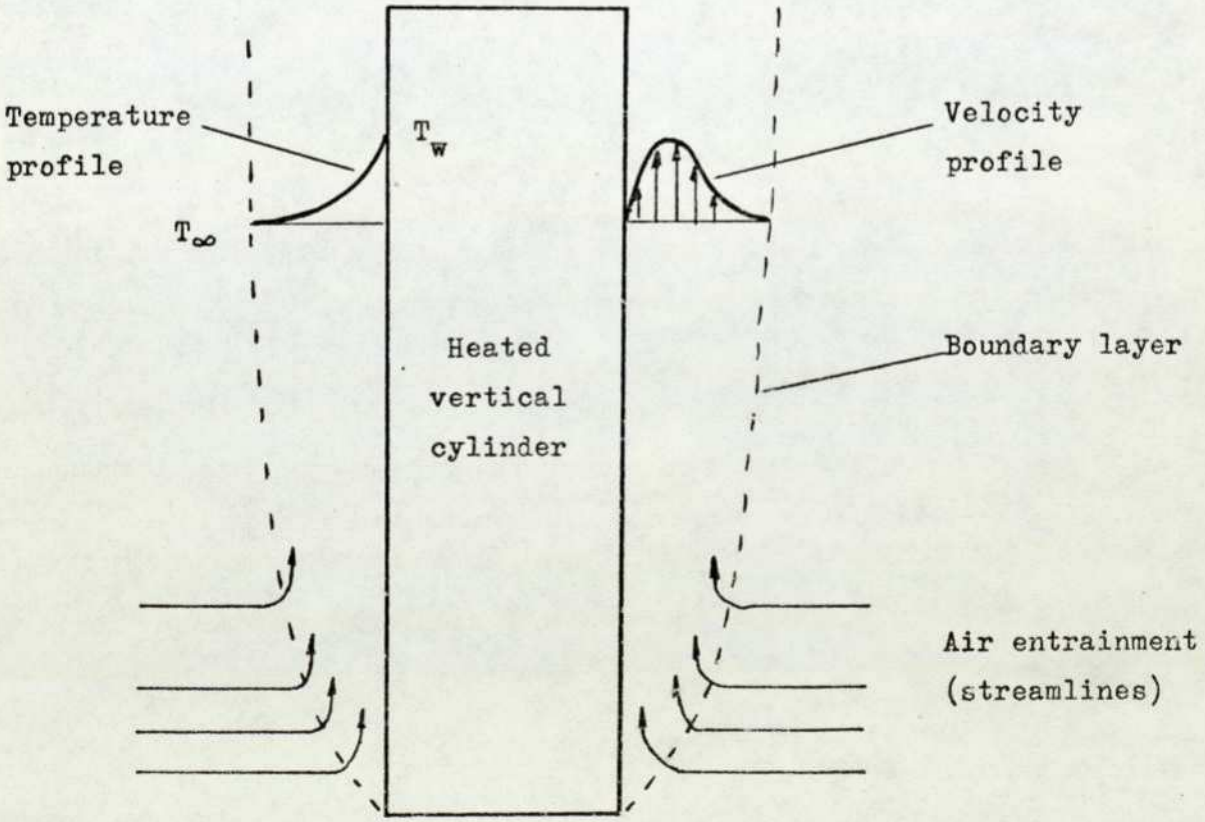
Under normal conditions, man is surrounded by a gas mixture (air) whose main constituents are Nitrogen (approx. 80%) and Oxygen (approx. 20%). In the case of the deep-sea diver in a hyperbaric diving chamber, a mixture of Helium and Oxygen is used at high pressure. In such a gas mixture it has been found that a higher environmental temperature is required for comfortable conditions Webb (10). This is known to be the result of changes in the convective heat loss from the body. In order to observe the convective changes associated with the above different gases, measurements were made with a surface plate calorimeter of the local free convection heat transfer coefficient h_c from the hand which was enclosed in (a) air, (b) Nitrogen, and (c) Helium.

Many of the physiological methods for measuring heat transfer, other than that of indirect calorimetry (appendix A), restrict body movement whilst measurements are in progress. However, the surface plate calorimeter offers little restriction and has been attached to the thigh of a runner. (Measurements were taken while the subject was running on a 'moving-belt' at an equivalent running speed of

4.5 ms^{-1}). The circumferential heat transfer distribution from the thigh of the runner are compared with results from a vertical heated cylinder in a cross-flow.

Since the convective flow pattern is known to be modified by the presence of clothing, Clark (4), measurements of the local heat transfer rates with different clothing fabrics on both a heated cylinder and the human body are presented for both free and forced convection conditions. Results are also presented of measurements of the local heat loss through different clothing assemblies, and also, for different spacings between the body and the covering material.

The sketch below shows diagrammatically the entrainment of the surrounding air into a natural convective boundary layer around a heated vertical cylinder.



2. CONVECTION HEAT LOSS FROM THE HUMAN BODY

A general discussion of the thermal balance that occurs between man and his environment will be developed in this chapter. This is discussed in relation to existing work on the particular type of human body heat loss of greatest interest in the present case, namely that due to convection.

Heat production and heat dissipation within the body have to be kept in balance by the thermoregulatory system if the internal body temperature is not to be allowed to rise to a dangerously high value. The gain in body heat may be considered to come from two sources;

(a) from the energy released per unit time from within the body, (Metabolic Rate, M),

(b) from the environment by convection (C), radiation (R), and conduction (K).

Since the environmental temperature is normally less than that of the body skin temperature the second of these sources is usually a negative one (a sink) and constitutes means by which heat is lost from the body. In addition body heat is also lost, in temperate climates, by evaporation (E) of water vapour from both lungs and skin surface (Appendix A).

If the body is not in thermal balance then the difference between heat production and heat dissipation will tend to change the average skin temperature, that is, a 'heat debt'* (S) will occur, Edholm and Burton (11). This heat debt will be positive when heat loss exceeds that of heat production and negative when heat production exceeds that of heat loss. This balancing of heat loss with heat gain per unit time may be expressed in an equation of the form;

---

* Gagge et al (12) originally introduced the term 'heat storage' to describe this thermal imbalance as positive when the heat loss exceeded heat production, but, since this term gives the erroneous impression that heat is permanently stored, the term 'heat debt' is considered a more accurate description.

$$M + S - C - R - K - E = 0 \qquad \ldots (2)$$

The heat loss or gain from the human body may be measured by one or more of the following calorimetric methods already used in physiology (Appendix A),

(i) Indirect Calorimetry --- measurement of the total heat produced per unit time by the method of gas analysis (that is, measurement of the Metabolic rate M);

(ii) Direct Calorimetry --- measurement of the total heat loss in a given time interval by all the heat transfer modes (that is, by convection, conduction, radiation, and evaporation);

(iii) Partitional Calorimetry --- evaluation of the individual heat transfer modes, usually by the process of elimination of such measurable quantities as evaporation, metabolism and heat debt in carefully controlled environments where either the radiation or the convection heat exchange can be reduced to zero*;

(iv) Internal Calorimetry --- not a useful method for determining heat transfer, rather for measuring thermal properties of body tissue;

(v) Model Calorimetry --- simulation of the human form by heated cylinders and life-size manikins for radiation and convection heat transfer studies.

According to this list of calorimetric techniques only the methods of Partitional and Model calorimetry are appropriate for studying the convective heat exchange, and it is one or other of these methods that have been used by many authors (refs 9-27) for evaluating the

---

* The convective heat exchange between a human body and its surroundings is evaluated by reducing both the radiation and conduction heat exchange to zero and measuring the Metabolic rate (M), evaporation (E), and heat debt (S) over a given time interval, thence from equation (2);

$$C = M + S - E \qquad \ldots (3)$$

overall convective heat transfer coefficient $(\bar{h}_c)^*$ for the human body.

The form this coefficient takes is usually decided by finding the best fit value for the results of the particular investigation. Where studies of the convective heat loss have been made under 'still air' conditions the value of $\bar{h}_c$ takes the form of a single value, but in other cases where the convective heat transfer resulting from various air velocities U has been studied, then $\bar{h}_c$ is given as an expression;

$$\bar{h}_c = A + B.U^n \qquad \ldots (4)$$

where A is the heat loss in 'still air' (air velocity $U \simeq 0$), and B and n are constants found from fitting experimental results.

In order to establish whether or not there is any relationship between different authors' results for the same convection condition an attempt to classify the results into two convective regimes, free convection and forced convection, have been made. This has been achieved by considering the velocity dependent part of the above expression $(B.U^n)$ as being due to forced convection, and the non-velocity dependent part (A) as the result of free convection.

2.1 FREE CONVECTION HEAT LOSS FROM THE HUMAN BODY

In 1928, Aldrich (13) published his results of a study of the radiation heat loss from (1) a vertical cylinder, and from (2) a horizontal cylinder, the idea being that these cylinders would be representative of the human body in the standing and supine postures respectively. From this study it was found that the vertical cylinder lost a rather greater proportion (about 7% more) by radiation than did the horizontal cylinder. (It follows that the horizontal cylinder

---

* $\bar{h}_c$ is the average amount of convective heat loss per unit area, per unit time, per degree Kelvin, from the body surface.

lost this same proportion more by free convection). If this is true also for the human body then significant changes in the convective heat loss may be expected for different body postures.

Since that time many investigators (refs. 9 – 27) have studied the convective heat exchange between the human body and its environment by measuring the overall convective heat transfer coefficient ($\bar{h}_c$) for the standing, reclining, and lying horizontal postures. From their results we might reasonably expect to find this convective difference becoming apparent, and in the cases where the same author has measured the heat loss from, for example, two postures, a difference is indeed noticeable.

Buttner (9) was, in 1934, one of the first to describe the features of a thermal boundary layer around the resting human form. This was achieved by comparing temperature gradients measured on heated horizontal cylinders and spheres to those measured on a nude horizontal subject, and he obtained an average value for $\bar{h}_c$ of 2.46 $W.m^{-2}.K^{-1}$ Different values for the same horizontal body posture have been published by Hardy & Dubois (14) in 1938, and recently by Missenard (15) in 1973. These authors have measured the convective heat loss by the method of partitional calorimetry and their results disagree; Hardy & Dubois recorded a value of between 0.9 -- 1.6 $W.m^{-2}.K^{-1}$ and Missenard a value of 3.05 $W.m^{-2}.K^{-1}$

Though small variations may have been expected in the results owing to the different methods used*, there is a rather wide range of values for the overall convection heat transfer coefficient ($\bar{h}_c$) for

---

* Buttner's method was different from the partitional calorimetric method used by the other authors in that (a) he measured temperature gradients at selected sites over the body surface and he averaged them in order to evaluate the convective heat loss for the entire body, and (b) his subject was lying on a bed and would, therefore, not have produced the same thermal flow field as if lying on the net support as used by Hardy & Dubois (14) and Missenard (15).

the same body posture.

For the standing posture, Hardy (16) measured values for the convection coefficient $\bar{h}_c$ of between 0.7 -- 0.93 $W.m^{-2}.K^{-1}$ by the method of partitional calorimetry. These values, if compared with the results of 0.9 -- 1.6 $W.m^{-2}.K^{-1}$ for the horizontal subject obtained by Hardy & Dubois (14), and 2.46 $W.m^{-2}.K^{-1}$ by Buttner (9), show that the heat loss from the body in the standing posture may be less than when lying horizontal; a fact supporting the earlier findings of Aldrich (13). This result is not supported by the results obtained by Missenard (15) who found that for a standing subject, the convection coefficient $\bar{h}_c$ was 3.5 $W.m^{-2}.K^{-1}$ and for the horizontal subject, 3.05 $W.m^{-2}.K^{-1}$

Again there are different results for the same posture (0.7 -- 0.93 $W.m^{-2}.K^{-1}$ in one case, and 3.5 $W.m^{-2}.K^{-1}$ in another), as well as two opposing trends, that is, (i) a higher heat loss for the supine subject than that for the standing subject, and (ii) a higher heat loss for the standing subject than that for the supine subject.

Only one theoretical solution appears so far to have been found for determining the convection heat loss from the human body in a standing posture. This is due to Clark (4). The approach is to consider the human body to be represented by a series of isothermally heated cylinders, Wissler (17). These cylinders may then be considered to be opened out into vertical flat plates so enabling the convective heat loss to be readily calculated by laminar boundary layer theory, Schlichting (50), Ostrach (51). By this method a convection heat loss (Q_{cv}) of 57.4 Watts was evaluated for a body surface temperature (T_w) of 33°C, and an environmental temperature (T_∞) of 15°C, and a body surface area (A_b) of 1.89 m^2. From these values an average convective heat transfer coefficient ($\bar{h}_c$) may be determined, since

$$\bar{h}_c = \frac{Q_{cv}}{A_b.(T_w - T_\infty)} = \frac{57.4}{1.89 \times (33 - 15)}$$

$$= \quad 1.7 \quad W.m^{-2}.\ K^{-1}$$

In the absense of data for other postures the only comment to be made is that this value is of the same order as those obtained by physiological measurements.

2.2 FORCED CONVECTION HEAT LOSS FROM THE HUMAN BODY

In this section the results of other investigations (refs.12-27) which have been classified represent the convective heat loss from the human body by the expression

$$\bar{h}_c = B.U^n \qquad \ldots \quad (5)$$

Furthermore, their results are divided into three sub-sections according to posture, that is, standing, reclining, and lying down.

2.2.1 CONVECTIVE HEAT LOSS FROM A STANDING SUBJECT

The results of Nelson et al (18) and Missenard (15) who both used partitional calorimetry as a method of evaluating the convective heat loss, demonstrate the widely differing values that have been found for the constants B and n in physiological heat loss experiments. For example, for a velocity range of $0.15 < U_\infty < 3.00$ m.s^{-1} Nelson et al (18) gives the expression

$$\bar{h}_c = 8.7\ U_\infty^{0.5} \qquad W.m^{-2}.\ K^{-1}$$

whereas Missenard (15) gives the following

$$\bar{h}_c = 3.5 + 4.9\ U_\infty \quad W.m^{-2}.\ K^{-1} \text{ for } U_\infty \leqslant 1.0 \text{ m.s}^{-1}$$

and

$$\bar{h}_c = 8.4\ U_\infty^{0.62} \quad W.m^{-2}.\ K^{-1} \text{ for } U_\infty \geqslant 1.0 \text{ m.s}^{-1}$$

An engineering approach to measuring the convection heat loss from a human body was used by Mitchel et al (19), who used a method first proposed by Carrol & Wisser (20) of measuring the temperature increase in the wake of a bluff body as a means of determining the convective heat exchange. From the results of this experiment, Mitchel found that values for B and n were:-

$$\bar{h}_c = 7.2\ U_\infty^{0.6} \quad W.m^{-2}K^{-1} \quad \text{for} \quad 0.5 < U_\infty < 5.0\ m.s^{-1}$$

This is a result similar to that found by Missenard for velocities greater than 0.25 $m.s^{-1}$.

The same type of expression has also been found by using models. For example, Hall (21) used a full size plastic manikin which he maintained at a constant temperature, in a low speed wind tunnel and he found that

$$\bar{h}_c = 2.9\ U_\infty^{0.8} \quad W.m^{-2}K^{-1} \quad \text{for} \quad 0.20 < U_\infty < 0.80\ m.s^{-1}$$

These values for B and n were not the same as those found by Tamari (22) who used a 1/4 scale segmented model of the human form which he was able to heat to 150°C. The model was then transferred to a wind tunnel and allowed to cool. The convection heat loss was then evaluated, for a range of air velocities, from the expression

$$Q_{cv} = m.Cp.\left(\frac{\partial T}{\partial t}\right)_{t=0} = h_c.A_b.(T_w - T_\infty) \qquad \ldots (6)$$

where $\left(\partial T/\partial t\right)_{t=0}$ is the rate of cooling of the body at time t = 0. By this method, Tamari found that the expression

$$\bar{h}_c = 7.1\ U_\infty^{0.643} \quad W.m^{-2}K^{-1} \quad \text{for} \quad 3.6 < U_\infty < 14.8\ m.s^{-1}$$

described the convective heat exchange for his 1/4 scale model. He then used a dimensional analysis to predict the convective heat loss from the human form as,

$$\bar{h}_c = 3.66\ U_\infty^{0.643} \quad W.m^{-2}K^{-1} \quad \text{for} \quad 0.85 < U_\infty < 3.54\ m.s^{-1}$$

In order to show more clearly the variation in the results for

predicting the convection heat loss from the human body in the standing posture, the above expressions have been plotted in Fig. 1, together with the results for the other postures.

2.2.2 CONVECTIVE HEAT LOSS FROM A RECLINING SUBJECT

The results obtained for this posture have been conducted in climatic chambers and the coefficients evaluated by the method of partitional calorimetry. Most of the measurements have been made at velocities less than 2.50 $m.s^{-1}$.

The early work of Gagge et al (23) suggested the relationship

$$\bar{h}_c = 11.6\, U_\infty^{0.5} \quad W.m^{-2}.K^{-1} \quad \text{for} \quad 0.05 < U_\infty < 0.11 \ m.s^{-1}$$

to hold for the human body in a reclining position. With the aid of a new improved climatic chamber in 1939, Winslow et al (24) measured the convective heat loss and suggested the relationship

$$\bar{h}_c = 12.8\, U_\infty^{0.5} \quad W.m^{-2}.K^{-1} \quad \text{for} \quad 0.046 < U_\infty < 0.075 \ m.s^{-1}$$

to hold for very low velocities. This was subsequently changed in 1940 (ref. 25), when higher convective velocities were considered, to

$$\bar{h}_c = 12.1\, U_\infty^{0.5} \quad W.m^{-2}.K^{-1} \quad \text{for} \quad 0.06 < U_\infty < 2.65 \ m.s^{-1}$$

A new formula put forward, quite recently, by Colin & Houdas (26) suggests that $\bar{h}_c$ does not follow a square root law as the other work implies, but rather depends on a 2/3 power law, thus

$$\bar{h}_c = 2.7 + 8.7\, U_\infty^{0.67} \quad W.m^{-2}.K^{-1} \quad \text{for} \quad 0.20 < U_\infty < 1.2 \ m.s^{-1}$$

Although the form of this expression is different to Winslow's the results are similar over the velocity range stated. Unfortunately Colin & Houdas's results are suspect since they measured their air velocities close to the skin surface instead of measuring the free-stream velocity, thereby obtaining a lower air velocity for the same measured body heat loss.

To facilitate comparisons the above results have been plotted in Fig. 1 with those for the standing subject.

2.2.3 CONVECTIVE HEAT LOSS FROM A SUPINE SUBJECT

The results obtained by various workers for this posture (refs. 9, 15, 22, 27) are presented in Table I together with those for the other two postures. From this table it will be seen that for a human subject in a horizontal position, a range of values have been found for the constants B and n (equation 5), from 2.54 to 11.4 for B, and from 0.5 to 1.0 for n.

The only two expressions that are similar are those put forward by Buttner (9) and Aikas & Pironen (27), that is,

$$\bar{h}_c = 7.3\ U_\infty^{0.5} \quad W.m^{-2}.K^{-1} \quad \text{for} \quad 0.15 < U_\infty < 0.50\ m.s^{-1}$$

by Buttner, and

$$\bar{h}_c = 7.9\ U_\infty^{0.5} \quad W.m^{-2}.K^{-1} \quad \text{for} \quad 0.15 < U_\infty < 0.22\ m.s^{-1}$$

by Aikas & Pironen.

These results, although they operate over a low velocity range, are plotted in Fig. 1 together with the results of Missenard (15),

$$\bar{h}_c = 3.05 + 10.6\ U_\infty \quad W.m^{-2}.K^{-1} \quad \text{for} \quad U_\infty \leqslant 0.25\ m.s^{-1}$$

$$\bar{h}_c = 11.4\ U_\infty^{0.5} \quad W.m^{-2}.K^{-1} \quad \text{for} \quad U \geqslant 0.25\ m.s^{-1}$$

and Tamari (22),

$$\bar{h}_c = 2.54\ U_\infty^{0.72} \quad W.m^{-2}.K^{-1} \quad \text{for} \quad 0.75 < U_\infty < 2.26\ m.s^{-1}$$

2.3 DISCUSSION

If equations of the type $\bar{h}_c = A + B.U_\infty^n$ are to be confidently used to estimate the convective heat loss from a human body, the spread of results among different investigators must be considered

rather than the reproducibility within one experimental series. McKerslake(28) has attempted to reduce the number of expressions by analysing several sets of results and reducing them to a square root relationship. He obtained the expression

$$\bar{h}_c = 8.3\ U_\infty^{0.5} \quad W.m^{-2}.K^{-1} \quad \text{for} \quad U_\infty > 0.25\ m.s^{-1}$$

Unfortunately only a limited number of results were studied and so this expression (which is also plotted in Fig. 1) is not a mean value of all the known results.

It is shown in Table I and in Fig. 1 that there are large differences between the results for both free and forced convection regimes, not only for the same posture but also for the different postures. It is impossible to say which value or expression is the more representative of the convection heat loss from the human body. Therefore, in order to improve our knowledge of the convective heat exchange a detailed study of the mechanism by which a body loses heat in the two convective regimes is required, as well as a description of the nature of the changes that occur within the thermal flow field. For example, in free convection it is known that the thermal boundary layer increases in thickness along the height of the body (ref 4). Increasing the thickness of this thermal 'overcoat' increases its insulating value thereby decreasing the convective heat loss, and vice versa. Therefore the local convection heat transfer coefficient h_c takes on different values at different heights according to this thickness. This is treated further in section 8.

In forced convection, the natural thermal boundary layer will be modified due to the boundary layer that will develop on the body as a result of the external flow, thereby increasing the local convective heat loss if the boundary layer decreases in thickness. In positions on the body which are sheltered from the external air-flow

the local convective heat loss may hardly alter.

By virtue of these arguments it would appear that if a detailed account of the local convection heat exchange from the human body could be provided then a clearer understanding of how the body may lose heat in any given circumstance may be possible. To attempt such an analysis on a mathematical basis would appear to be impossible, therefore an experimental method must be found for measuring the local convection heat transfer coefficient (h_c).

The only available experimental techniques that enable localised measurements to be made are those for measuring the convection and radiation heat losses from regional areas. For example, Burton (29) used a temperature gradient calorimeter for measuring the heat loss from the head, Forster et al (30) used a plethysmo-calorimeter* for heat loss from the hand, and Clifford (31) used a series of small heat flow meters for measuring the heat loss from arms, legs, and trunk.

For the present experiments it was decided to investigate more closely this latter method as a first step to finding an instrument capable of measuring local convection heat losses from the human body. But before taking measurements from a human this instrument was first tested under known convective heat transfer conditions in order to investigate its measuring capabilities (see section 4). To establish a convective flow pattern in which the local heat losses are known it is necessary to appreciate the fundamental laws of free and forced convection and to understand how the local convective heat loss changes with body geometry, orientation, and flow condition. For this reason a non-dimensional analysis for both convective regimes is included in section 3 together with a description of :-

---

* An instrument for measuring the blood flow through the hand as well as the heat loss from it.

(a) how the local convective heat transfer coefficient h_c varies

(i) along a vertical cylinder in free convection;

(ii) around a horizontal cylinder in free convection;

(iii) around a vertical cylinder in forced convection;

(b) how the total convective heat loss from a model (geometrically similar in shape and size to a human) may be determined from the local heat loss coefficient for

(i) a standing model in free convection;

(ii) a horizontal model in free convection.

Finally, it is worth commenting on the effect of humidity (water content) of the air flowing around the various bodies to be studied.

Although it is obvious, subjectively, that humidity has a large influence on heat loss rates and comfort, the reason for this is that it significantly affects the evaporative heat loss rate. Humidity has only a very small effect on convective heat loss from the human body, and what effect it does have results from changes in the Prandtl number (see page 21). For the present purposes the variation due to changes in humidity may be ignored and it suffices to state that all the author's tests were carried out in atmospheres of relative humidity varying from 40 per cent to 80 per cent, corresponding approximately to a range of Prandtl number of 0.72 to 0.78.

3. CONVECTION HEAT LOSS FROM FLAT PLATES AND CYLINDERS

In this section the convective heat loss from heated vertical flat plates and cylinders and horizontal cylinders in free and forced convection will be analysed. Dimensional analysis is used to find the physical variables that influence the two convective regimes and in each case the convective flow pattern and the heat transfer distribution is described.

The reasons for considering the convective heat loss from such bodies as heated cylinders are as follows:-

(i) the convective flow pattern around the human body in the standing and supine postures in free convection may be described by the flow patterns around heated vertical and horizontal cylinders respectively;

(ii) assuming that both the human body and heated cylinders lose heat by convection in a similar manner then the description of the local convection heat transfer distribution around heated cylinders in free and forced convection will indicate the way in which convective heat is lost from localised positions on the human body;

(iii) heated cylinders can be used in free and forced convection to check that the instruments we choose for measuring the local convection heat loss from the human body are indeed capable of measuring the correct magnitude of convection heat transfer.

3.1 DIMENSIONAL ANALYSIS FOR FREE CONVECTION

The free convective flow about a body of given geometry may be influenced by the physical variables listed below. These variables may be formed, by the method of dimensional analysis, into non-dimensional groups, allowing the convective heat transfer description for one particular body to be applicable to all bodies of the same

geometrical shape having the same values of the non-dimensional groups.

The variables that are listed below may be considered to affect in some way the convective heat loss from a body. For instance, consider a warm body immersed in a cool fluid; we may confidently assume that the shape of the body will have some effect on the convective heat loss, as well as,

(i) the density, viscosity and thermal conductivity of the surrounding fluid,

(ii) the temperature difference between the body and fluid,

(iii) the specific heat of the surrounding fluid,

(iv) the gravitational buoyancy $(g\beta)^{*}$ of the fluid,

(v) a convective heat transfer coefficient (that is, the rate at which the body loses heat per unit area per degree Kelvin).

QUANTITY	SYMBOL	UNITS
Typical body length	X	L
Density of the surrounding environment	ρ	ML^{-3}
Dynamic viscosity " " " "	μ	$ML^{-1}t^{-1}$
Thermal conductivity " " "	k	$JL^{-1}t^{-1}\theta^{-1}$
Temperature difference	θ	θ
Specific Heat of surrounding environment	C_p	$JM^{-1}\theta^{-1}$
Gravitational buoyancy " " "	$g\beta$	$Lt^{-2}\theta^{-1}$
Heat transfer coefficient	h_c	$JL^{-2}t^{-1}\theta^{-1}$

Where the units express length L, mass M, time t, temperature θ; and heat J.

---

* For a given mass of gas the coefficient of thermal expansion for that gas (β) represents the relative change in volume of a fluid element per degree temperature increase, and $g\beta$ represents the buoyancy force per unit mass on that fluid element; where $\beta = \frac{1}{T}$.

Although this is only strictly true for a perfect gas it may be safely assumed to apply to Air at normal temperatures and pressures (NTP).

These variables may be considered to be related in an equation of the form,

$$f(X^{a}, \rho^{b}, \mu^{c}, k^{d}, \theta^{e}, C_p^{m}, g\beta^{n}, h_c^{r}) = 0 \qquad \ldots (7)$$

Since there are 5 units for the 8 variables involved a unique solution is impossible, but a non-dimensional solution may be found such that there will occur $8 - 5 = 3$ undetermined functions in the form of non-dimensional groups, Buckingham's II Theorem (32).

$$\Pi_1 = X^{a_1} . \rho^{b_1} . \mu^{c_1} . k^{d_1} . \theta^{e_1} . C_p^{m}$$
$$\Pi_2 = X^{a_2} . \rho^{b_2} . \mu^{c_2} . k^{d_2} . \theta^{e_2} . g\beta^{n}$$
$$\Pi_3 = X^{a_3} . \rho^{b_3} . \mu^{c_3} . k^{d_3} . \theta^{e_3} . h_c^{r}$$

The actual variables involved in these groups may be found by the method of dimensional homogeneity, that is, by solving for the indices in each of the above equations, taking each unit separately. By this method, three possible solutions are given below,

$$\Pi_1 = \frac{g\beta . \theta . X^3 . \rho^2}{\mu^2} \qquad (G_r) \quad \text{Grashof Number}$$

$$\Pi_2 = \frac{C_p . \mu}{k} \qquad (Pr) \quad \text{Prandtl Number}$$

$$\Pi_3 = \frac{h_c . X}{k} \qquad (Nu) \quad \text{Nusselt Number}$$

Therefore equation (7) may be rewritten as,

$$f(Nu, Pr, G_r) = 0$$

or,
$$Nu = f(Pr, G_r) \qquad \ldots (8)$$

The Prandtl number is a non-dimensional grouping which depends only on the surrounding environment in which the body is immersed. Although it is temperature dependent it is approximately constant over

the temperature range of interest in this work, that is, between $10^{o}C$ - $40^{o}C$, and for air it has a value of Pr = 0.72. (The table below gives an example of the various Prandtl numbers for a range of fluids).

FLUID	PRANDTL NUMBER
Mercury	0.03
Air	0.72
Water	7.0
Oil	110.0

Since the Prandtl number takes on a particular value for air, the non-dimensional convective heat transfer coefficient (Nu) becomes dependent only on the Grashof number (Gr) which relates the buoyancy forces to the viscous forces within the natural convective boundary layer.

$$Nu = f(Gr) \qquad \ldots (9)$$

The particular relationship between the Nusselt number and the Grashof number is dependent upon whether the convective flow is laminar or turbulent*, Eckert & Jackson (33), Cheesewright (34). The change from laminar flow to turbulent is dependent on the value of the Grashof number. For a Grashof number below $Gr = 10^{8}$ the convective flow is generally laminar, and above 10^{10} generally turbulent. Between these values the flow is in a transitional state, although Cheesewright (34) has extrapolated his results for a vertical flat plate to give a precise value of 2×10^{9} for the change from laminar to turbulent.

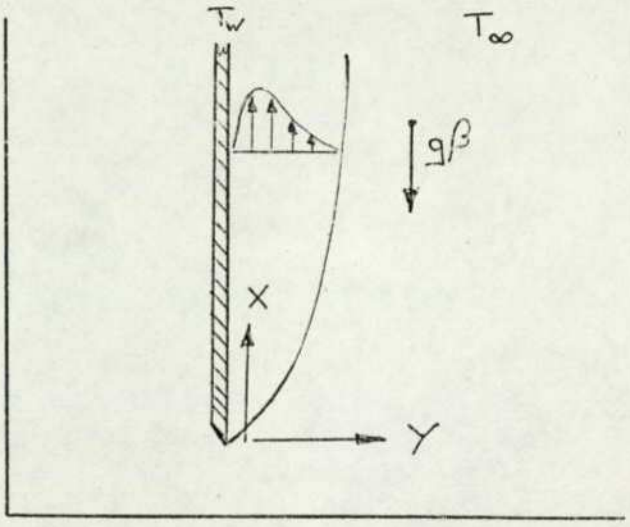
3.1.1 LAMINAR FREE CONVECTION FLOW FROM A VERTICAL FLAT PLATE

The laminar free convection flow from an isothermally heated vertical flat plate, with the coordinate system as shown below, is described

---

* For laminar free convection flow it may be shown that the Nusselt number is proportional to $Gr^{0.25}$, Ostrach (51), whereas for turbulent flow a semi-empirical relationship exists such that $Nu \propto Gr^{0.1}$, Cheesewright (34). Throughout the present work we will only consider the case of laminar free convective flows.

by the solution of the following boundary layer equations, refs (50) and (51).



Momentum in the X - direction,

$$u\frac{\partial u}{\partial x} + v\frac{\partial u}{\partial y} = \nu\frac{\partial^2 u}{\partial y^2} + g\beta(T_w - T_\infty) \qquad \ldots(10)$$

Energy in the X - direction

$$u\frac{\partial \theta}{\partial x} + v\frac{\partial \theta}{\partial y} = P_r\frac{\partial^2 \theta}{\partial y^2} \qquad \ldots(11)$$

Continuity

$$\frac{\partial u}{\partial x} + \frac{\partial v}{\partial y} = 0 \qquad \ldots(12)$$

with the boundary conditions,

$u = v = 0$ and $T = T_w$ at $y = 0$

$u = 0$ and $T = T_\infty$ at $y = \infty$

Ostrach (51) reduced these partial differential equations, by introducing a stream function ψ such that

$$u = \frac{\partial \psi}{\partial y} \qquad \text{and} \qquad v = -\frac{\partial \psi}{\partial x}$$

and the following similarity transforms,

$$\eta = \left(\frac{G_{T_x}}{4}\right)^{1/4}\frac{Y}{X}$$

$$\psi = (4X)^{3/4} \cdot F(\eta) \qquad \text{and} \qquad \theta = \frac{H(\eta)}{\beta T_\infty}$$

into two ordinary differential equations,

$$F''' + 3FF'' - 2F'^2 + H = 0 \qquad \ldots(13)$$

$$H'' + 2Pr.FH' = 0 \qquad \ldots(14)$$

where the primes denote differentiation with respect to η .

For these equations the boundary conditions become

$$F'(0) = F(0) = 0$$

$$H(0) = 1$$

$$F'(\infty) = H(\infty) = 0$$

The solution of these two equations (13) & (14) yields the non-dimensional velocity and temperature distributions within the thermal boundary layer, that is, the velocity profile is described by

$$F'(\eta) = u X / 2\nu\sqrt{G_{r_x}}$$

and the temperature profile by

$$H(\eta) = \left(\frac{T - T_\infty}{T_w - T_\infty} \right)$$

} Ostrach (51)

From these non-dimensional results, which are shown in Fig. 2, the actual velocity and temperature profiles for laminar free convection flow on an isothermally heated vertical flat plate may be obtained by substituting the values of height X, body temperature T_w, ambient temperature T_∞, and transverse distance away from the wall y into the respective expressions.

The local heat loss may be found from the local heat transfer parameter $H'(0)$, where

$$- H'(0) = Nu_x \Big/ (Gr_x/4)^{0.25}$$

For air , Pr = 0.72, the value of $- H'(0)$ was computed to be -0.5046. Hence the local Nusselt number at height X on a flat plate is

$$Nu_x = 0.3568\ Gr_x^{0.25} \qquad \ldots(15)$$

Furthermore, the average Nusselt number for a vertical flat plate

of height X is,

$$Nu_{av} = \frac{4}{3} Nu_x = 0.476\ Gr_x^{0.25} \qquad \ldots(16)$$

From these expressions the convection heat transfer coefficients h_c (local) and $\bar{h}_c$ (average) may be computed, since

$$Nu_x = h_c.x/k \qquad \text{and} \qquad Nu_{av} = \bar{h}_c.X/k$$

Fig. 3 shows how the local Grashof number, Nusselt number and heat transfer coefficient vary with increasing height X on a vertical flat plate, wall temperature $T_w = 33^oC$, air temperature $T = 15^oC$. From this figure it is shown that as the Grashof number and the Nusselt number increase the local convection heat transfer coefficient decreases. The reason for this is that at the lower edge of the plate, where local Grashof and Nusselt numbers are small, the temperature gradients are steep and the coefficient h_c large. With increasing height X, the boundary layer thickens and the temperature gradients become smaller with a consequent reduction in the value of the coefficient h_c.

3.1.2 LAMINAR FREE CONVECTION FLOW FROM CYLINDERS

Since a human body in the standing and lying horizontal postures may be represented by a vertical and horizontal cylinder respectively, a study of the free convective heat transfer for such cylinders will be useful as an initial stage in our understanding of the heat transfer process from a human subject. Thus we next report a consideration of,

(a) the difference between the local heat loss from vertical cylinders and flat plates, and,

(b) the local convective heat loss from horizontal cylinders.

3.1.2.1 VERTICAL CYLINDERS

The solutions of the equations of motion for the laminar free convection boundary layer on an isothermally heated vertical cylinder, in cylindrical coordinates, provided a local convective heat transfer rather higher than that for a vertical flat plate under the same conditions, Sparrow & Gregg (35). These authors found that the ratio of the Nusselt number for the cylinder to that for the flat plate was determined as a function of the cylinder radius, r_o, such that,

$$\left(Nu_x\right)_{cyl} = \left(Nu_x\right)_{fp} + \left(Nu_x\right)_{fp} \cdot \frac{0.98}{\sqrt[4]{Gr_x}} \left(\frac{X}{r_o}\right)$$

Since $\left(Nu_x\right)_{fp} = 0.3568\ Gr_x^{0.25}$ for $Pr = 0.72$, Ostrach (51), this expression reduces to

$$\left(Nu_x\right)_{cyl} = \left(Nu_x\right)_{fp} + 0.35\left(\frac{X}{r_o}\right) \qquad \ldots(17)$$

The local Nusselt number Nu_x and the convective heat transfer coefficient h_c are plotted for the case of two heated cylinders (one 0.10 m diameter, the other 0.20 m diameter) in Fig. 4 as a comparison with values for a flat plate. From this figure it will be seen that, for the same Grashof number, the convective heat loss for the 0.10 m diameter cylinder is some 14% greater than that for the 0.20 metre diameter cylinder. This implies that if the human body is assumed to be made up of a series of cylinders of different diameters, Wissler (17), for purposes of estimating the convective heat loss then each cylinder must be treated separately. The convective heat from a cylindrical model of the human form is computed from the above equation in section 3.2.

3.1.2.2 HORIZONTAL CYLINDERS

In 1933 Jodlbauer (36) measured both velocity and temperature profiles normal to the wall of an isothermally heated horizontal cylinder, and his results are shown in Fig. 5 together with the isotherms (i.e. constant temperature contours) around a heated cylinder given by Eckert & Soehngen (37). At the bottom of the cylinder the convective boundary layer is thin and the temperature gradients steep. As the flow progresses around the cylinder the boundary layer thickens until a heated plume is developed above the cylinder. The temperature gradients within this plume are markedly reduced.

Although it is possible to evaluate the local convective heat transfer coefficient h_c from the local temperature gradients, that is,

$$q_c/A = -k\left(\frac{\partial T}{\partial y}\right)_{y=0} = -h_c\,(T_w - T_\infty) \quad \ldots(18)$$

the method devised by Schmidt (38), using a schlieren technique, allows both the convective heat transfer envelope and the thermal boundary layer to be visualised, and enables the coefficient h_c to be determined. With this method, light rays from an arc lamp situated at a great distance from the body (approximately 30 m) fall axially upon the circumference of the horizontal cylinder and its silhouette is projected onto a screen. The light rays touching the heated surface are refracted by an amount proportional to the temperature gradient normal to the body, Fig. 6.

A theoretical solution for the case of the horizontal cylinder has been obtained by Hermann (39). This was accomplished by solving the boundary layer equations in cylindrical coordinates by an approximation method. This theoretical solution is plotted non-dimensionally in Fig. 7 as a comparison with the measured values obtained by Schmidt (38).

Of these two results the measured values of Schmidt are possibly the more accurate since in the approximation method of Hermann the boundary layer assumptions at the upper stagnation point strongly deviate from the actual conditions.

3.2 APPLICATION OF LAMINAR FREE CONVECTION HEAT TRANSFER THEORY TO THE HUMAN FORM

By considering the human body to be represented by a series of cylinders as proposed by Wissler (17) and Newling (40) we can compute the convective heat loss for the standing and horizontal cases. In this way an answer may be found to the question of whether or not the human body loses more heat when lying down than when standing.

3.2.1 DIMENSIONS USED IN THE MATHEMATICAL MODEL AND ASSUMPTIONS USED IN COMPUTATION

In the analysis given below the human form is represented by six separately heated cylinders the dimensions of which are shown in Fig. 8. The difference between this proposed model and that used in Newling's experiment is that the body trunk is considered a circular cylinder in our case rather than an elliptical cylinder. (The circular shape lends itself more easily to analysis).

The following table gives the dimensions and curved surface areas of the present model.

Cylinders	Model Part	Length m.	Diameter m.	Surface Area m^2
1	Leg	0.80	0.115	0.29
2	Leg	0.80	0.115	0.29
3	Arm	0.68	0.063	0.135
4	Arm	0.68	0.063	0.135
5	Trunk	0.68	0.305	0.65
6	Head	0.23	0.18	0.13
Total Body Area				1.63

The total body area involved in the calculations given below is 1.63 m^2 (total curved surface area of the six cylinders) which is a value lower than that for an average male of 1.8 m^2. The reason for this is that only the curved areas of the cylinder walls are used in the calculations and not the flat surfaces. (The total area of the flat surfaces is 0.16 m^2 which when added to the total cylindrical area of 1.63 m^2 gives an area for the complete model of 1.79 m^2, a value in good agreement with the above value of 1.8 m^2 for the average male).

The assumptions used in the calculations for the standing and lying horizontal postures are as follows:-

(i) constant cylinder wall temperature of 33°C,

(ii) constant ambient temperature of 15°C,

(iii) each cylinder loses heat as an isolated cylinder, that is, there is no interaction between the convective flow of one cylinder and another,

(iv) in the case of the standing model, laminar boundary layer theory was assumed to apply (although in fact the convective flow will go turbulent at approximately 1.2 m, we are only considering each cylinder separately and for the longest of these (the legs) the Grashof number is 1.6×10^9, that is below the critical value of 2×10^9 suggested by Cheesewright (34) for the change from laminar flow to turbulent),

(v) in the case of the horizontal model, the experimental results of Schmidt (38) were used in the analysis.

3.2.2 FREE CONVECTION HEAT LOSS FOR THE STANDING CASE

The convective heat loss for each cylinder was computed in the following way:-

(a) Each cylinder was first considered as a flat plate and the average Nusselt number evaluated from expression (16),

$$Nu_{av} = 0.476\ Gr_X^{0.25} = Nu_{fp}$$

(b) The Nusselt number for each cylinder was then calculated from equation (17), Sparrow & Gregg (35),

$$Nu_{cyl} = Nu_{fp} + 0.35 \frac{X}{r_o}$$

(c) From this Nusselt number the average convective heat transfer coefficient $\bar{h}_c$ was evaluated

$$\bar{h}_{c\ cyl} = Nu_{cyl} \cdot \left(\frac{k}{X}\right) \qquad W.m^{-2}.K^{-1}$$

(d) The total heat loss from each cylinder was computed by multiplying the coefficient by the area of the cylinder and the temperature difference,

$$Q_{cyl} = \left(\bar{h}_c\right)_{cyl} \cdot A_{cyl} \cdot (T_w - T_\infty) \qquad \text{Watts}$$

From this analysis the following convective heat losses were found for the standing case.

Model Part	Convective Heat Loss Q_{cyl} Watts	% of Total
Leg	16.5	16.9
Leg	16.5	16.9
Arm	8.5	8.7
Arm	8.5	8.7
Trunk	37.5	38.5
Head	10.0	10.3
Total	97.5	100

This value of 97.5 Watts is some 30% higher than an expected value of 70 Watts for a standing nude subject under the same environmental conditions. The reason for this difference may be attributed to:-

(i) assuming an isothermal body temperature of 33°C (in the real situation the skin temperature of a nude human subject in an environmental temperature of 15°C would take on different values over the body surface area;

(ii) assuming that there is no interaction between the convective flows around each cylinder (on the human body the convective flow pattern must be extremely complicated in such regions as the peripheral areas, between the legs and under the arms, and in these latter 'stagnation' regions the convective heat loss will be lower than that calculated for the 'freely suspended' limbs).

Even with this relatively high value of 97.5 Watts, the overall convective heat transfer coefficient $\bar{h}_c$ is of the correct magnitude, that is,

$$\bar{h}_c = \frac{Q_{cyl}}{A_t \cdot (T_w - T_\infty)}$$

$$= \quad 3.3 \quad W.m^{-2}.K^{-1}$$

where Q_{cyl} is the total heat loss, A_t is the total cylindrical area, and $(T_w - T_\infty)$ is the temperature difference between the body and the surrounding environment.

This is a value similar to that found by Missenard (15).

3.2.3 FREE CONVECTION HEAT LOSS FROM THE HORIZONTAL MODEL

The following method was used to calculate the free convective heat loss from each cylinder in turn:-

(a) From Schmidt's (38) results of the heat transfer distibution around the circumference of a heated horizontal cylinder, the average value for the non-dimensional heat dissipation was found to be

$$\frac{Nu}{Gr^{0.25}} = 0.42$$

(b) The Nusselt number (Nu_d) for each cylinder (diameter d) was obtained by first evaluating the Grashof number (Gr_d) for each cylinder in turn, $Gr_d = g\beta(T_w - T_\infty)d^3/\nu^2$, and substituting the value in the above expression.

(c) From this average Nusselt number for each cylinder the average convective heat transfer coefficient $\bar{h}_c$ was evaluated from the expression

$$\bar{h}_c = Nu_d \frac{k}{d}$$

and the total convective heat loss for each cylinder evaluated from

$$Q_{cyl} = \bar{h}_c \cdot A_{cyl} \cdot (T_w - T_\infty)$$

where A_{cyl} is the circumferential area of the cylinder, and $(T_w - T_\infty)$ is the temperature difference between the cylinder wall and the environment.

The results for the horizontal model obtained by this method are given in the table below.

Model Part	Surface Area m^2	% of total Area	Convective Heat Loss Q Watts	% of total Heat Loss
Leg	0.29	17.8	22.5	18.9
Leg	0.29	17.8	22.5	18.9
Arm	0.135	8.2	12.5	10.5
Arm	0.135	8.2	12.5	10.5
Trunk	0.65	40.0	40.0	33.6
Head	0.13	8.0	9.0	7.6
Total	1.63	100	119	100

With this analysis the total convective heat loss from the horizontal model is 119 Watts, a value some 21.5 Watts higher than for the standing case.

The overall convection heat transfer coefficient $\bar{h}_c$ for the complete model may be computed from,

$$\bar{h}_c = \frac{Q_{cyl}}{A_t \cdot (T_w - T_\infty)}$$

$$= \quad 4.0 \quad W.m^{-2}.{}^{o}K^{-1}$$

By comparing coefficients for the standing and horizontal models, that is,

$\bar{h}_c = 3.3 \quad W.m^{-2}.K^{-1}$ for the standing model

and $\bar{h}_c = 4.0 \quad W.m^{-2}.K^{-1}$ for the horizontal model

we see that the standing model loses approximately 17% less heat than that of the horizontal model. Since both models were of the same surface area and temperature, this difference can only be due to the convective flow pattern that surround the two bodies.

In the above analysis the human body has been considered as a simple, segmented cylindrical model and one of the dominant assumptions that have been used is that the convective heat loss from each cylinder has no effect on the heat loss from the other cylinders. This assumption is obviously not valid but it is shown in Appendix B that (for the standing model) by considering the cylinders separately the maximum laminar convective heat loss is obtained. In which case this assumption of independence will almost certainly mean that we have a greater overestimate for the convective heat transfer for the standing position than for the horizontal position, and we may therefore be fairly confident that in the real situation there is significantly more heat lost in the horizontal position than in the standing position.

3.3 DIMENSIONAL ANALYSIS FOR FORCED CONVECTION

In the method of dimensional analysis for a heated body immersed in a flowing medium of freestream velocity U_∞, we may assume that the buoyancy force $g\beta$ is negligible and can be replaced by the forcing velocity U_∞ in the list of variables, (section 3.1). Therefore no more dimensionless parameters become involved and that one set of parameters found to be useful is,

$\Pi_1 = h.X/k$ (Nu) Nusselt number

$\Pi_2 = U_\infty .X \rho/\mu$ (Re) Reynolds number

$\Pi_3 = C_p . \mu/k$ (Pr) Prandtl number

Since the Nusselt number may be considered to represent the non-dimensional convective heat transfer, this number may be expressed as a function of the other two numbers, such that,

$$Nu = f(Re, Pr) \quad \ldots(19)$$

For air the Prandtl number is very nearly constant at Pr = 0.72, therefore the Nusselt number (Nu) is dependent only on the Reynolds number of the fluid,

$$Nu = f(Re) \quad \ldots(20)$$

The particular relationship between the Nusselt number and the Reynolds number may be considered to depend on the following:-

(a) whether the overall heat loss or the local heat loss (sections 3.3.1 & 2) from the body is considered;

(b) the scale of freestream turbulence (section 3.3.3);

(c) for air velocities that are similar in magnitude to the convection velocities, the direction of the external air flow (section 3.3.4).

Since it is the aim of this work to find an instrument that can measure the local convective heat loss from a human body, it will be

necessary to first test the instrument in a situation where the local convective heat losses are known. This being the case, the following sub-sections deal with the local forced convection heat loss distribution around a heated circular cylinder in a cross-flow (this being the simplest and most documented study).

3.3.1 FORWARD STAGNATION POINT HEAT TRANSFER FROM A HEATED CYLINDER IN FORCED CONVECTION

Numerous approximate methods have been proposed for calculating the forced convection heat transfer coefficients at points on the surface of an isothermal body. Spalding & Pun (41) have analysed and classified fifteen theoretical methods but without more reliable experimental data than Schmidt & Wenner's (42), they could draw no final conclusion about the relative accuracy of the methods.

The exact prediction of the local heat transfer rate from the body, through the two dimensional, steady, laminar boundary layer is given by the solution of the following partial differential equations, ref (41).

Momentum

$$u\frac{\partial u}{\partial x} + v\frac{\partial u}{\partial y} = \nu\frac{\partial^2 u}{\partial y^2} \qquad \ldots(21)$$

Energy

$$u\frac{\partial T}{\partial x} + v\frac{\partial T}{\partial y} = P_r\frac{\partial^2 T}{\partial y^2} \qquad \ldots(22)$$

Continuity

$$\frac{\partial u}{\partial x} + \frac{\partial v}{\partial y} = 0 \qquad \ldots(23)$$

with the boundary conditions that the wall is isothermal and that

$u = v = 0$ and $T = T_w$ at $y = 0$

$u = U_\infty$ and $T = T_\infty$ at $y = \infty$

Frössling (43) solved these equations by a series method and obtained the only known exact solution for the non-dimensionalised

local convection heat transfer at the forward stagnation point of a heated cylinder in a cross-flow, that is,

$$Nu = 0.9449\ Re^{0.5} \qquad \ldots(24)$$

Other workers, such as Squire (44), Lighthill (45), Eckert (46), Lees (47), Ambrok (48), Allen & Look (49), have either reduced the above partial differential equations into ordinary differential equations by integration, or, have considered boundary layers with similar profiles but whose solution is given by ordinary differential equations. A comparison of these theoretical solutions is shown in the table given below, together with the experimental results of Schmidt & Wenner (42).

Author	Year	$Nu/\ Re^{0.5}$
Frössling	1940	0.9449
Squire	1942	0.90
Eckert	1942	0.945
Allen & Look	1943	1.87
Lighthill	1950	1.125
Lees	1956	0.80
Ambrok	1957	0.80
Schmidt & Wenner (Experimental)	1941	1.01

These latter authors measured the forward stagnation point heat transfer from a cylinder with a plug-type calorimeter inserted into a cavity within the cylinder wall, but insulated from it. The plug was heated electrically and maintained at the same temperature as that of the cylinder wall. The electrical energy supplied to the plug for this condition is equal to the local heat transfer from

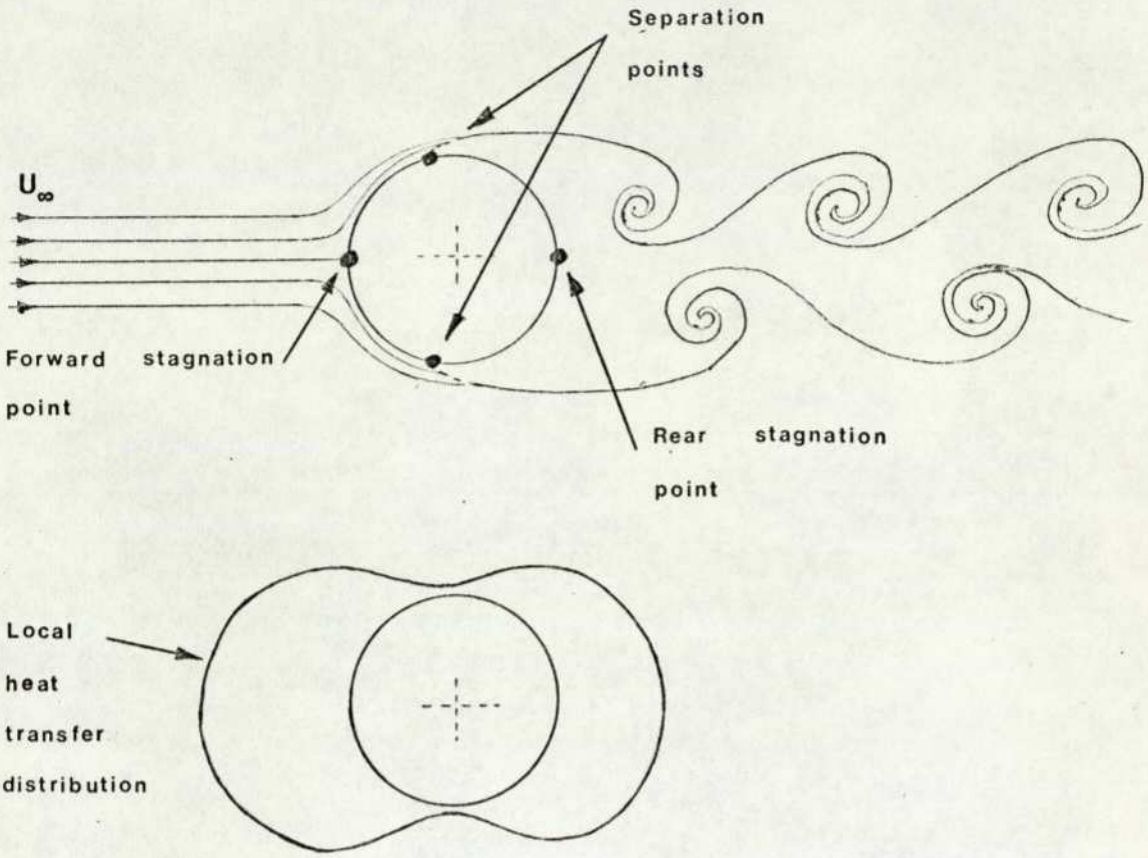
that position on the body, and it is this electrical quantity which is measured.

Direct comparisons between the theoretical and the experimental results are difficult since the effect of freestream turbulence (section 3.3.3) on the local heat transfer was almost certain to be present in the experiment, although of course no account is taken of this in the theory.

3.3.2 LOCAL HEAT TRANSFER DISTRIBUTION AROUND A HEATED CYLINDER IN FORCED CONVECTION

The distribution of the local convection heat transfer around the circumference of an isothermally heated cylinder in a cross-flow has been studied both theoretically and experimentally. The theoretical solutions as given by the authors already cited, (refs. 43 to 49) can only be considered to apply to the laminar boundary layer on the surface of the cylinder. Of these authors, only Frössling's (43) solution is exact, and this was assumed by Spalding & Pun (41) to be correct for the region $0 < X/D \leqslant 0.45$, where X is the distance around the circumference of the cylinder from the forward stagnation point, and D is the cylinder diameter. (No theoretical solution exists for the heat transfer in the region $0.45 < X/D \leqslant 1.0$ due to the complexity of the flow behind the cylinder, see sketch below).

The value of the local heat transfer coefficient (h_c) around a circular cylinder in a cross-flow is not constant but depends on the local thickness of the boundary layer on the cylinder surface. Since the greatest heat loss occurs where the boundary layer is thin (such as at the stagnation points where the temperature gradients are steep) and least where the boundary layer is thickest (at the separation points where the temperature gradients are less steep) the heat transfer distribution around the cylinder takes on an appearance similar to that shown in the sketch below.



In 1938 Krujilin (52) published his experimental results showing the reduction in the heat transfer coefficient in the neighbourhood of the separation points compared to that measured at the forward stagnation point. Schmidt & Wenner (42), in 1941, reported similar findings to those of Krujilin, although their actual values, especially at the forward stagnation point, were as much as 30% lower; their results were also in agreement with some published theoretical work of Squire (44). These authors, again using the plug-type calorimeter in the surface of a cylinder, showed that for a Reynolds number less than the critical value* of 3×10^5 the heat transfer is largest at the forward stagnation point where the boundary layer is thin and the temperature gradients steep. To either side of the stagnation point the laminar boundary layer thickens and the heat transfer decreases until the boundary layer flow reaches a position approximately 80° behind the stagnation point. At this position the flow separates

---

* Above a critical Reynolds number of 3×10^5 the flow behind a circular cylinder becomes fully turbulent; when this occurs the drag of the cylinder is markedly reduced and the heat loss over the rear half of the cylinder increases (ref. 50).
(Throughout the present work we will only be considering flows below this critical value).

and vortex shedding occurs. The heat transfer increases in value to a local maximum at the rear stagnation point.

3.3.3 EFFECT OF FREESTREAM TURBULENCE ON THE HEAT TRANSFER FROM A CYLINDER

As early as 1925 Reiher (53) reported that under various conditions of air turbulence (which was not measured quantitatively) the effect on the heat loss from cylinders could be increased by 100%. Goukhman (54) and McAdams (55) both state that an increase in heat transfer between 23% and 30% occurs from a single heated cylinder if two or more cylinders are placed upstream of the original cylinder.

Some quantitative work on the effect of turbulence on heat transfer was performed in 1949 by Comings, Clapp & Taylor (56); these authors observed that increasing the freestream turbulence level from 1 to 20% resulted in an increase in the rate of heat transfer from a cylinder, at a constant Reynolds number, of 25%.

The effect of increasing the intensity of the freestream turbulence ε, where $\varepsilon = \sqrt{\frac{1}{3}(\overline{u'^2} + \overline{v'^2} + \overline{w'^2})} \Big/ u_\infty$, on the local heat transfer from a cylinder has since been studied in more depth by Kestin et al (57), and Kestin & Maeder (58). These authors found that it was possible for the local heat flux from a cylinder to increase by as much as 80% for a freestream turbulence intensity of 2.5% compared to the turbulence free case as predicted by Frössling (43).

For the present purposes it is sufficient to note these results and to be aware that any measurements taken in forced convection can be expected to yeild higher results than the theoretical values.

3.3.4 EFFECT OF FLOW DIRECTION

Both the free and the forced convection regimes may be considered

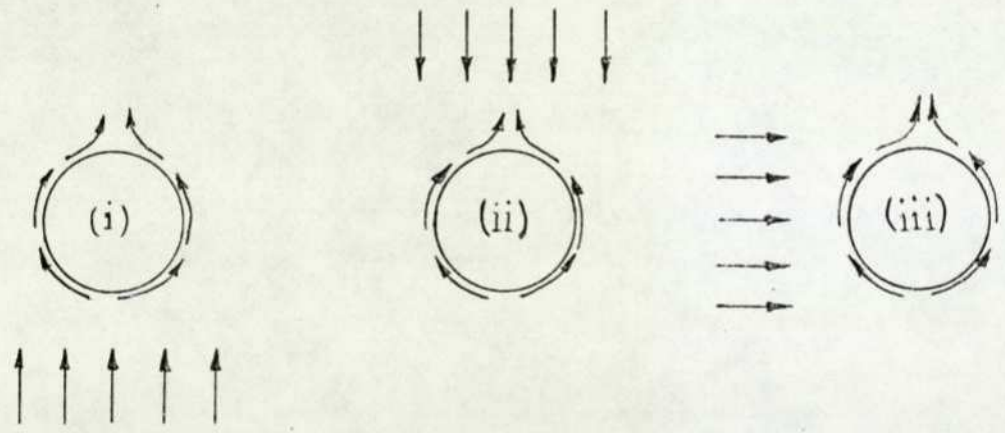
to be the limiting cases of the mixed free and forced convection regime, Collins (59), and since either of these limiting cases may be approached from within this mixed convection regime, one of the convective heat transfer modes will predominate over the other. In the case of the forced convection approaching the free convection mode, the direction of the forcing velocity will have some effect on the heat transfer, Hatton et al (60), Sparrow (61), since in one case it may be aiding heat transfer and in another opposing.

The direction of the forcing velocity may be defined in three cases, Sparrow et al (62);

(1) Aiding flow, in the same direction as the free convection flow,

(2) Opposing flow, in the opposite " " " " " "

(3) Cross flow, in the direction perpendicular to the free " "



In the following experiments on heat loss from the human body in forced convection, the subject stood in a low speed wind tunnel and therefore the flow can only be classified as a cross-flow.

3.4 EFFECT OF RADIUS OF CURVATURE ON THE HEAT TRANSFER

The effect of radius of curvature of a body on the convection heat loss in both free and forced convection is best demonstrated by the following examples.

3.4.1 LAMINAR FREE CONVECTION

For this case consider a heated horizontal cylinder losing heat by free convection. This cylinder will lose heat according to the relationship between the Nusselt number (Nu) and the Grashof number (Gr), that is,

$$Nu \propto Gr^{0.25} \qquad \text{(section 3.1.1)}$$

By basing both of these non-dimensional numbers on the cylinder radius, that is,

$$Nu_r = \frac{h_c.r}{k} \qquad \text{and} \qquad Gr_r = g\beta.(T_w - T_\infty).r^3/\nu^2$$

we obtain

$$Nu_r \propto Gr_r^{0.25}$$

or

$$\frac{h_c.r}{k} \propto \left\{ \frac{g\beta.(T_w - T_\infty).r^3}{\nu^2} \right\}^{0.25}$$

giving

$$h_c \propto 1/r^{0.25}$$

The local convection heat transfer coefficient h_c is therefore inversely dependent on $r^{0.25}$. Increasing the radius of curvature, results in a reduction in the value of the coefficient.

3.4.2 LAMINAR FORCED CONVECTION

For a heated cylinder in a cross-flow, the Nusselt number $Nu_r = h_c.r/k$ is dependent on the Reynolds number $Re_r = U_\infty.r/\nu$, such that

$$Nu_r \propto Re_r^{0.5}$$

We may rewrite this proportionality as

$$\frac{h_c.r}{k} \propto \left\{ \frac{U_\infty.r}{\nu} \right\}^{0.5}$$

giving

$$h_c \propto 1/r^{0.5}$$

Therefore the local convection heat transfer coefficient h_c is inversely proportional to $r^{0.5}$. This means that by doubling the

radius of curvature, the convective heat loss decreases by 29% in forced convection, and by 16% in free convection.

4. METHODS FOR MEASURING THE LOCAL CONVECTIVE HEAT LOSS FROM WARM BODIES

In order to find an instrument for measuring the local convective heat loss from the human body it is first necessary to examine the existing methods used in convective heat transfer studies. If any of these methods appear to be suitable then they must satisfy the following criteria:-

(a) the method of attachment of any instrument to the skin surface must not cause discomfort to the subject;

(b) the presence of any instrument in the thermal and velocity flow fields should cause only insignificant disturbance to these flow fields.

4.1 SELECTION OF INSTRUMENT

A variety of methods is available for measuring the local free and forced convection heat transfer from warm inanimate models, but few methods are suitable for use on a human body. For example, the following methods are used in many engineering applications but are unsuitable for the present purposes.

(1) Interferometric methods, using either Zehnder-Mach (Schardin, 63) or Schlieren (Sernas & Fletcher, 64), are mainly suitable for measuring temperature gradients in two-dimensional thermal flow fields (the flow field around the human body is three-dimensional).

(2) Temperature gradient methods (Cheesewright 65) using either thermocouples or hot-wire anemometers are satisfactory for fixed wall boundaries but would cause some discomfort to a human subject since he would have to keep extremely still whilst measurements were being taken.

(3) Surface temperature distribution methods (Giedt 66, VanMeel 67) are only suitable for bodies of known thermal conductivity and are

therefore certainly not applicable to the human body.

(4) Local calorimetric methods using either

(a) a plug-type heat sensor, such as the thin walled, transient response calorimeter (Gordon 68) which replaces part of the wall of the body and whose temperature-time gradient is proportional to the local heat flux (clearly an impractical method for use on the human body), or

(b) heated plug-type calorimeters of the type used by Schmidt and Wenner (42), and Coustanceau (69), which are only suitable where a cavity exists in the body surface. The plug is inserted into this cavity and is made flush with the external wall surface. The local heat loss rate is obtained by electrically heating the plug to the same temperature as that of the surrounding body temperature, and recording the electrical energy supplied for this condition, section 4.5; (Although this is an impracticable method for measuring the convective heat loss from a human body in the form described, it will be shown later that a similar device may be designed which is practicable, that is, a surface plate calorimeter, section 4.8).

Not all heat flux sensors fall into the categories described above, and Clifford (31) has measured the heat loss from different regional areas of the human body with a heat flow disk of the type described by Hatfield and Wilkins (70). In his experiment, Clifford attached several of these disks to a region of the body and covered them with one layer of surgical bandage. The presence of the bandage was found to damp the fluctuations in the readings caused by the external air currents over the exposed face of the disk. Other than stating that these fluctuations were only transient changes in the temperature of the outer face of the disk, and did not represent variations in the heat loss from the skin, no explanation is given for the fluctuating

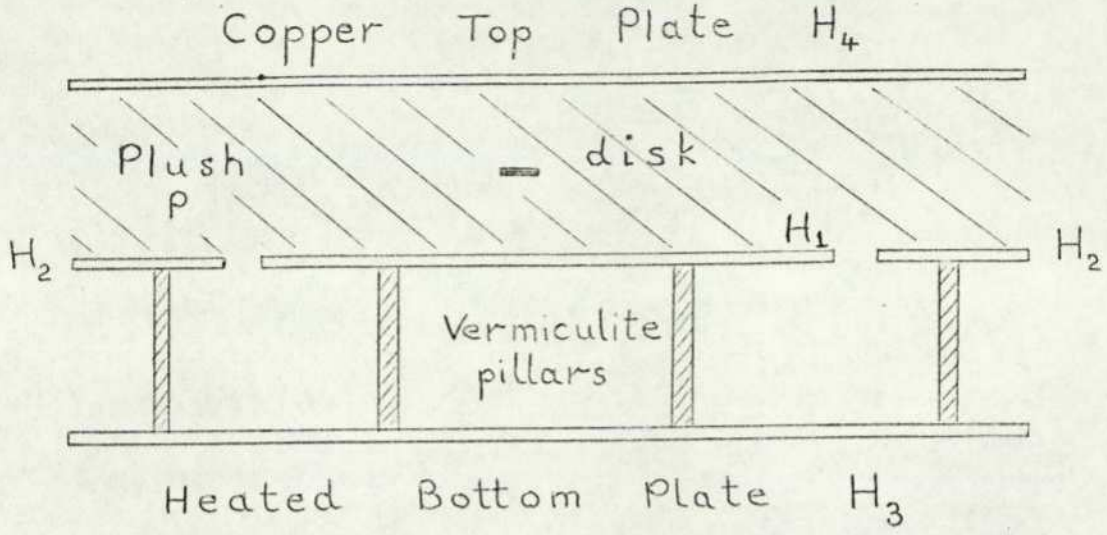
component, or to the exact position of the disk on the body. Since these disks may have been recording the local convective heat losses it was thought that a more detailed investigation of this instrument would be valuable since it also appears from Clifford's description to be sensitive to convective currents as well as being easily attached to the human body with 'plastic skin'.

4.2 HEAT FLOW DISK

The heat flow sensor, designed by Hatfield & Wilkins (70), is of the form of a small disk, measuring approximately 12 mm in diameter and 1.5 mm thick, of Tellurium-Silver alloy with a thin copper gauze coating on its two faces. By attaching the disk with its plane at right angles to the flow of heat to be measured, a temperature difference proportional to the heat flow through the disk occurs between the two faces. This temperature difference may be monitored on a galvanometer which is connected via copper leads to the two copper faces of the disk. (Tellurium-Silver has a high thermal electromotive force relative to copper, and a heat flow of 10 $W.m^{-2}$ will be recorded as 6.0 μV on a galvanometer).

4.2.1 DISK CALIBRATION

The disk, in its commercial form, is supplied with the manufacturers own calibration. The calibration is carried out by placing the disk in a one-dimensional heat flow field and measuring the potential difference across the two faces on a sensitive galvanometer. The calibration rig, which was designed by Hatfield & Wilkins, consisted of an electrically heated flat plate H_1, guard ring H_2, bottom plate H_3, a uniform pile of plush P, a uniform copper top plate H_4, and Vermiculite. The disk was inserted in the pile of plush above the heated plate H_1. (This rig is shown diagrammatically in the sketch below)



For the condition where the central plate H_1 and its guard ring H_2 and the bottom plate H_3 are all at the same temperature, the heat lost from the central plate, through the layers of plush*, produces a uniform one-dimensional heat flow field. This heat may be expressed by the one-dimensional heat flow equation,

$$q = -k_p . A_p . \frac{dT}{dy} \qquad \ldots(25)$$

where q is the electrical energy supplied to the heated plate H_1 and dissipated in the form of heat, k_p the thermal conductivity of the furniture plush, A_p the area of the heated plate H_1, and dT/dy the temperature gradient across the layers of plush.

This method of setting up a one-dimensional heat flow field, and then inserting a disk into this known heat flux for calibration purposes, is correct only if the presence of the disk does not interupt or disturb the heat flow field, that is, if the thermal resistance of the plush and disk combination is the same as that of the plush alone. However, if the field is disturbed then the disk may give an incorrect indication of the heat flux, and this would lead to inaccuracies in measurements taken from the human body. An investigation of what effect the disk has on the heat flow within the calibration rig is discussed below.

---

x Plush was used because of its low thermal conductivity.

4.2.2 THE CALIBRATION OF THE HEAT FLOW DISK

Since there is no radial heat flow in the centre portion of the calibration rig, the effect of the disk on the heat flow field may be investigated using the simple one-dimensional heat flow equation. This is achieved by considering the steady state condition, with the top plate H_4 and the heated central plate H_1 at constant temperatures T_1 and T_2, with the plates spaced at a distance d_1 apart by several layers of plush of constant thermal conductivity k_p. The heat flow per unit area across the plush is given by,

$$\left(\frac{q}{A}\right)_1 = k_p \cdot \frac{(T_2 - T_1)}{d_1} \qquad \ldots(26)$$

It is now possible to consider a heat flow disk of thermal conductivity k_d and of thickness d_2 to be inserted into the plush. In our analysis the following assumptions will be made:-

(1) that the diameter of the disk is far less than that of the flow field and that the temperature of the copper plate H_1 and the top plate H_4 remains unchanged,

(2) since the temperature difference between the two plates H_1 and H_4 also remain unchanged a one-dimensional heat flow $(q/A)_2$ acts separately through the plush and disk combination. (If the thermal resistance* of this combination is the same as that of the plush alone, then the heat flow will remain unchanged, that is, $(q/A)_1$.)

---

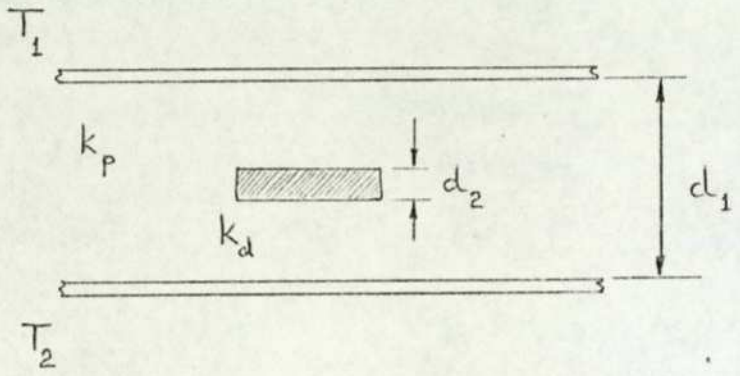
* If the heat flow equation $q = kA(T_1 - T_2)/d$ is stated in the form $(T_1 - T_2) = q.d/kA$, then this may be compared with Ohm's law, $E = RI$, where the potential difference E correspond to the temp. diff. $(T_1 - T_2)$, the electric current I correspond to the heat flow q, and the resistance R corresponds to the thermal resistance d/kA. Furthermore, the same laws that apply in electrical circuits apply in thermal ones, for example, the total resistance R of two resistors in series r1 and r2, is R = r1 + r2; similarly the total thermal resistance d/kA of two thermal resistors $(d/ka)_1$ and $(d/kA)_2$ is given by

$d/kA = (d/kA)_1 + (d/kA)_2$

For the heat flow through the plush without the disk being present equation 26 may be rewritten as

$$(T_2 - T_1) = \Delta T = \frac{d_1}{k_p} \cdot \left(\frac{q}{A}\right)_1 \qquad \ldots(27)$$

where d_1/k_p is considered to be the thermal resistance* of the plush. The sketch below shows a section through the calibration rig where the one-dimensional heat flow is assumed to apply, that is, above the heated central plate H_1.



For the case of the disk being present in the plush, consider the total thermal resistance of the combination, that is,

thermal resistance of plush = $(d_1 - d_2)/k_p$

thermal resistance of disk = $(d_2)/k_d$

thermal resistance of combination = $(d_1 - d_2)/k_p + (d_2)/k_d$

Since the temperature difference ΔT is assumed to remain unchanged, the one-dimensional heat flow equation for the plush and disk combination is

ΔT = (total thermal resistance) x heat flow

$$= \left\{\frac{(d_1 - d_2)}{k_p} + \frac{d_2}{k_d}\right\} \cdot \left(\frac{q}{A}\right)_2 \qquad \ldots(28)$$

* Since we are considering a heat flux per unit area we have adopted (d_1/k_p) as the thermal resistance.

By equating these two equations 27 & 28, and reducing them to the form

$$\left(\frac{q}{A}\right)_1 = \left(\frac{q}{A}\right)_2 \left\{ 1 - \frac{d_2}{d_1}\left(1 - \frac{k_p}{k_d}\right)\right\} \quad \ldots(29)$$

it may be seen that the heat flow through the disk is correct only if

(i) $d_2 \ll d_1$

or (ii) $k_p \simeq k_d$

otherwise the heat flux through the plush alone will be greater than that recorded by the metering disk. In the event that the calibration rig was designed so as to allow the disk to record the true value of the heat flux $(q/A)_1$, the disk may only be used under similar conditions where the above equation may be satisfied.

In the absence initially of a more satisfactory instrument it was decided to test the disk in the free and forced convection regimes despite the fact that it may give erroneous answers in situations other than one-dimensional heat flows.

4.3 EXPERIMENTAL APPARATUS FOR TESTING THE HEAT FLOW DISK IN FREE AND FORCED CONVECTION

In order to test the heat flow disk in a free convection regime, and in one in which results are already known, the disk was attached to the surface of a heated horizontal cylinder. For this test, a brass cylinder 7 cms diameter, 1.0 mm wall thickness, 50 cms in length was used. Its surface temperature was maintained constant at $34^{\circ}C \pm 0.2^{\circ}C$ (as monitored with an electric thermometer), by circulating warm water from a reservoir, through the cylinder, via a pump. The cylinder was mounted horizontally in a position in the laboratory where the external air currents were less than 0.05 $m.s^{-1}$, as found

from the output of a hot-wire anemometer. In this position, the cylinder was rotated axially through 360° in 30° intervals and the convection heat transfer distribution around the cylinder examined with the heat flow disk. The results were then compared to the well accepted experimental results of Schmidt (38).

For the forced convection experiment, the same cylinder was used, but in this case was mounted vertically in the octagonal working section of a low-speed wind tunnel. Air velocities in the wind tunnel were measured with a hot-wire anemometer of the type described by Clark (4). (The calibration of these anemometers was achieved using the rig described in Appendix C). With the disk attached to the cylinder surface measurements were taken of the forward stagnation point heat transfer and the results compared to the theoretical solution of Frössling (43).

4.3.1 FREE CONVECTION TEST FOR THE HEAT FLOW DISK

Hatfield & Wilkins (70) had found that the thickness and nature of the cement used for attaching the disk had no serious effect on the heat flow reading. Therefore, double-sided adhesive tape was used to attach the disk to the cylinder surface. (This means of attachment was chosen because the same method could be applied to the human body). To the side of the disk, a copper-constantan thermocouple was attached to the surface of the cylinder and the surface temperature measured.

In the steady state condition, the measured heat flow at the outer surface of the disk is equivalent to the convection and radiation heat loss from the disk surface, and in order that the radiation heat loss from the disk and the cylinder surfaces are the same the emissivity of both surfaces were made similar. This was done by painting them both matt black.

With the disk attached to the cylinder surface, measurements were taken of the cylinder wall temperature T_w, the environmental air temperature T_∞, and the heat flux (q/A). This measured heat loss may then be expressed by the following equation,

$$(q/A) = \text{convection} + \text{radiation}$$

$$= h_c.(T_w - T_\infty) + \sigma \varepsilon_o \varepsilon_i \left\{ \left(\frac{T_w}{100}\right)^4 - \left(\frac{T_\infty}{100}\right)^4 \right\} \quad ..(30)$$

where σ ($= 5.67\ W.m^{-2}K^{-4}$) is the Stefan-Boltzmann radiation constant, ε_o and ε_i the emissivities of the surroundings and the body surface respectively. Since the radiation term in this equation may be calculated, the local convective heat transfer coefficient h_c may be evaluated.

4.3.1.1 RESULTS OF THE FREE CONVECTION TEST

The results for the distribution of the heat transfer coefficient h_c around the cylinder were reduced to the non-dimensional form, Nusselt number $Nu_D = h_c.D/k_a$, where D is the cylinder diameter and k_a is the thermal conductivity of air. Since the Nusselt number is known to be dependent on the Grashof number, $Gr_D = g\beta(T_w - T_\infty)D^3/\nu^2$, by an equation of the form,

$$Nu_D \propto Gr_D^{0.25}$$

the heat transfer distribution was plotted as $Nu_D/Gr_D^{0.25}$ around the circumference of the cylinder. The results are shown in Fig. 9 together with the more reliable results of Schmidt (38). (Only one half of the cylinder is shown since symmetry is assumed).

The results for the convection heat transfer distribution as measured with the disk were obtained with a standard deviation of about 8% and are shown in Fig 9 to be approximately 25% higher than the experimental values of Schmidt, except near the upper stagnation

point where the flow breaks away into a plume. At this position the measured heat flow is much lower than that measured by Schmidt.

4.3.1.2 DISCUSSION OF THE RESULTS OF THE FREE CONVECTION TEST

The temperature within the free convective boundary layer falls from that of the wall to that of the surrounding environment, and the local convective heat loss is given by the temperature gradient at the wall,

$$\left(\frac{q}{A}\right) = h_c.(T_w - T_\infty) = - k_a \left(\frac{\partial T}{\partial y}\right)_{y = 0}$$

At the lower stagnation point on the circumference of the horizontal cylinder, the boundary layer is thin and the temperature gradient steep. It is at this point that the largest heat transfer rate occurs and this fact is also indicated by the heat flow disk.

At the upper stagnation point, the flow has broken away into a heated plume where the temperature gradients are shallow. This result is again shown by measurements taken with the disk.

The discrepancy between the results obtained with the disk and those of Schmidt cannot be explained simply by an incorrect calibration constant, since the results at the upper stagnation point are higher than Schmidt's results, and at the lower stagnation point, they are lower. One possible explanation for this difference may be the method by which the disk was calibrated. For instance, the disk was originally calibrated, by the manufacturers, in a one-dimensional heat flow situation, but this condition does not exist at the surface of a heated cylinder in free convection. Here the disk is cooled by the convective flow, not only from the face of the disk but also from its periphery, (the area of the face of the disk is twice that of the edges) as well as by radiation heat loss. Assuming that the radiation heat loss is constant around the cylinder then the heat flux

measured by the disk will depend on the amount of heat removed from the disk's face and edges by the convective boundary layer. The thickness of this boundary layer is considerably larger than the thickness of the disk over the upper half of the cylinder and is of similar thickness over the lower half. Furthermore, if we assume for the sake of simplicity that the heat flow is mainly lost through the face of the disk, that is a one-dimensional heat flow condition, equation 29 may be applied in order to explain the difference in the results,

$$\left(\frac{q}{A}\right)_{air} = \left(\frac{q}{A}\right)_{disk} \left\{1 - \frac{d_2}{d_1}\left(1 - \frac{k_a}{k_d}\right)\right\}$$

where d_1 is the boundary layer thickness (which corresponds to the plush thickness in the calibration rig), d_2 is the disk thickness, k_a and k_d the thermal conductivities of the air and disk respectively (the choice in these terms is governed by the derivation of equation 29 since we must consider the analogy of the air replacing the furniture plush)*.

In this equation the measured heat flux $(q/A)_{disk}$ will only measure the true heat flux $(q/A)_{air}$ if,

$$d_2/d_1 = 0 \qquad \text{or} \qquad k_a/k_d \simeq 1$$

The ratio of the thermal conductivities (k_a/k_d), in this case air to that of Tellurium-Silver, is fixed at approximately 1/200, therefore it is necessary that d_2/d_1 should be as small as possible for the true heat flux to be measured.

---

* The analogy we are applying in the above argument is that since the disk measures the heat lost across the plush in the calibration rig it may also be considered to measure the heat lost through a 'still air' layer (the boundary layer), and therefore, the boundary layer in our situation replaces the plush.

Over the upper half of the cylinder the boundary layer thickness d_1 is probably larger than the disk thickness d_2, due to the breaking away of the heated plume. Consequently, the measured heat flux $(q/A)_{disk}$ will tend towards the true value. For the lower half of the cylinder the ratio of d_2/d_1 will be larger than that for the upper half, consequently $(q/A)_{disk}$ will overestimate the true heat flux $(q/A)_{air}$, which has been found to be the case, Fig 9.

Without actually measuring the boundary layer thickness it is difficult to estimate by how much the measured heat flux will overread the true value. Furthermore, there are other factors involved which have not been taken into consideration; for example, the boundary layer does not compare precisely with the plush since the temperature distribution through it is far from linear.

4.3.2 FORCED CONVECTION TEST FOR THE HEAT FLOW DISK

For this test the 7 cm diameter cylinder was mounted vertically in the working section of a wind tunnel. The heat flow disk and a copper-constantan thermocouple were attached to the cylinder surface at the forward stagnation point. Measurements were recorded of the cylinder wall temperature T_w, the freestream air temperature T_∞, and the forward stagnation point heat flux (q/A) for different air velocities U_∞. (The freestream velocity U_∞ was measured* with a hot-wire anemometer at a position 30 cms upstream of the cylinder). The local convection heat transfer coefficient h_c was evaluated from equation 30

$$\left(\frac{q}{A}\right) = h_c \cdot (T_w - T_\infty) + \sigma \varepsilon_o \varepsilon_1 \left\{ \left(\frac{T_w}{100}\right)^4 - \left(\frac{T_\infty}{100}\right)^4 \right\}$$

* Throughout this work the wind tunnel velocity (U_t) was, in fact, measured and a blockage correction applied to it in order to evaluate the freestream velocity (U_∞), Appendix D.

since the radiation heat loss may be evaluated as in the previous case.

4.3.2.1 RESULTS OF THE FORCED CONVECTION TEST

After reducing the local convection heat transfer coefficient h_c to the non-dimensional number Nusselt number $Nu_D = h_c.D/k_a$, and the freestream velocity U_∞ to the equivalent Reynolds number $Re_D = U_\infty D/\nu$, the above results were plotted in the form Nu_D against $\sqrt{Re_D}$ in Fig. 10 together with the theoretical solution of Frössling (43). From this figure it may be seen that throughout the Reynolds number range tested, $10^2 < Re_D < 10^4$, the measured heat transfer rate underestimated the predicted heat flux in a non-linear manner. (This is the opposite effect to that found in the free convection regime). In order to explain this reduced heat flux, the effect of the disk on the boundary layer at the forward stagnation point must be considered and this is discussed below.

4.3.2.2 DISCUSSION OF THE RESULTS OF THE FORCED CONVECTION TEST

The boundary layer on a circular cylinder in a cross-flow is thinnest at the forward stagnation point (azimuth angle equal to zero) and increases in thickness around the forward half of the cylinder circumference until the flow separates at an azimuth angle of approximately 80°, section 3. The thickness of the boundary layer at the stagnation point decreases with increasing Reynolds number and, as the boundary layer decreases the temperature gradient between the cylinder wall and the surrounding environment also decreases, resulting in an increased convective heat loss.

Unfortunately, with the heat flow disk attached at this position the boundary layer growth is affected for three reasons:

(a) the disk produces a surface discontinuity to the freestream velocity,

(b) the thickness of the disk is comparable to that of the boundary layer,

(c) the boudary layer produced by the disk will affect the boundary layer of the cylinder.

Even assuming that the disk does not cause the flow to separate at the forward stagnation point and also assuming that increasing the Reynolds number will reduce the boundary layer thickness, it is unlikely that the reduction will be the same as that of a smooth cylinder. This hypothesis is given strength since if we assume a thicker boundary layer being produced as a result of introducing the disk, the measured heat transfer will be lower; and this is reflected in the results of Fig 10.

4.4 CONCLUDING REMARKS ON THE HEAT FLOW DISK

Although the heat flow disk was found to be small enough to measure local convection heat losses and could be attached comfortably to a human body, the following reasons are given for not continuing with this instrument in the present experiments:-

(A) the calibration of the instrument, as supplied commercially, was only applicable for a one-dimensional heat flow situation;

(i) by using the calibration constant as supplied, the disk overestimated the free convection heat loss from a horizontal cylinder by as much as 25% compared to the more accurately measured values of Schmidt (38),

(ii) for the forced convection test the disk under-estimated, by a variable amount, the local heat transfer at the forward stagnation point of a vertical cylinder in a cross-flow as compared to the theoretical prediction of Frössling (43);

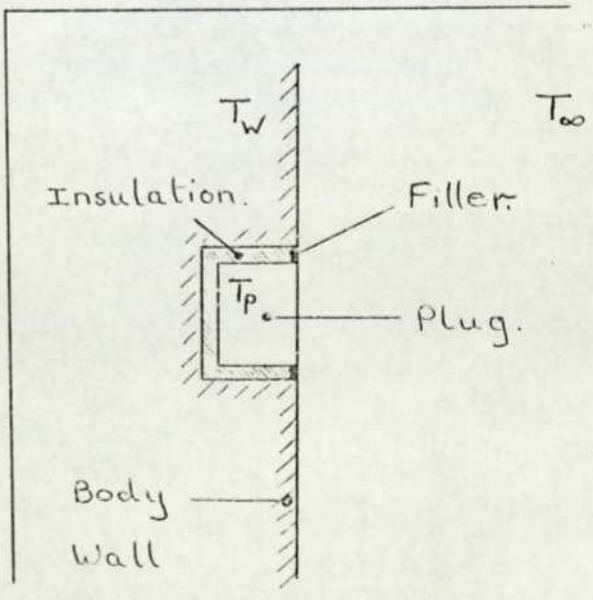
(B) even though it may be argued that the disk could be recalibrated from the curves of Figs. 9 and 10, this would give rise to two diff-

erent calibration curves, one for free convection and one for forced convection. Though this may be suitable for isothermally heated models, such as flat plates and cylinders in which the convective flow may be assumed to be free or forced with some confidence, it would be difficult in the case of the human body to be certain that the body was losing heat by either free or forced convection in order to use the correct calibration factor.

Since it was decided not use the heat flow disk an alternative instrument had to be found. This was achieved by first examining the methods adopted by Schmidt & Wenner (42) and Coustanceau (69) for measuring convective heat transfer and then designing and developing a surface plate calorimeter.

4.5 THE METHOD OF PLUG-TYPE CALORIMETRY

In 1941 Schmidt & Wenner (42) employed a method for measuring the local convective heat transfer around the circumference of a heated vertical cylinder in forced convection, and more recently (1967) Coustanceau (69) measured the local free convective heat loss from a vertical flat plate using a plug-type calorimeter. This instrument may be described as a small plug inserted into a cavity in the wall of a body at a position where the local heat transfer rate is to be found. This plug is heat-insulated from the rest of the body, except for one face of the plug and this is made flush with the external body surface. By supplying electrical power to a heater in the plug, the plug temperature T_p is raised to that of the body



temperature T_w. When this condition is achieved, the heat exchanged between the body and the plug is zero and the electrical energy is transformed into thermal energy and is lost from the one exposed face of the plug. This heat is lost by radiation and convection and may be expressed as

$$I^2R = Q_{rad} + Q_{conv} \qquad \ldots(31)$$

The local convective heat loss Q_{conv} may be evaluated by subtracting the radiation heat loss Q_{rad} (which may be calculated from the Stefan-Boltzmann radiation law, $Q_{rad} = \sigma \varepsilon_o \varepsilon_i ((T_w/100)^4 - (T_\infty/100)^4)$ from the electrical power supplied to the calorimeter.

This instrument has proved successful for both free and forced convection heat transfer measurements, but in order to develop a surface plate calorimeter so that it is independent of a cavity being in the body surface, it had to be decided whether the plug-type calorimeter is limited to one, two or three-dimensional heat flows. This is discussed in the following sub-sections.

4.5.1 LIMITATIONS TO THE USE OF THE PLUG-TYPE CALORIMETER

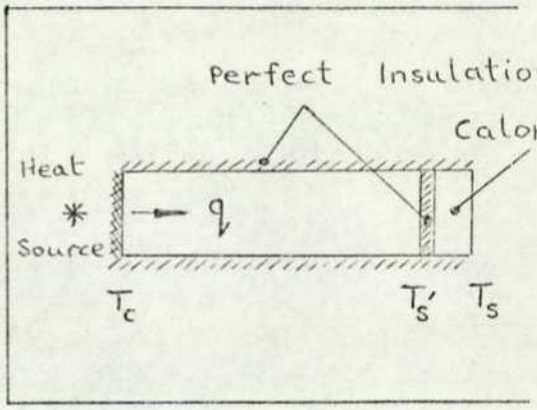
In order to investigate more fully the operation of the plug-type calorimeter consider first a one-dimensional heat flow system, and then a two/three-dimensional system.

4.5.1.1 ONE-DIMENSIONAL HEAT FLOW SYSTEM

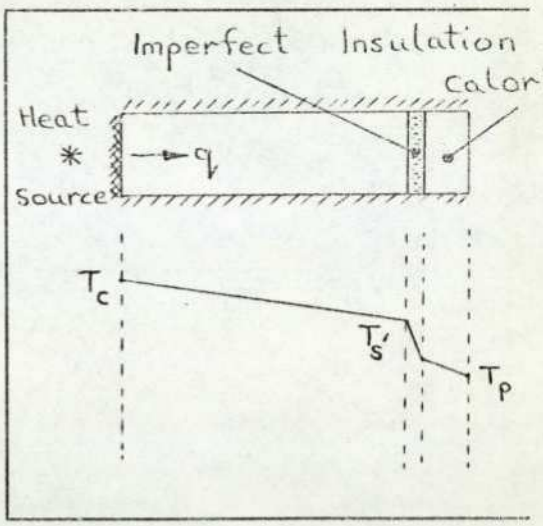
Consider an internally heated homogeneous body perfectly insulated from its surroundings except at one face; in the steady state condition, the internal temperature will be T_c, and at the free face T_s, where $T_c > T_s$. The heat conducted through the material per unit area is dependent on the thermal conductivity k of the body and the temperature gradient. For constant thermal properties, the temperature gradient will be linear, and $(q/A)_{cond} = -k.(dT/dY)$.

With the calorimeter inserted at the free face and having the same area as that of the free surface the consequences are:-

(1) If perfect insulation is used between the plug and the body surface, then the temperature of the body behind the calorimeter T_s' will rise to that of the core temperature T_c, and the heat flow will be reduced to zero (this situation is impractical since no insulation is perfect, and also the core temperature itself would rise because heat is being produced inside the body and is being prevented from escaping.)



(2) If poor insulation is used, the temperature of the body behind the calorimeter T_s' will be higher than that of the plug surface T_p due to the temperature gradient across the insulation, shown diagramatically in the sketch. This will remain as a steady state condition as long as the plug is not internally heated.

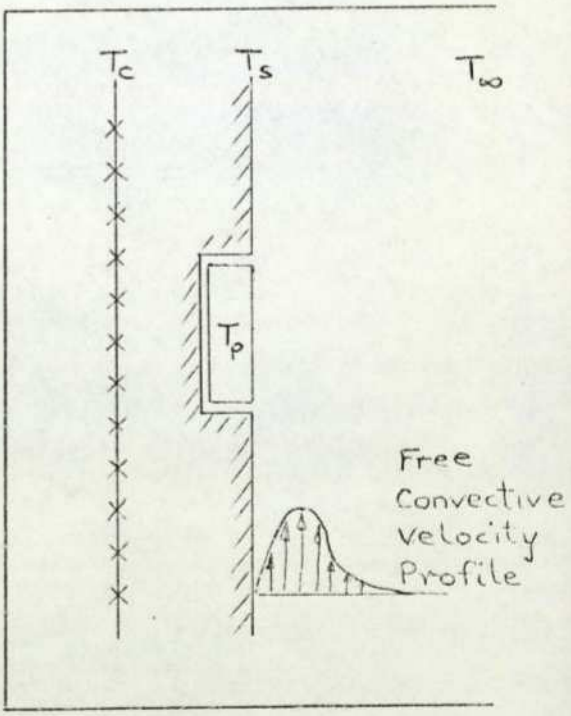


Since the required condition is where the plug temperature T_p is the same as that of the body surface temperature T_s', the electrical energy supplied to the plug, in order to attain this condition, will not only raise the temperature T_p but will also reduce the heat flow q in the body. This in turn raises the temperature T_s', and if the core temperature remains unaltered, more electrical energy will be required to raise the temperature T_p again. In this way, the electrical energy being supplied to the plug will reduce the heat flowing through the body material and the final result will be that, when $T_p = T_s'$,

then the plug temperature will also equal the core temperature T_c, that is, an isothermal situation will arise. (In the real case, the core temperature would also have to rise since heat is again being prevented from escaping). Therefore this method of measuring the heat transfer in a one-dimensional situation cannot be used since it dramatically affects the heat flow from the body. (An instrument using this one-dimensional heat flow phenomena has been used to measure the deep-body temperature of a human body, Fox et al (71). This is acceptable in such situations where locally isothermal conditions are approximated).

4.5.1.2 TWO-OR-THREE DIMENSIONAL HEAT FLOW SYSTEM

Consider a plug inserted into a cavity in the surface of a heated body as described previously. If a heat flow is produced within the body such that the internal core temperature T_c is higher than that of the surface temperature T_s, which is in turn higher than that of the surrounding environment T_∞, then a steady state condition will be obtained. For the case where the plug is perfectly insulated from the body, the temperature of the plug T_p will be close to that of the ambient temperature T_∞, (although in a convective flow the air moving over the plug surface may serve to increase the plug temperature above that in the far field) and under these circumstances the temperature and heat flow field within the body will be distorted from the original distribution which existed before the cavity was produced, Fig. 11 (a) and (b). This distortion will be minimal if



the size of the plug is small compared to that of the body since the heat produced within the body will be free to escape to the environment on either side of the plug, Fig. 11 (b).

Having considered the insulation to be perfect, raising the temperature of the plug T_p to that of the surrounding surface temperature T_s will not produce any increase in the temperature of the body behind the plug, therefore, further distortion of the thermal flow field within the body cannot occur. The electrical energy supplied to the plug in order to raise its temperature to that of the body surface T_s will, therefore, be lost by radiation and convection to the surrounding environment from the one exposed face of the plug. (If the nature of the plug's surface is similar to that of the body surface, then the heat loss from the plug is equivalent to the heat that would be lost from the body surface if the plug were not there).

If poor insulation is used between the plug and the body the distortion of the thermal flow field will be less than for a perfect insulator since some of the heat can flow through the insulation and the plug. In this case, heating of the plug to the temperature of the surrounding surface T_s will have the effect of reducing the conduction heat transfer through the insulation, the result being that this insulation will then act as a perfect insulator. Therefore, the final distortion of the temperature field will be similar to that shown in Fig. 11 (b), and the electrical energy supplied for this condition will again be equal to the radiation and convection heat loss from the exposed surface of the plug.

Since the plug-type calorimeter has proved successful in 2 or 3 dimensional heat flows (a condition which is certainly satisfied in the case of a human body) but cannot be used on a human subject, it was decided to investigate the possibility of developing a surface instrument on the same principles but capable of being attached to the human body.

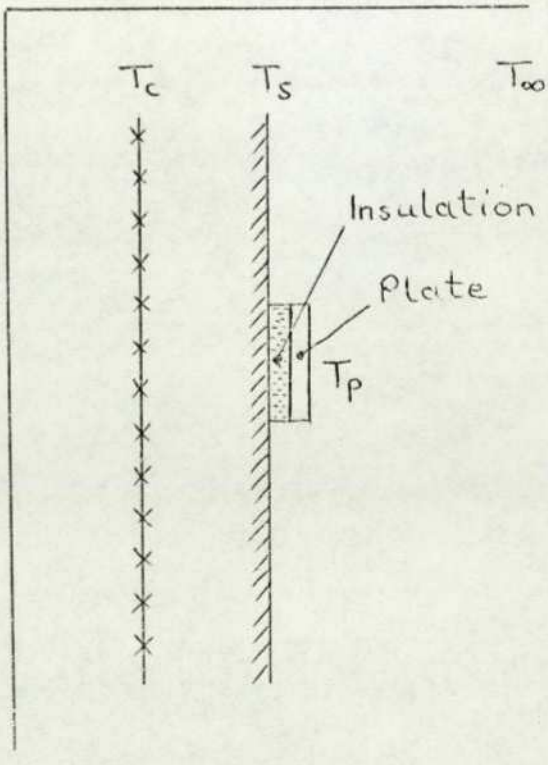
4.6 THE CONCEPT OF A SURFACE PLATE CALORIMETER

The initial considerations in designing a surface instrument were based on developing a small plate that could be attached to a body surface but insulated from it. Further criteria were that it should be capable of being electrically heated internally and that it should be small in comparison to the body; also it had to be small if it were not to suffer from the same problems of the Hatfield-Turner heat flow disk, namely the disturbance of the convective flow due to the presence of the instrument. A similar discussion to that given above for the plug-type calorimeter is given below.

4.6.1 PLATE PERFECTLY INSULATED FROM A HEATED BODY

Consider an internally heated homogeneous body in the steady state condition. Before a surface instrument is attached to it the internal heat flow field may be considered uniform as shown in the isothermal heat flow diagram, Fig. 11 (a).

With the plate attached to the body surface but perfectly insulated from it, as shown in the sketch below, the thermal flow field in the body behind the insulation will appear as shown in the isothermal heat flow diagram in Fig. 11 (c) when the steady state condition is reached. It is shown from this figure that the temperature of the body surface behind the insulation will be expected to rise, but because this is a two-dimensional heat flow situation the rise in temperature will depend on the area of the surface instrument;



the smaller the area of the plate covering the body surface the lower will be the temperature increase.

Since a perfect insulator is being considered, the plate temperature T_p will, in the absence of any heat being supplied to the calorimeter, be lower than that of the surface temperature of the body T_s, and apart from the convective heat gained from the natural convective flow, will be close to the temperature of the surrounding environment T_∞. Increasing the temperature of the plate T_p to that of the body surface temperature T_s, by electrically heating the plate, will not affect the thermal flow field behind the insulator, and consequently, this electrical energy may be considered to be lost to the environment from the free face of the plate by radiation and convection. This heat lost being equivalent to that which the body surface would lose if the calorimeter were not attached to the body.

4.6.2 PLATE IMPERFECTLY INSULATED FROM A HEATED BODY

For this case, some heat will be conducted through the insulation and the plate to the surrounding environment, and the thermal flow field within the body will not be so distorted as in the previous case, Fig. 11 (c). Heating of the plate to the same temperature as that of the body surface T_s will result in the conduction heat loss through the insulation being reduced to zero, and for this condition, this imperfect insulator will then act as a perfect one. Consequently the thermal flow field in the body will also be similar to that for a perfect insulator, and the electrical energy supplied will again be lost, by radiation and convection, to the environment from the free face of the plate.

4.7 DESIGN AND CONSTRUCTION OF A SURFACE PLATE CALORIMETER

Up to this point the concept of a surface plate calorimeter for

measuring the local convection and radiation heat loss from the surface of a warm body has only been considered as a hypothetical instrument devoid of any technical details of its actual construction. Assuming that such an instrument could be constructed to satisfy the conditions given above, that is, that it should be small in order not to distort to any appreciable extent either the convective flow pattern or the heat flow field within the body, then the next consideration must be the actual physical size of the calorimeter and the components for its construction.

Since the surface plate calorimeter was modelled, for its operation, on the plug-type calorimeter the following components needed to be found:-

(1) a surface plate to replace the copper plug in the latter instrument;

(2) a heater in order to increase the plate temperature to that of the surrounding body;

(3) a thermo-sensor for recording the temperature of the plate for comparison with the temperature of the surrounding body;

(4) suitable insulation in order to insulate the plate from the body surface.

To select the right material for each of these components several arguments had to be considered and these are outlined below.

4.7.1 SELECTION OF PLATE MATERIAL

The function of the plate is to dissipate the heat generated within the calorimeter by the electric heater to the surrounding environment by convection and radiation from the external face of the plate. To do this efficiently the plate must be heated as uniformily as possible without causing steep temperature gradients to occur across either the thickness of the plate or along the plate surface.

Therefore the plate itself must be thin and the material selected of high thermal conductivity.

The range of possible materials which are commercially available in sheet form are listed in the table below, together with their thermal conductivities for $0^{o}C$, Kaye & Laby (72).

Material	Thermal Conductivity k $W.m^{-1}.K^{-1}$
Brass	96
Constantan	22
Copper	385
Gold	310
Platinum	73
Silver	418
Stainless Steel	24.5

From this list only copper, silver and gold are of high thermal conductivity, but since it was considered that many instruments were to be used, the cost of using either silver or gold was considered prohibitive. Therefore available copper sheet of thickness 0.05 mm, thermal conductivity k = 385 $W.m^{-1}.K^{-1}$, was selected as the most promising plate material.

4.7.2 SELECTION OF ELECTRIC HEATER

The points that had to be considered in selecting this particular component were,

(i) that the heater must be thin as possible (so that the overall thickness of the calorimeter is thin to prevent the convective flow pattern being distorted),

(ii) in order not to create hot spots within the calorimeter it is

essential that the heating grid be of a uniform resistance.

To meet these requirements attempts were made at winding narrow gauge high resistance wire uniformily around a former. This proved unsuccessful on two counts:-

(a) inability to obtain a uniform resistance field,

(b) the heater produced by this method was too bulky, being some 20 times thicker than the copper plate.

The solution to these problems was to use a component normally used for measuring strain in structures under load, that is, the strain gauge. This commercially available component is manufactured to within very close tolerance levels as regards size and resistance, and the ones selected for use in the calorimeter were made by Hottinger & Baldwin, type LE 11. This gauge had the resistance grid (120 Ohms $\pm$ 0.2%) encapsulated for electrical insulation and short leads already attached. (Since the gauge is used simply as a heater any other similar type of strain gauge would be suitable).

4.7.3 SELECTION OF THERMOSENSOR

In order to monitor the temperature of both the copper plate and the surrounding body surface, copper-constantan thermocouples were selected as the most convenient form of thermosensor. The reasons for selecting this particular combination were:-

(i) this type of thermocouple could be easily attached to the copper plate without the need for insulating the thermocouple from the plate (with any other combination this would not have been the case since extra thermal electromotive forces would arise between the copper plate and the combination giving incorrect results),

(ii) wire of diameter 0.10 mm could be easily handled and attached to the plate.

4.7.4 SELECTION OF INSULATOR

Other workers who used plug-type calorimetry, such as Schmidt & Wenner (42) and Coustanceau (69), have used air and air-wool respectively as the insulator between the body and the plug. Although the thermal conductivities of these two insulators are low (being 0.026 $W.m^{-1}.K^{-1}$ and 0.04 $W.m^{-1}.K^{-1}$ respectively) they were found to be impossible to use with the surface plate calorimeter. Alternatively, other low thermal conductive materials were tried as the possible insulator, such as mica, cork, balsa, and paper, but difficulty was experienced in shaping and fixing the insulator to the back of the plate as well as keeping the insulator thin in the process.

These difficulties were finally overcome by deciding to use an Epoxy Resin not only as the bonding agent for attaching the strain gauge to the plate but also as the insulator, since the thermal conductivity of this material is approximately $k = 0.5\ W.m^{-1}.K^{-1}$ (Roff & Scott, 73). This material was considered ideal since it could be poured in its liquid state over the already assembled copper plate, heater and thermocouple to a known depth and allowed to harden. On hardening, any excess resin may be trimmed and the calorimeter, apart from attaching the heater leads, is thus complete.

4.8 DESCRIPTION OF THE COMPLETED SURFACE PLATE CALORIMETER

A completed calorimeter is shown in Fig. 12 and in diagrammatic form in Fig. 13. An electric heating element (the strain gauge) is attached to one surface of a copper plate 0.05 mm thick and approximately 8 mm by 12 mm in area. Since we are mainly concerned with comparing the temperature of the copper plate to that of the surrounding body surface a differential thermocouple was incorporated into the calorimeter. This was achieved by spot soldering an insulated copper lead (1.0 m long, 0.10 mm diameter) and an insulated constantan lead

(5.0 cm long, 0.10 mm diameter) to the copper plate on either side of the heating element. The copper plate then acts as one junction, A, of a differential thermocouple, the other junction, B, being formed by joining a second copper wire (1.0 m long, 0.10 mm diameter) to the free end of the constantan lead. The heater element and junction A are both protected with a layer of Epoxy Resin approximately 0.15 mm thick. Typical dimensions of a surface plate calorimeter are 8 mm x 12 mm x 0.20 mm.

4.8.1 METHOD OF USE

The calorimeter is normally attached to the body surface with double-sided adhesive tape, with the insulated side of the calorimeter towards the body surface. Thermocouple junction B is attached to the body surface close to the calorimeter so as to form the reference junction for the differential thermocouple. Because of the conduction heat loss through the insulation and the convection and radiation heat losses from the exposed surface, a temperature difference is established between junctions A and B and the resulting potential difference is monitored on a galvanometer. The calorimeter is then electrically heated until a null reading is obtained on the galvanometer. No heat can then flow between the calorimeter and the body surface, and the electric power supplied is therefore a measure of the convection and radiation heat loss from the exposed copper surface. If the emissivity of this surface is the same as that of the body surface, then the electric power supplied is equal to the convective and radiative heat loss from the equivalent area of the body surface covered by the calorimeter, that is,

$$i^2R = h_c.A_c.(T_w - T_\infty) + \sigma \varepsilon_o \varepsilon_1 A_c \left\{ \left(\frac{T_w}{100}\right)^4 - \left(\frac{T_r}{100}\right)^4 \right\} \quad ..(32)$$

where i^2R is the electrical power supplied as heat to the calorimeter; $h_c.A_c.(T_w - T_\infty)$ is the convective heat loss from the calorimeter surface; and $\sigma \varepsilon_o \varepsilon_1 \; A_c.\left\{\left(\frac{T_w}{100}\right)^4 - \left(\frac{T_r}{100}\right)^4\right\}$ is the radiative heat loss.

If the emissivities ε_o and ε_1 are known, and also the surrounding temperature T_r, it is possible to calculate the radiative heat loss from the Stefan-Boltzmann equation (given above) and hence obtain the local convective heat transfer coefficient, h_c.

4.8.2 RADIATION CORRECTION

In many situations it is possible to calculate the radiative heat loss for use in equation 31, but in the case where neither the surrounding radiative temperature T_r nor the emmisivity of the surrounding environment ε_o is known, the following method may be used.

The local heat loss from the body surface is measured with two calorimeters each with a different known surface emissivity at the point at which the local convective heat loss is required to be evaluated. Each of the calorimeters will radiate heat to the surroundings proportional to the emissivity of their respective surfaces, and furthermore, since neither the convective heat loss nor the calorimeter surface temperature will change, the only other variable to counterbalance the differing radiative heat losses due to these different surface emissivities is the electrical energy supplied to the heater.

For calorimeter (1) with surface emissivity ε_1, thermal balance is obtained when

$$(i^2R)_1 = h_c.A_c.(T_w - T_\infty) + \sigma \varepsilon_o \varepsilon_1 \; A_c.\left\{\left(\frac{T_w}{100}\right)^4 - \left(\frac{T_r}{100}\right)^4\right\}$$

and for calorimeter (2) with surface emissivity ε_2,

$$(i^2R)_2 = h_c.A_c.(T_w - T_\infty) + \sigma \varepsilon_o \varepsilon_2 \; A_c\left\{\left(\frac{T_w}{100}\right)^4 - \left(\frac{T_r}{100}\right)^4\right\}$$

During the measuring period, if the emissivity of the surroundings (ε_o) and the radiative temperature T_r remains unchanged, then these equations may be combined to give:-

$$\frac{(i^2R)_1 - h_c.A_c.(T_w - T_\infty)}{(i^2R)_2 - h_c.A_c.(T_w - T_\infty)} = \frac{\varepsilon_1}{\varepsilon_2} = \bar{\varepsilon}$$

where $\bar{\varepsilon}$ is the ratio of the surface emissivities.

Therefore the local convective heat transfer coefficient h_c may be obtained from

$$h_c = \frac{(i^2R)_1 - \bar{\varepsilon}\ (i^2R)_2}{A_c.(T_w - T_\infty).(1 - \bar{\varepsilon})} \qquad \ldots(33)$$

It is obviously important to chose the emissivities of the two calorimeters (ε_1 and ε_2) to be very different from one another otherwise the ratio of $\varepsilon_1/\varepsilon_2$ will tend to unity making expression 33 inaccurate, that is, the value of h_c will tend to infinity as $(1 - \bar{\varepsilon})$ tends to zero. This may be overcome by using one calorimeter with a surface emissivity $\varepsilon_1 = 1$ (black body radiator), and the other calorimeter with a surface emissivity $\varepsilon_2 = 0.3$ (silver body radiator).

4.8.3 CONDUCTION CORRECTION

In the event of some heat escaping through the insulation at the back of the calorimeter and increasing the body surface temperature, a correction may be applied if we know the temperature of the body surface behind the calorimeter before and after the calorimeter is heated for thermal balance. This is possible by considering the following assumptions:-

(i) if the temperature difference between the body and the environment is less than 30^oC, then the radiative heat loss from the body surface may be expressed as:-

$$(q/A)_{rad} = \sigma \varepsilon_o \varepsilon_1 (T_w - T_\infty)(T_w^3 - T_w^2.T_\infty - T_w.T_\infty^2 - T_\infty^3) \times 10^{-8}$$

and the bracket $(T_w^3 - T_w^2.T_\infty - T_w.T_\infty^2 - T_\infty^3)$ may be considered to be approximately constant. (That is, for a wall temperature of 30°C, $T_w = 273 + 30$ °K, and say two ambient temperatures of 10°C and 20°C, $T_\infty = 283$°K and 293°K respectively, the value of this bracket only changes by some 6%. Therefore we may rewrite equation 32 as

$$q_t = (T_w - T_\infty).A_c.\left\{h_c + \sigma\varepsilon_o\varepsilon_1 f(T_w, T_\infty)\right\}$$

where q_t is the true heat loss from the body surface, that is,

$$(q/A_c)_{true} = (T_w - T_\infty) \text{ x constant Z}$$

where constant $Z = \left\{h_c + \sigma\varepsilon_o\varepsilon_1 f(T_w, T_\infty)\right\}$

(ii) In the case where the calorimeter is attached to the body surface and electrical energy supplied for thermal balance raises the temperature of the body surface behind the calorimeter to T_w', then the measured heat loss $(q/A_c)_{meas.}$ may be expressed as,

$$(q/A_c)_{meas.} = (T_w' - T_\infty) \text{ x constant Z}$$

Assuming that the value of the constant Z remains approximately the same value, then the true heat loss may be expressed as,

$$(q/A_c)_{true} = (q/A_c)_{meas.} \times \frac{(T_w - T_\infty)}{(T_w' - T_\infty)} \qquad \ldots(34)$$

Therefore by measuring the temperature of the body surface behind the calorimeter (T_w) before applying heat to it, and then again on thermal balance (T_w'), a more accurate heat loss value is obtained.

5. EXPERIMENTAL TESTS FOR THE SURFACE PLATE CALORIMETER

In order to check that the surface plate calorimeter was capable of measuring the local convective heat transfer coefficient of the surface of a heated body in free and forced convection, the following tests were made:-

(i) Free convection test:- the local convective heat loss from the surface of an isothermally heated cylinder was measured with the calorimeter and the results compared with results obtained by other workers;

(ii) Forced convection test:- measurements were taken with the calorimeter at various positions around the circumference of a vertical isothermally heated cylinder in a cross-flow, and the results compared with accepted values of known authors.

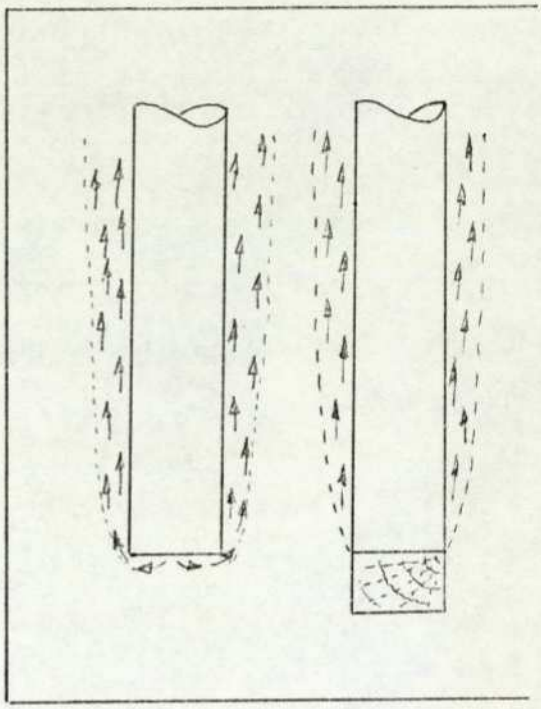
Both of these tests were conducted in a similar manner to the experiments described for the heat flow disk, section 4.3.

5.1 FREE CONVECTION TEST

The surface plate calorimeter was used to measure the local convection heat transfer coefficient h_c at different vertical positions on the surface of a heated vertical cylinder as well as at different positions around the circumference of a heated horizontal cylinder. In both conditions, a thin walled brass cylinder was isothermally heated to a temperature of approximately 33°C by circulating warm water, through a pump, from a reservoir. The value of 33°C was chosen because in an environment of some 20°C, this represents a mean skin temperature value for a human subject, Newburgh (74). In order that the cylinder may lose heat by radiation in a similar manner to that of a human body, the cylinder surface was painted matt black making the value of the surface emissivity (ε_1) equal to 0.96, Newburgh (74).

5.1.1 FREE CONVECTION TEST ON A VERTICAL HEATED CYLINDER

The brass cylinder (0.10 m diameter, 1.20 m long) was mounted vertically, on an insulating base of the same diameter, in a position within the laboratory where no external draughts were observed (a hot-wire anemometer was used to help locate such a position). This insulating base, which was made from balsa wood (thermal conductivity $k_b \simeq 0.055$ W.m^{-1}.K^{-1}), was used to improve the starting conditions for the convective flow from the lower edge of the cylinder. For a cylinder freely suspended in air the convective flow pattern is influenced by the flow around the lower edge of the base of the cylinder, see sketch.



The calorimeter was attached to the surface of the cylinder with double-sided adhesive tape with junction B behind the calorimeter and in contact with the cylinder wall. A second copper-constantan thermocouple was attached to the cylinder close to the calorimeter in order to monitor the cylinder wall temperature. The height at which the calorimeter was attached above the base of the cylinder was measured to the centre of area of the copper plate. At each of the positions at which the calorimeter was attached the local free convection heat transfer coefficient h_c was evaluated as described in section 4.8.1, and also the local Grashof and Nusselt numbers, that is,

$$Gr_x = \frac{g\beta\,(T_w - T_\infty)\,X^3}{\nu^2} \quad \text{, and} \qquad Nu_x = \frac{h_c \cdot X}{k}$$

5.1.1.1 RESULTS OF THE VERTICAL FREE CONVECTION TEST

From section 3. it has been shown that the Nusselt number in laminar free convection is dependent on the Grashof number in a relationship of the form,

$$Nu = f(Gr)^m$$

By reducing the results obtained with the calorimeter to non-dimensional form a direct comparison with published results for the same geometrical shape is possible. This being so the experimental results have been plotted in a logarithmic manner in Fig. 14, that is,

$$Log_{10} Nu_x = m\ Log_{10} Gr_x + const.$$

and compared with the theoretical results for an isothermally heated vertical cylinder, Sparrow & Gregg (35).

From these experimental results, the value of the index m in the above equation was found to be 0.27 compared with 0.25 for the theoretical results. This represents a difference of about 8% between the experimental results and that of the theoretical prediction. This was a particularly encouraging result because,

(a) we could not reasonably expect an instrument which caused a small step change in the surface of the cylinder to give results which were very close to a theoretical prediction based on a smooth cylindrical surface,

(b) the convective boundary layer around the cylinder may have been influenced by,

(i) external air flows such as natural convection air currents within the laboratory,

(ii) the starting conditions for the natural convection boundary layer on the cylinder (the balsa wood on which the cylinder was supported did increase in temperature and would therefore have produced its own convective boundary layer).

Any of these conditions could account for the 8% difference, especially the latter two.

5.1.2 FREE CONVECTION TEST ON A HORIZONTAL HEATED CYLINDER

For this test, the surface plate calorimeter was attached to the surface of an isothermally heated brass cylinder (0.07 m diameter) which was mounted with its axis horizontal in a draught-free position within the laboratory. The free convection heat transfer distribution around the circumference of the cylinder was measured by rotating the cylinder itself (axially in steps of 30^{o}) in preference to detaching and re-attaching the calorimeter. At each axial position the local heat loss (i^2R), the cylinder wall temperature (T_w) and the environmental temperature (T_∞) were measured and the local convection heat transfer coefficient h_c evaluated from equation 32.

In order to compare the results of the heat transfer distribution obtained with the calorimeter with those given by other workers, such as, Schmidt (38), Eckert & Sohngen (37), Hermann (39), the results were again reduced to the non-dimensional form of the Nusselt number, $Nu_D = h_c.D/k_a$, and plotted in polar form in Fig. 15. The distribution of the convective heat transfer boundary around the cylinder, as found from the calorimeter results, is similar to that already observed by Schmidt (38), Eckert & Sohngen (37) in Figs. 5 & 6, that is, at the lower stagnation point where the temperature gradients between the body surface and the environment are steep the local convective heat loss is large, and at the upper stagnation point where the temperature gradients within the plume are small, the corresponding convective heat loss is reduced in magnitude.

Since the Nusselt number Nu, in free convection, is directly proportional to the fourth root of the Grashof number Gr, the heat transfer distribution around the cylinder is plotted in the form $Nu_D/(Gr_D^{1/4})$

against azimuth angle ϕ in Fig. 16, together with the theoretical results of Hermann (39) and the experimental results of Schmidt (38).

The results obtained with the calorimeter are about 12% higher than those predicted by Hermann who solved the polar form of the laminar boundary layer equations (section 3.) for the velocity and temperature profiles by an approximation method. From his analysis, which was originally compared with the experimental results of Jodlbauer (36), Hermann found that his prediction method was in error by approximately 5% which he attributed to the difference between the theoretical and experimental conditions in the neighbourhood of the stagnation points. From these predicted temperature profiles, Hermann evaluated the local convection heat transfer distribution and, as shown in Fig. 16, arrived at a value for the convection heat loss of zero at the upper stagnation point. This implies that the approximation method used by Hermann over-simplified the boundary conditions. Therefore, it was decided to rely on the more acceptable experimental results of Schmidt (38). Schmidt's optical method for visualising the convective heat transfer boundary around two-dimensional bodies in free convection (Fig. 5) allows the local convective heat transfer coefficient h_c to be found.

At each angular position around the circumference of the cylinder some 20 readings were taken and the standard deviation of each set of data was found to be st. dv. $\leqslant 0.05$. These results for the convection heat transfer distribution are shown in Fig. 16 to be within 10% of the reliable experimental results of Schmidt (38).

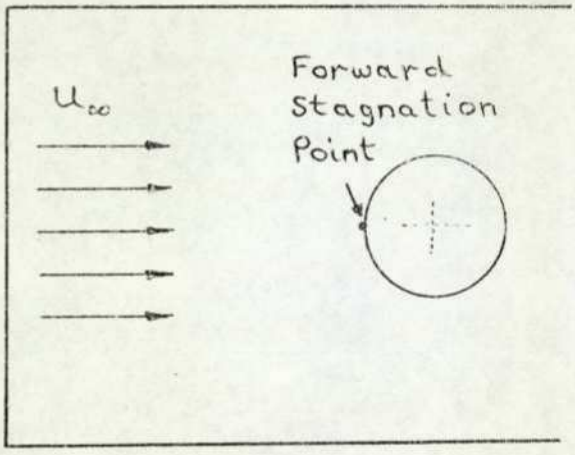
5.2 FORCED CONVECTION TEST

Both theoretical and experimental results are known for the forward stagnation point heat transfer from a circular cylinder in a cross flow, Frössling (43), Schmidt & Wenner (42). Their results form a basis for checking that the local heat loss from a heated body in forced con-

vection may be measured with a surface plate calorimeter. For this purpose the calorimeter was attached to the surface of an isothermally heated cylinder which was mounted vertically in the working section of a low velocity wind tunnel. The cylinder was mounted such that it could be rotated axially in order that the local heat transfer distribution around the circumference of the cylinder might be measured.

5.2.1 STAGNATION POINT HEAT TRANSFER FROM A VERTICAL HEATED CYLINDER

With the calorimeter attached to the cylinder surface, in a manner similar to that already discussed in section 4.8.1, the cylinder was rotated in order that the calorimeter was positioned at the forward stagnation point and the local heat transfer rate measured for a range of air-speeds $0.15 < U_\infty < 3.50$ ms^{-1}. (The air velocity in the tunnel was measured with a hot-wire anemometer of the type described by Clark (4). The turbulence level was also determined and found to be approximately 0.2% .



In forced convection, the Nusselt number $Nu_D = h_c D/k_a$, is dependent on the Reynolds number $Re_D = U_\infty D/\nu$ in a relationship of the form

$$Nu_D \propto Re_D^{1/2}$$

This being so, the results for the local convection heat transfer coefficient h_c were reduced to this non-dimensional form and are plotted in Fig. 17 together with the experimental results of Schmidt & Wenner (42) and the theoretical predictions of Frössling (43).

5.2.1.1 RESULTS FOR THE FORWARD STAGNATION POINT HEAT TRANSFER TEST

The laminar boundary layer equations for the forward stagnation

point on a cylinder in a cross-flow were solved by an exact method by Frössling, and his predictions for a range of air-speeds are shown in Fig. 17. From this plot, the relationship between the Nusselt number and the Reynolds number is

$$Nu_D = 0.95\ Re_D^{1/2}$$

By comparing the results obtained with the surface plate calorimeter at the forward stagnation point of a heated cylinder with the above expression, we are able to estimate whether or not the calorimeter behaves in a satisfactory manner. Bearing in mind that the theoretical prediction for the local convection heat loss is based on the solution of the laminar boundary layer equations we may expect the experimental results to be larger due to the presence of turbulence in the air-stream, Kestin & Maeder (58).

It may be seen from Fig. 17 that the experimental results* are approximately 5% higher than the theoretical results, but are in agreement with the experimental results of Schmidt & Wenner. Both of these sets of experimental results overlap in the Reynolds number range $9 \times 10^3 < Re_D < 2 \times 10^4$, and give for the relationship between the Nusselt number and Reynolds number;

$$Nu_D = 1.0\ Re_D^{1/2}$$

over the entire Reynolds number range for which each set of results were obtained.

These results obtained with the surface plate calorimeter were considered satisfactory because:-

(a) the calorimeter had been designed in a similar form to that of the plug-type calorimeter and had given similar results under similar conditions,

(b) the presence of the surface plate calorimeter within

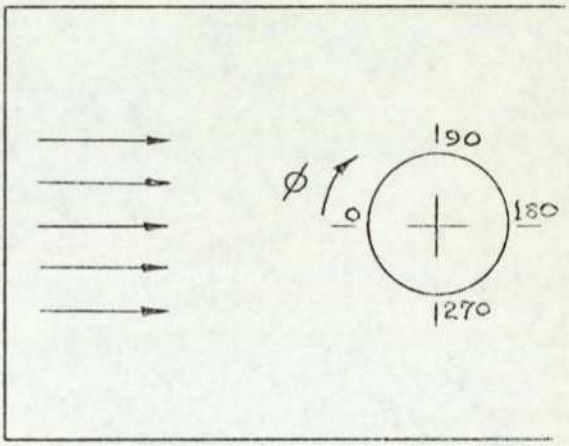
---

* For this case the standard deviation was again, st. dv. $\simeq$ 0.05

the thermal boundary layer does not appear to influence the local heat loss to a significant extent.

5.2.2 HEAT TRANSFER DISTRIBUTION AROUND A VERTICAL CYLINDER

This last test was conducted with the calorimeter attached to the surface of the vertical cylinder described in the previous subsection. The cylinder was mounted through the walls of the tunnel in such a way that it could be easily rotated axially through 360^{o} in steps of 30^{o} to the direction of the flow. At each angular position the local heat loss (q/A) and the cylinder wall temperature (T_w) was measured, together with the surrounding environmental temperature (T_∞) and the wind velocity (U_∞). Using these measurements the local convection heat transfer coefficient h_c was evaluated from equation 30, and reduced to the non-dimensional form of the Nusselt number for each constant Reynolds number in the range $2.1 \times 10^3 < Re_D < 1.5 \times 10^4$.



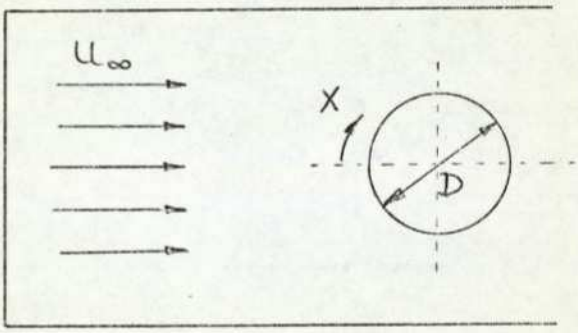
5.2.2.1 RESULTS FOR THE HEAT TRANSFER DISTRIBUTION

For each constant Reynolds number the heat transfer distribution is plotted in polar form in Fig. 18 with the radial (r) coordinate corresponding to the Nusselt number (Nu_D), and the angular (Θ) coordinate to the azimuth angle (ϕ).

As described previously in section 3.3.2, the local heat transfer rate is greatest at the forward stagnation point, where the boundary layer is thin and the temperature gradients steep. It is very much less near the separation point, and increases again over the rear half of the cylinder to a maximum value at the rear stagnation point. Also plotted in Fig. 18 is the heat transfer distribution obtained by

Schmidt & Wenner (42) with their plug-type calorimeter for a constant Reynolds number of 8300. From this figure it may be seen that the distribution obtained with the surface plate calorimeter for a constant Reynolds number of 8600 is in good agreement with their results.

In forced convection the Nusselt number is known to be dependent on the square root of the Reynolds number ($Nu_D \propto Re_D^{1/2}$). By employing non-dimensional similarity to all geometrically similar bodies subjected to the same flow conditions, the local value for the ratio of $Nu_D/Re_D^{1/2}$ will be the same. This being so, the results obtained with the surface plate calorimeter over the forward half of the cylinder have been reduced in this manner and plotted in Fig. 19, together with the results of Schmidt & Wenner and the theoretical prediction of Frössling (43). Since Frösslings exact solution is only correct in the region $0 < X/D < 0.45$, Spalding & Pun (41), this is the range selected for the comparison.



The results obtained with the surface plate calorimeter were recorded with a standard deviation of s.d.$\simeq 0.05$, and are shown to be in good agreement with those obtained by Schmidt & Wenner. Both sets of experimental results are higher in value than the theoretical values predicted by Frössling, but, since Frössling's solution was based on laminar flow conditions, this discrepancy may be attributed at least in part, to the presence of free-stream turbulence. In the case of the experimental results of Schmidt & Wenner, the turbulence intensity within their wind tunnel has been estimated (since no detail of this quantity was recorded in their original paper) by Kestin & Maeder (58) to be approximately 0.9%: for our own wind tunnel, the turbulence intensity was measured and found to be approximately 0.2%.

In summary, the surface plate calorimeter has been tested in both free and forced convection and the results obtained by this method are shown to agree well with other known results. This being so, it was decided to use this instrument for measuring the local convective heat loss from the human body and the results of our studies are reported in the following sections.

6. PRELIMINARY TESTS FOR THE CALORIMETER ON THE HUMAN BODY

Although successful results were obtained with the surface plate calorimeter from heated cylinders in free and forced convection, it is necessary to know whether the calorimeter itself would behave in a satisfactory manner when attached to a human body. Therefore, before attempting to measure convection heat losses from a human subject, the following questions had to be answered.

(1) Is there any discomfort to the subject once the calorimeter is attached to the skin, before or after the calorimeter is heated?

(2) Is the combined radiation and convection heat loss measured with the calorimeter of the correct magnitude for that part of the anatomy to which the calorimeter is attached?

(3) Is there a change in the local skin temperature when,

(a) the calorimeter is first attached?

(b) the calorimeter is attached for a given time interval?

(c) the calorimeter is attached and measuring the local heat loss?

(4) Is the calorimeter sensitive to convective heat loss changes on the human body?

These questions are dealt with below.

6.1 SUBJECTIVE TESTS AS TO THE COMFORT OF THE CALORIMETER ON SKIN

In order to check whether discomfort was caused by the presence of the calorimeter on a subjects skin, the following tests were conducted.

The area of skin where the calorimeter was to be attached was first cleaned with dry cotton wool. This was to remove any moisture which could prevent the adhesion of the calorimeter to the skin. The calorimeter was then firmly attached with double-sided adhesive tape and the subject asked whether its presence was uncomfortable, before and after it was heated to its null reading. The calorimeter was then moved to a new position and the procedure repeated.

This test was conducted on the legs, arms and face of two subjects, one male (CB), the other female (EC), and both reported that the calorimeter caused no discomfort at all.

6.2 COMBINED CONVECTION AND RADIATION HEAT LOSS MEASUREMENTS FROM THE HUMAN BODY

This test was to determine if the calorimeter measured the correct magnitude for the combined convection and radiation heat loss from a human subject. To do this, measurements were taken with the calorimeter of the heat loss from the legs and forearms of two subjects (CB and EC), and the results compared with those of Clifford (31). For each subject a calorimeter and a thermocouple was attached to the prepared skin surface and the local heat loss and skin temperature measured. These instruments were then moved to another position on the limb and new measurements recorded.

The results of this test are shown with those of Clifford in Figs. 20 and 21, where the local heat loss is plotted as a function of the local skin temperature. At this stage we have not attempted to associate the local heat loss with position of the calorimeter on the skin (that is, with local convective variations) but have simply shown that our results are in agreement with those of Clifford for the two limbs.

6.3 OBSERVATIONS TO DETERMINE WHETHER THE CALORIMETER AFFECTS THE LOCAL SKIN TEMPERATURE

In order to observe whether the local skin temperature was affected by attaching the surface plate calorimeter to the skin the following tests were conducted.

(1) The local skin temperature of different areas of the body was monitored on an infra-red radiation camera, which was capable of measuring the surface temperature with an error of less than $0.5^{\circ}C$. This

was done both before and after attaching the calorimeter to the same skin surface area.

It was observed that the local skin temperature remained unchanged when the calorimeter was (a) first attached, (b) measuring the heat loss from the body for a 20 minute period, and (c) removed.

(2) A surface plate calorimeter was attached to the forearm in a position shown in Fig. 22. Close beside the calorimeter a thermocouple was attached to the skin surface for measuring the local skin temperature. This temperature was monitored with an electric thermometer for a period of 30 minutes, whilst the calorimeter was measuring the local combined convection and radiation heat loss. The results of this test are shown in Fig. 23. and it can be seen that both the skin temperature and the heat loss remain fairly constant during this time interval. (The peaks in the heat loss measurements were probably due to local movements of the body which changed the local convective heat loss.)

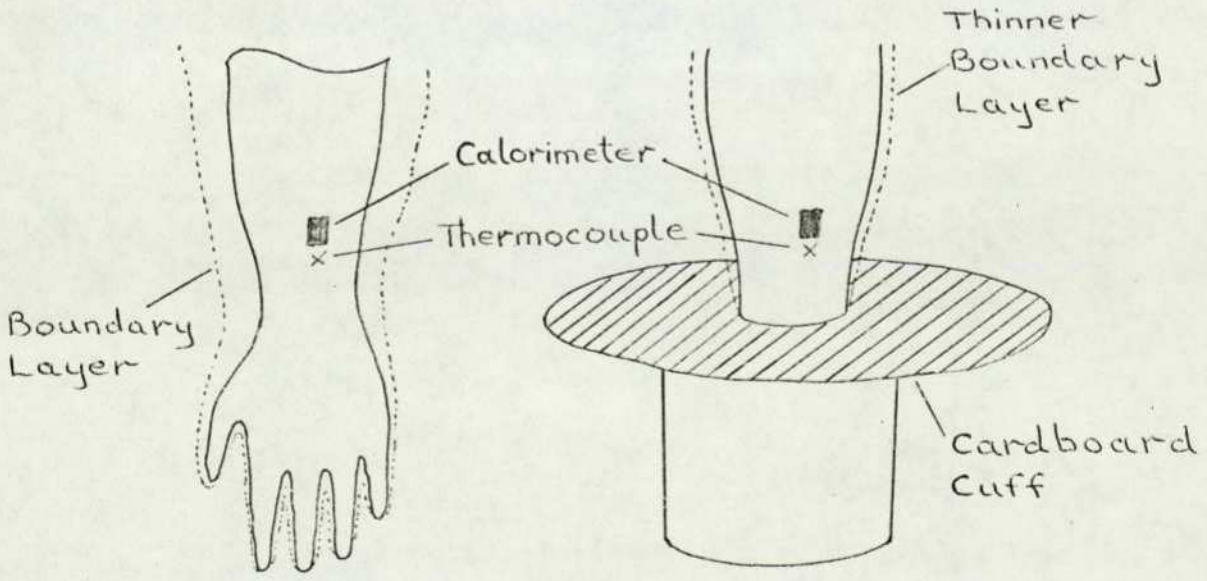
From these observations, it was concluded that the presence of the calorimeter did not affect the local skin temperature by any significant amount. This being so, the only test that had to be performed before using the calorimeter for free and forced convection heat transfer studies was to ensure that the calorimeter was capable of responding to local convective changes on the human body. Tests were therefore carried out and are presented in the next sub-section.

6.4 CONVECTIVE HEAT TRANSFER TESTS

In order to justify using the calorimeter for free and forced convection studies it was necessary to determine whether the calorimeter responded to local convective changes on the human body. To do this we attempted to measure the change in the convection heat loss from a limb when the convective flow pattern around that limb was altered.

For this purpose, a bare forearm was held vertically downwards in free convection, in a position away from the convective flow of the rest of the body. A surface plate calorimeter and a thermocouple was then attached to the forearm in a similar position to that shown in Fig. 22. The local convective heat transfer was then measured over a period of approximately 20 minutes, Fig. 24. With the arm in this position the calorimeter should be responding to the convective flow rising from the hand over the lower forearm, see sketch below.

The next step was to alter this convective flow pattern, and this was accomplished by placing a cardboard cuff around the wrist, below the calorimeter, and in such a way so as not to cause any constriction of the blood vessels in the arm. This cuff had the effect of stopping the convective boundary layer from the hand reaching the calorimeter, and also starting a new boundary layer on the lower forearm at the wrist-cuff interface. The new boundary layer, which develops closer to the calorimeter, will be much thinner than before, and therefore the temperature gradients steeper at the position of the calorimeter. Therefore, it is to be expected that the local convective heat loss at this position will be larger than the previous condition.



With the cuff in position, the local convective heat loss was measured for a further 20 minutes and the results plotted in Fig. 24. It can be seen from this figure that the local convective heat loss from the forearm increased as expected thereby confirming that local changes in the convection heat loss from the human body may be measured with the surface plate calorimeter.

6.5 SUMMARY

It has been shown in this section that the surface plate calorimeter may be attached to a human body with double-sided adhesive tape and cause neither discomfort to the subject, nor any increase in the local skin temperature. Furthermore, tests were carried out to determine whether the calorimeter was capable of measuring (a) the local combined convection and radiation heat loss from the leg and forearm of two subjects, and (b) the local changes in the convection heat loss from a human body. In each case the answer was affirmative. This being so, the following two sections report the measurements of free and forced convection heat transfer from the human body with this instrument.

7. FREE CONVECTIVE HEAT TRANSFER FROM THE HUMAN BODY

The preliminary experiments of the previous section showed that the surface plate calorimeter could be used to measure the local convective heat loss from the human body. This being so it was decided to use this instrument to measure the local heat loss from selected areas of the body and to form a detailed picture of the convective heat loss mechanism for each of these areas. This was achieved by:-

(i) studying how the local heat loss varies with body posture,

(ii) comparing the results with the local heat loss from heated cylinders,

(iii) using the results to describe the convective boundary layer,

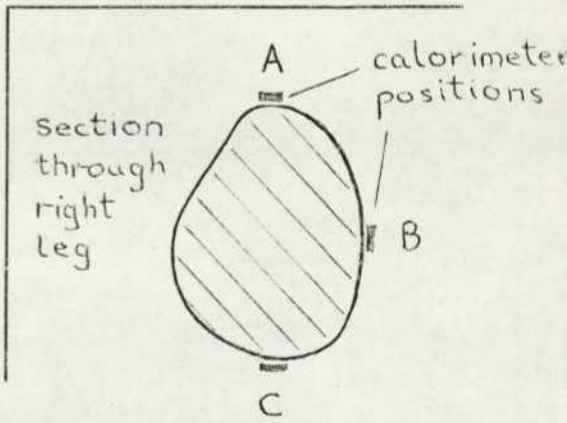
(iv) using the results, where appropriate, to estimate the total heat loss from the area where measurements are being made, and to compare this value with a theoretical value found from considering the area as a cylinder and calculating the heat loss using boundary layer theory.

For the convenience of the personnel from whom heat transfer measurements were taken the following areas were selected for different body postures, (a) the leg, and (b) the head.

7.1 FREE CONVECTION HEAT LOSS FROM THE LEG

As a preliminary experiment three surface plate calorimeters were attached to the leg of a subject (SB) and the combined convection and radiation heat losses for the leg in the vertical and horizontal positions measured.

Each of the three calorimeters was attached to the right leg at a height of 30 cms above the ground in the positions shown in the sketch opposite. Measurements of the combined convection and radiation heat loss at each



circumferential position were taken for approximately 15 minutes with the leg in the vertical position (the subject being seated), for 20 minutes with the leg in the horizontal position (the leg being supported at the thigh and ankle), and for a further 10 minutes with the leg again in the vertical posture.

Results for the three positions on the leg are shown in Fig. 25 and the first observation shows that at each circumferential position on the leg, for each posture, there is thermal stability during the measuring period. With the leg vertical, there is a difference in the results for each of the positions on the leg which is possibly due to the different starting conditions for the natural convective boundary layer. For example, the starting condition of the boundary layer at the back of the leg (position C) is the heel, whereas that for the front of the leg (position A) is the bridge of the foot. (The convective flow pattern over the leg is described in more detail in the following sub-section).

With the leg horizontal, the minimum heat transfer occurs on the top of the leg at position A, and the heat losses at the sides and bottom of the leg, position B & C, are similar, giving a heat transfer distribution that might be expected for a heated horizontal cylinder. When the leg is returned to the vertical, the previous heat transfer patterns are re-established.

The results of this simple experiment showed that the local heat loss from the surface of a human leg did change according to the orientation of the leg, and this change could be measured with the surface plate calorimeter. This being so, further experiments were conducted for the case of the vertical leg and for the horizontal leg.

7.1.1 CONVECTIVE HEAT LOSS FROM A VERTICAL LEG

From the results of the above preliminary test it was observed

that for the case of the vertical leg, the heat loss from the back of the leg was different from that at the front, and it was suspected that this difference was possibly due to the different starting conditions for the convective boundary layer. To investigate this further, we considered taking measurements from the vertical leg and comparing the results with those obtained theoretically by utilizing boundary layer theory to evaluate the convective heat loss from a vertical heated circular cylinder. Since boundary layer theory is only applicable for the laminar free convection flows we further considered taking measurements only from positions on the leg which we assumed to be within this type of flow regime. In order to take measurements within this laminar free convection region it was first necessary to estimate the maximum height on the body for which laminar flow may be considered to exist.

It was discussed in section 3. that the height over which laminar free convection exists is dependent on the value of the local Grashof number, $Gr_x = g\beta(T_w - T_\infty)X^3/\nu^2$. On an isothermally heated vertical flat plate, laminar flow is known to exist below $Gr_x = 10^8$, and turbulent flow above $Gr_x = 10^{10}$, (between these two limits a transitional region is established) Cheesewright (34). By assuming that the same conditions apply to the human body the maximum height X_m on the human leg may be obtained by inserting the appropriate values for the environmental temperature T_∞ and the skin temperature T_w for the leg in the local Grashof number corresponding to this limit, $Gr_x = 10^8$.

The mean skin temperature T_w for the leg was obtained by simply measuring the skin temperature with a copper-constantan thermocouple at 15 different positions on the leg and averaging the results; by this method an average skin temperature of $32^\circ C$ was recorded. The environmental temperature was measured with another thermocouple and

found to be approximately 26°C. Utilizing these measurements in the local Grashof number equivalent to $Gr_x = 10^8$ gives the maximum height that is required, that is,

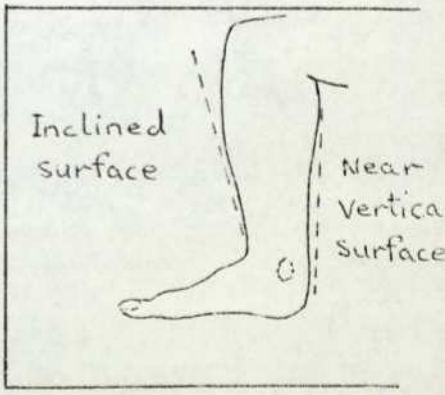
$$Gr_x = 10^8 = g \frac{(T_w - T_\infty)}{T_\infty} \cdot \frac{X_m^3}{\nu^2}$$

$$= \frac{g}{\nu^2} \frac{(32 - 26)}{299} \cdot X_m^3$$

From this expression $X_m = 0.46$ m. is the maximum height below which laminar flow may be considered to exist.

Since this height corresponded to the position of the knee of our subject, measurements had to be taken from the lower portion of the leg.

In order to compare measured results with theoretical calculations it was necessary to take measurements on a portion of the leg which was nearly vertical and had a starting condition for the convective flow pattern which was not influenced by the flow around the foot. With the subject seated comfortably it was observed that the rear part of his leg nearly satisfied these conditions although the front part of his leg was then inclined as shown in the opposite sketch (due to the leg being more conical in shape than cylindrical).



The combined convection and radiation heat loss and skin temperature was recorded at the front and rear of the leg for vertical positions X = 0.10, 0.20, & 0.33 metres. From these measurements the local convection heat transfer coefficient h_c was evaluated using equation 32.

7.1.1.1 RESULTS FOR THE VERTICAL LEG EXPERIMENT

The results for the rear of the leg are shown in Fig. 26 where the convective heat transfer coefficient h_c is plotted as a function of time to show the thermal stability of the readings. Also plotted

in this figure is the local skin temperature at the three positions and it can be seen that the temperature in this region is fairly constant over the entire rear surface of the leg. The variations in the local convective heat loss is probably due to small body movements and therefore an average value for h_c from this figure has been computed and replotted in Fig. 27 against its local position.
The local Nusselt number is also plotted in this figure and has been evaluated at each position from the expression $Nu_x = h_c.X/k_a$, where k_a is the thermal conductivity of air at 26°C, (the temperature of the environment in the experiment).

Theoretical values for the local convective heat loss from the surface of a vertical circular cylinder have been computed and are plotted with the above experimental results in Fig. 27. These values were obtained by first calculating the local Grashof number at each height X cms, $Gr_x = g\beta(T_w - T_\infty)X^3/\nu^2$, where the surface temperature T_w is taken as the mean value of the experimental results ($T_w = 31.2°C$) and T_∞ is the average room temperature ($T_\infty = 26.0°C$); the local Nusselt number at each height was then evaluated from the expression given by Sparrow & Gregg (35),

$$\left(Nu_x\right)_{cyl} = \left(Nu_x\right)_{fp} + 0.35(X/r_o)$$

where $\left(Nu_x\right)_{fp} = 0.3568\ Gr_X^{0.25}$ (Ostrach's solution for a flat plate), and r_o is taken as the local radius of curvature of the rear half of the leg.

The convective heat loss from the rear of the leg and the cylinder

Vertical Height	Rear of Leg (Experimental)		Cylinder (Theoretical)	
X m.	h_c $Wm^{-2}.K^{-1}$	Nu_x	h_c $Wm^{-2}.K^{-1}$	Nu_x
0.10	5.0	19	3.6	14
0.20	3.3	25	2.8	22
0.33	2.1	27	2.4	30

The results for the front of the leg are not so easy to interpret since the inclination of this area of the leg was some 15^{o} to the vertical and the convective boundary layer from the foot affects the boundary layer over the leg. It was found that the local convective heat transfer coefficient h_c was greater at X = 0.33 m than at X = 0.10 m, a result that is opposite to that found for the vertical portion of the leg. The probable reasons for this effect are discussed in the next sub-section.

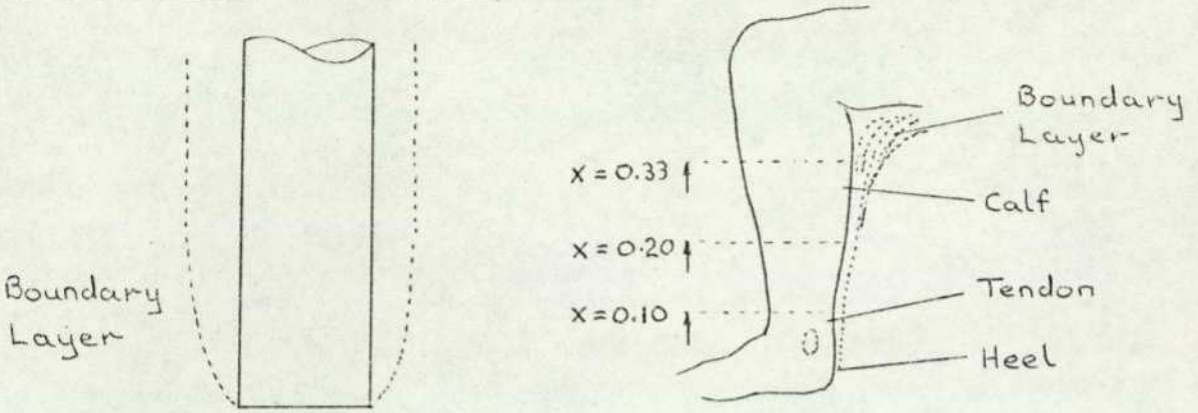
The values of the coefficient h_c for the front and rear portions of the leg are presented in the following table.

Vertical Height X m.	Experimental Results	
	Front of Leg h_c $Wm^{-2}.K^{-1}$	Rear of Leg h_c $Wm^{-2}.K^{-1}$
0.10	2.7	5.0
0.20	4.9	3.3
0.33	6.3	2.1

7.1.1.2 DISCUSSION OF THE RESULTS FOR THE VERTICAL LEG

It was discussed in section 3. that the convective boundary increases its thickness with height up a vertical heated cylinder, and where the boundary layer is thin, the temperature gradients are steep and the local convective heat transfer large. If we assume this effect to be similar over the human body then we may expect that the local convective heat transfer coefficient h_c for the rear of the leg to be greater at X = 0.10 m and decrease in value at X = 0.20 m, and reduce still further at X = 0.33 m. The results for the rear of the leg plotted in Fig. 27 shows that this does occur. By comparing the experimental and theoretical results in this figure the experimental results are seen to be higher than the theoretical values at X = 0.10 m and lower at X = 0.33 m. The reason for this may be due to the complicated starting condition for the convective flow from the area around the heel and tendon. The boundary layer over the first 0.10 m will probably be thin-

ner and less vigorous than it would be on an isothermally heated cylinder where the starting condition is clearly defined, (see sketch below).



As the convective flow gains momentum over the calf (X = 0.20 m) the boundary layer thickens and the convective heat loss decreases. At X = 0.33 m, the experimental result for the convective heat loss is lower than that from a vertical cylinder at the same height; this is possibly due to the influence of the convective flow pattern below the thigh. That is, a stagnation region tends to develop in the bend of the knee thus increasing the boundary layer thickness downstream of this position (thereby decreasing the convective heat loss).

At the front of the leg, the convective flow from the forefoot will help to form a thicker boundary layer in the ankle region. As the flow gathers momentum it tends not to flow up the inclined surface of the leg, but breaks away and flows vertically over the leg section, thus causing a thin boundary layer to form over the front surface of the leg with a corresponding large heat loss. (Fig. 28 shows in diagrammatic form the convective flow pattern that exist over the lower leg in this posture; part of this flow pattern is visualised on the schlieren film produced by Clark (4)).

7.1.2 CONVECTIVE HEAT LOSS FROM A HORIZONTAL LEG

For this experiment the subject was seated comfortably with his right leg supported in the horizontal position at the ankle and thigh.

Measurements were taken with the surface plate calorimeter of the local free convective heat loss at 4 positions around the circumference of the leg at each of 3 longitudinal positions (these positions are shown in Fig. 29a together with the cross-sectional area of the leg at each position).

7.1.2.1 RESULTS FOR THE HORIZONTAL LEG EXPERIMENT

The local convective heat transfer coefficient h_c at each position is plotted normal to the circumference of the cross-section of the leg in Fig. 29b. From this figure it is shown that the results for the anterior positions at sections B and C are very low (0.10 and 0.12 $W.m^{-2}.K^{-1}$ respectively). These low convective heat losses from the two positions is due to the shallow temperature gradients that exist within the heated plume that develops above the leg.

The convective heat transfer boundary is drawn through the measured points in a similar form to that found for a heated horizontal cylinder, Fig. 15.

7.1.2.2 DISCUSSION OF THE RESULTS FOR THE HORIZONTAL LEG

From Fig. 29b it is shown that at each section of the leg the convective heat transfer coefficient h_c has a different value for a given azimuth angle. For example, at the rear of the leg, the values for h_c are 4.4, 4.0, and 3.4 $W.m^{-2}.K^{-1}$ at sections A, B and C respectively. To explain these somewhat different results we must consider the local radius of curvature (r_o) at each section, that is,

at section A, $r_o = 0.02$ m

" B, $r_o = 0.04$ m

" C, $r_o = 0.05$ m

From the discussion in section 3.4.1 the coefficient h_c may be written as

$$h_c = 1/(r_o)^{\frac{1}{4}} \times \text{Constant}$$

provided that the same temperature difference and similar geometrical locations on a body are considered.

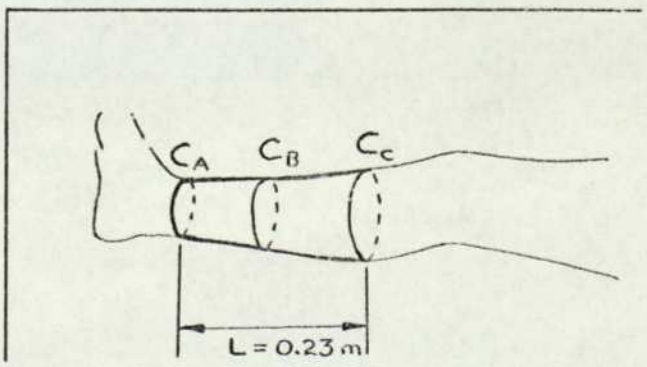
Therefore by considering the particular case of the three posterior positions on the leg, that is, at sections A, B & C, we may expect that $h_c.r_o^{1/4}$ = constant for the three positions. Since the skin temperature at each of the three positions was $31^{\circ}C \pm 0.2^{\circ}C$, the value of the constant in the above expression was computed using the experimental results for h_c and the local radius of curvature r_o and is shown in the following table.

Position on Leg	Coefficient h_c $Wm^{-2}.K^{-1}$	Radius r_o m.	$h_c.r_o^{1/4}$
A	4.4	0.02	1.65
B	4.0	0.04	1.79
C	3.4	0.05	1.61

We may conclude that the local radius of curvature of the body plays an important role in the mechanism by which the body loses heat by convection.

In order that a comparison may be made between the experimental results and a theoretical model, the convective heat transfer distribution around the leg was used to compute the total convective heat loss from the lower leg in the horizontal posture. This was then compared with the value computed for an equivalent horizontal cylinder.

This analysis is effected by considering only that portion of the leg between sections A & C, giving a length of leg L = 0.23 m. The circumference of the leg at each of the sections was found to be as follows, C_A = 0.21 m, C_B = 0.27 m, C_C = 0.33 m



From these measurements the approximate surface area of the leg was found to be $A_L = 0.062\ m^2$.

From the convective heat transfer distribution around the leg, an average value for the coefficient h_c was computed to be

$$\overline{h_c} = 3.0\ Wm^{-2}.K^{-1}$$

The total convective heat loss for the portion of the leg between sections A & C may be computed from,

$$Q_L = \overline{h_c}.\ A_L.\ (T_w - T_\infty)$$

where $(T_w - T_\infty)$ is the average temperature difference between the leg and the surrounding environment, and was found to be 5.0^oC.

Therefore $Q_L = 0.93$ Watts

In order to compute the convective heat loss from an equivalent horizontal cylinder, a cylinder of the same length and surface area of the leg, that is, $L_{cyl} = 0.23$ m, $A_{cyl} = 0.062\ m^2$, was considered. Using these values the circumference of the equivalent cylinder was found to be $C_{cyl} = 0.27$ m, and its diameter, $D = 0.086$ m.

By considering the same temperature difference to occur between the cylinder and the environment as in the previous case, that is $(T_w - T_\infty) = 5.0^oC$, then the Grashof number for the cylinder may be obtained from the expression

$$Gr_D = g\beta (T_w - T_\infty) \frac{D^3}{\nu^2} = 5.0 \times 10^5$$

From an analysis of Schmidt's results for the convective heat loss from horizontal cylinders (ref. 38) an average Nusselt number for the cylinder may be found, that is,

$$\overline{Nu_D} = 0.42\ Gr_D^{1/4}$$

$$= 11.2$$

Since the Nusselt number is also defined as $\overline{Nu}_D = \overline{h}_c.D/k_a$ then an average convective heat transfer coefficient $\overline{h}_c$ for the cylinder may also be calculated,

$$\overline{h}_c = 3.4 \quad Wm^{-2}.K^{-1}$$

and the total convective heat loss from an equivalent cylinder will be,

$$Q_{cyl} = \overline{h}_c . A_{cyl} . (T_w - T_\infty)$$

$$= 1.05 \quad \text{Watts}$$

In the foregoing, the total convective heat loss from a horizontal leg has been computed using,

(a) the local convective heat transfer coefficient h_c obtained from measurements taken with the surface plate calorimeter, and

(b) an equivalent size horizontal cylinder.

Good agreement is noted between the results.

7.2 CONVECTIVE HEAT LOSS FROM THE HEAD

The way in which the convective boundary layer around the human head changes with body posture is shown diagrammatically in Fig. 30 for a standing and supine subject. For the standing subject the convective flow will have developed over the entire body surface and will leave the top of the head as a heated plume.* For the supine subject, the convective flow will not have had this initial flow and must develop around the head in a similar way to that for a horizontal cylinder, with the heated plume leaving the facial region. (Both of these flow conditions have been observed with a schlieren optical system, Clark (4), Clark & Toy (75). It may be expected then that measurements of the convective heat lost from the face in the standing posture to be larger than that for the supine posture, since in the latter case the temperature gradients within the heated plume will be shallow. As an

---

* The amount of convective flow will depend on the clothing worn, since clothing is known to produce a thicker boundary layer resulting in a lower convective heat loss.

example of this phenomena a single calorimeter and a thermocouple was attached to the centre of the forehead of a subject (CB) and the local convective heat transfer coefficient and skin temperature was measured for a period of approximately 15 minutes with the subject standing, and for a further 15 minutes with the subject supine. The results of this experiment are shown in Fig. 31 with both the local convection and radiation heat loss and skin temperatures against time to show the thermal stability of the readings. By subtracting the calculated radiation heat loss from these results, the local heat transfer coefficient h_c for the standing subject was evaluated to be approximately 3.7 $Wm^{-2}K^{-1}$, and for the supine subject, approximately 1.7 $Wm^{-2}K^{-1}$.

7.2.1 HEAT TRANSFER DISTRIBUTION AROUND THE HEAD

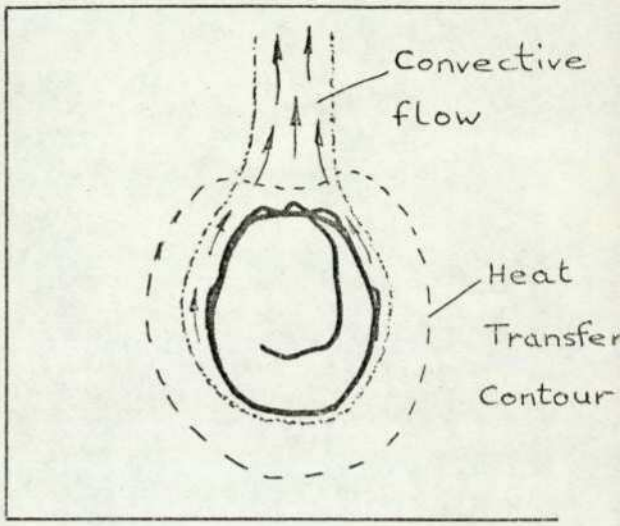
In order to investigate the local convective heat transfer distribution over the head of a standing and lying horizontal subject, the following experiment was conducted. Calorimeters were attached to the facial region of a subject (CB), Fig. 32, and measurements taken of the local heat loss with the subject in the supine and prone positions (the prone position was used in order to measure the convective heat loss below the head since difficulty was experienced in attaching the calorimeter to the head in the presence of hair). Since this only provided a heat transfer distribution around the circumference of the head and did not give results for the convective heat loss over the cranium, the distribution was also measured along the median line of the head of a partially bald subject (OE) in the standing and supine postures.

7.2.1.1 RESULTS AND DISCUSSION OF THE HEAT TRANSFER DISTRIBUTION TEST

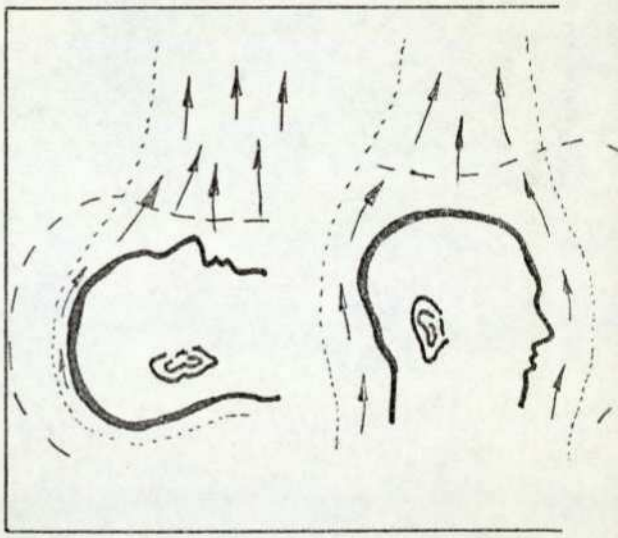
The results of the local convective heat transfer distribution around the head of two subjects are plotted in polar form in Figs. 33 &34.

From a study of these figures the following remarks can be made.

(a) For the subject in the supine and prone positions, the heat loss from the head is similar to that for a horizontal cylinder. Thus the greatest heat loss occurs at the bottom of the head where the convective boundary layer is thin and the temperature gradients steep. At the top of the head where the plume breaks away the temperature gradients are shallow and the local heat loss is markedly reduced.



(b) For the subject in the standing and supine positions, the heat loss from the top of the head for the standing posture is lower in value than that for the face due to the shallow temperature gradients within the heated plume above the head; and for the supine posture, the heat loss from the median line of the face is less than that at the cranium due to the face now being within the heated plume, and the heat loss at the cranium position is increased due to the local convective boundary layer developing around the head of the subject.



To complement this work the total convective heat loss from the head of a subject in the standing and supine postures has been evaluated from the local heat loss measurements in the following manner.

7.2.2 TOTAL HEAT LOSS FROM THE FACE OF A STANDING SUBJECT

In this experiment the combined convection and radiation heat loss from the face of a standing subject was measured and the result

compared to a calculated value.

The facial region of a standing subject was considered to be divided up into areas as shown in Fig. 35a, and from each area the local combined convection and radiation heat transfer rate was measured. By summing the heat losses for each of the areas shown in the following table the total heat loss from the face was evaluated.

Position on face	Area $\times 10^{-3}$ m^2	Local heat loss $W.m^{-2}$	Heat lost from area Watts
A	5.6	130	0.73
B	3.0	103	0.31
C	8.4	79	0.66
D	9.0	116	1.04
E	6.0	88	0.53
F	8.0	132	0.64
B	3.0	103	0.31
C	8.4	79	0.66
E	6.0	88	0.53
Total heat lost from face =			5.4 W

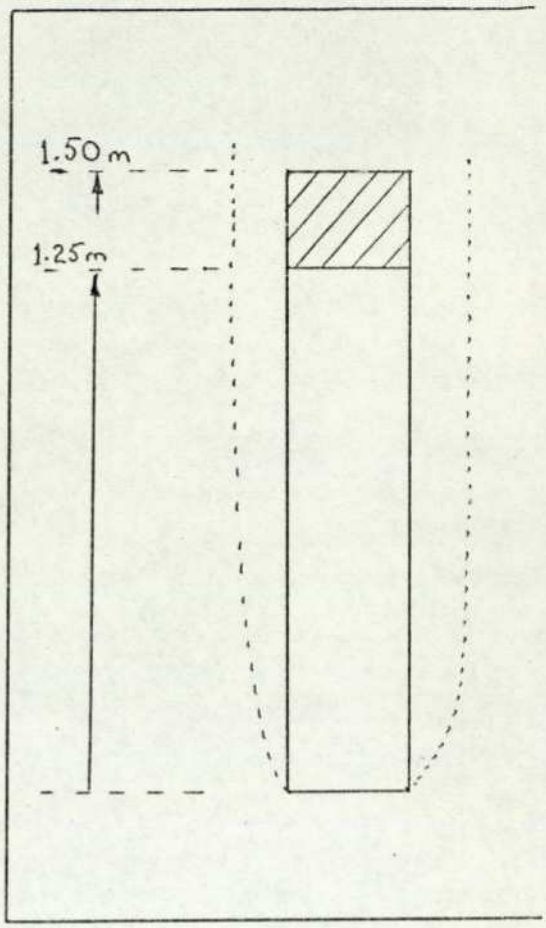
By this method the total combined convection and radiation heat loss from the face of a standing subject was found to be

$$Q_{face} = 5.4 \text{ Watts}$$

As a theoretical comparison, a heated vertical cylinder (0.25 m long, 0.17 m in diameter) was considered to be representative of the shape of the human head. Furthermore, in this analysis, this cylinder was considered to be placed on top of another heated cylinder 1.25 m long and of the same diameter (see sketch).

The following assumptions will be made in this analysis:-

(1) that the convective flow pattern from the bottom cylinder sim-



ulates the same conditions as those which occur between the lower part of the human body and the facial region,

(2) the surface temperature of both cylinders is constant at 33°C (a value similar to the average skin temperature of our subject),

(3) that laminar boundary layer theory can be used to calculate the average convective heat transfer rate between the limits X = 1.25 m and X = 1.50 m,

(4) that the Stefan-Boltzmann radiation law can be used to calculate the radiation heat loss from the cylinder surface employing a surface emissivity similar to that of skin, that is, $\varepsilon_1 = 0.96$.

For an environmental temperature of $T_\infty = 22^\circ C$, the average convection heat transfer rate for the height range X = 1.25 m to X = 1.50 m was found from boundary layer theory (section 3) to be

$$(q/A)_{conv} = 24 \ W.m^{-2}$$

The radiation heat transfer rate was evaluated from the Stefan-Boltzmann radiation law and found to be

$$(q/A)_{rad} = \sigma \varepsilon_o \varepsilon_1 \left\{ \left(\frac{T_w}{100}\right)^4 - \left(\frac{T_\infty}{100}\right)^4 \right\}$$

$$= 78 \ W.m^{-2}$$

where ε_o is the emissivity of the surroundings and equal to unity. The total heat transfer rate from the 0.25 m long cylinder is then

$$(q/A)_{total} = (q/A)_{conv} + (q/A)_{rad}$$

$$= 102 \ W.m^{-2}$$

If we now consider only half of the area of the 0.25 m long cylinder to represent the face, then the area of this portion will be,

$$A_{cyl} = 0.067 \quad m^2$$

and the total heat loss from this area will be,

$$Q_{total} = 102 \times 0.067$$

$$= 6.83 \quad \text{Watts}$$

This theoretical value of 6.8 watts for the cylinder compares favourably with the estimated value of 5.4 watts for the face of our subject. The difference between these values may be due to,

(a) the area of the cylinder chosen to represent the face was incorrect (an area of 1/3 of the cylinder surface would result in a heat loss of some 4.6 watts);

(b) incorrect assumptions for our cylinder model;

(c) incorrect area weighting factors for the subjects face.

7.2.3 HEAT LOSS FROM THE HEAD OF A HORIZONTAL SUBJECT

For this experiment, the subject lay on a thin canvas camp bed in the supine posture with his head supported by a thin leather sling. The head was then considered to be segmented as shown in Fig. 35b and from each of the segmented regions the local combined convection and radiation heat loss was measured. The following table gives both the local heat transfer rate and the overall heat loss for each region. (The area of each segment was approximately 0.0165 m^2).

By summing the individual values for each region the total convective and radiative heat loss from the head was found to be

$$Q_{head} = 16.76 \quad \text{Watts}$$

Facial Region	Local Heat Loss Rate $W.m^{-2}$	Heat Lost from area Watts
I	81	1.34
II	110	1.81
III	135	2.22
IV	145	2.40
V	155	2.56
VI	145	2.40
VII	135	2.22
VIII	110	1.81
Total heat lost from the head = 16.76 W		

As a simple theoretical comparison, consider a heated horizontal cylinder 25 cms long, 17 cms diameter to be representative of the human head. Furthermore, let us assume that the cylinder wall temperature is constant at 33°C (average skin temperature) and the surrounding environmental temperature is 22°C. If the cylinder is supported from its two ends (in this analysis we will ignore the heat lost from these extremities) the cylinder will only lose heat by radiation and convection and the total heat lost will be

$$Q_{cyl} = Q_{rad} + Q_{conv}$$

Consequently, the radiative heat loss was evaluated from the Stefan-Boltzmann law and found to be

$$Q_{rad} = 10.45 \text{ Watts}$$

The convective heat loss was evaluated using the heat transfer analysis given in section 3, that is by evaluating an average Grashof and Nusselt number and then an average heat transfer coefficient $\overline{h}_c$. By this method the convective heat loss was found to be

$$Q_{conv} = 6.43 \text{ Watts}$$

The total heat lost from the cylinder was therefore

$$\underline{Q_{cyl} = 16.88 \text{ Watts}}$$

This total heat loss compares favourably with that found for the head of our subject and is approximately 1% higher in value. Had we assumed that heat is also lost by one end of the cylinder, the total heat lost would have been some 18.92 Watts, that is, some 12% higher.

8. FORCED CONVECTION HEAT TRANSFER FROM THE HUMAN BODY

In this section results are presented of the distribution of the local forced convection heat transfer around two particular regions of the human body. The regions selected for study were the same as in the preceding section, namely, the leg and the head.

The local heat loss from the leg of a subject was measured at specified positions on the right lower leg (below the knee). For these measurements to be taken in forced convection the subject was comfortably seated above a wind tunnel, with his right leg outstretched across the octagonal working section of the tunnel, with the foot pointing upstream. (Fig. 36 shows a subject (RNC) seated above the wind tunnel). Measurements of airspeed inside the tunnel were taken with a constant temperature hot-wire anemometer positioned on the centre-line of the tunnel one metre upstream of the subject's leg: 10 cms below this instrument a copper constantan thermocouple was positioned to record the ambient air temperature (T_∞) through the tunnel. Four other similar thermocouples were attached to the matt black walls of the tunnel to record the radiative temperature (T_r) for use in the radiative heat transfer equation.

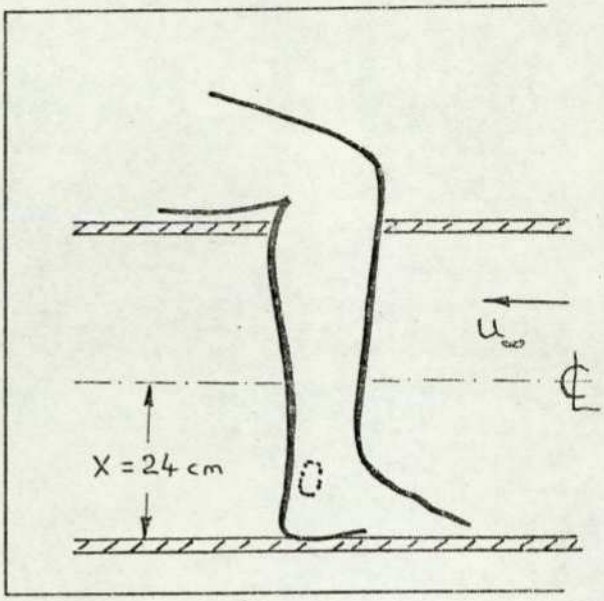
For the forced convection heat loss measurements from the head, a subject (OE) was seated in a 2.4 x 2.4 x 1.8 m^3 working section of a closed return wind tunnel*, as shown in Fig. 37. Measurements were taken at velocities between 0 and 4 ms^{-1} at an ambient temperature of $22.4^\circ \pm 0.2^\circ C$.

---

* This tunnel formed part of an environmentally controlled suite at the National Institute for Medical Research. Permission to use this wind tunnel is gratefully acknowledged.

8.1 HEAT TRANSFER DISTRIBUTION AROUND THE LEG

With a subject seated comfortably above the wind tunnel eight surface plate calorimeters and eight thermocouples were attached around the circumference of the leg at a height of 24 cms (this height being co-incident with that of the tunnel centre line). Measurements were then taken enabling the local convective heat transfer coefficient h_c to be determined for three air velocities, U_∞ = 1.0, 2.0 and 4.0 ms^{-1}. The wind tunnel air and wall temperatures remained constant throughout the experiment at $21.5^\circ \pm 0.2^\circ C$.



RESULTS AND DISCUSSION

The results of this experiment are presented in polar form in Fig. 38 and in cartesian form in Fig. 39.

Fig. 38 shows a cross-section of the leg at a height of X = 24 cms, and the radial lines drawn normal to the circumference of the leg are the coordinates for the local heat transfer coefficient h_c. The contour lines surrounding the leg are the heat transfer coefficient envelope for each tunnel velocity. This figure simply shows that the forced convective heat loss distribution around the leg is similar to that of a heated vertical cylinder with the greatest heat loss occurring at the front of the leg (forward stagnation region) and falling to a minimum at the lateral and medial positions.

With the results plotted in cartesian form (Fig. 39) it is shown that although the heat loss is minimal at the lateral and medial positions (some 90° behind the front of the leg) the distribution is not

symmetrical for both sides of the leg (as it is for a heated cylinder, shown by the dashed line in this figure). This means that the convective boundary layer around the leg is also not symmetrical, and from this figure the following may be deduced:-

(a) since both the cylindrical results and those for the lateral side of the leg are nearly coincident, the convective flow around the lateral side will separate in a similar manner to that for a cylinder at a position some $80^{o} \rightarrow 90^{o}$ behind the forward stagnation point;

(b) the convective flow does not appear to separate at a corresponding position on the medial side; this is probably due to the flow remaining laminar much farther around this part of the leg.

8.1.1 FORWARD STAGNATION POINT HEAT TRANSFER FROM THE LEG

To measure the local forced convection heat loss from the forward stagnation point of a subjects leg, a calorimeter and a thermocouple was attached at the front of the leg at three different heights, X = 10, 20, and 33 cms. Measurements were then taken of the local heat transfer coefficient h_c for various air velocities, $0 \leqslant U_\infty < 2.0$ ms^{-1}

RESULTS AND DISCUSSIONS

Since it has been shown in section 3 that a body in forced convection loses heat roughly in proportion to the square root of the forcing velocity of the fluid, the results of this experiment have been plotted in Fig. 40 in the form (h_c) against $\sqrt{U_\infty}$. From these results it is seen that the coefficient h_c is not simply dependent on $\sqrt{U_\infty}$ but takes on different values according to the different heights on the leg. This apparent discrepancy may be explained by considering what effect the local radius of curvature has on the local convective heat loss.

From section 3.4.2, it has been shown that the local convective heat transfer coefficient h_c in forced convection is proportional to $\sqrt{U_\infty/r}$, where r is the local radius of curvature. That is,

$$h_c \propto \sqrt{U_\infty/r}$$

or,

$$h_c = \sqrt{U_\infty/r} \times \text{const } D$$

The value of this constant D may be evaluated from the gradient of the curves plotted in Fig. 40 and the local radius of curvature at each height on the leg. These values are shown in the table below.

Vertical Height X cms	Radius of Curvature r cms	$\sqrt{r}$	Gradient $h_c/\sqrt{U_\infty}$	Constant D
10	2.4	1.55	3.35	5.2
20	3.0	1.73	2.90	5.0
33	4.0	2.00	2.25	4.5
			Average value	4.9

As a comparison with results for a heated cylinder in forced convection the value of the constant D has been computed for a vertical cylinder in a cross-flow using Frössling's result, that is, $Nu = 0.9449\sqrt{Re}$, and $Nu = h_c d/k$ (section 3). For example, for a 10 cms diameter cylinder in a 1.0 ms^{-1} cross-flow, the Reynolds number for the cylinder is $Re_d = 7000$, and the Nusselt number is $Nu_d = 79$, and the convection coefficient $h_c = 20.5$ $W.m^{-2}.K^{-1}$. The constant D may then be shown to be,

$$D = h_c \sqrt{r}/\sqrt{U_\infty}$$

$$= 4.6$$

The difference between this theoretical value and the average value for the leg is only $6\frac{1}{2}$ percent, which shows that the leg results may be considered to be in good agreement with those for a vertical cylinder

under the same flow conditions. This may be further emphasised by plotting the local convective heat loss results for the leg in non-dimensional form and comparing them with experimental results for a heated cylinder in forced convection. This has been achieved by reducing the results for the leg into local Nusselt numbers, $Nu_d = h_c d/k$, where $d = 2r$ (twice the local radius of curvature), and plotting them against the Reynolds number, $Re_d = U_\infty d/\nu$, in logarithmic form. These results are shown in Fig. 41 together with the experimental results obtained for a heated cylinder in a uniform cross-flow. From this figure it may be seen that the results for the position X = 10 cms are not completely linear over the entire air velocity range (a result which is also shown in the previous figure 40). This is probably due to the complicated air flow over the foot affecting the boundary layer around the leg at this height. The results for the other two positions show good agreement between the heat loss from the forward stagnation point of a stationary leg in the presence of a wind and that for a heated vertical cylinder under the same flow conditions, as well as with the theoretical results for a heated cylinder predicted by Frössling (43).

8.2 CONVECTION HEAT LOSS FROM THE HUMAN HEAD

All of the experiments conducted in this section were performed in the environmental wind tunnel at the National Institute for Medical Research (Hampstead Laboratories).

The first experiment that was conducted was to determine whether or not there were any significant differences in the results obtained from the human head in forced convection and those obtained from a heated cylinder. Since the average diameter of an adult head is approximately 14 cms (measured around the forehead, ref 17) results were obtained of the heat transfer distribution around a 14 cms diameter cylinder in an airstream of 0.80 ms^{-1}, air temperature $22.0^\circ \pm 0.2^\circ$ C.

This was achieved by attaching a calorimeter and a thermocouple to its surface and determining the local convective heat transfer coefficient h_c around the circumference of the cylinder by rotating it about its longitudinal axis in 30^o intervals.

To measure the heat transfer distribution around the head a similar procedure was adopted. This time the calorimeter and thermocouple was attached at the centre of the forehead of a standing subject. The subject was then rotated in steps of 30^o in the 80 $cm.s^{-1}$ airstream. Although this method does not give the true distribution around the head it does allow a simple comparison with the cylinder results to be made. Both distributions are presented in cartesian and polar form in Fig. 42.

RESULTS AND DISCUSSION

A direct comparison of the results obtained from the head with those of the cylinder is not possible. This is because the local heat loss was measured from the forehead with the head at different orientations to the flow, and not from different locations around the circumference of the head. This latter case was not set-up since problems arose due to (i) air disturbances caused by the flow of air over the ears, and 'flapping' hair, and (ii) difficulty in attaching the calorimeter to areas around and on the ears and scalp. However, one can conclude from this simple experiment that it would appear that the convective heat loss from the head is similar to that of a heated cylinder under the same conditions. The greatest heat losses occurred from the forehead with the subject facing directly into and directly away from the freestream velocity. Certainly over the front half of the head (between $-90^o < \phi < +90^o$) the two sets of results (from head and cylinder respectively) are close, and is possibly due to the forehead over this region being smooth like that of the cylinder surface.

8.2.1 HEAT TRANSFER DISTRIBUTION ALONG THE MEDIAN PLANE OF THE HEAD

The heat transfer distribution was measured along the median plane of the head of a bald subject (OE) in a range of freestream velocities between 0.15 and 1.40 ms^{-1}. This was achieved by attaching four calorimeters and four thermocouples to the subject's head in the following positions; one of each on the chin, on the forehead, and two near the crown of the head. With the subject centrally positioned in the environmental wind tunnel, the freestream velocity was measured with a low-velocity anemometer. The average air temperature within the tunnel was measured upstream of the subject with six equally spaced thermocouples, and for each of the air velocities the air temperature was found to be $22.0^{o} \pm 0.2^{o}C$. The local convection and radiation heat loss was then measured in freestream velocities of 0.15, 0.60, 0.90, and 1.40 ms^{-1}. From these measurements the local convection heat transfer coefficient h_c was determined (using equation 30) and the results plotted in polar form in Fig. 43.

RESULTS AND DISCUSSION

It may be seen from Fig 43 that at the higher air velocities of 0.60, 0.90, and 1.40 $m.s^{-1}$, the heat transfer distribution around the head takes the form of the usual heat loss contour plot around a heated cylinder. The greatest heat losses then occurred at the chin and the forehead (corresponding to the forward stagnation point on a vertical heated cylinder), and a minimum on the crown of the head where the convective boundary layer may be expected to separate.

The more interesting result is that for the lower air velocity of 0.15 $m.s^{-1}$. Here the convective heat loss appears to be uniform over the face and crown, and one possible reason for this result may be the combined effect of the natural and forced convection velocities. For example, if the velocity within the natural convective boundary layer is much greater than the forcing velocity (it can be as high as

0.5 $m.s^{-1}$, Clark (4)) a convective plume develops above the subject's head. Conversely, if the forcing velocity is the greater a heated wake occurs behind the subject. But for the case where neither the forcing velocity nor the natural convective velocity is dominant then a rising heated wake occurs behind the subject. Fig.44 shows in diagrammatic form the above three effects. (These effects have been observed from (i) an oscillating heated cylinder in still air, and (ii) a traversing vertical cylinder in still air, with the schlieren system at the N.I.M.R. (Hampstead laboratories).

8.2.2 FORWARD STAGNATION POINT HEAT TRANSFER FROM THE FACE

To complete this section measurements were taken of the forward stagnation point* heat loss from the face of a subject. These were obtained by attaching a calorimeter and a thermocouple to the centre of the forehead, and to the chin of a subject (CB) who then stood facing upstream in the environmental wind tunnel. Measurements were recorded of the local convection heat loss from these areas for the range of air velocities $0.20 < U_\infty < 3.0$ $m.s^{-1}$. (During this experiment the freestream air temperature was measured at five positions upstream of the subject and remained constant at $23.5^\circ \pm 0.2^\circ C$).

RESULTS AND DISCUSSION

Since it has already been shown in section 3.4 that the local radius of curvature affects the local heat transfer, the radius of curvature of the chin and the forehead were measured and found to be 3.5 and 7.0 cms respectively. These values were used together with the measured local heat transfer coefficient h_c for each of the regions to define a local Nusselt number, and Reynolds number for the chin and forehead. Thus, if we let d_c and d_f be the diameters of the chin and forehead respectively, then

* The point at which the flow is assumed to be brought to rest.

$$(Nu_d)_{chin} = \frac{h_c \cdot d_c}{k} \quad \text{and} \quad (Re_d)_{chin} = \frac{U_\infty \cdot d_c}{\nu}$$

and $$(Nu_d)_{f'head} = \frac{h_c \cdot d_f}{k} \quad \text{and} \quad (Re_d)_{f'head} = \frac{U_\infty \cdot d_f}{\nu}$$

By reducing the results to this form and plotting them logarithmically, a comparison may be made between these results and those obtained for the forward stagnation point of a heated cylinder. Fig. 45 shows such a comparison. Although the results for the chin and the forehead appear to be similar to those for the cylinder, the gradients of the slopes of the graphs are different for the two cases; and since the gradient gives the relationship between the two non-dimensional groups, it also gives the relationship between the convective heat loss and the freestream velocity. That is, the heat loss from the cylinder may be described by the expression

$$\text{Log}_{10} Nu_d = 0.5 \text{ Log}_{10} Re_d + \text{constant}$$

giving $$Nu_d = 0.95 \ Re_d^{0.5}$$

and the heat loss from the face by the expression

$$\text{Log}_{10} Nu_d = 0.56 \text{ Log}_{10} Re_d + \text{constant}$$

giving $$Nu_d = 0.80 \ (Re_d^{0.56})$$

From the definition of the Nusselt number and the Reynolds number the heat transfer coefficient h_c for the chin and forehead may therefore be described by the empirical expression,

$$h_c = 0.80 \left(\frac{d}{\nu}\right)^{0.56} \cdot \left(\frac{k}{d}\right) \cdot (U_\infty)^{0.56}$$

where d is twice the local radius of curvature of the region.

To test the validity of this expression another experiment was conducted using three calorimeters. These were attached to the forehead, chin and nose of a second subject (CB) under the same environmental conditions as before, and measurements taken of the local convection heat loss for a range of air velocities, $0.15 < U_\infty < 4.0$ m.s^{-1}. The results obtained for the local heat transfer coefficient h_c were then plotted against $U_\infty^{0.56}$ in Fig. 46. From this figure the gradient of the curves for these three regions was evaluated and compared with the computed values predicted by the above expression. The table below shows this comparison and the % error betwen the experimental results and the computed values.

Region	Local diameter d metre	Exptl constant	Computed constant $0.8\left(\frac{d}{\nu}\right)^{0.56} \cdot \frac{k}{d}$	% Error
Forehead	0.15	23.5	23.0	2.5
Chin	0.07	32.0	33.5	5.0
Nose	0.025	15.0	47.0	61.0

From the experimental results for the chin and forehead the value of the constant for the above expression is shown to be less than 5% in error of the predicted value. Unfortunately this good agreement does not hold for the results obtained from the nose, where an error of 61% was found. Although this same experiment was repeated many times on different occasions this same result always occurred. One explanation that can be offered as to why the nose loses more convective heat for air velocities up to approximately 2.0 m.s^{-1}, and less heat for velocities above this value, may be found from a typical plot of the difference between the local skin and ambient temperatures ($T_s - T_\infty$) against increasing air velocity (U_∞). Fig 47 shows that the temp-

erature of both the forehead and the chin fall with increasing air velocity to a near constant skin temperature some $3^{\circ} \rightarrow 4^{\circ}C$ above the ambient temperature; whereas that of the nose falls quite rapidly to a temperature close to ambient. (Once the skin temperature is at ambient no convection heat loss can occur; and this appears to be what happens for the case of the nose).

In order to observe this phenomenon occurring on a subject in more detail an experiment was conducted using an infra-red radiation camera to photograph the local skin temperature over the face of the subject in free and forced convection. The subject was seated in the working section of the environmental wind tunnel facing upstream, and the camera, which was capable of resolving to within $1^{\circ}C$, was positioned 2 metres in front of the subject.*

With no wind the subject was considered to be cooling in free convection, and a series of 20 photographs were taken. From these photographs one complete isothermal map of the subjects face, resolved to within $1^{\circ}C$, was obtained.

The subject was then subjected to an air velocity of 2.5 $m.s^{-1}$ and allowed to cool by forced convection for approximately five minutes, another series of photographs were then taken to produce a second isothermal map. This procedure was again repeated for an air velocity of 4.0 $m.s^{-1}$.

The results of this experiment are shown in Fig. 48 where each colour in this case represents $1^{\circ}C$, with ambient temperature ($T_{\infty} = 24.0^{\circ}C$) being represented by white, and the warmest skin area of $35^{\circ}C$ by the colour 'nut brown'.

---

* Note:- The resolution of this camera was in fact $2^{\circ}C$ per colour change on the colour monitor, but it also had an 'enhance' facility that could be used to enhance with white light any part of the entire colour range. This enhance facility when reduced to cover a $1^{\circ}C$ range could be used to highlight half of each colour thus giving the facility of resolving to within $1^{\circ}C$ an isothermal map of the viewed area.

From this figure it can be seen that the nose has again cooled down very near to ambient for the 2.5 $m.s^{-1}$ air velocity, and to ambient for the 4.0 $m.s^{-1}$ airspeed, whereas the chin and the forehead have both remained between $3^{o} \rightarrow 6^{o}C$ above the ambient temperature for both air velocities. Also from this figure the values for the temperature difference between the local skin and ambient temperature was estimated for the three facial areas of interest for each of the air velocities, and the results are shown in the table below.

Velocity U_{∞} $m.s^{-1}$	Temperature difference $(T_s - T_{\infty})\ ^{o}K$		
	(Forehead)	(Chin)	(Nose)
0	11.0	10.0	9.0
2.5	6.0	4.0	2.0
4.0	5.0	3.0	0

These values are plotted to provide a comparison with the results already obtained with thermocouples in the previous figure 47. It may be observed that the values obtained by a non-contact temperature measuring method are similar to those obtained during the heat transfer measurement experiment.

9. APPLICATIONS OF THIS HEAT TRANSFER MEASURING TECHNIQUE

It has been shown in the preceeding sections that a surface plate calorimeter may be used to obtain information on how the human body loses heat by convection to its surroundings. This has been achieved by taking measurements in free and forced convection and showing that large areas of the human body lose heat in a similar manner to the surface of a heated cylinder. Moreover agreement exists between these experimental results and theoretical values obtained by applying boundary layer theory to cylindrical shapes. In order to show that the calorimeter is not restricted to taking measurements in experiments of the above type, three further fields of study were chosen in which some contribution may be made by taking heat loss measurements with this instrument. It must be emphasised that since each topic could easily command a complete project of its own, these studies were meant only as examples although it is hoped that further work may be performed at some later date.

The three topics investigated were as follows:-

(1) the convective heat loss from the hand in different gaseous environments,

(2) the convective heat loss from the thigh of a long distance runner,

(3) the heat loss through clothing.

9.1 CONVECTIVE HEAT LOSS FROM THE HAND IMMERSED IN DIFFERENT GASEOUS ENVIRONMENTS.

The purpose of this section is to show that the calorimeter is not only confined to measuring heat losses in air but may also be used to measure the difference in the free convective heat loss from a body experienced by changing the gaseous content of the environment from a Nitrogen-rich one to a Helium-rich one.

Men who spend days in a hyperbaric helium gas environment require much warmer environmental temperatures, typically above 29°C, than the normal air temperature of say 20°C for comfortable thermal conditions, and they are also quick to sense small changes in temperature, Flynn et al (76), Timbal et al (77), Raymond et al (78), and Webb (79). The reason for requiring this rather high environmental temperature is attributed to the convection heat loss mode, that is, for the same environmental temperature and pressure, a man in a helium rich environment loses more heat by convection than in a nitrogen rich one. Although not in a position to test hyperbaric gas environments we decided to investigate this particular phenomenon by measuring the local convective heat loss from the hand in two environments, that is, a helium gas environment and a nitrogen gas one.

In order to explain why the convective heat loss should be different for the two gases we looked first at the differences between the physical properties of the two gases, and then compared these results with the measurements taken from the hand.

The properties of the two gases, and those of air, at a temperature of 20°C are listed below.

Properties	Helium	Nitrogen	Air	Units
Specific heat C_p	5230	1040	1006	J/Kg^oC
Dynamic viscosity μ	1.94×10^{-5}	1.74×10^{-5}	1.82×10^{-5}	Ns/m^2
Thermal conductivity k	0.147	0.026	0.0257	$W/m^2\ ^oC$
Density ρ	0.166	1.250	1.205	Kg/m^3
Derived property				
Prandtl number Pr	0.69	0.70	0.72	

From section 3 we have seen that the non-dimensional free convective heat loss from a body is dependent on the Grashof number and Prandtl number of the fluid, that is,

$$Nu = f(Gr, Pr)$$

Since the Prandtl number for both helium and nitrogen are similar to that of air then we may assume for simplicity that

$$Nu = f(Gr)$$

and that the same velocity and temperature profiles occur in both gases, (Ostrach, ref 51).

In order to evaluate what effect the gas has on the local free convection boundary layer on a heated body, the local Grashof number has been calculated along the wall of an isothermally heated vertical flat plate immersed in the different environments. For this calculation a vertical flat plate 1.0 m high was assumed to be heated isothermally to a temperature of 33^oC and immersed in each of the above gases, which were themselves assumed to be at a temperature of 20^oC. The local Grashof number $Gr_x = g\beta(T_w - T_\infty)\, x^3/\left(\frac{\mu}{\rho}\right)^2$ was evaluated at 5 cm intervals, and the results plotted in Fig. 49. From this figure it can be seen that at any particular height on the flat plate the value of the local Grashof number for helium is two orders of magnitude less than that for nitrogen and air. This means that the convective boundary layer in the helium environment will be thinner

than that for the other two environments, and therefore the temperature gradients steeper, giving rise to a higher convective heat loss.

To evaluate how much more convective heat is lost in a helium environment to that of a nitrogen one it is only necessary to consider the expression $Nu = f(Gr)$. In free convection the Nusselt number is approximately proportional to the fourth root of the Grashof number, that is,

$$Nu_x \propto Gr_x^{1/4}$$

Since the Nusselt number may also be expressed as $Nu_x = h_c.X/k$ we may rewrite the above proportionality as

$$h_c.X/k \propto \left\{ g\beta(T_w - T_\infty)X^3/\left(\frac{\mu}{\rho}\right)^2 \right\}^{1/4}$$

Furthermore, since we are considering the effect of the different gases on the local convective heat transfer coefficient h_c, we may assume the values of $g\beta$, $(T_w - T_\infty)$, and X to be constant, and therefore

$$\frac{h_c}{k} \propto \frac{1}{\left(\frac{\mu}{\rho}\right)^2}^{1/4}$$

or

$$h_c = \frac{k}{\sqrt{\frac{\mu}{\rho}}} \cdot \text{Const}$$

From this we may compare the convective heat loss from a warm body in any two gas environments as long as the values of k, μ, and ρ are known, for example

for helium $$(h_c)_{He} = \left(\frac{k}{\sqrt{\frac{\mu}{\rho}}}\right)_{He} \cdot \text{Const}$$

for nitrogen $$(h_c)_N = \left[\frac{k}{\sqrt{\frac{\mu}{\rho}}}\right]_N \cdot \text{Const}$$

and therefore

$$\frac{(h_c)_{He}}{(h_c)_N} = \frac{k_{He}}{k_N}\left\{\frac{\left(\frac{\mu}{\rho}\right)_N}{\left(\frac{\mu}{\rho}\right)_{He}}\right\}^{1/2}$$

From the values given in the previous table

$$\frac{(h_c)_{He}}{(h_c)_N} = 1.95$$

We may therefore expect to lose about twice as much heat by convection in a helium environment compared with that of a nitrogen one, under otherwise similar circumstances.

For comparative purposes, we measured the local convective heat from the back of the hand of a subject (CB) in the two different gaseous environments, as well as in air. This was achieved by inserting the hand in a nitrogen filled perspex chamber Fig. 50, and measuring the local convective heat loss from the hand with a surface plate calorimeter; then refilling the chamber, via the inlet nozzle with helium (the gas inside being allowed to escape from the one-way gas valve), and measuring the local heat loss once more. The results are shown below together with the results for the heat loss from the hand in air.

Convection coefficient (h_c) $Wm^{-2}K^{-1}$	Helium	Nitrogen	Air
	3.2	1.8	1.7

The results in the table below show the ratio of the convective heat losses in the different environments.

$(h_c)_1/(h_c)_2$	Theory	Experiment	% Error
Air : Nitrogen	0.95	0.94	1.5
Helium : Air	2.05	1.88	8.3
Helium : Nitrogen	1.95	1.78	8.7

From this table it may be seen that the experimental values are within 10% of the theoretical results and this error may be attributed to the very complicated flows which would exist within such a closed chamber. This may be especially true for the lighter helium gas since it is the comparison with these results that the largest discrepancy occurs. This simple experiment, utilizing a surface plate calorimeter clearly demonstrates the increase in convective heat loss resulting from helium enrichment.

Although we are not in a position to measure the convective heat loss from a body immersed in high pressure surroundings we can, nevertheless, estimate what the effect may be. This may be achieved by considering the expression for the free convective heat loss from a body as given on page 119, that is, $Nu_X \propto Gr_X^{1/4}$.

If we rewrite this expression in full,

$$\frac{h_c X}{k} \propto \left\{ g\beta (T_w - T_\infty) X^3 \frac{\rho^2}{\mu^2} \right\}^{1/4}$$

For a given body geometry (X) and surface (T_w) and ambient temperatures (T_∞), this expression may be reduced to

$$h_c \propto \frac{k}{\sqrt{\mu}} \rho^{1/2}$$

Furthermore, if we assume the gas to be ideal, then the gas pressure $Pg = \rho RT_\infty$ (universal gas law) and we can simply substitute Pg for ρ in the above expression (since RT_∞ may be considered constant in this case).

$$h_c \propto \frac{k}{\sqrt{u}} Pg^{1/2}$$

This expression shows that the convective heat loss from a body will increase as the square root of the gas pressure.

9.2 CONVECTIVE HEAT LOSS FROM THE THIGH OF AN ATHLETE

The following experiment was performed in order to study the convective heat loss from the thigh of an athlete whilst he was running on a treadmill, with and without wind blowing over him. The reason for the interest shown in this topic was due to some earlier work (unpublished) of Dr Pugh at the National Institute for Medical Research (Hampstead Laboratories) in which he found by partitional calorimetry, that for an athlete running outdoors at 4.5 ms^{-1} the convection coefficient was 29.8 $Wm^{-2}K^{-1}$, whereas the corresponding value for a standing subject in an equivalent airstream was some 17.6 $Wm^{-2}K^{-1}$ (McKerslake, 28). On further discussion with Dr Pugh he suggested that this increase was due to the increased work level done by the thigh muscles whilst running and that if measurements could be taken of the convection heat loss from the thigh alone, then interesting results may occur. Therefore the experiment took the form of measuring the convective heat loss distribution around the thigh of an athlete* in action using surface plate calorimeters, and this is more fully described below.

9.2.1 EXPERIMENTAL SET-UP

Four surface plate calorimeters and thermocouples were attached equally spaced around the circumference of the right thigh of an athlete, 30 cms below the hip joint. Measurements of the local heat loss were taken with the athlete first standing still in a climatic chamber, with an air temperature of 11°C, in a 4.5 ms^{-1} airstream, and then whilst running on a treadmill at 4.5 ms^{-1}. The running tests were done both under still air conditions and facing into a 4.5 ms^{-1} airstream. From these measurements the local convective heat loss was obtained by estimating the radiation heat loss using the local skin temperatures and chamber wall temperatures, and subtracting this

* Throughout these tests the subject was dressed only in running shorts.

value from the measured heat loss. The results are plotted in Fig. 51. and from this figure the following observations may be made for the above three conditions.

Subject standing, facing into the wind

(1) With the subject standing facing into a 4.5 ms^{-1} airstream (curve 1 of Fig. 51) the greatest loss of heat from the thigh is at the anterior position (which may be as expected since this position corresponds to the forward stagnation point of a heated cylinder in an airstream).

(2) At the lateral position the convective heat loss is considerably reduced (the same phenomena occurs at a similar position on a heated cylinder).

(3) Although a similar result may be expected to occur from the medial position as that of the lateral, that is if the thigh is to be thought of as a free cylinder, it is found that the heat loss is nearly as high as that found at the anterior position. It is not clear why this should be so but one possibility is that the air-flow through the legs is fully turbulent, giving rise to a higher convective heat loss.

Subject running on a treadmill, facing into the wind

(1) For the subject running on a treadmill at 4.5 ms^{-1} facing into a 4.5 ms^{-1} airflow the distribution of heat loss around the leg (curve 2 of Fig. 51) is very similar to that found for a heated cylinder in a cross-flow, with the greatest heat losses occurring at the anterior and posterior positions (corresponding to the forward and rear stagnation points on a heated cylinder) and a minimum occurring at the lateral and medial positions some 90^{o} behind the anterior position.

(2) For this condition the medial position appears to lose less

heat than the lateral. This may be due to an improved flow condition through the legs, since the legs are now in-line for only a small fraction of the total time (a condition that may give rise to turbulence at the medial position). From a cine film taken of the thigh of a subject running at 4.5 ms^{-1} it was found that the legs were in-line once every 0.325 secs. This is demonstrated in Fig. 52(a) and (b) in which the sequential positions of the right thigh is plotted together with a sine wave; it may be seen from this figure that the movement of the thighs is simple harmonic (as might be expected), except where the body weight is about to be transferred from one leg to the other (period A --- D). It may be seen from Fig. 52(b) that the thighs are only momentarily in-line at an angle of approximately 29^{o} to the vertical.

(3) The average heat loss around the thigh for the standing and running conditions was obtained by integrating the area under curves 1 and 2 of Fig. 51. By this means the average heat loss for the stationary thigh in a 4.5 ms^{-1} wind was found to be 35 $Wm^{-2}K^{-1}$ and for the running subject 44 $Wm^{-2}K^{-1}$, representing an increase in heat loss of some 25%. This increase may be explained by considering the extra velocity of the limbs during running, that is, for a body forward speed of 4.5 ms^{-1} the point on the thigh at which measurements were taken (some 30 cms below the hip joint) has to move approximately 1.5 ms^{-1} faster (this value was calculated from the cine film results plotted in Fig. 52(a) and (b)). For air blowing over the subject whilst he is running the velocity of the air flow over the thighs is the sum of the wind velocity and the thigh velocity giving a value of some 6.0 ms^{-1} over the thighs when the athlete is running in the wind.

Subject running on a treadmill, no wind

(1) With the subject running on the treadmill at 4.5 ms^{-1} with no wind the heat loss distribution is as shown in curve 3 of Fig. 51. From this figure it is seen that the greatest heat loss occurs at the anterior position on the thigh, and the least at the posterior. The reason for this heat loss distribution being different in this case to the previous two cases (curves 1 and 2 of Fig. 51) is that even though the thigh may look as though it is moving forward and backwards (as a pendulum), it is in fact only moving forwards, and therefore the only airflow around the thigh is that created by the thigh alone moving forward through still air. In other words, the running sequence is that once the thigh has swung forward (see period I → O in Fig. 52(b)) and the foot has made contact with the ground (period A) the weight of the body is transferred to that leg (period A → D) with that leg then remaining fixed relative to the treadmill, until period H. As the treadmill then moves the leg backwards the forward movement of the other leg and the trunk in relation to it gives the 'pendulum' effect.

(2) The average heat loss around the thigh for this case was found to be 24 $Wm^{-2}K^{-1}$.

Since the thigh of a runner can be thought of as being essentially in a forced convection regime, the heat loss will be proportional to the square root of the air velocity (section 3). As a consequence, the results for the above three cases were corrected for the natural convection case*, and these results then plotted against the square root of the average air velocity for each case in Fig. 53. That is, for the standing subject the average air velocity was 4.5 ms^{-1}, for

---

* Note:- This correction meant subtracting the natural convection heat loss of the thigh (measured with the subject standing in still air conditions) from the three sets of results so that the heat loss was zero for zero air velocity.

the running subject (+ wind) the average air velocity was taken as 6.0 ms^{-1}, and for the running subject (no wind) the velocity was taken as 1.5 ms^{-1}. It may be seen from this figure that although the results were obtained in three quite distinct cases they do lie roughly along a straight line, thus allowing the heat loss from the thigh to be described by the expression,

$$\bar{h}_c = 13.6 \sqrt{U_{av}} \qquad Wm^{-2}K^{-1}$$

The value of the constant in this expression is much higher than that given by McKerslake (28) for the whole body subjected to a uniform air stream, that is,

$$\bar{h}_c = 8.3 \sqrt{U_{\infty}} \qquad Wm^{-2}K^{-1}$$

With the aid of these two expressions a comparison may now be made with the earlier results found by Pugh. This may be achieved by comparing the ratios of:-

(a) the constants in the above expressions, with

(b) the results of Pugh for the subject running at 4.5 ms^{-1} and the results of McKerslake for the subject standing in an equivalent airstream.

That is, the ratio of the constants in the above expression is

1.6 : 1.0

For a subject running at 4.5 ms^{-1}, Pugh found that the overall convection heat transfer coefficient $\bar{h}_c$ was 29.8 $Wm^{-2}K^{-1}$, whereas that suggested by McKerslake for a body in an equivalent airstream was 17.6 $W.m^{-2}K^{-1}$; the ratio of these results being

1.7 : 1.0

Although there is good agreement between these two ratios thereby showing that the results obtained with the surface plate calorimeters support the earlier findings of Pugh, far more work is required in order to explain fully how this heat is lost. Thus it is not just the action of running that produces the increase in the loss of heat from

the thighs since, in the first case when the athlete was standing still in an airstream the heat loss was found to be higher than the predicted whole body value. It would appear that the nature of the air flow around the thighs must account for this increase, although further investigations are needed to quantify this conclusion.

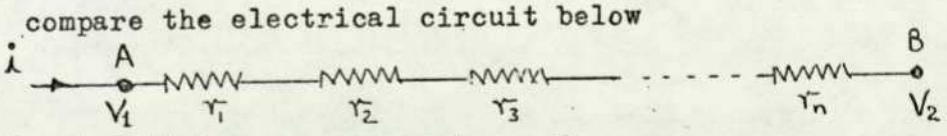
9.3 HEAT LOSS THROUGH CLOTHING

This section is not intended as a complete investigation into either the physical or functional properties of fabrics but only as an introduction to the means by which measurements may be made using the surface plate calorimeter when clothed subjects are to be studied.

For this series of experiments two distinct sets of tests were performed. In the first set, the surface of a heated horizontal cylinder was used as the subject on which clothing material could be assembled, and in the second set, measurements were taken from a human subject. With a calorimeter attached to the surface of a 'subject', either with or without clothing, measurements of the overall heat loss were taken, that is, the heat loss by convection, together with radiation and conduction (where the clothing is in contact with the calorimeter). The inverse of the overall heat loss was then found, since this gives a measure of the insulation value of the clothing assembly worn. For the present series of experiments the insulation value has been expressed in terms of the "clo"*, which is a unit generally used in physiological work. The definition is:-

---

* Note:- Since the 'clo' is a unit of thermal insulation or thermal resistance, this system of units has a distinct advantage over the transmittance units for clothing in as much that the resistance of each fabric may be added together to give the total resistance of the clothing assembly; in an analogous manner to the electrical resistance of a circuit.
For example: compare the electrical circuit below



Electrical potential difference across A —— B,

$$V_2 - V_1 = \sum_{n=1}^{n} r_n \cdot i$$

with a thermal circuit



Thermal potential difference across A --- B,

$$T_2 - T_1 = \sum_{n=1}^{n} I_n \cdot (q/A)$$

Where voltage is analogous to temperature, resistance to insulation, and current to the heat flux.

'one clo unit of thermal insulation will maintain a resting-sitting man, whose metabolism is 50 Kcal/m^2/hr, indefinitely comfortable in an environment of 21°C, relative humidity less than 50%, and air movement 20 ft/min', (Burton and Edholm, ref 11),

and represents a value of:-

$$1 \text{ clo} = 0.155 \quad {}^{o}Cm^{2}W^{-1}$$

As an introduction into the use of the clo unit, measurements were first taken of the value for air insulation and the results compared with a value given by the empirical formula of Burton and Edholm (11), that is,

$$I_a = \frac{1}{0.61 \times \left(\frac{T}{298}\right)^3 + 0.19\, U_\infty^{1/2} \times \left(\frac{298}{T}\right)}$$

Where I_a is the thermal insulation of air, U_∞ is the freestream air velocity in cm/sec, and T the ambient air temperature in degrees Kelvin. This equation, which was obtained empirically from measuring the overall heat loss from subjects in a climatic chamber, indicates that air insulation depends only on the freestream air velocity and ambient air temperature, and on neither the boundary layer around a body nor the wall temperature of a body.

9.3.1 HEAT LOSS THROUGH CLOTHING FROM A CYLINDER

Test 1. Insulation of air around a cylinder.

For this experiment a surface plate calorimeter was attached to the surface of a uniformly heated 7 cm diameter cylinder. The cylinder was then mounted horizontally in a low speed wind tunnel and measurements were taken of the local convection and radiation heat loss at 30° intervals around the circumference of the cylinder for three different cylinder wall temperatures of 35°, 45°, and 55°C at an ambient temperature of 23° ± 1°C, and freestream velocity of 1.7 ms^{-1}. These heat loss results were then converted into local insulation values

and plotted in Fig. 54 against the local azimuth angle on the cylinder. Also plotted in this figure is the value of the air insulation as given by the above equation, with $U_\infty = 1.70\ ms^{-1}$, and $T = 273^o + 23^oK$.

Results and Discussion of Test 1.

It may be observed from figure 54 that:-

(1) since the results for each cylinder wall temperature are similar then the insulation value for air is indeed independent of the body wall temperature;

(2) for a heated cylinder in a uniform air flow, the insulation value for air is not constant around its circumference but is distributed around the cylinder in a reciprocal manner to the heat transfer distribution (that is, being lowest at the forward stagnation point of the cylinder, and highest at a position some 90^o behind this point on the cylinder). Consequently not only does the boundary layer around a body play an important role in the evaluation of the air insulation, but also the external air flow condition (i.e. laminar or turbulent flow) since this affects the convective heat loss from a body (ref.58) and in turn the air insulation;

(3) an average value for the air insulation may be obtained from these results by integrating the area under the curves. By this method the value was found to be $I_a = 0.27$ clo. This is approximately 18% lower than the value given by the formula due to Burton & Edholm (11), $I_a = 0.32$ clo. Use of a high value for I_a would lead to an underestimation of the amount of clothing a subject would require for comfort in a particular environment.

Test 2. Thermal insulation of a cylinder in free convection

An experiment was next conducted in order to establish whether or not the method of using a surface plate calorimeter could be used to measure the insulation value of a particular material. For this purpose a light weight cotton fabric (typical of shirt material) was

chosen as the test piece.

A calorimeter and a thermocouple were then attached to the surface of a uniformly heated, 7 cm diameter, cylinder (wall temperature $T_w = 34^o \pm 0.2^oC$) which was freely supported horizontally at both its ends. The local radiative and free convective heat loss (q/A) distribution was measured at 30^o intervals around the cylinder from the lower stagnation point. These results were then converted to local insulation values (I) and plotted in Fig. 55 against local azimuth angle.

One layer of the cotton fabric was then wrapped around the circumference of the cylinder, covering the calorimeter and thermocouple. Since the calorimeter measures heat loss to the environment from the body to which it is attached it will, in this case where the fabric is touching the calorimeter, measure the combined local radiative, convective, and conductive heat loss. This total heat loss is indeed the loss of greatest interest. The distribution of this heat loss loss was measured around the cylinder and the results reduced to local insulation values (I) and plotted in Fig. 55 together with the results for the free surface of the cylinder.

Results and Discussion of Test 2.

The results for the free surface of the cylinder (curve 1 of Fig. 55) may be considered as the local air insulation value (I_a) around the cylinder, whereas the results shown in curve 2 are for the combined air plus cotton ($I_a + I_c$). From these two curves the following information may be obtained.

(1) The air insulation around a heated body in free convection is not constant, and is lowest where temperature gradients are steepest (i.e. at the bottom half of the cylinder), and highest where the gradients are shallowest (i.e. within the convective plume).

(2) With the cotton fabric attached around the cylinder the value for

the insulation is increased around the bottom half of the cylinder and decreased at the top. The reason for this change will be due to the new convective boundary layer that is established at the outer surface of the fabric. This surface will have a lower temperature than that of the free cylinder surface (because of the conductive heat loss across the fabric) and the temperature gradients at the bottom of the cylinder will be shallower and the convective boundary layer thicker; at the top of the cylinder the plume will be less vigorous and the temperature gradients steeper thereby giving a lower insulation value; (3) Integrating the area under curve (1) gives the average value for the air insulation as

$$I_a = 0.700 \pm 0.005 \text{ clo}$$

Since we may add thermal insulation values in series the measurements we have taken with the cotton fabric (curve 2) will be the combined air and cotton values, i.e. $I_a + I_c$. Average values for this combination are

$$I_a + I_c = 0.750 \pm 0.005 \text{ clo}$$

This gives an insulation value for the cotton material of

$$I_c = 0.050 \pm 0.005 \text{ clo}$$

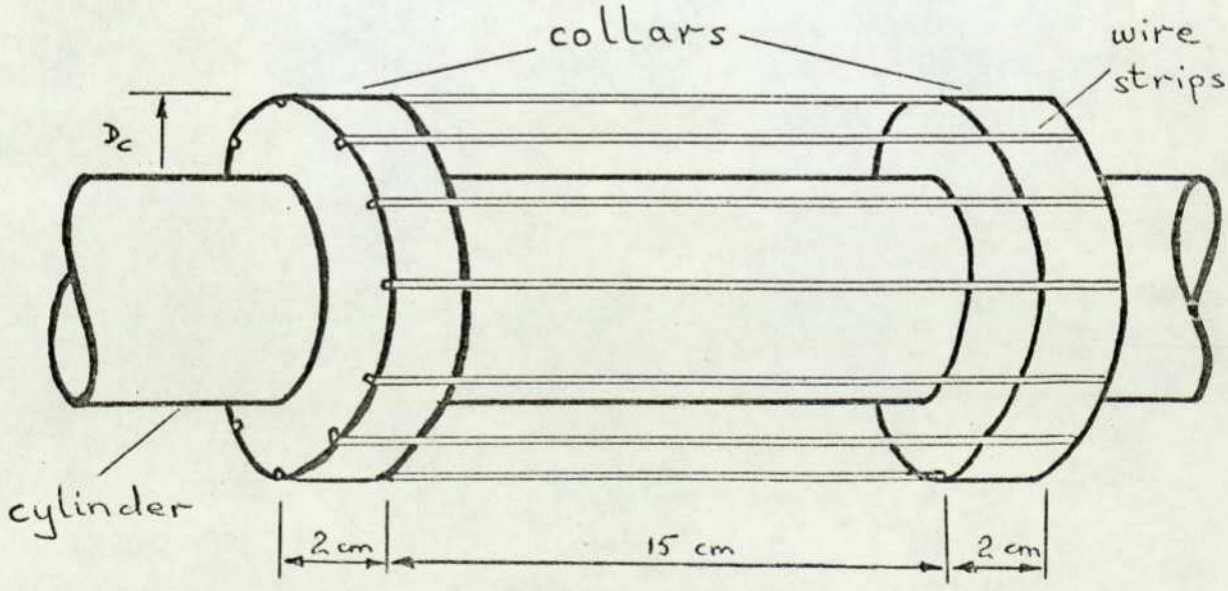
A value for cotton used in poplin shirting given in Newburghs book (ref. 74, p 299) is $I_c = 0.051$ clo. This was obtained by placing the fabric between two plates of known temperature with a constant heat flux between them. Since this heat flux must also pass through the material the value for the insulation will be given by the expression $I_c = (T_1 - T_2)/(q/A)$, where T_1 and T_2 are the plate temperatures and (q/A) the heat flux. The insulation value for cotton obtained using a surface plate calorimeter is shown to be in good agreement with this latter value.

Test 3. Thermal insulation of a cylinder in forced convection

In order to investigate what effect the cotton fabric may have

on insulating a heated cylinder in forced convection, two experiments were performed. The first experiment was to observe how the local heat loss (and hence the thermal insulation) from the forward stagnation point of a heated cylinder in a cross-flow was affected by the cotton material being positioned a known distance from the cylinder wall (i.e. producing an air gap between the fabric and wall). The second was to observe how the local heat loss and insulation varied around the circumference of the cylinder in a cross-flow with the material, once again, at different set distances from the cylinder wall.

For these two experiments five pairs of nylon collars, 2 cm thick, were made to fit snugly around the cylinder. Each pair of collars were of uniform depths of either 4, 8, 12, 16, or 20 mm and had twelve 1.0 mm deep groves machined across the width of the collars and equally spaced around the outer circumference. With a pair of collars attached approximately 15 cms apart, twelve 19 cm long, 0.914 mm diameter, wire strips (20 s.w.g.) were positioned in the machined grooves, thus giving the cylinder a 'caged' appearance. This cage was robust enough to hold one layer of the cotton fabric stretched in such a way that the fabric could be considered to be D_c cm away from the cylinder wall, where D_c is the depth of the collars. See sketch below.



Expt. 1. Stagnation point heat transfer through cotton fabric

A calorimeter and a thermocouple was attached to the wall of a heated cylinder which was mounted horizontally across the working section of a low-speed wind tunnel. The combined convection and radiation heat losses were measured from the forward stagnation point of the cylinder for a range of air velocities between $0.15 < U_\infty < 2.00$ ms^{-1}. In order to observe whether or not the presence of the cage had any effects on the local heat losses, the 4 mm deep cage was then attached around the cylinder with the collars equally spaced on either side of the calorimeter, and the above measurements repeated.

One layer of the cotton fabric was then attached around the cylinder surface (D_c = 0 mm) and the local heat loss again measured over the same velocity range. Each of the cages was then placed around the cylinder in-turn and a layer of cotton material attached to it; measurements were again taken for the same velocity range for each of the different air gaps (that is, for D_c = 4, 8, 12, 16, 20 mm).

The above results are presented in two figures: Fig. 56 shows how the local heat loss, from the forward stagnation point of a cylinder covered with a cotton material set at prescribed distances from the cylinder surface, varies with increasing velocity; and Fig. 57 shows the corresponding local insulation values.

Results and Discussion of Expt. 1, Test 3.

From the heat loss results plotted in Fig. 56 the following observations may be made.

(1) The presence of the cage around the cylinder has no noticeable affect on the local heat loss from the forward stagnation point. (Although we may expect the cage to increase the local turbulence level around the cylinder, and thereby increase the convective heat loss, this increase is insufficient to affect the local heat loss appreciably.

(2) By attaching the cotton fabric on the surface of the cylinder a

heat loss reduction at the forward stagnation point of only 20% at 0.50 ms^{-1} and 40% at 2.00 ms^{-1} may be obtained, whereas by attaching the fabric 4 mm from the surface the local heat loss is reduced by as much as 55% over the entire velocity range, and as much as 65% if placed 8 mm from the surface. Above this value of D_c = 8 mm the saving in the heat loss from the cylinder is not significantly increased.

With the local heat loss results converted into local insulation values and plotted against increasing velocity in Fig. 57 further information may be obtained.

(1) The value of the insulation for all of the combinations falls monotonically but non-linearly with increasing velocity.

(2) The difference between the insulation for the clean cylinder and that for the cotton covered cylinder (D_c= 0 mm) gives the insulation value for the cotton alone (I_c). That is, the local value for the clean cylinder is given by curve 1 (the insulation value for air, I_a), and with the cotton attached to the cylinder by curve 2 (the insulation of the cotton plus air combination, $I_a + I_c$). The difference between these two curves represents the insulation value for the cotton and is approximately constant throughout the velocity range at a value of I_c = 0.05 clo.

(3) With the cotton attached around each of the cages in-turn the value of the insulation measured is that of:-

(i) the air (I_a),

(ii) the cotton (I_c),

(iii) the air gap between the cotton and the cylinder wall (I_{ag}).

From the results of this combination it can be seen that:-

(A) there is insignificant gain in the combined insulation by attaching the cotton further than D_c= 12 mm from the cylinder surface;

(B) since the difference between the combined insulation results for D_c = 4, 8, and 12 mm ($I_a + I_c + I_{ag}$) and that obtained for D_c= 0 ($I_a + I_c$)

is the insulation value for the air gap alone (I_{ag}), we observe that I_{ag} does not remain constant over the velocity range (in contrast to the behaviour of I_c) but rapidly falls off with increasing velocity. This is due to the trapped air between the cylinder and the cotton becoming increasingly mobile as the airspeed outside increases with the result that the convection heat loss from the cylinder increases as the outside airspeed increases.

Expt. 2. Heat loss distribution around a heated cylinder, with and without the cotton fabric

As in the previous experiment a calorimeter was used to measure the local heat loss from the surface of a heated cylinder with and without the cotton material attached at different distances from the cylinder surface. By rotating the cylinder axially in steps of 30^{o} the distribution of heat transfer from the surface of the cylinder in a cross-flow was determined. The freestream velocity was maintained constant at 0.90 ms^{-1} as measured with a hot-wire anemometer placed one metre upstream of the body.

Measurements were made with the bare cylinder and with the cotton material attached to the surface of the cylinder ($D_c = 0$), as well as to the five 'cages' (i.e. for D_c = 4, 8, 12, 16, 20 mm). The results have been plotted in Fig. 58 and Fig. 59. Fig 58 shows how the local heat transfer is distributed around the cylinder in the various situations while in Fig 59 the distribution of local insulation is presented.

Results and Discussion of Expt. 2, Test 3.

The results for the heat transfer distribution plotted in Fig 58 shows that:-

(1) with the cotton attached around the cylinder the local heat loss is considerably reduced, and that the shape of the distribution is

basically unaltered;

(2) this reduction in the local heat loss increases as the air gap is increased up to D_c = 12 mm. Above this value there is little further reduction in the heat loss.

With the heat loss results converted into insulation values and plotted against azimuth angle in Fig 59, the following information may be obtained.

(1) As the air-gap increases to a value of D_c = 12 mm, the angular positions for maximum insulation appear to move further around the cylinder from the forward stagnation point. (If we assume that these angular positions are related to the separation points, then it would seem that the laminar boundary layer over the front half of the cylinder remains attached for a greater distance around the cylinder, with the result that the wake formed behind the cylinder may be narrower).

(2) For the air-gap of D_c = 16, and 20 mm the position for maximum insulation return to the same angular position as for the free cylinder. This is probably due to the increased air flow between the cylinder wall and the fabric.

By integrating the areas under the curves from both of the figures it is possible to estimate (a) the amount of heat per unit time saved for each of the cotton/air-gap configurations, and (b) the insulation value of the cotton and the air-gap. The following table summarises these results together with the percentage of heat saved from the cylinder as the air-gap increases and it may be observed that:-

(1) The average insulation value for the cotton (obtained from the difference between the total insulation for the cotton fabric attached to the cylinder wall ($I_a + I_c$) and the air insulation (I_a) obtained from the free cylinder) is

$$(I_a + I_c) - I_a = 0.055 \text{ clo}$$

This result is consistent with the value for cotton obtained in the previous experiment.

(2) The average insulation for the air-gap (obtained from the difference between the insulation of the cylinder - fabric - air-gap combination ($I_a + I_c + I_{ag}$) and the cylinder - fabric combination ($I_a + I_c$)) increases as the depth of the air-gap increases up to D_c = 16 mm, above this value there is a reduction in the insulation. This may be expected since above an optimum depth of air-gap (approximately 12 mm, ref 11 p 54) the amount of air penetrating the cotton will increase and help to re-establish the original convective pattern around the cylinder.

(3) By using one layer of material around a heated cylinder the amount of heat conserved is shown to be as much as 52% if a 4mm air-gap is used between the cylinder wall and the fabric, and as high as 70% for a 16 mm air-gap.

Average values of the heat loss and insulation around a cylinder in a 0.90 ms^{-1} airstream, air temperature T_∞ = 23.5° ± 0.2°C

curve No.	Heat loss ($W\ m^{-2}K^{-1}$)	% Heat saved	Insulation (clo)
1 free cyl.	20.0	0	0.38 (I_a)
2 D_c = 0 mm	15.5	22	0.42 ($I_a + I_c$)
3 = 4 "	9.5	52	0.75 ($I_a + I_c + I_{ag}$)
4 = 8 "	8.0	60	0.86 (")
5 = 12 "	6.5	67	1.10 (")
6 = 16 "	6.0	70	1.25 (")
7 = 20 "	6.3	68.5	1.15 (")

9.3.2 HEAT LOSS THROUGH CLOTHING FROM A HUMAN SUBJECT

As an introduction to the type of measurements that could be taken from the human body the following experiment was conducted. A subject was dressed in different clothing assemblies and measurements of the local heat loss from the skin of the subject through the garments were taken with the subject standing in streams of differing velocity.

A calorimeter and a thermocouple were attached to the skin over the area of the left pectoral muscle of a subject (CB). With the subject unclothed above the waist and facing upstream in an environmental wind tunnel, in which the air temperature remained constant at $T_\infty = 20.5^\circ \pm 0.3^\circ C$, local heat transfer measurements were taken at various air velocities, $0 \leqslant U_\infty < 1.75\ ms^{-1}$.

The subject then dressed in the following clothing assemblies:-

(1) a cotton singlet;

(2) " " " + a cotton shirt;

(3) " " " + " " + a laboratory overcoat.

For each of the above combinations local heat transfer measurements were again taken over the same velocity range.

The cotton singlet was then replaced by a string vest and a second series of measurements taken.

The results of this experiment are given in two figures. In Fig 60 the local heat loss is presented, and in Fig 61 the local insulation is given. In each case the results for the various clothing assemblies are given as functions of airspeed.

Results and Discussion

The following observations may be made from the heat loss results plotted in Fig 60.

(1) From curves 2 and 3 it is shown that rather less heat is lost from this area of a human body when a string vest is worn instead of a cotton singlet. A similar observation (obtained qualitatively using a schlieren

optical system) has been described by Clark (4), who found that the convective flow over the surface of a string vest is inhibited due to pockets of air trapped between the string fibres, resulting in small 'convective cells'. Thus the convective boundary layer over a string vest is thicker than that over a cotton singlet, with correspondingly shallower temperature gradients and therefore a lower heat loss.

(2) With a cotton shirt worn on top of each of the vests in turn, the local heat loss was reduced by approximately 30% over the entire velocity range, as compared to the heat loss from the subject wearing the vests alone. It was also observed that more heat was lost with the singlet - shirt combination (curve 4) than with the string vest and shirt (curve 5). The reason for this was attributed to the 'air pockets', trapped by the string vest, producing an air-gap between the shirt and the body (similar to the air-gap in the previous experiment) and thereby increasing the insulation of the assembly by the addition of the air-gap insulation.

(3) For the subject wearing the laboratory overcoat on top of either of the two-garment combinations it may be observed that ,

(a) the local heat loss is approximately constant at 8 W m^{-2} K^{-1} for the velocity range tested,

(b) there is little difference between the local heat losses for the clothing combination wearing the cotton singlet, and the combination wearing the string vest.

A more quantitative approach to the above observations may be obtained from the local insulation values plotted in Fig 61. Using the fact that the total insulation value of a clothing assembly is the sum of the insulation values for each of the garments, the following values for the separate clothes in this experiment have been evaluated for the three different air velocities of U_∞ = 0.50, 1.00, and 1.50 ms^{-1}, and are shown in the table below.

Velocity U (ms^{-1})	Insulation (clo)						
	curve no.						
	1	2	3	4	5	6	7
	I_a	I_a+I_c	I_a+I_{sv}	$I_a+I_c+I_s$	$I_a+I_{sv}+I_s$	$I_a+I_c+I_s+I_L$	$I_a+I_{sv}+I_s+I_L$
0.50	.33	.39	.40	.60	.64	.90	.95
1.00	.27	.34	.35	.56	.60	.84	.88
1.50	.24	.32	.33	.55	.58	.80	.80

From this table the average values for the cotton singlet, string vest, shirt and laboratory overcoat may be determined and are shown in the following table (note that the shirt and the overcoat have two insulation values for each air velocity depending on the undergarment worn: the first value in each of the respective columns relates to the cotton singlet, and the second to the string vest).

Velocity U (ms^{-1})	Insulation (clo)			
	c'singlet I_c	s'vest I_{sv}	shirt I_s	L'overcoat I_L
	(2) - (1)	(3) - (1)	(4) - (2) / (5) - (3)	(6) - (4) / (7) - (5)
0.50	.06	.07	.21 / .24	.30 / .31
1.00	.07	.08	.22 / .25	.28 / .28
1.50	.06	.07	.23 / .25	.25 / .22
Av. value	.06	.07	.22 / .25	.28 / .27

The numbers in the brackets refer to the curve numbers in Fig 61.

It was observed from Fig 60 that a subject loses less heat when wearing a string vest than for a cotton singlet. The reason for this may be attributed to the 'air pockets' trapped between the fibres of the string vest, and it may be assumed therefore that these pockets of relatively still air would also have an insulation value. This value is given indirectly from the results in the above table, since both the singlet and the string vest are made of cotton the difference between the average insulation for these garments may be considered to be equivalent to the extra insulation of the 'air pockets'. That is,

$$I_{sv} - I_c = I_{\text{air pocket}}$$
$$= 0.01 \text{ clo}$$

It may also be observed from this table that the average insulation value for the shirt is greater by 0.03 clo for the subject wearing the string vest combination as opposed to the singlet combination. This difference is again attributed to the trapped air between the fibres of the string vest, but, in this case, because the air is also trapped between the shirt and the subject's skin (in a similar manner to the air-gap produced in the previous experiment) a more efficient insulation layer is produced resulting in a higher insulation value for the trapped air. That is,

$$(I_s)_{sv} - (I_s)_{cs} = I_{\text{trapped air}}$$
$$= 0.03 \text{ clo}$$

The insulation values found when the laboratory overcoat was worn show no consistent effect attributable to the string vest replacing the cotton singlet. Thus at an airspeed of 0.50 ms^{-1} wearing the string vest next to the skin gives slightly greater insulation than when the cotton singlet is worn but for an airspeed three times larger the reverse is true. An explanation for these different values is that the overcoat was not held firmly enough against the subject during the experiment, but was allowed to 'flap' in the wind, with the consequence

that the amount of air trapped between the clothes varied for each tunnel speed and clothing assembly. This was not true for the shirt and undergarments since these articles were tucked into the trousers thus holding these clothes firmly against the body.

From the above experiments it has been shown that the local heat transfer through cotton material from a heated cylinder and through various clothing assemblies from a human subject may be obtained using a surface plate calorimeter. Although these experiments were not intended as complete investigations in themselves, several interesting points are raised which are worthy of further study. For instance, since the insulation value for air at a known airspeed and temperature varies around the circumference of a heated cylinder, it would be interesting to study how this insulation varies around the human body. Also, since this (calorimetric) method has shown that the insulation value for cotton may be determined simply using a heated cylinder in free convection, a similar experiment could be arranged to determine the insulation properties of other fabrics.

The effect of an air-gap between the skin of a human subject and different fabrics could also be investigated.

It is worth remarking on the fact that use of the surface plate calorimeter enables measurements of insulation values and heat transfer rates through various clothing assemblies to be made on a human body in different environments without the need to measure overall heat losses.

To enable a more informed interpretation of the results it would be valuable to conduct an investigation of the wake behind a cylinder surrounded by a porous material.

The above remarks on further work are not meant to be exhaustive but simply to illustrate that the surface plate calorimeter could prove to be a fruitful instrument in this particular field.

10. CONCLUDING REMARKS

The overall convective heat transfer coefficient ($\bar{h}_c$) for the human body obtained by other workers have been classified into either free or forced convection heat loss. It is shown that conflicting results have occurred and that an investigation of the local convective heat transfer coefficient (h_c) from the human body enables a more consistent approach to the study of heat transfer.

As a first step the local convective heat loss for heated cylinders in free and forced convection has been described. Using this knowledge a theoretical value for the free convective heat loss from a human body in the supine and standing posture has been computed by representing the human form as a series of 6 cylinders. It was found that 17% more convective heat was lost in the supine posture compared to the standing.

Since the methods available for measuring the local convection heat transfer from flat plates and cylinders were found to be inappropriate for use on the human body, a new instrument, a surface plate calorimeter, was developed. Measurements taken with this instrument on heated cylinders in free and forced convection have shown that the results are within 10% of other known data, and that the standard deviation of the results for any particular experiment is st. dv. = 0.05.

Measurements of the local convective heat loss has been taken from the leg and head of a subject in both free and forced convection. From the results of these measurements it is shown that:-

(i) The thermal boundary layers around the leg and head may be described in a similar manner to the thermal boundary layers around heated cylinders;

(ii) The overall convective and radiative heat loss from the face of a standing subject, and the head of a supine subject, in free convection may be computed from the measured local heat losses. These values are shown to be comparable to the theoretical values derived for a heated vertical and horizontal cylinder of similar size, respectively.

(iii) The radius of curvature is important in assessing the heat loss from highly curved surfaces such as the anterior position on the leg, and the chin.

In forced convection the skin temperature of the nose falls rapidly to that of the surrounding air as the air velocity is increased. (The convective heat loss also falls rapidly with increasing air velocity). Temperature measurements of the face in free and forced convection have been taken with an infra-red radiation camera and the above observations noted.

The calorimeter has been used to measure the local heat loss in the following three fields:-

(1) Measurements have been taken from a hand immersed in two different gaseous environments. It was found that the results were within about 10% of the theoretical results based on an analysis of the physical properties of the gases.[X]

(2) The convective heat loss from the thigh of an athlete running on a treadmill has been measured. From these measurements it was found that about 25% more heat is lost from the thigh of a subject running into a 4.5 ms^{-1} airstream than that for the stationary thigh in the same airflow. The associated heat losses around the thigh are described in conjunction with frames of a film of the sequential leg positions during running.

(3) Finally, the effect of clothing on the convective heat loss from a human body has been described. Measurements have been taken of the insulation value of air and of various clothing assemblies in both free and forced convection. From these measurements it is shown that for a

---

X Since this work has applications in the diving industry, the heat loss from personnel inside a hyperbaric, Helium filled, diving chamber is the subject of a continuing study. It is also hoped to extend the study to the heat loss from personnel immersed in cold water.

body in a 0.9 ms^{-1} airstream a heat saving of some 70% may be made if a cotton garment is attached around the body at a distance of 16 mm from it. The comparitive differences in the heat losses through such garments as a cotton singlet and a string vest are described in relation to the air-gaps produced by the string fibres.

Appendix (A) - 1

Glossary of Physiological terms.

Metabolic rate: - The sum of the external work and heat produced by a human being. It may be measured by a calorimetric technique but is more frequently measured by oxygen consumption.

Evaporation heat loss: - There are two forms of evaporation heat loss from the human body, sensible and insensible evaporation. The former allows heat to be lost by 'sweating', and the latter by evaporation of water vapour from the lungs due to respiration and diffusion of water vapour through the eperdermis from the deeper layers of the skin. - The latent heat of vaporization is 4.82 J/Kg at $33^{\circ}C$, and for temperate climates a body loses about 0.030 Kg/hr of water vapour by insensible perspiration, that is, about 20 watts of heat is lost by this method alone.

Indirect Calorimetry: - This method requires knowledge of the amount of oxygen inhaled and the amount of carbon dioxide released due to respiration, Benedict (80), Haldane(81). Provided the proportion of carbohydrate, fats and protein utilised in the combustion process are known, the heat output from the body (Q) may be determined from the Respiratory Quotient (r.q), since $Q \propto r.q$

where r.q = ratio of $\frac{\text{Carbon Dioxide released}}{\text{Oxygen consumed}}$

Direct Calorimetry: - This method allows the total heat loss by convection, conduction, evaporation, and radiation from the human body to be measured. Two techniques have been used for these measurements, gradient layer calorimetry,Benzinger (82), and adiabatic calorimetry, Rubner (83). Both methods require the body to be enclosed in a specially designed room or suit.

Gradient Layer Calorimeter: - A subject is placed inside the calorimeter and the heat flow (q/A) from the subject through the walls of the calorimeter is evaluated by measuring the temperature gradient $(\Delta T/\Delta y)$ across the walls, that is, $(q/A) \propto \Delta T/\Delta y$

Adiabatic Calorimeter: - This technique allows no heat from the subject to pass through the walls of the calorimeter. Instead, the temperature increase per unit time ($\Delta T/\Delta t$) of the air passing through the calorimeter is a measure of the total heat loss (Q) from the subject, hence

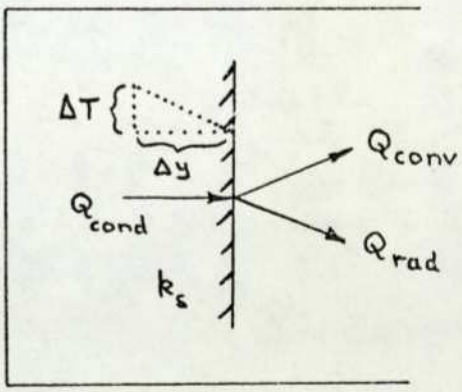
$$Q \propto \Delta T/\Delta t$$

Partitional Calorimetry: - This method was developed in order to measure the different heat losses from the body separately, Winslow (24). The subject was placed in an experimental room in which the radiative or convective heat loss from the body could be minimised by either heating the walls or the surrounding environment respectively. By measuring the Metabolic rate (M), the evaporative heat loss (E), and the heat storage (S) independently, (the heat storage may be computed from the mean changes in rectal and skin temperature, Hardy (84) , the convective or radiative heat loss may be computed from, $\pm C = M - E \pm S$ (where the radiation $R \simeq 0$), and $\pm R = M - E \pm S$ (where the convection $C \simeq 0$).

Internal Calorimetry: - At the interface between a heated body and air the conduction heat transfer that occurs within the body is converted into radiation and convection heat loss,

$$Q_{cond} = Q_{rad} + Q_{conv}$$

Therefore it is justifiable to assume that measurements of the conduction heat transfer will contribute to this realisation.



$$(q/A)_{cond} = - k_s . \Delta T/\Delta y$$

where k_s is the skin thermal conductivity and $\Delta T/\Delta y$ the temperature gradient within the body. Although thermal conductivities and temperature gradients have been measured in skin tissues using needle thermocouples (Grayson (85), Cooper (86), Bazett (87)) the structure of the epidermis and dermis layer, as shown diagrammatically in Fig 62, Lewis (88), and its non-homogeneity discourages any attempt to use this method as a means of indirectly measuring the local convective heat transfer.

Appendix (B) - 1

Effect of cylinder height on the overall convective heat loss.

In free convection a body loses heat as described by the following proportionality, (section 3),

$$Nu \propto \sqrt[4]{Gr}$$

Expanding these non-dimensional numbers, we find that

$$h_c.L/k \propto \sqrt[4]{(g\beta.\Delta T/\nu^2)\ L^3}$$

For different sizes of body with other parameters constant, the convection coefficient h_c may be described by,

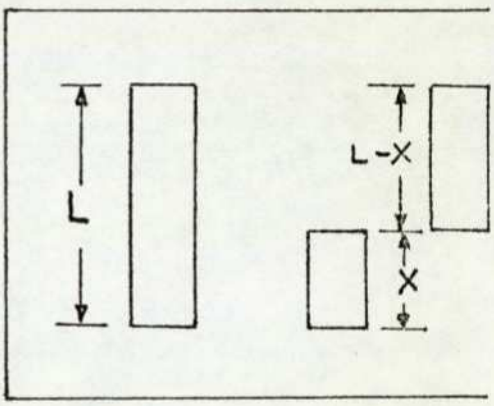
$$h_c \propto \sqrt[4]{1/L}$$

Now consider the convective heat loss from two isothermally heated cylinders of diameter d, and the same wall temperature T_w. Let one of the cylinders be of length L and the other of height X.

The ratio of the average convection heat transfer coefficients of these two cylinders may be written as,

$$(h_c)_X/(h_c)_L = \sqrt[4]{L/X}$$

This ratio is plotted in Fig. 63 against the non-dimensional height X/L.



In order to ascertain what the effect of cylinder height will be on the overall convective heat loss consider the total heat loss from a cylinder of height L and two smaller cylinders (of the same diameter) of combined height L.

The total heat loss from a cylinder of length L, diameter d, and temperature difference ΔT, is

$$Q_L = (\bar{h}_c)_L.\pi\, d.L.\Delta T$$

and from two separate cylinders of height X and L - X,

$$Q_{total} = Q_X + Q_{(L-X)}$$

$$= (\bar{h}_c)_X.\pi\, d.X.\Delta T + (\bar{h}_c)_{L-X}.\pi\, d.L-X.\Delta T$$

We may now write the ratio of Q_{total}/Q_L as,

$$\frac{Q_{total}}{Q_L} = \frac{(\bar{h}_c)_X \cdot X + (\bar{h}_c)_{L-X} \cdot (L - X)}{(\bar{h}_c)_L \cdot L}$$

$$\frac{(\bar{h}_c)_X}{(\bar{h}_c)_L} \cdot \frac{X}{L} + \frac{(\bar{h}_c)_{L-X}}{(\bar{h}_c)_L} \cdot \frac{(L - X)}{L}$$

As an example consider two cylinders of height $X = 0.2\ L$ and $(L - X) = 0.8\ L$. (see Fig. 63). If the values shown in Fig 63 are substituted in the above expression then this ratio will be,

$$\frac{Q_{total}}{Q_L} = 1.1449$$

This means that for two separate cylinders of combined height L, the total heat loss will be approximately 15% more than for a single cylinder of height L.

The greatest heat loss from two such cylinders occurs when $X = 0.5\ L$, in which case $Q_{total}/Q_L = 1.189$, that is approximately 19% more heat is lost.

This analysis shows that by considering the human form as a cylindrical model with each of the cylinders losing heat separately, the maximum total heat loss was evaluated, and any interaction effects would almost certainly lead to lower heat losses.

Appendix (C) - 1

Calibration of the hot-wire anemometer

The constant temperature hot-wire anemometer used throughout the present work has been described by Clark (4) and consists of a hot-wire probe and a servo-amplifier circuit, commercially denoted by DISA 55D05. The probe is constructed of a 5 μm diameter tungsten wire welded across two nichrome wire prongs approximately 3 mm apart. The amplifier circuit contains a Wheatstone bridge network, one arm of which is the hot-wire probe. When electrical energy is supplied to the bridge the probe heats up to a constant temperature. If the probe is placed in an airstream the wire cools and more electrical energy is supplied to the bridge from the amplifier in order to maintain the wire at its constant temperature.

For the present experiments it was assumed that the wire cools in accordance with King's Law, that is,

$$V^2 = A.U_\infty^{0.5} + V_o^2$$

where V is the voltage across the wire in an airstream of U_∞,

V_o is the no-flow voltage across the wire,

A is a constant and is a function of the dimensions and properties of the wire.

To calibrate the voltage across the wire in terms of velocity the probe was placed in a known airstream. Since we were concerned only with measuring air velocities between $0.15 < U_\infty < 5.0$ ms^{-1} the probe was calibrated by two methods. For velocities above 1.5 ms^{-1} the anemometer was calibrated against a pitot-static tube in a small wind tunnel, and for velocities below 1.5 ms^{-1} in a laminar parabolic velocity field. Such a velocity field occurs within a smooth-bore cylindrical tube at some distance greater then 100 diameters downstream of the inlet if the Reynolds number, based on the internal tube diameter, is $Re_d \leq 2000$.

The volume flow rate of air through such a tube is given by

$$\dot{V} = \Pi r^2 \bar{U}$$

where $\bar{U}$ is the mean velocity.

For a parabolic velocity profile

$$\bar{U} = \tfrac{1}{2} U_m$$

where U_m is the maximum velocity on the axis of the tube.

$$\therefore \quad \dot{V} = \tfrac{1}{2} \Pi r^2 . U_m$$

or

$$U_m = \frac{2 \dot{V}}{\Pi r^2}$$

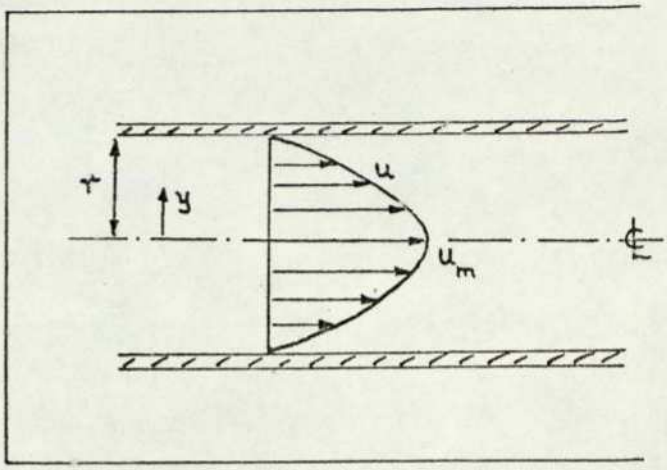


Fig. 64 shows a diagrammatic sketch of the apparatus for calibrating the probe for velocities below 1.5 ms^{-1}. It consists of a 1.908 cm diameter, smooth bore, tube, 2.5 m long, a traversing mechanism for positioning the probe in the tube, a medical rotameter, and a suction pump. The probe was mounted in the traversing mechanism above a 5 mm diameter hole in the wall of the tube, 2.1 m from the tube entrance. The other end of the tube was connected to the rotameter, and this in turn to the suction pump. The probe was then traversed through the hole and positioned on the axis of the tube with the wire at right angles to the airstream. The volume flow rate of air drawn through the tube by the pump was measured with the rotameter.

To check the shape of the velocity profile in the calibration tube the probe was traversed across the tube diameter for a constant volume flow rate. The voltage output was then converted into the non-dimensional velocity function $\left\{(V^2 - V_o^2)/(V_m^2 - V_o^2)\right\}^2 = U/U_m$ and plotted against y/r in Fig. 65. (Where V is the voltage output from the wire at position y in the tube, and V_m is the maximum voltage in the tube). From this figure it may be seen that the velocity profile is parabolic in nature, but is slightly skewed away from the entrance hole for the probe. The reason for this skewness is probably due to this discontinuity in the wall surface, as well as the effect of the prongs in the velocity field.

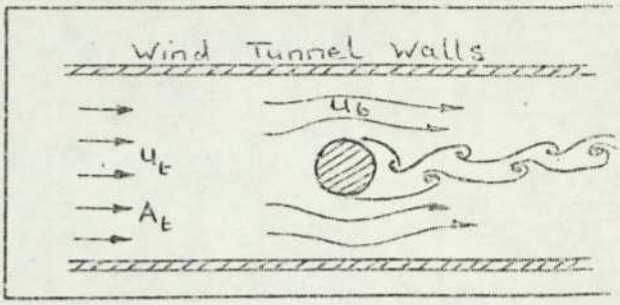
Fig. 66 shows a typical calibration curve for a hot-wire anemometer obtained by the two methods. It may be seen from this figure that the

two calibration curves do overlap but the results are not linear as given by King's Law, $V^2 - V_o^2 = A.U^{0.5}$

Although there are many reasons for this discrepancy, such as temperature loading, and wrong power function for the wire, Collis & Williams (89), they are outside the scope of this work. It was sufficient for the present purposes to use the calibration curve to evaluate the freestream velocity from anemometer voltages rather than use the above law.

Wind tunnel blockage correction

It is known that the air flow around a body inside a closed working section of a wind tunnel is constrained by the tunnel walls (ref.32). The effect of these constraints causes the air velocity (U_b) around the body to be higher than that measured upstream (U_t) of the body position. In order to correct for this anomaly two types of wind-tunnel blockage corrections have to be applied to all measured wind tunnel velocities, that is, (a) solid blockage (ε_{sb}), correction due to presence of the body in the tunnel, and (b) wake blockage (ε_{wb}), correction due to the influence of the wake downstream of the body.



From the analysis of wind tunnel blockage corrections given by A. Thom (R & M 2033, 1943) for a two-dimensional model in a wind tunnel of cross-sectional area A_t, the solid blockage is,

$$\varepsilon_{sb} = \Delta u_1 / u_t = K_1 (\text{Model Volume}) / A_t^{3/2}$$

where $K_1 = 0.74$ and Δu_1 is the velocity correction due to solid blockage: the wake blockage is,

$$\varepsilon_{wb} = \Delta u_2 / u_t = (d/4H) C_d$$

where d = cylinder diameter, H = height of tunnel section, Δu_2 is the velocity correction due to wake blockage, and C_d is the cylinder drag coefficient. (Throughout this work the value of C_d was taken as unity since the Reynolds number of the cylinder was maintained between the limits $8 \times 10^2 < Re_d < 2 \times 10^4$, and never exceeded the critical Reynolds number of 3×10^5).

The total blockage correction is the sum of these two terms

$$\varepsilon_t = \Delta u / u_t = \Delta u_1 / u_t + \Delta u_2 / u_t$$

and the velocity at the position of the body is given by

$$u_b = \Delta u + u_t$$

For the human subject in the environmental wind tunnel, the total blockage correction was computed from the form suggested by A. Pope & J.J. Harper (Low-Speed Wind Tunnel Testing, Wiley, 1966) for unusual shaped bodies, that is,

$$\varepsilon_t = \Delta u / u_t = \frac{1}{4} \left(\frac{\text{Model Frontal Area}}{\text{Test Section Area}} \right)$$

(The "model frontal area" was estimated from measurements using a planimeter around a photograph of the subject in the environmental wind tunnel).

REFERENCES

(1) Lewis, H.E.
Journal of Physiology, 188, 6, (1967)

(2) Lewis, H.E., Foster, A.R., Mullan, B.J., Cox, R.N., & Clark, R.P.
Lancet (i), 1273 - 1277, (1969)

(3) Foster, A.R.
M.Sc Thesis, City University, (1973)

(4) Clark, R.P.
Ph.D Thesis, City University, (1973)

(5) Clark, R.P., Baker, C.R., & Glover, D.D.
Engineering in Medicine, 3, No 1, 1 - 3, (1974)

(6) Toy, N., & Cox, R.N.
Revue Generale de Thermique, 145, 37 - 41, (1974)

(7) Clark, R.P., Cox, R.N., & Toy, N.
Journal of Physiology, 223, 10 - 12, (1972)

(8) Plummer, J.H.
Publication of the Climatology and Environmental Protection Branch, Office of the Quartermaster General, (1944)

(9) Buttner, K.
Publication of the Prussian Meteorological Institute, 10, 404, (1934)

(10) Webb, P.
Aerospace Medicine, 1282 - 1288, (1970)

(11) Burton, A.C., & Edholm, O.G.
Man in a Cold Environment.
Edward Arnold (Publishers) Ltd, (1955)

(12) Gagge, A.P., Winslow, C.E.A., & Herrington, L.P.
Am. J. of Physiology, 124, 30, (1938)

(13) Aldrich, L.B.
Smithsonian Miscellaneous Collections, 81, 6, 1 - 54, (1928)

(14) Hardy, J.D. & Dubois, E.F.
J. of Nutrition, 15, 477, (1938)

(15) Missenard, F.A.
Actes du Colloque International Collection des Colloques Internationaux du C.N.R.S., 15 Quai Anatole France. (1972)

(16) Hardy, J.D.
The Harvey Lectures, 49, 242 - 270, (1953 - 54)

(17) Wissler, E.H.
Temperature: Its measurement and control in Science and Industry, 3, 603, (1963)

(18) Nelson, N., Eichna, L.W., Horvath, S.M. & Shelley, W.B.
Am. J. Physiol. 151, p 626 - 652, (1947)

(19) Mitchel, D., Wyndham, C.H., Vermeulen, A.J., Hodgson, T., Atkins, A.R. & Hofmeyr, H.S.
J. Appl. Physiol., 26, p 111 - 118, (1969)

(20) Carroll, D.P. & Wisser, J.
Rev. Sci. Instr., 37, p 1174 - 1180, (1966)

(21) Hall, J.
Wright Patterson A.F.B., Ohio,
Memo Rpt., MCREXD - 696 - 105P, (1950)

(22) Tamari, Y.
M.Sc Thesis, Columbria University, (1969)

(23) Gagge, A.P., Herrington, L.P. & Winslow, C.E.A.
Am. J. Physiol., 126, p 84 - 102, (1937)

(24) Winslow, C.E.A., Gagge, A.P. & Herrington, L.P.
Am. J. Physiol., 127, p 505 - 518, (1939)

(25) Winslow, C.E.A., Herrington, L.P. & Gagge, A.P.
Am. J. Physiol., 131, p 79, (1940)

(26) Colin, J. & Houdas, Y.
J. Appl. Phys., 22, p 31 - 38, (1967)

(27) Aikas, E. & Piironen, P.
Wright Patterson A.F.B., Ohio,
Tech. Rpt., AMRL - TDR - 63 - 86, (1963)

(28) McKerslake, D.
The Stress of Hot Environments
Cambridge University Press, (1972)

(29) Burton, A.C.
Sixth Commonwealth Defence Conference on Clothing and General Stores
CDA - 8, Australia (1959)

(30) Forster, R.E., Ferris, B.G. & Day, R.
Am. J. Physiol., 146, p 600, (1946)

(31) Clifford, J.M.
Flying Personnel Research Committee FPRC/1261, (1966)

(32) Duncan, W.J., Thom, A.S. & Young, A.D.
Mechanics of Fluids, 1st Ed., p 193,
Edward Arnold (Publishers) Ltd., (1962)

(33) Eckert, E.R.G., & Jackson, T.W.
N.A.C.A. Rpt. 1015, (1951)

(34) Cheesewright, R.
J. Heat & Mass Transfer, 10, p 1847 - 1859, (1968)

(35) Sparrow, E.M. & Gregg, J.L.
J. Heat Transfer, 84, p 1823 - 1829, (1956)
(36) Jodlbauer, K.
Forsch. Geb. Ing., 4, p 157 - 172, (1933)
(37) Eckert, E.R.G., & Soehngen,
50 Jahre Grenzschicht forschung., p 407 - 418,
Freidr. Vieweg & Sohn, Brunswick, Germany, (1955)
(38) Schmidt, E.
Forsch. Ing - Wes., 3, p 181 - 189, (1932)
(39) Hermann, R.
V.D.I. - Forsch., 379, (1936)
(40) Newling, P.S.B.
M.R.C. Spec. Rpt. 54, (1954)
(41) Spalding, D.B. & Pun, W.M.
J. Heat & Mass Transfer, 5, p 239 - 249, (1962)
(42) Schmidt, E. & Wenner, K.
R.A.E. Library Trans. No. 280, (1948)
(43) Frössling, N.
N.A.C.A. Tech. Memo 1432
(44) Squire,
A.R.C. R & M 1986, (1942)
(45) Lighthill, M.J.
Proc. Roy. Soc., London A 202, p 359- 377, (1950)
(46) Eckert, E.R.G.
V.D.I. - Forsch., 416, p 1 - 23, (1942)
(47) Lees, L.
Jet Propulsion, 26, p 295 - 269, (1956)
(48) Ambrok, G.S.
Soviet Phys. Techn. Phys., 2, p 738 - 748, (1957)
(49) Allen, H.J. & Look, B.C.
N.A.C.A. Rpt. 764, (1943)
(50) Schlichting, H.
Boundary Layer Theory,
McGraw Hill, 6th Ed., (1968)
(51) Ostrach, S.
N.A.C.A. Tech. Note., 2635, (1952)
(52) Kroujilin, G.
Tech. Phys., USSR 5, p 289 - 297, (1938)
(53) Reiher, H.
V.D.I. - Forsch., 269, p 47, (1925)

(54) Goukhman, A., Joukovsky, V. & Lonziansky, L.
Tech. Phys. USSR 1, p 221 - 242, (1934)

(55) McAdams, W.H.
Heat Transmission,
McGraw, 3rd Ed., (1954)

(56) Comings, E.W., Clapp, J.T. & Taylor, J.F.
Ind. & Eng. Chem., 40, p 1076 - 1082, (1948)

(57) Kestin, J., Maeder, P.F. & Sogin, H.H.
Z.A.M.P. 12, p 115 - 132, (1961)

(58) Kestin, J. & Maeder, P.F.
N.A.C.A. Tech. Note 4018, (1954)

(59) Collins, M.
Research Memo. No. ML 15, City University, (1968)

(60) Hatton, A.P., James, D.D. & Swire, H.W.
J. Fluid Mech., 42, 1, p 17 - 31, (1970)

(61) Sparrow, E.M. & Gregg, J.L.
J. Appl. Mech., p 133 - 134, (1959)

(62) Sparrow, E.M., Eichhorn, R. & Gregg, J.L.
Physics of Fluids, 2, 3, p 319 - 328, (1959)

(63) Schardin, H.
Z. Instr., 53, p 396 - 403, (1933)

(64) Sernas, V. & Fletcher, L.S.
J. Heat Transfer., 92, p 202 - 204, (1970)

(65) Cheesewright, R.
J. Heat Transfer., 90, p 1 - 8, (1968)

(66) Geidt, W.H.
J. Heat Transfer., 71, p 375 - 381, (1949)

(67) VanMeel, D.A.
J. Heat & Mass Transfer., 5, p 715 - 722, (1962)

(68) Gordon, S.A.
J. Heat Transfer., 86, p 291 - 293, (1964)

(69) Coustanceau, J.
C.R. Hebd. Seanc. Acad. Sci., Paris 264, Serie B, p 1537 - 1540 (1967

(70) Hatfield, H.S. & Wilkins, F.J.
J. Sci. Instr., 27, p 1 - 3, (1950)

(71) Fox, R.H. & Solman, A.J.
J. of Physiol., 212, 8 - 10 P, (1970)

(72) Kaye, G.W.C. & Laby, T.H.
Tables of Physical and Chemical Constants,
Longmans, Green & Co. Ltd., (1968)

(73) Roff, W.J. & Scott, J.R.
Fibres, Films, Plastics and Rubbers: Handbook of Common Polymers,
London Butterworth & Co. (1971)

(74) Newburgh, L.H.
Physiology of Heat Regulation,
Hafner Publishing co., (1968)

(75) Clark, R.P. & Toy, N.
J. of Physiol., 244, p 283 - 302, (1975)

(76) Flynn, E.T., Vorosmarti, J. & Modell, H.I.
N.E.D.U. Res. Rpt. 21 - 73, p 1 - 42, (1974)

(77) Timbal, J., Vieillefond, H., Guenard, H. & Varene, P.
J. Appl. Physiol., 36, p 444 - 448, (1974)

(78) Raymond, L.W., Thalmann, R., Lindgren, G., Langworthy, H.C., et al
Und. Bio. Res., 2, 1, p 51 - 67, (1975)

(79) Webb, P.
Aerospace Med 41 (11), p 1282 - 1288, (1970)

(80) Benedict, F.G.
Boston Med. & Surg. Jnl., 178, p 667 - 678, (1918)

(81) Haldane, J.S.
J. of Physiol., 13, p 419 - 430, (1892)

(82) Benzinger, T.H., & Kitzinger, C.
Temperature: Its Meas. & Control in Sci. & Ind., 3, 3, p 87, (1963)

(83) Rubner, M.
Handbuch d. Biol., IV, 10, (1926)

(84) Hardy, J.D., & Dubois, E.F.
J. of Nutrition, 15, p 461, (1938)

(85) Grayson, J.
J. of Physiol., 118, p 52 - 72, (1952)

(86) Cooper, T.E.
Ph.D. Thesis, University of California, (1970)

(87) Bazett, H.C., & McGlone, B.
Am. J. of Physiol., 82, p 415, (1927)

(88) Lewis, H. in 'Principles of Human Physiology'
Ed. Davson, H., & Eggleton, M.G.
Churchill Ltd, 14th edition, (1968)

(89) Collis, D.C., & Williams, M.J.
J. Fluid Mech., 6, p 357 - 384, (1959)

Table 1. List of expressions for predicting the overall convection heat transfer coefficient $\bar{h}_c$ from a human body in three postures.

STANDING POSTURE

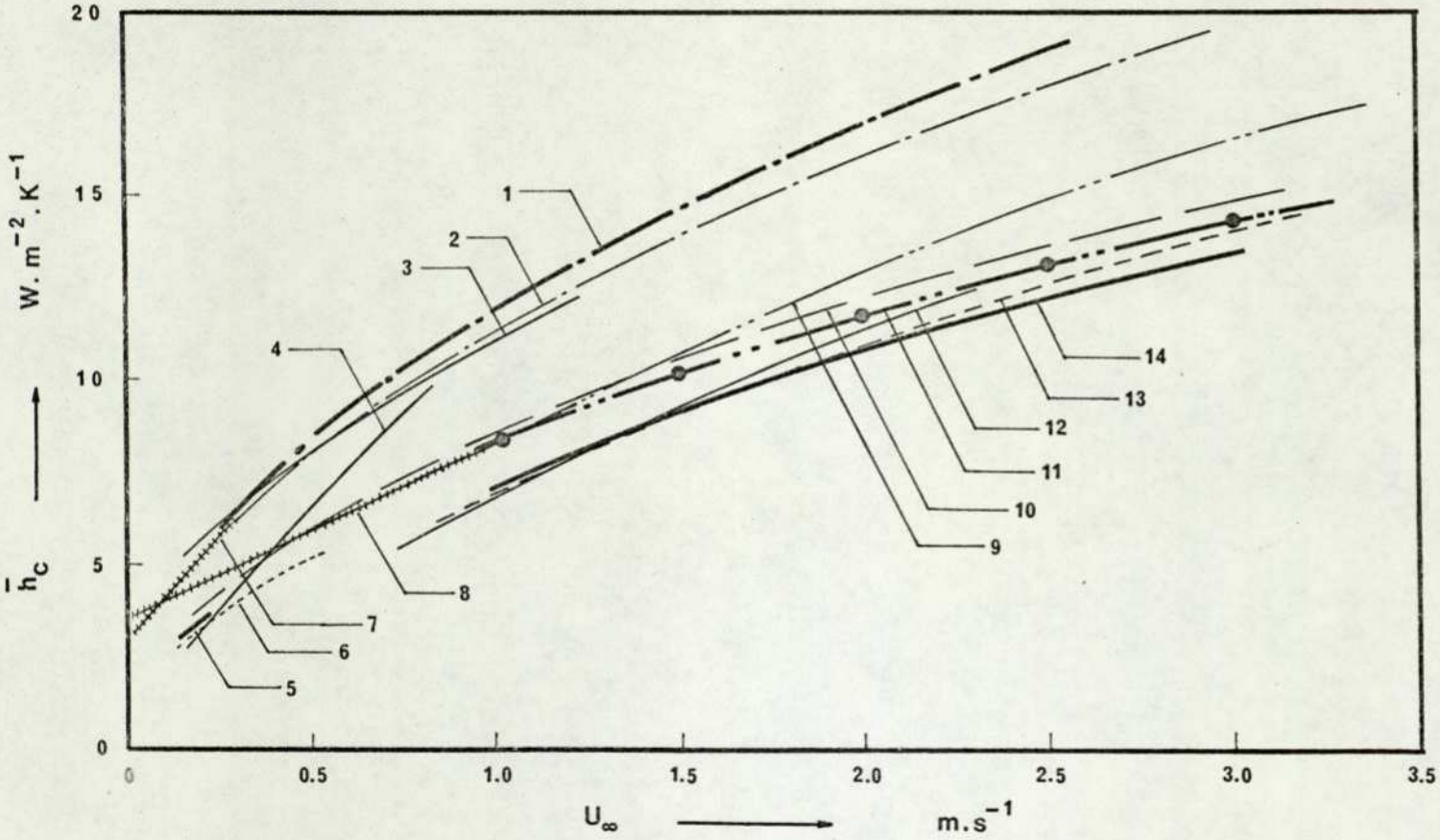
AUTHOR	EXPRESSION FOR $\bar{h}_c$ $W.m^{-2}K^{-1}$		CONSTANTS			VELOCITY RANGE
	FREE	FORCED	A	B	n	U ms^{-1}
Hardy (16)	A	—	0.7 - 0.93	—	—	—
Nelson (18)	—	$B.U^n$	—	8.7	0.5	0.15 - 3.00
Mitchel (19)	—	$B.U^n$	—	7.2	0.6	0.50 - 5.10
Hall (21)	—	$B.U^n$	—	2.9	0.8	0.20 - 0.80
Tamari (22)	—	$B.U^n$	—	7.1	0.643	3.6 - 14.8
Tamari (22)	—	$B.U^n$	—	3.66	0.643	0.85 - 3.54
Missenard (15)	A +	$B.U^n$	3.5	4.9	1.00	$U \leqslant 1.00$
Missenard (15)	—	$B.U^n$	—	8.4	0.62	$U \geqslant 1.00$
Clark (4)	A	—	1.7	—	—	—

RECLINING POSTURE

Gagge (12)	—	$B.U^n$	—	10.6	0.5	0.03 - 0.5
Gagge (12)	—	$B.U^n$	—	11.6	0.5	0.05 - 0.11
Winslow (24)	—	$B.U^n$	—	12.8	0.5	0.046 - 0.075
Winslow (24)	—	$B.U^n$	—	12.1	0.5	0.06 - 2.65
Colin (26)	A +	$B.U^n$	2.7	8.7	0.67	0.20 - 1.20

SUPINE POSTURE

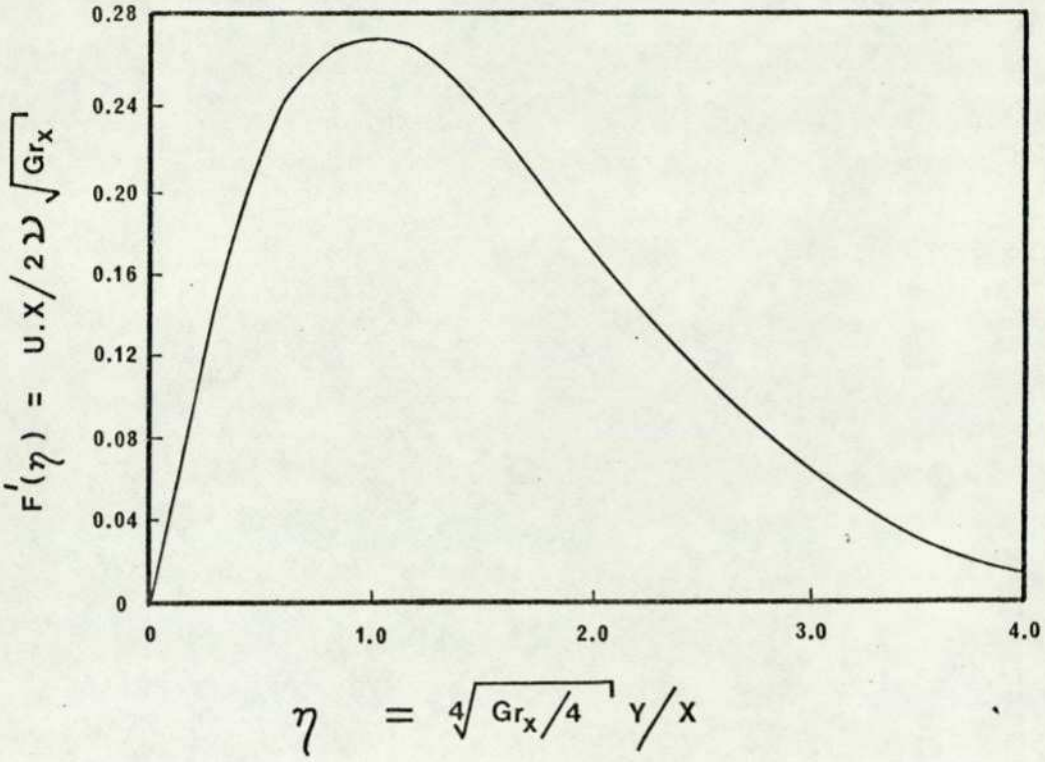
Buttner (9)	A	—	2.46	—	—	—
Buttner (9)	—	$B.U^n$	—	7.3	0.5	0.15 - 0.50
Hardy (14)	A	—	0.9 - 1.6	—	—	—
Aikas (27)	—	$B.U^n$	—	7.9	0.5	0.15 - 0.22
Tamari (22)	—	$B.U^n$	—	4.4	0.72	3.15 - 9.50
Tamari (22)	—	$B.U^n$	—	2.54	0.72	0.75 - 2.26
Missenard (15)	A +	$B.U^n$	3.05	10.6	1.00	$U \leqslant 0.25$
Missenard (15)	—	$B.U^n$	—	11.4	0.5	$U \geqslant 0.25$



No	Author	Posture
1	Winslow (24)	Reclining
2	Missenard (15)	Supine
3	Colin et al (26)	Reclining
4	Hall (21)	Standing
5	Aikas et al (27)	Supine
6	Büttner (9)	"
7	Missenard (15)	"
8	"	Standing
9	"	"
10	Nelson (18)	"
11	McKerslake (28)	Unspecified
12	Tamari (22)	Supine
13	" "	Standing
14	Mitchel (19)	"

Fig. 1 The overall convective heat transfer coefficient $\bar{h}_c$ for the human body plotted against freestream air velocity U_∞ for three body postures

VELOCITY PROFILE



TEMPERATURE PROFILE

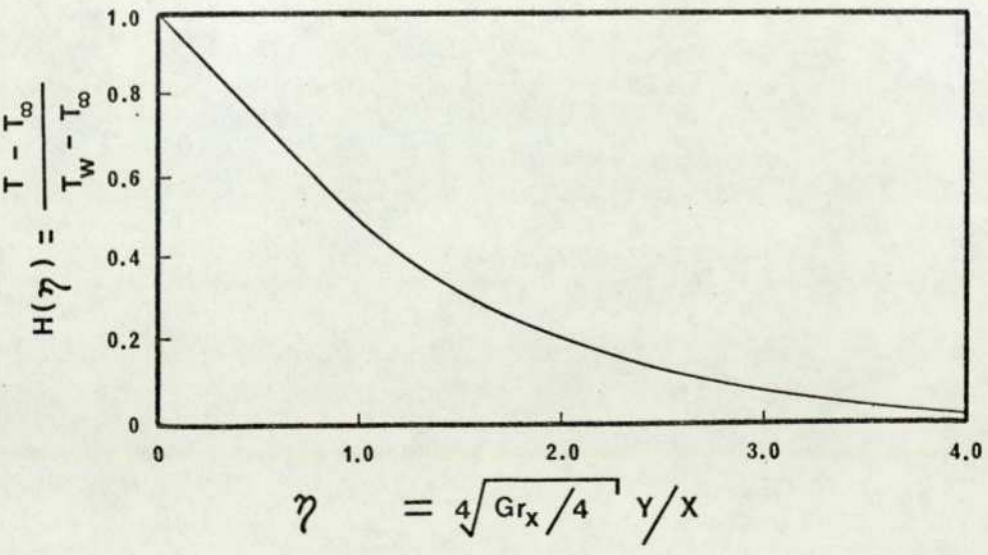


Fig. 2 Non-dimensional velocity and temperature profiles in laminar free convection flow

Fig. 3 Plot of the Local Value of Gr_x, Nu_x, and h_c with increasing Height X for Laminar Free Convective Flow on an Isothermally Heated Vertical Flat Plate

Wall Temperature $T_w = 33^\circ C$

Air " $T_\infty = 15^\circ C$

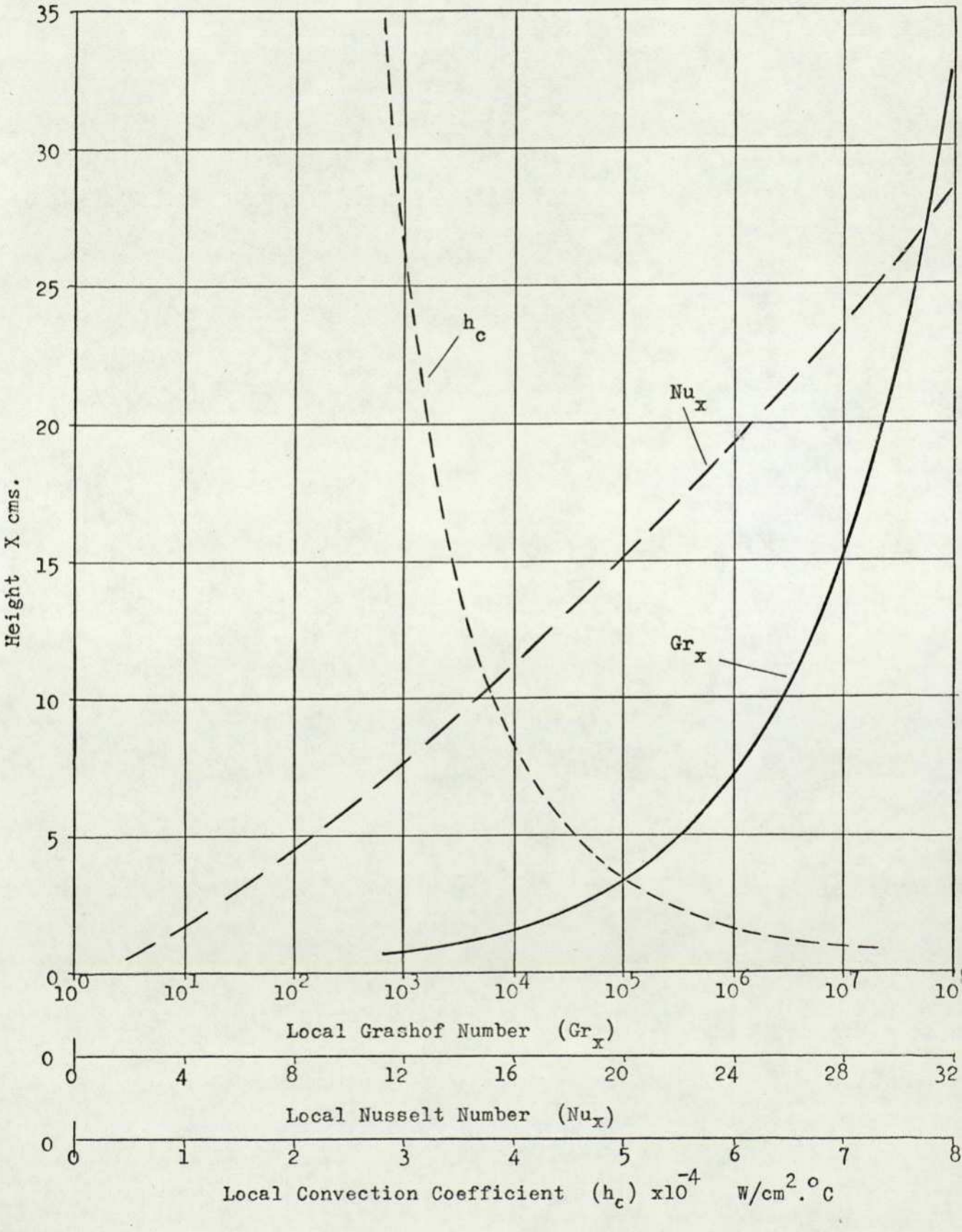
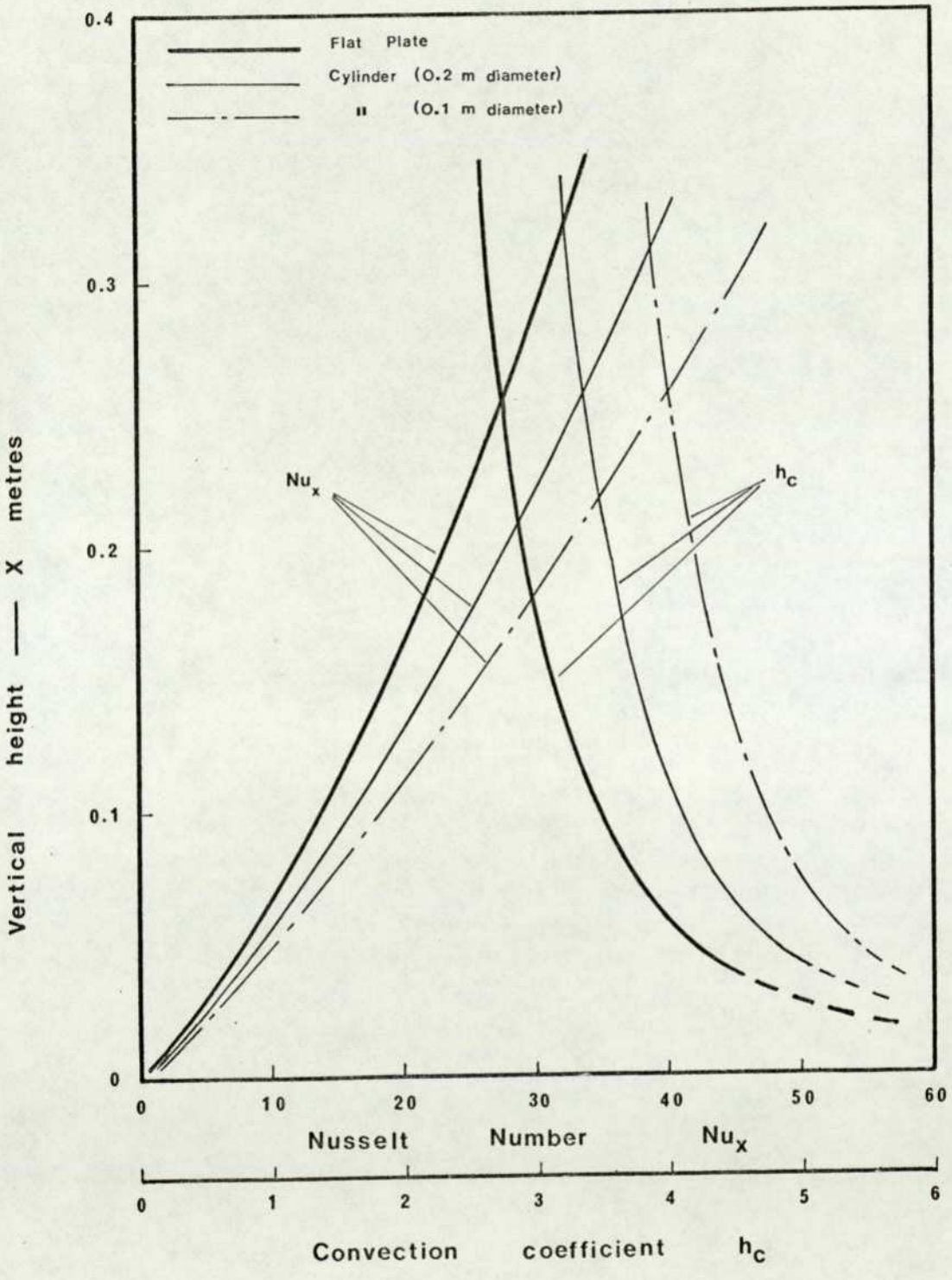


Fig. 4 Variation of the local convection coefficient h_c and Nusselt number on an isothermally heated vertical cylinder and flat plate



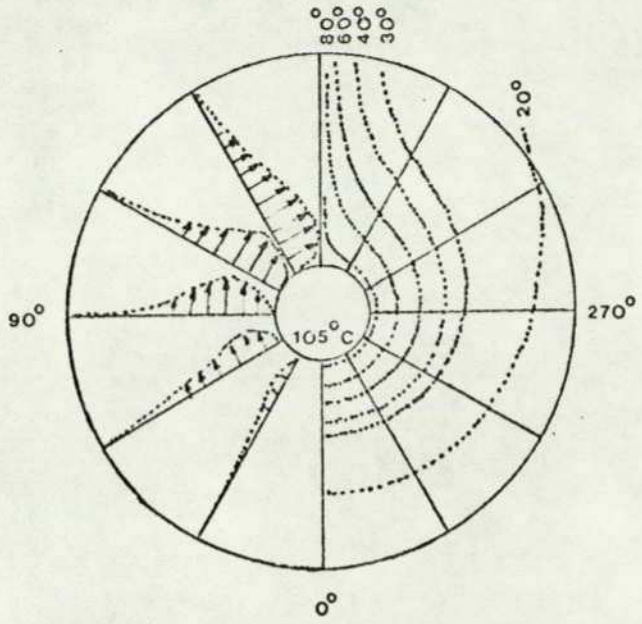
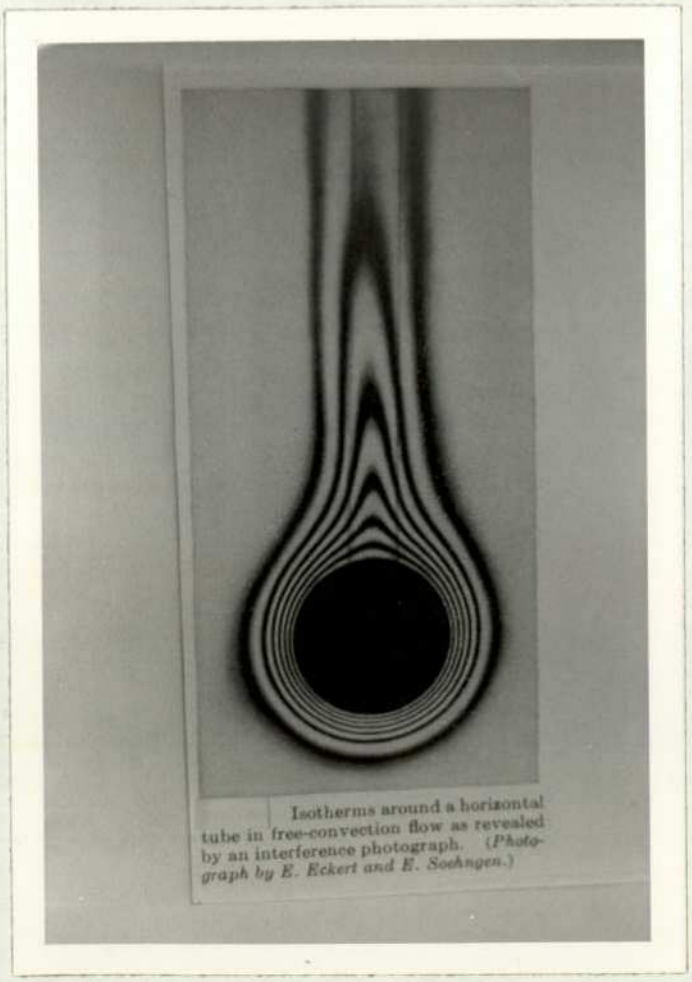


Fig. 5 Velocity profiles and isotherms around a heated horizontal cylinder in free convection (measurements by Jodlbauer (36), Photograph by Eckert and Soehngen (37))



Isotherms around a horizontal tube in free-convection flow as revealed by an interference photograph. (*Photograph by E. Eckert and E. Soehngen.*)



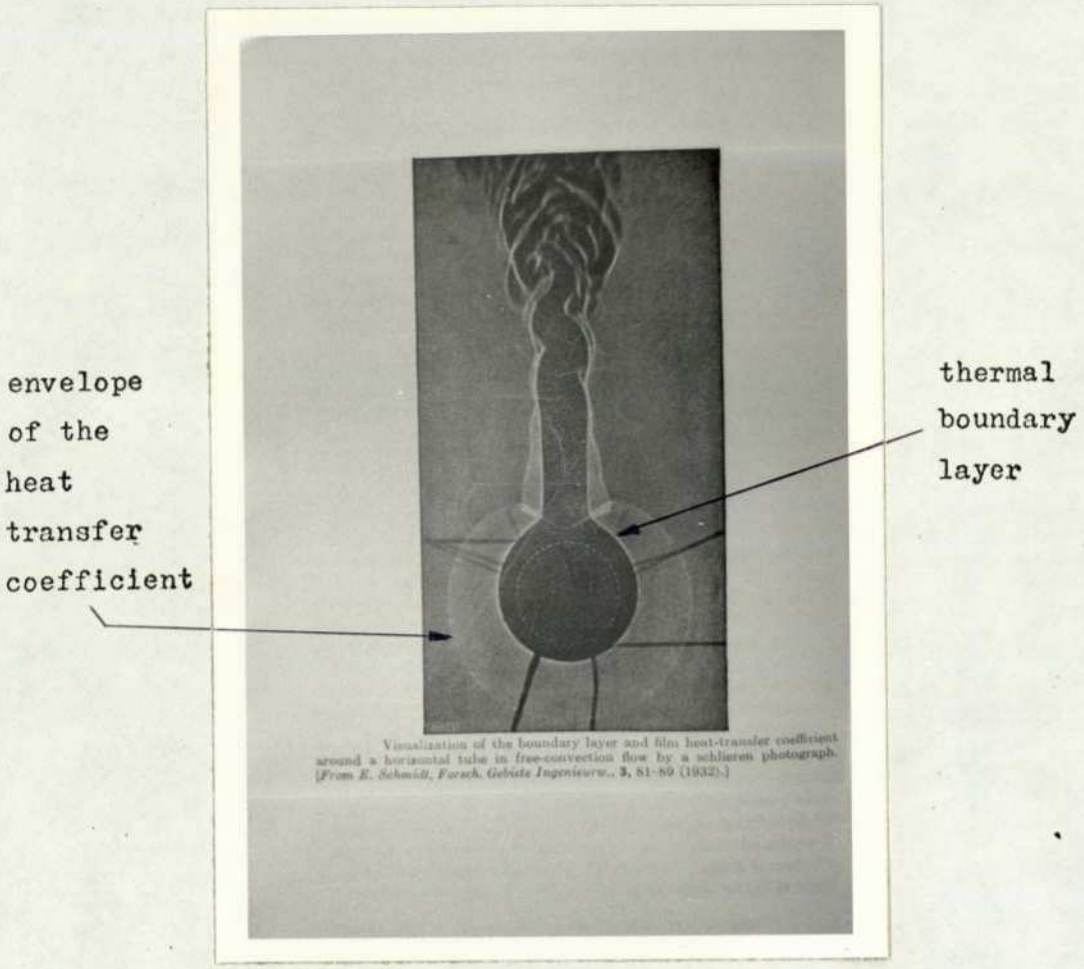


Fig. 6 Schlieren photograph of free convection around a heated horizontal cylinder (Schmidt (38))

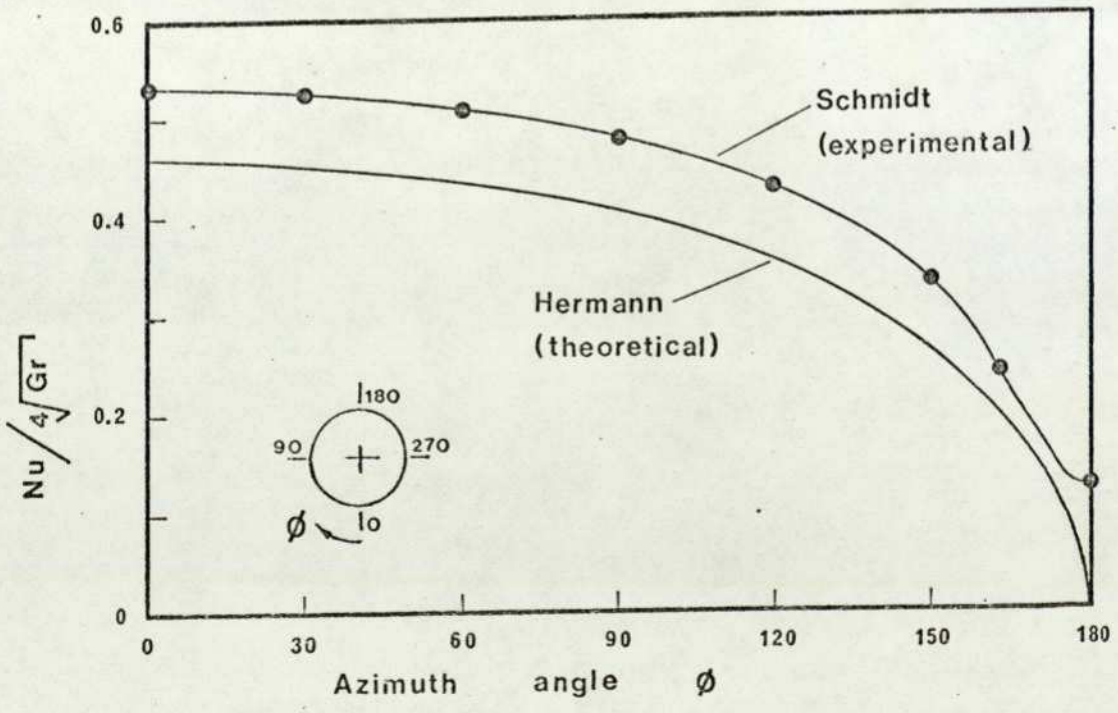


Fig. 7 Theoretical and experimental results for free convection heat loss around a heated horizontal cylinder



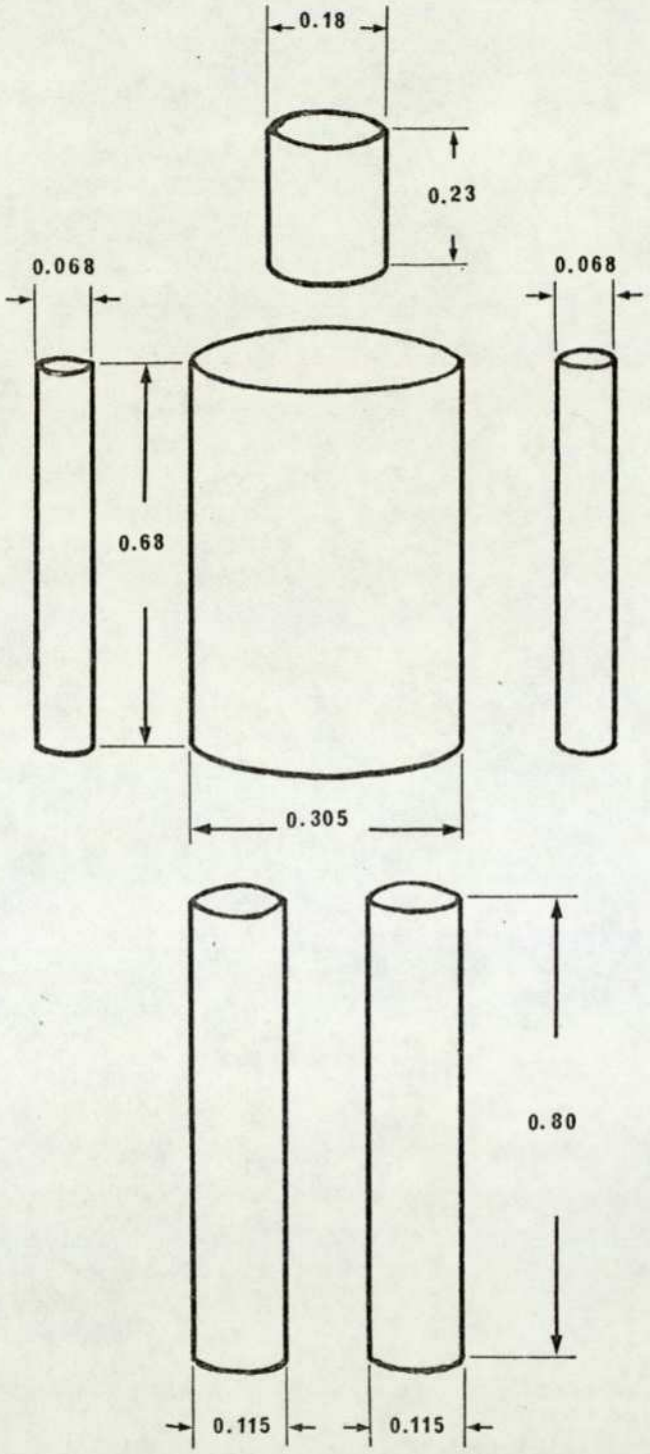


Fig. 8 Dimensions of model in metres (theoretical)

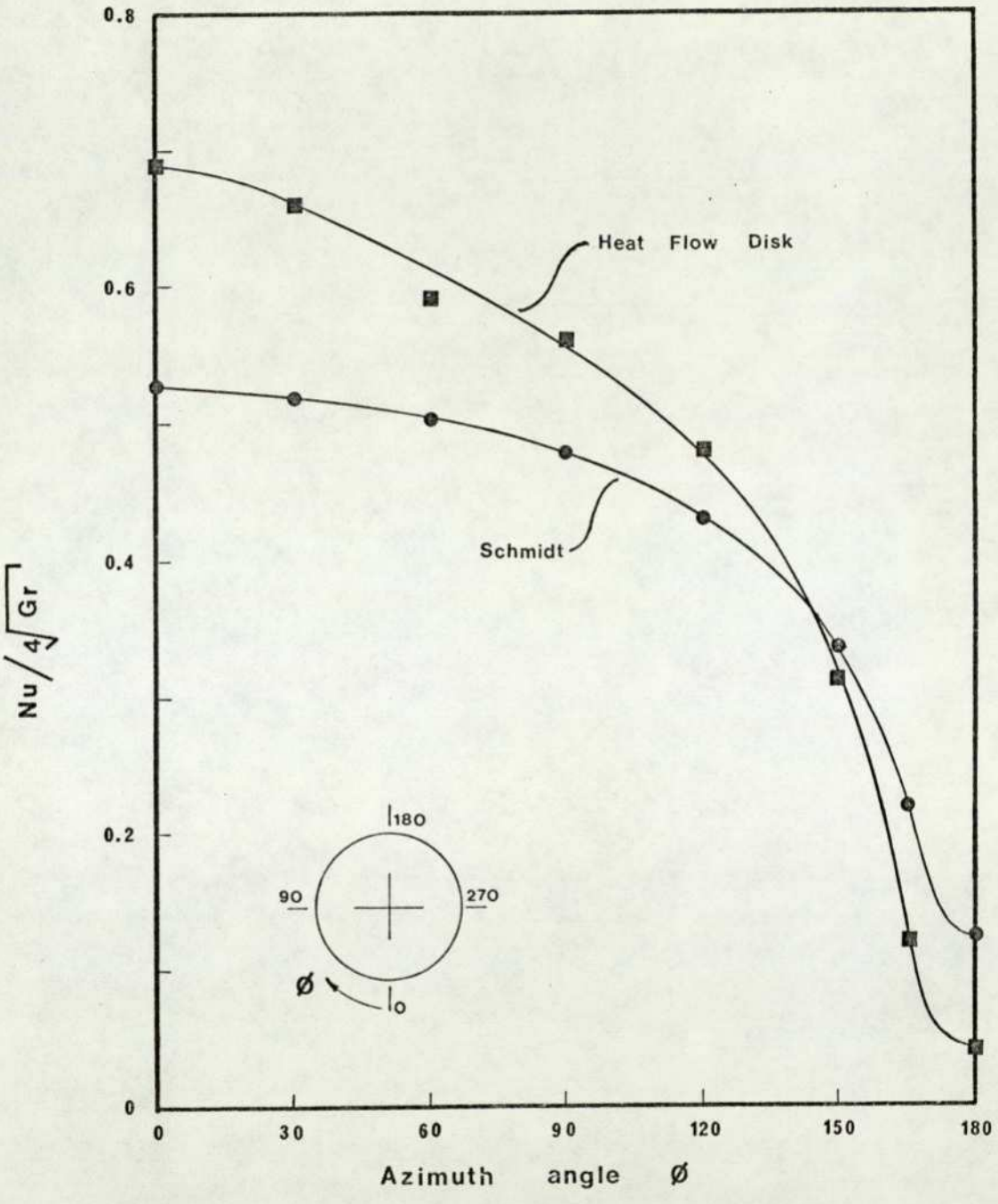


Fig. 9 Measurement of the convection heat loss around a heated horizontal cylinder using a heat flow disk

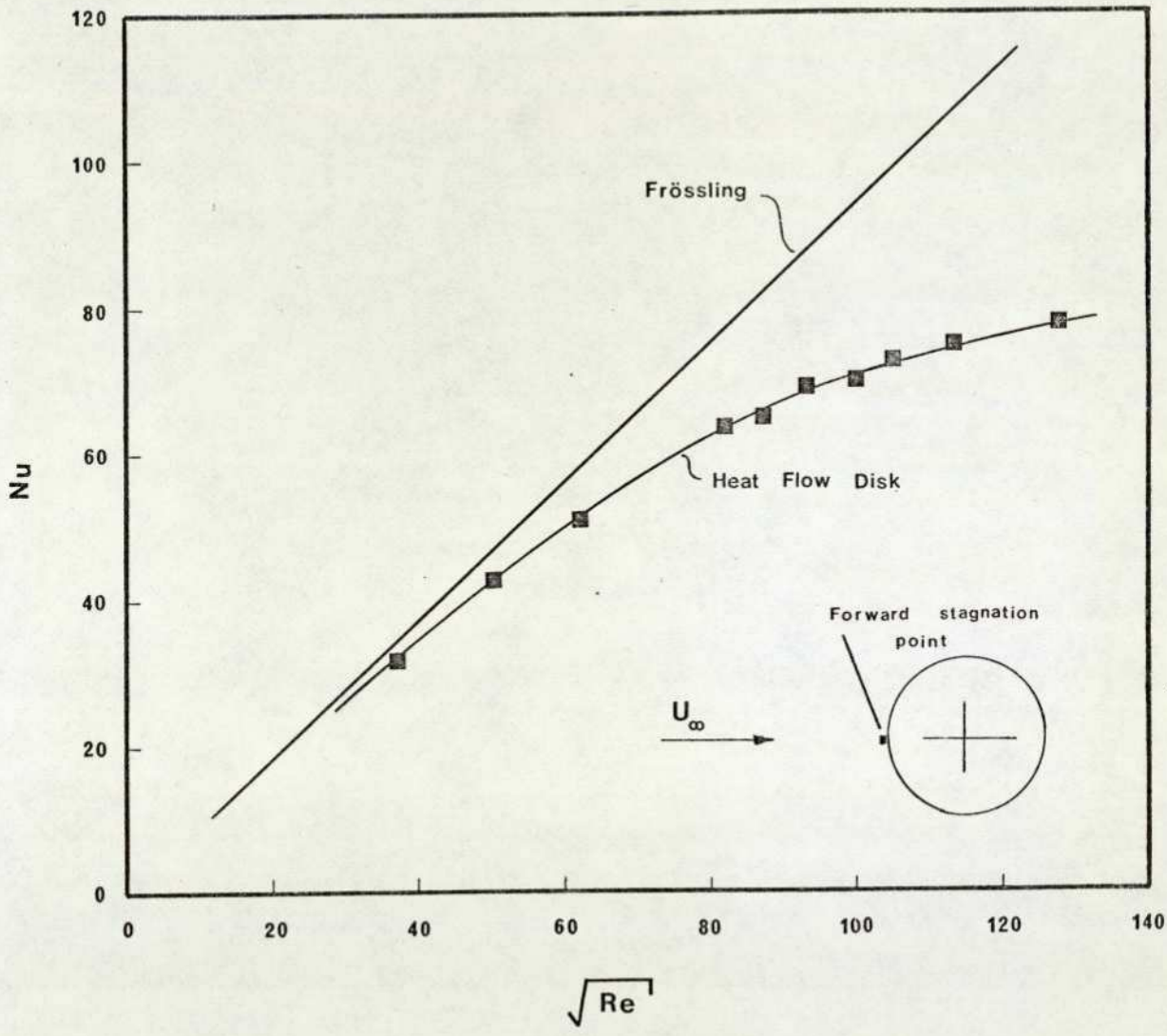


Fig. 10 Measurements of the forced convective heat loss from the forward stagnation point on a heated cylinder

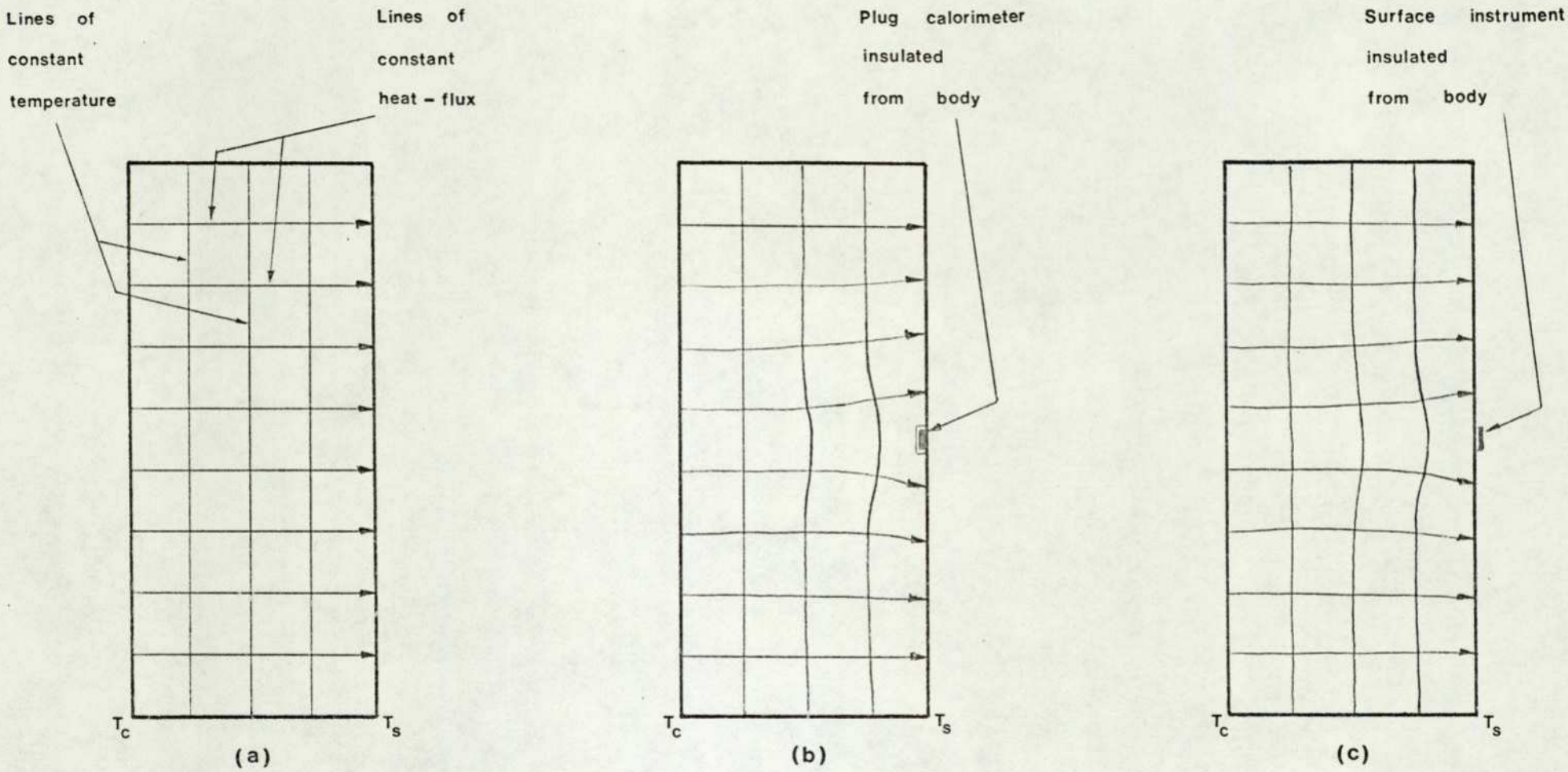


Fig. 11 Orthographical construction of the heat flow field in a heated body for three conditions;

(a) a uniform temperature – heat flux field,

(b) temperature – heat flux field behind the plug,

(c) " " " " " " surface instrument.

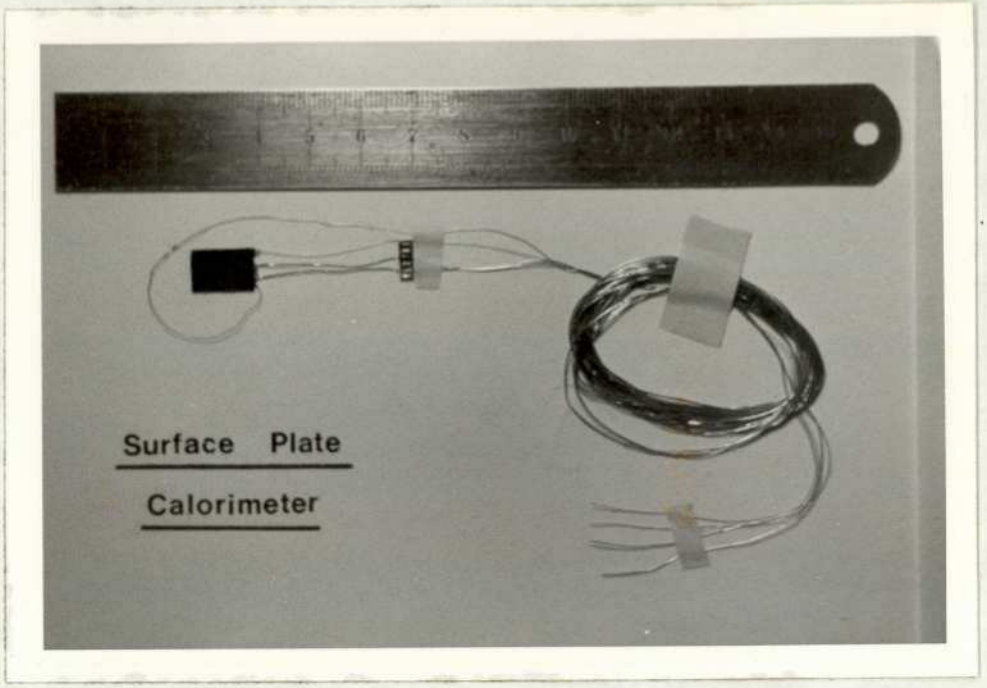


Fig. 12 Typical size of a Surface Plate Calorimeter.
($12 \times 8 \times 0.05$ mm^3)



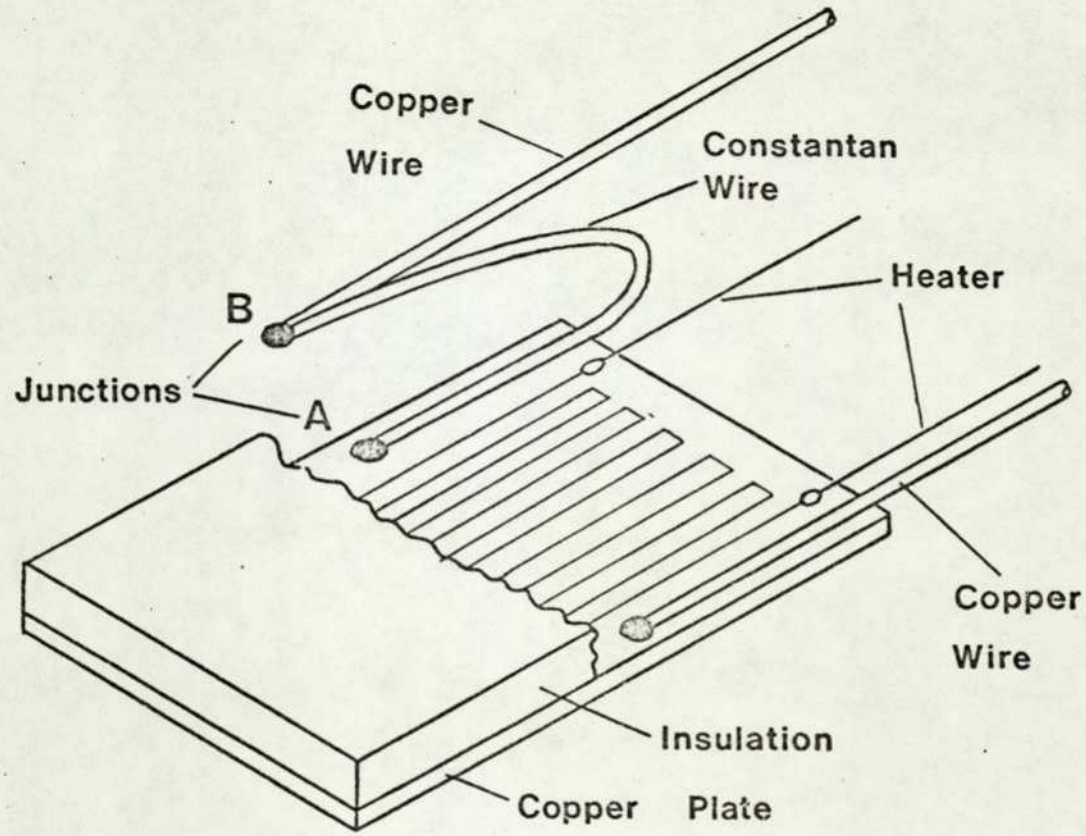


Fig 13 Diagram of the Surface Plate Calorimeter

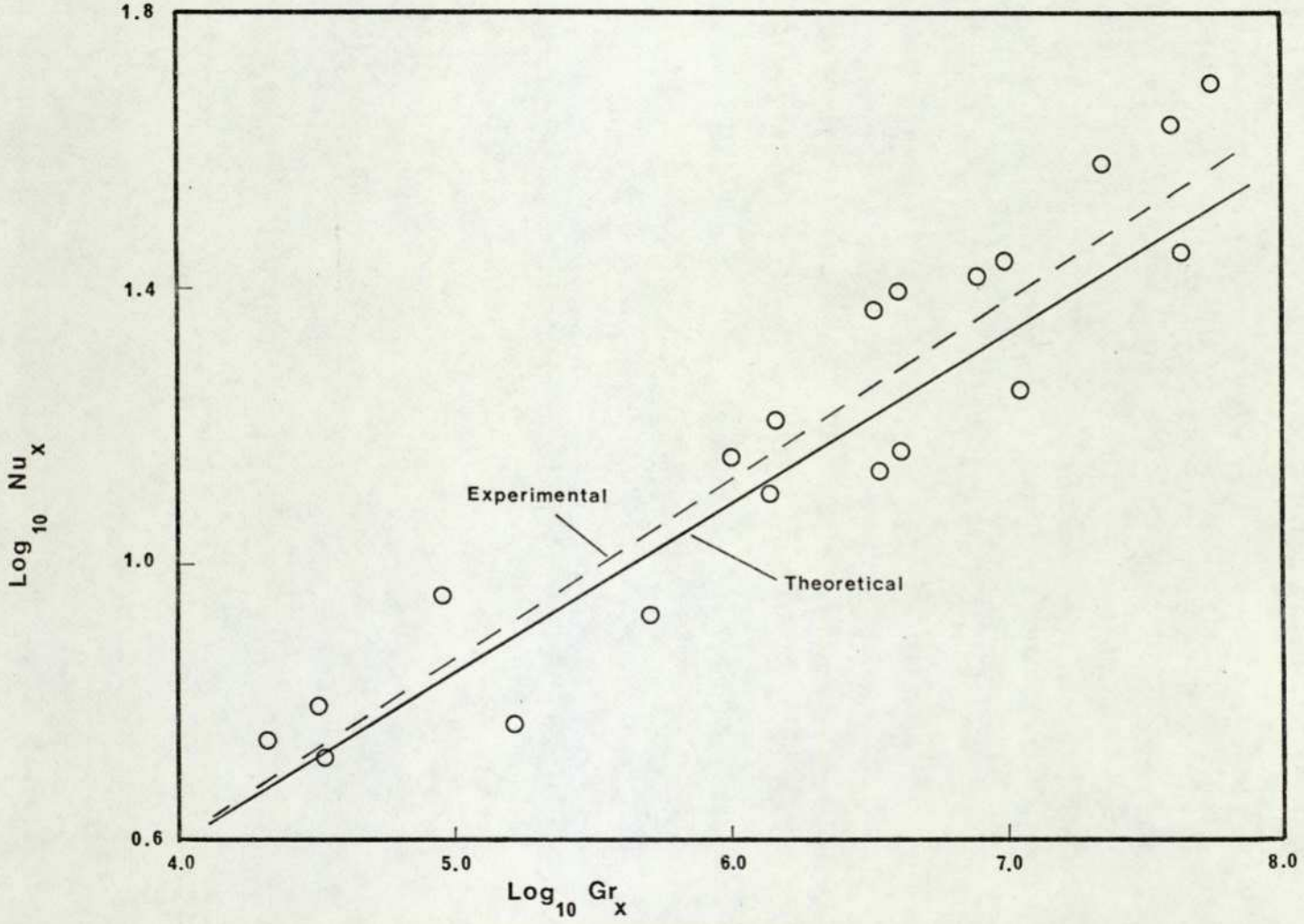


Fig. 14 Natural convective heat loss from a heated vertical cylinder

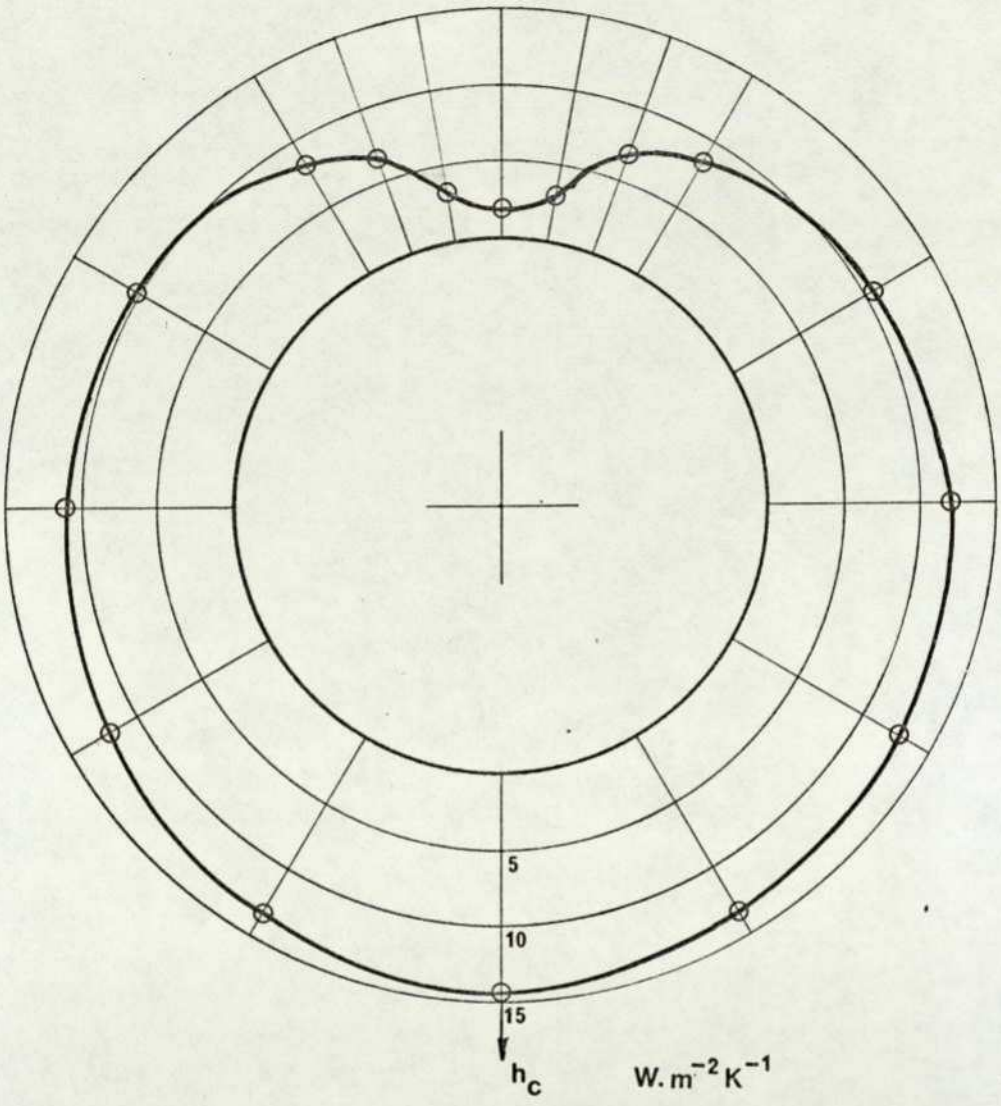


Fig. 15 Local convection heat transfer coefficient h_c around a heated horizontal cylinder.

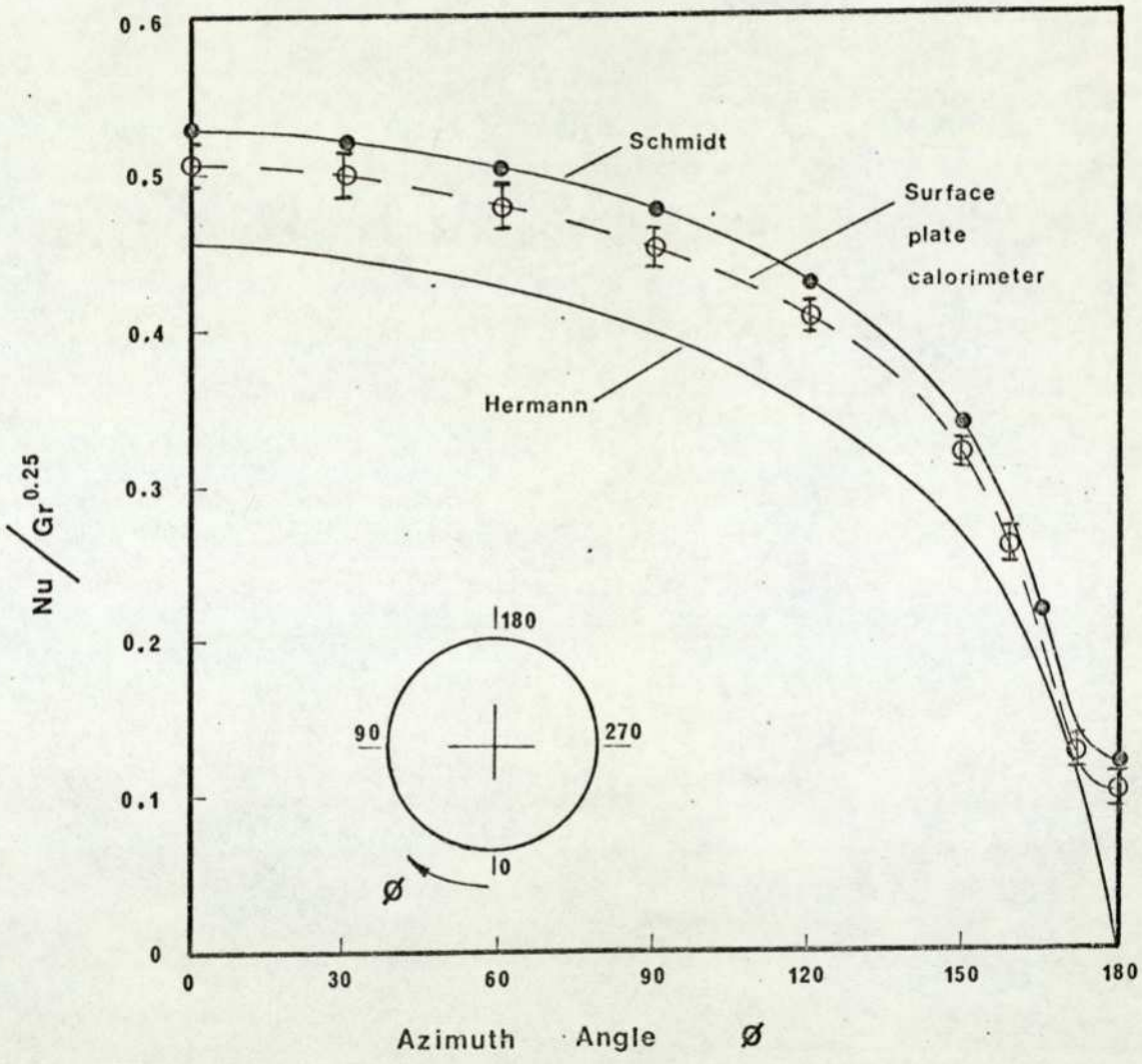


Fig. 16 Natural convection heat transfer from a horizontal cylinder.

{ Bars indicate the range of the 'standard error of the mean'
i.e. $\left(\text{mean value} \pm \frac{\text{st. dv.}}{\sqrt{n}} \right)$ where n = number of
observations, in this case n = 20. }

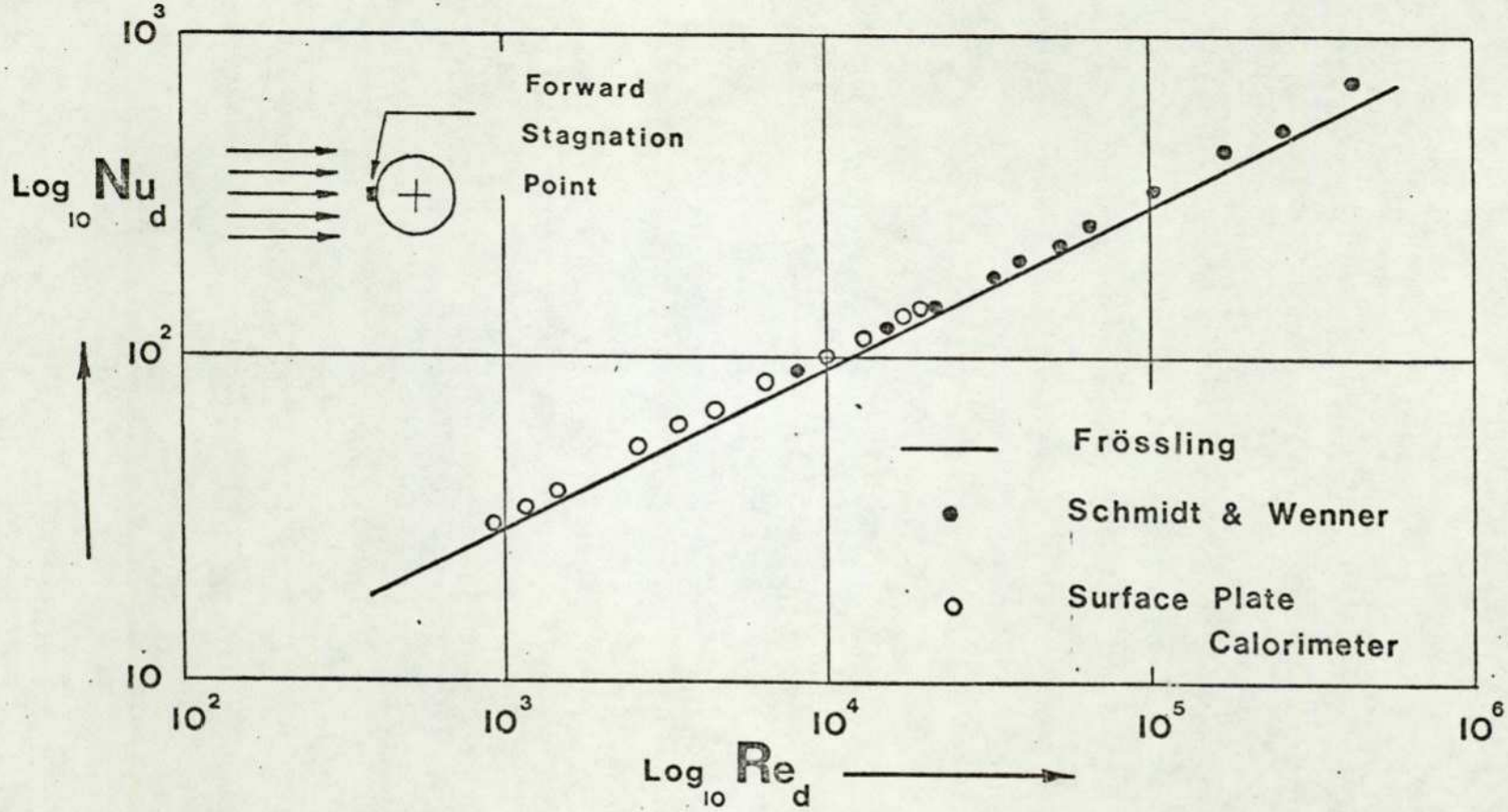


Fig. 17 Forced Convection Heat Transfer

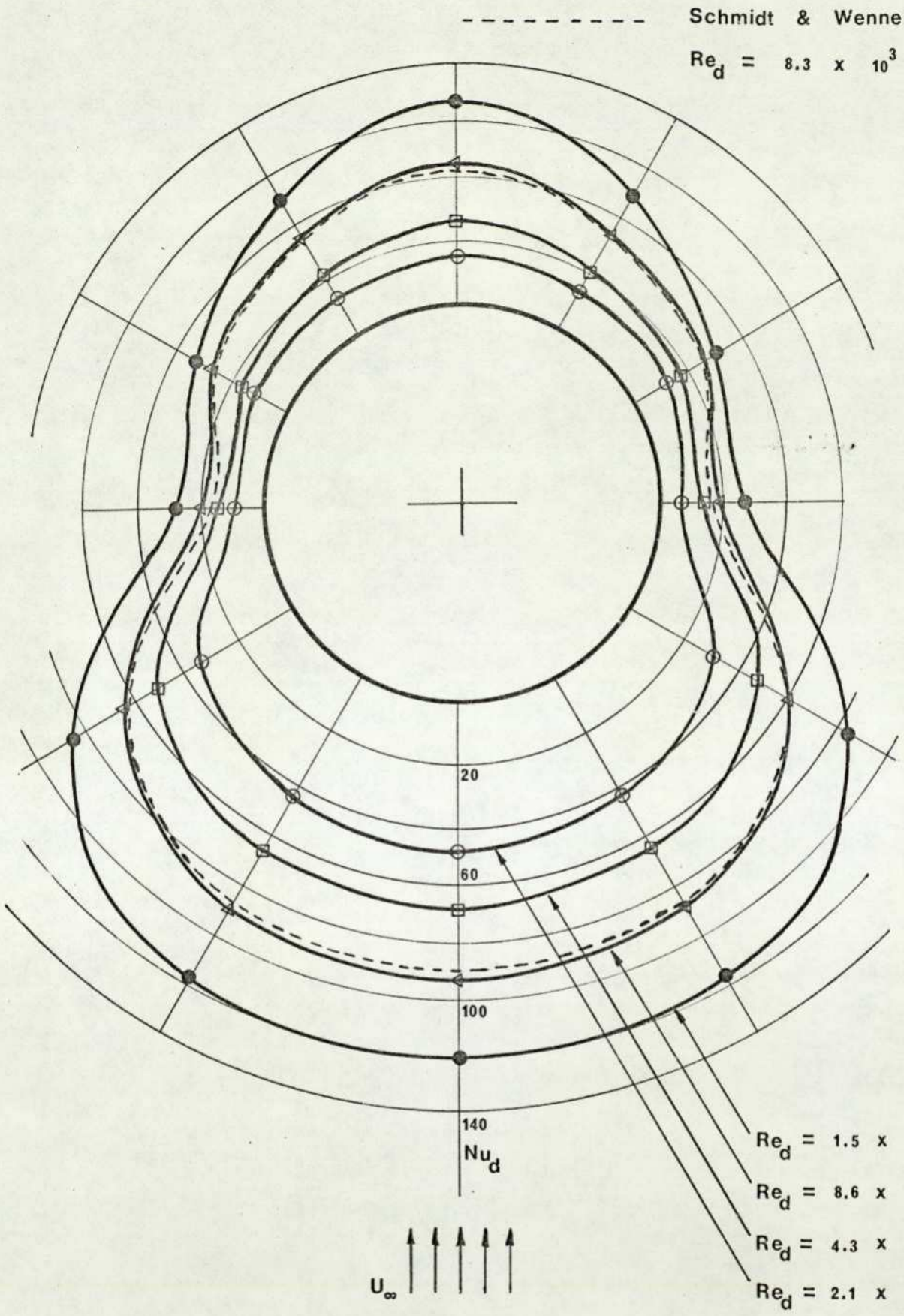


Fig. 18 Forced convection heat transfer distribution around a heated vertical cylinder.

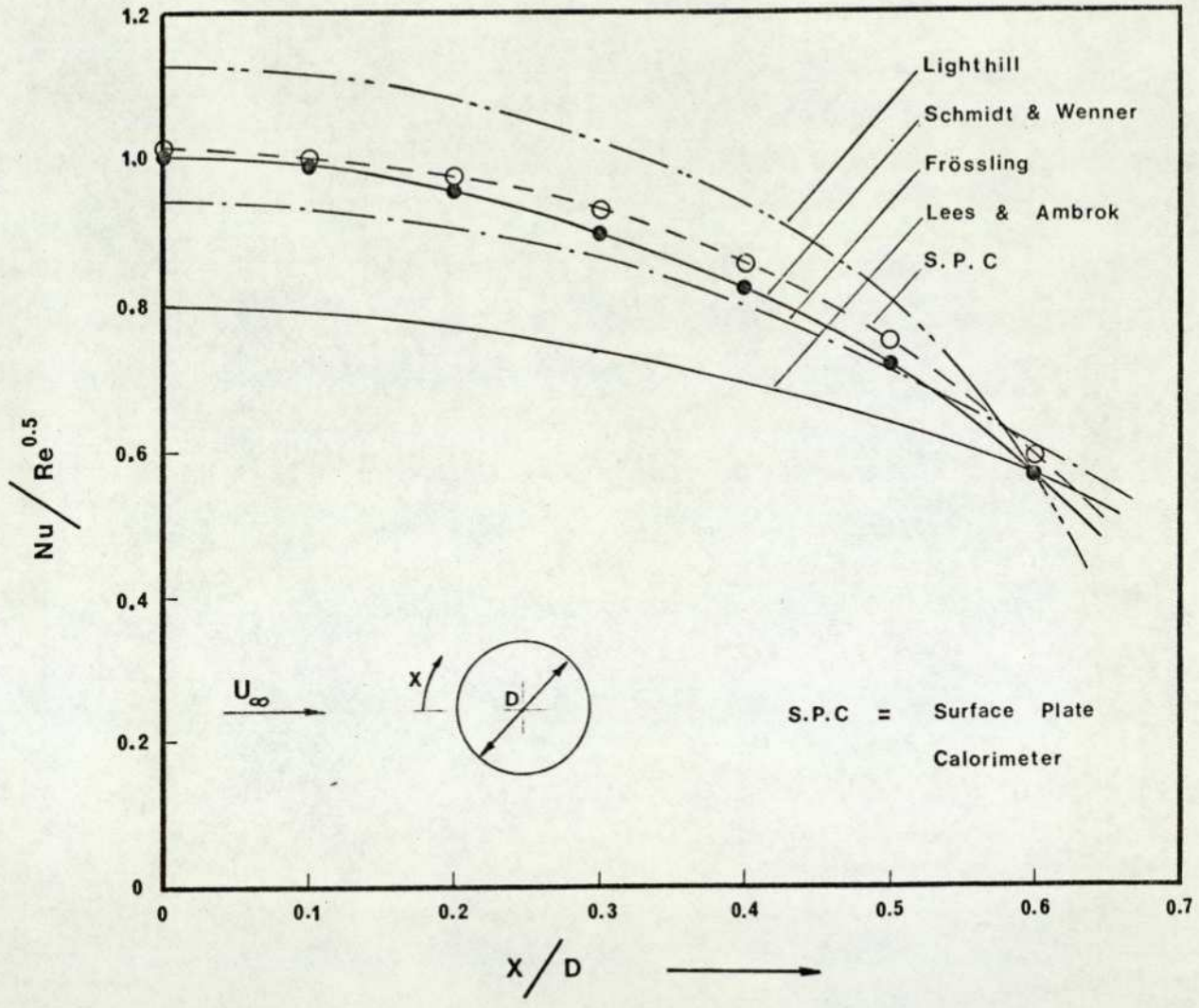


Fig. 19 $Nu/Re^{0.5}$ plotted against X/D for a circular cylinder in forced convection as predicted by different methods.

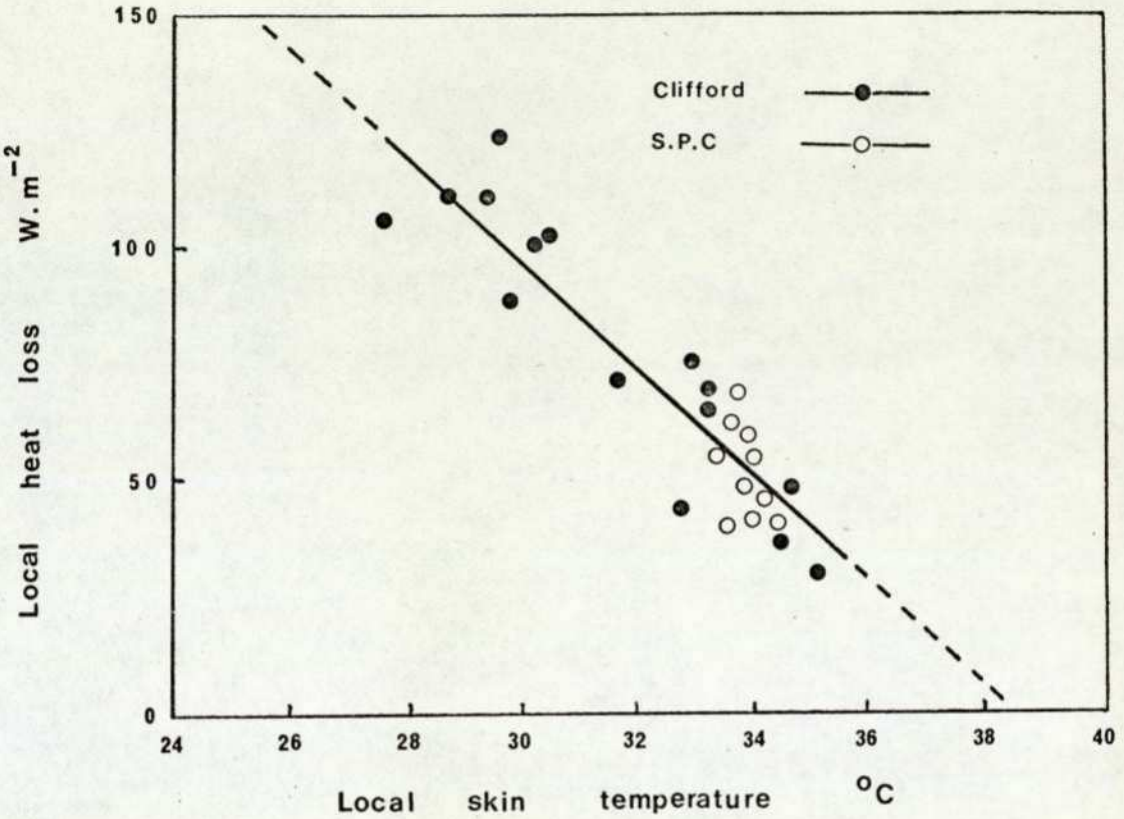


Fig. 20 Local heat loss by convection and radiation from the lower forearm of a subject. Present results compared with those of Clifford, the continuous line being the regression line given by Clifford.

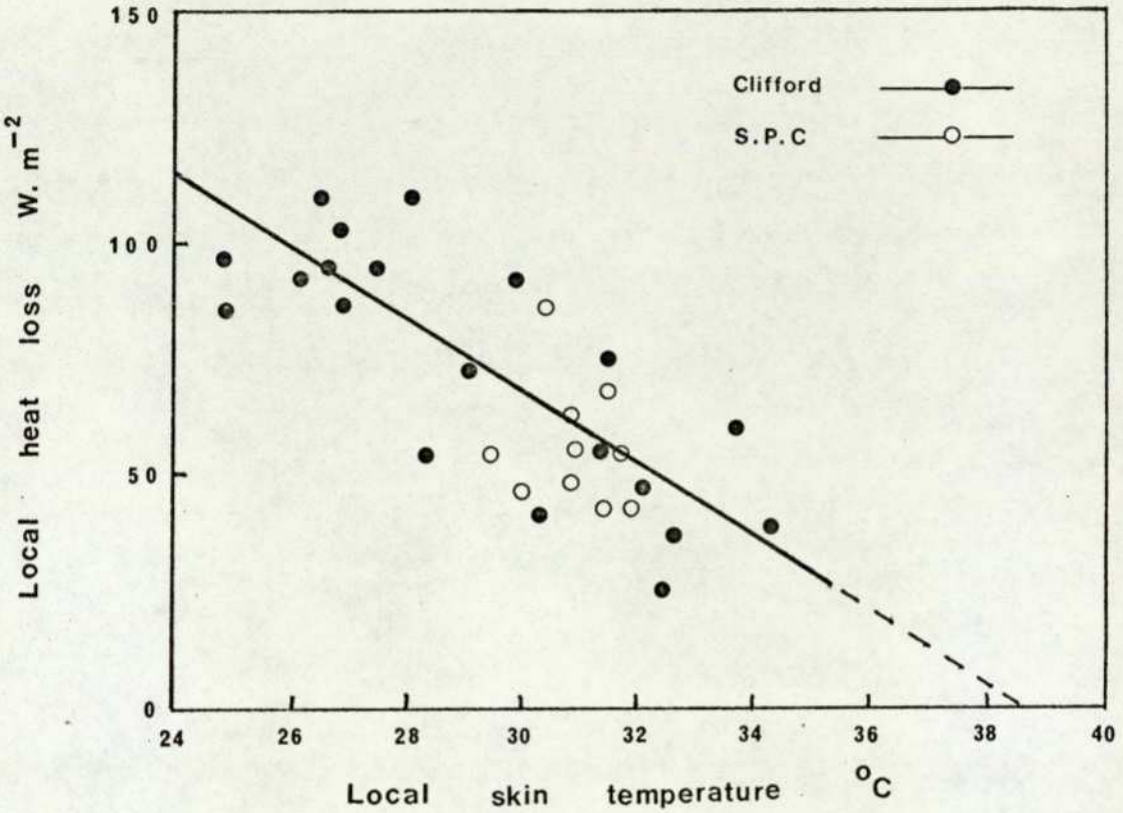


Fig. 21 Local heat loss by convection and radiation from the leg of a subject. Present results compared with those of Clifford, the continuous line being the regression line given by Clifford.

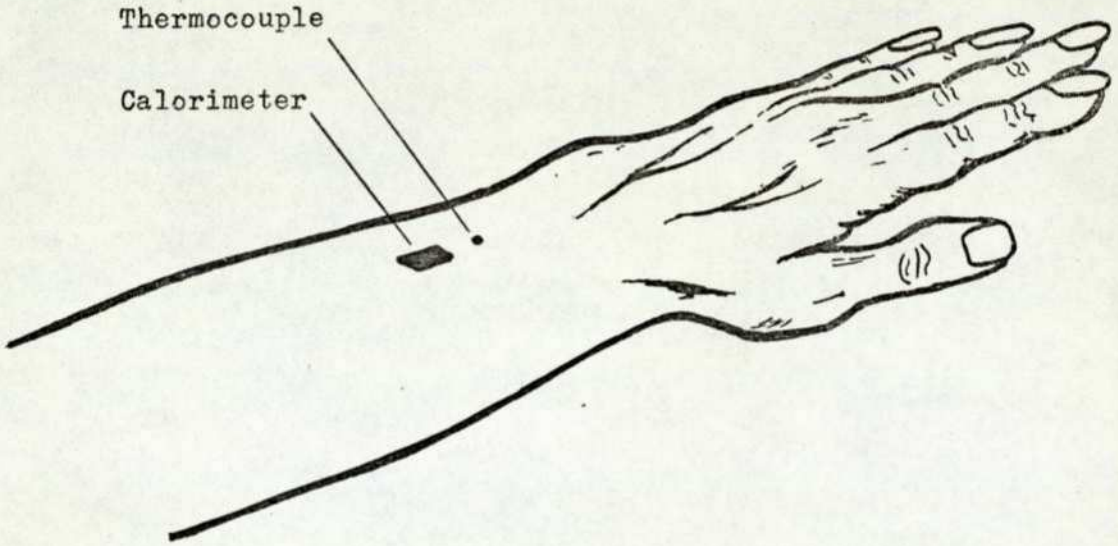


Fig. 22 Position of the calorimeter and thermocouple on the left forearm of a subject.

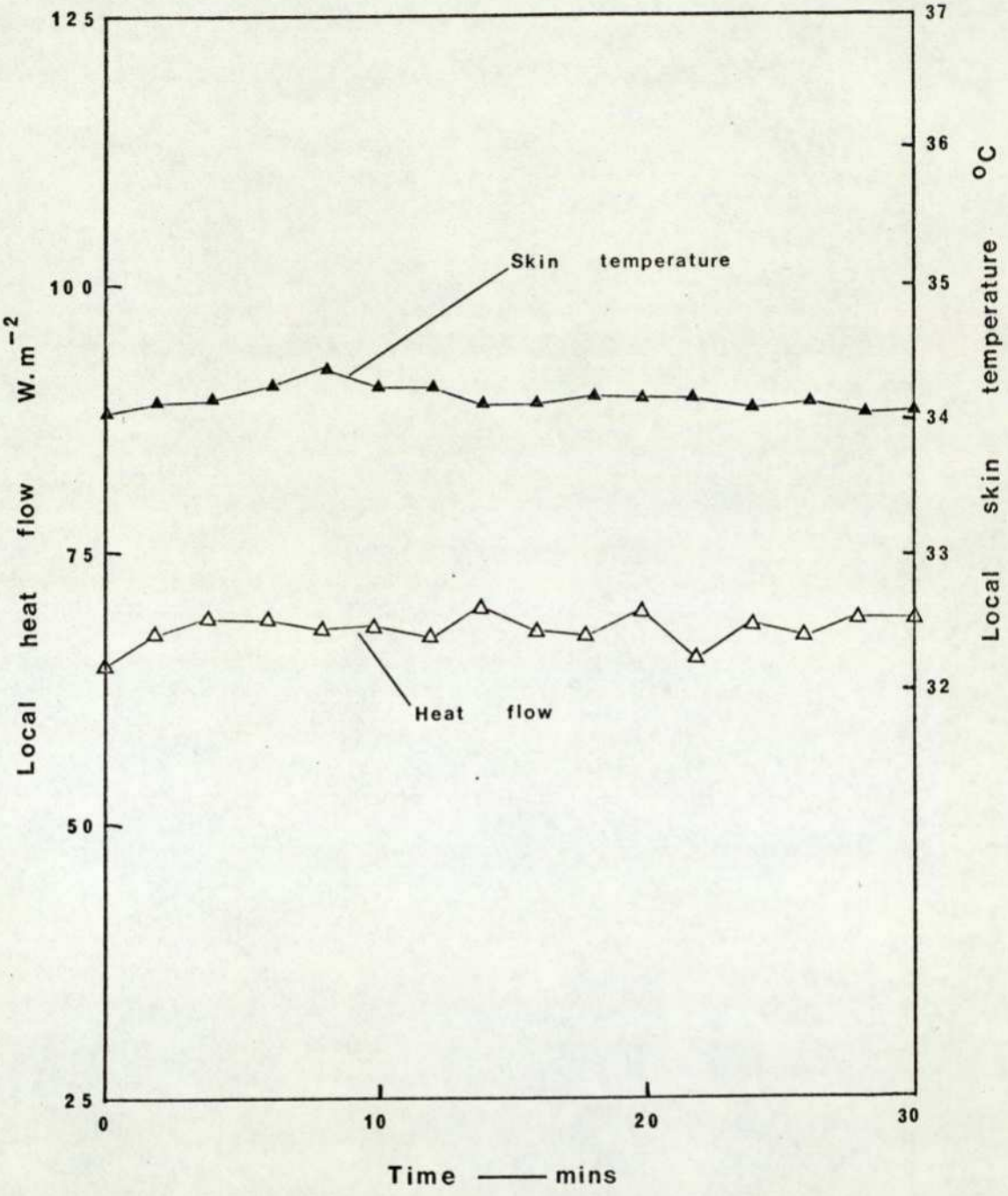


Fig. 23 Plot of the local convection and radiation heat loss and skin temperature from the forearm of a subject.
(The arm was kept still in a horizontal position)

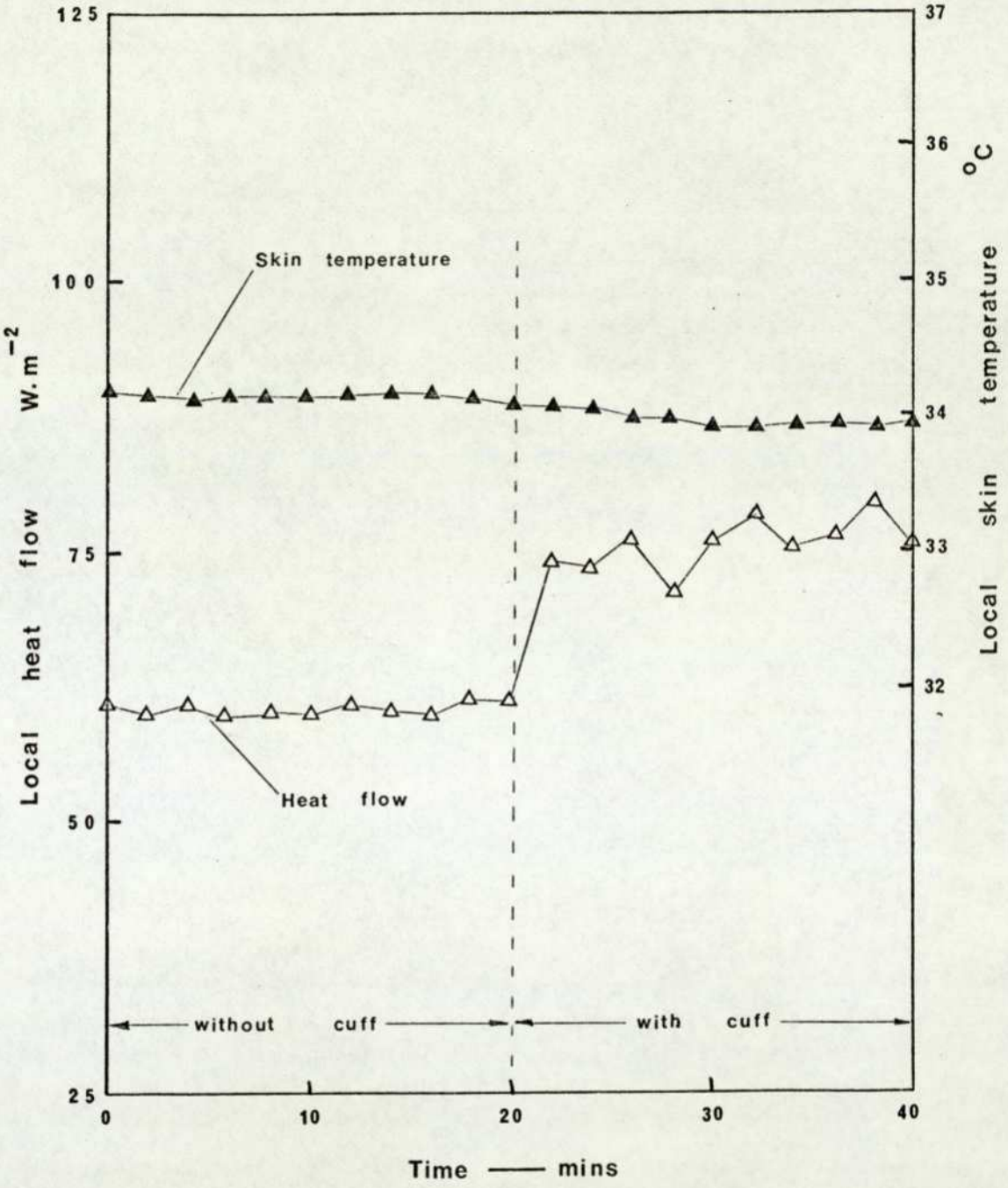


Fig. 24 Variation of the local heat loss and skin temperature from the forearm of a subject. The arm was suspended vertically and a cuff was placed around the wrist at t = 20 minutes.

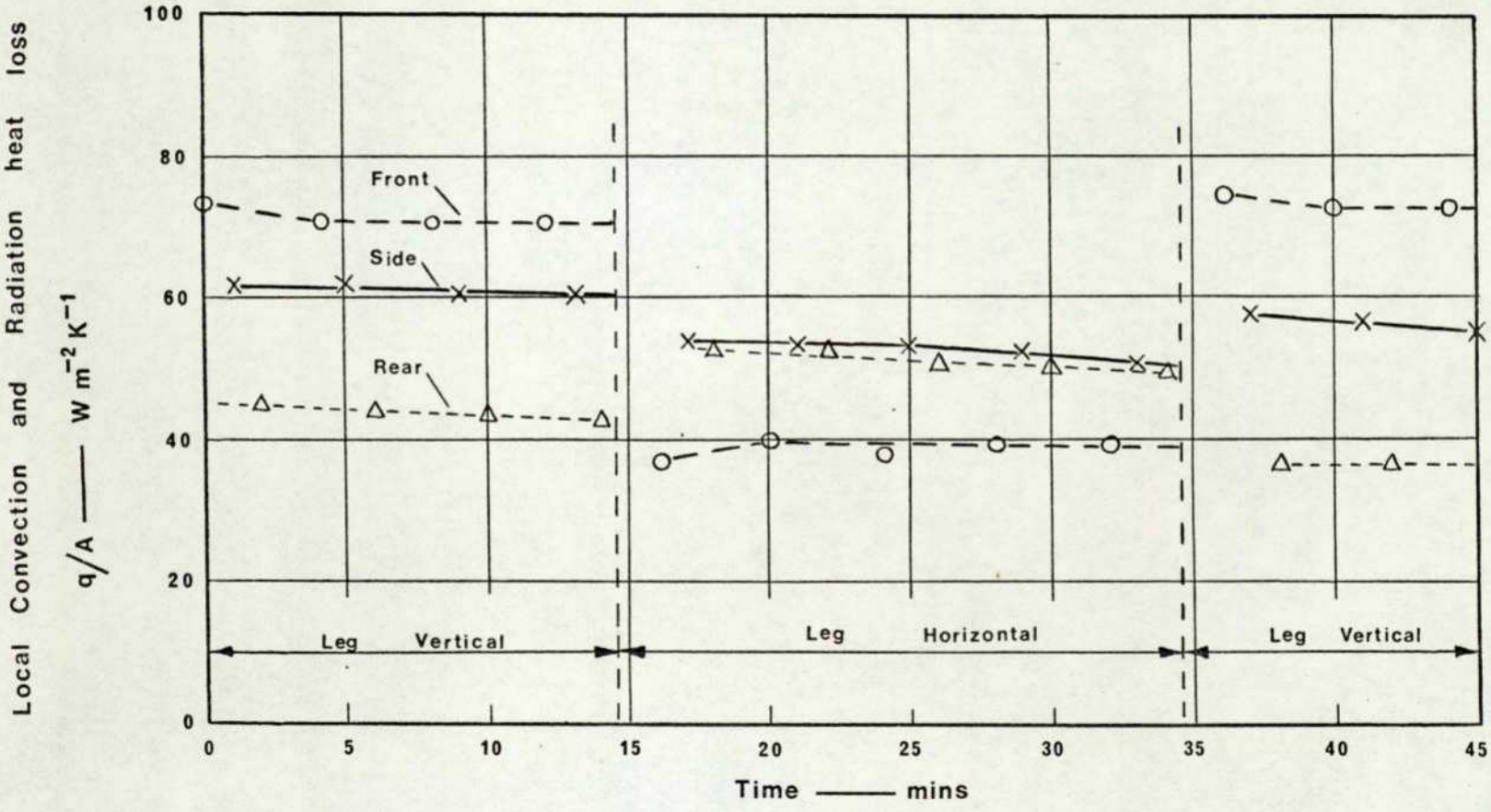
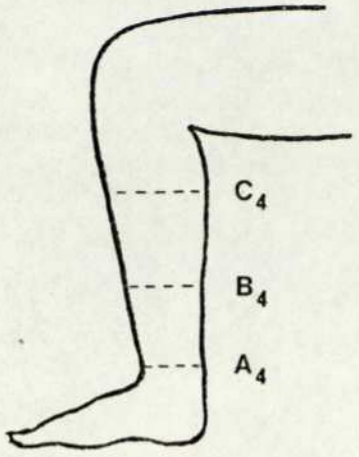


Fig. 25 Variation of the heat loss around the leg with posture.



Position of 3 calorimeters on the right leg.

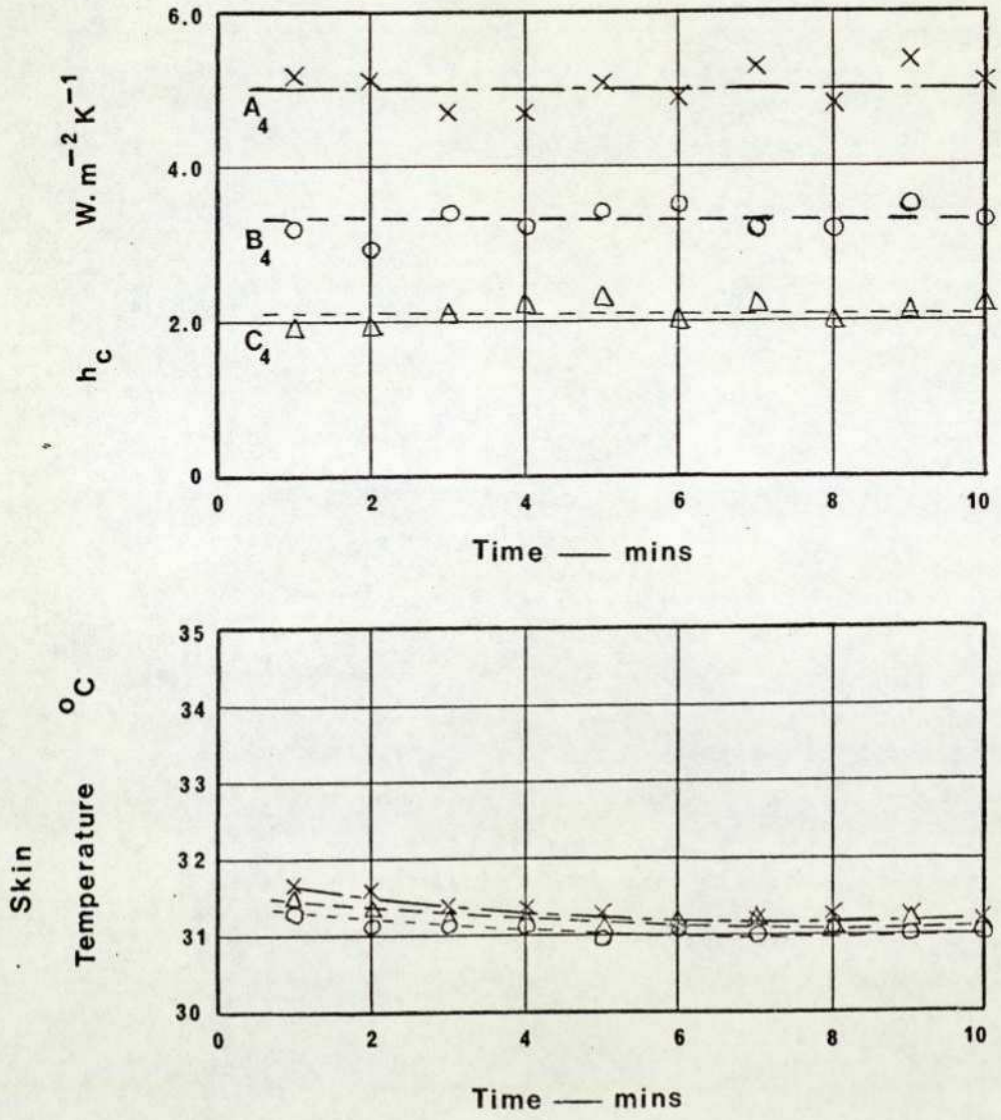


Fig. 26 Variation in the local convective heat loss and skin temperature from the rear of a leg in the vertical posture.

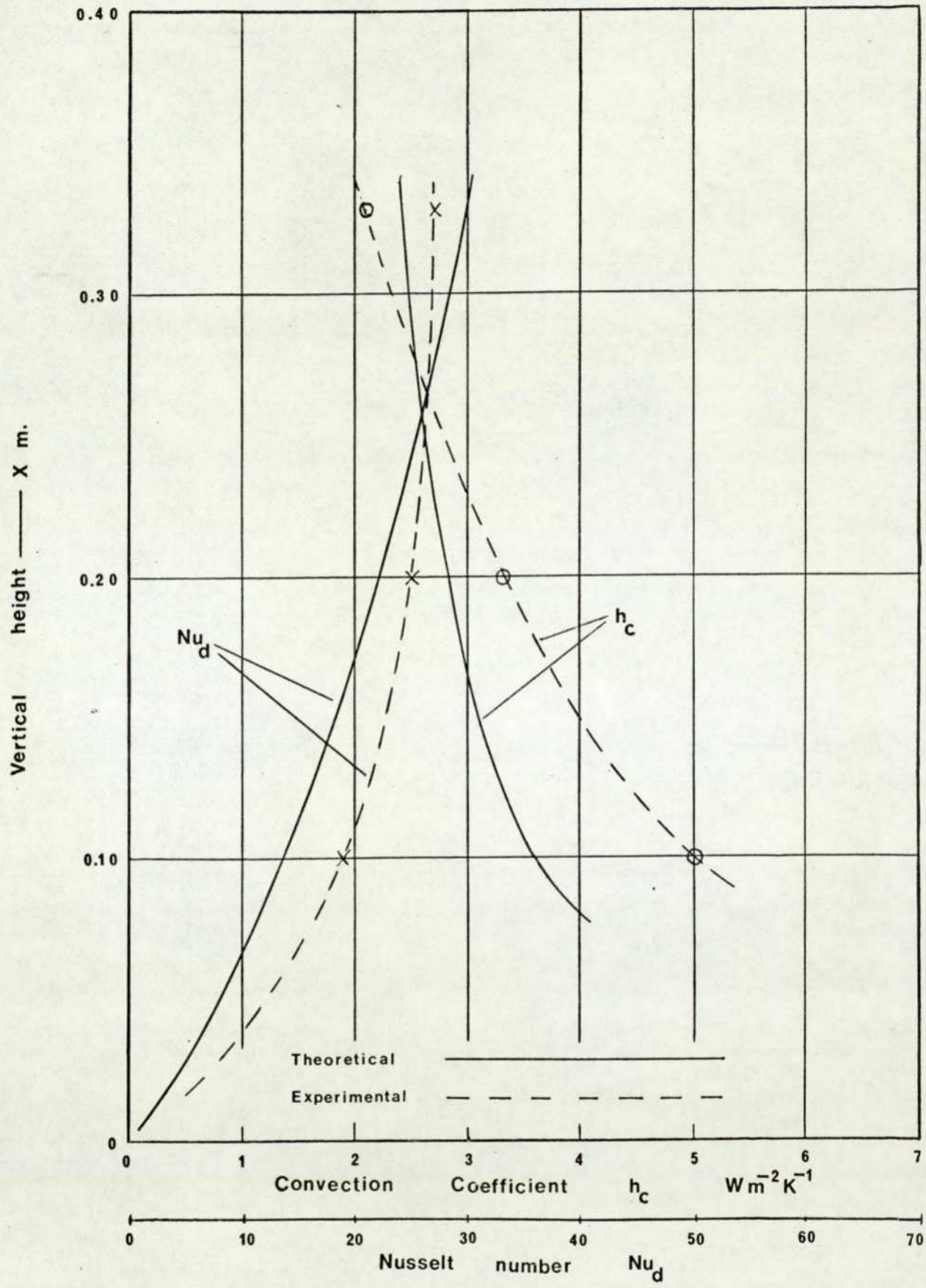


Fig. 27 Experimental results for the free convective heat loss along the vertical leg of a subject together with the theoretical results for a vertical cylinder.

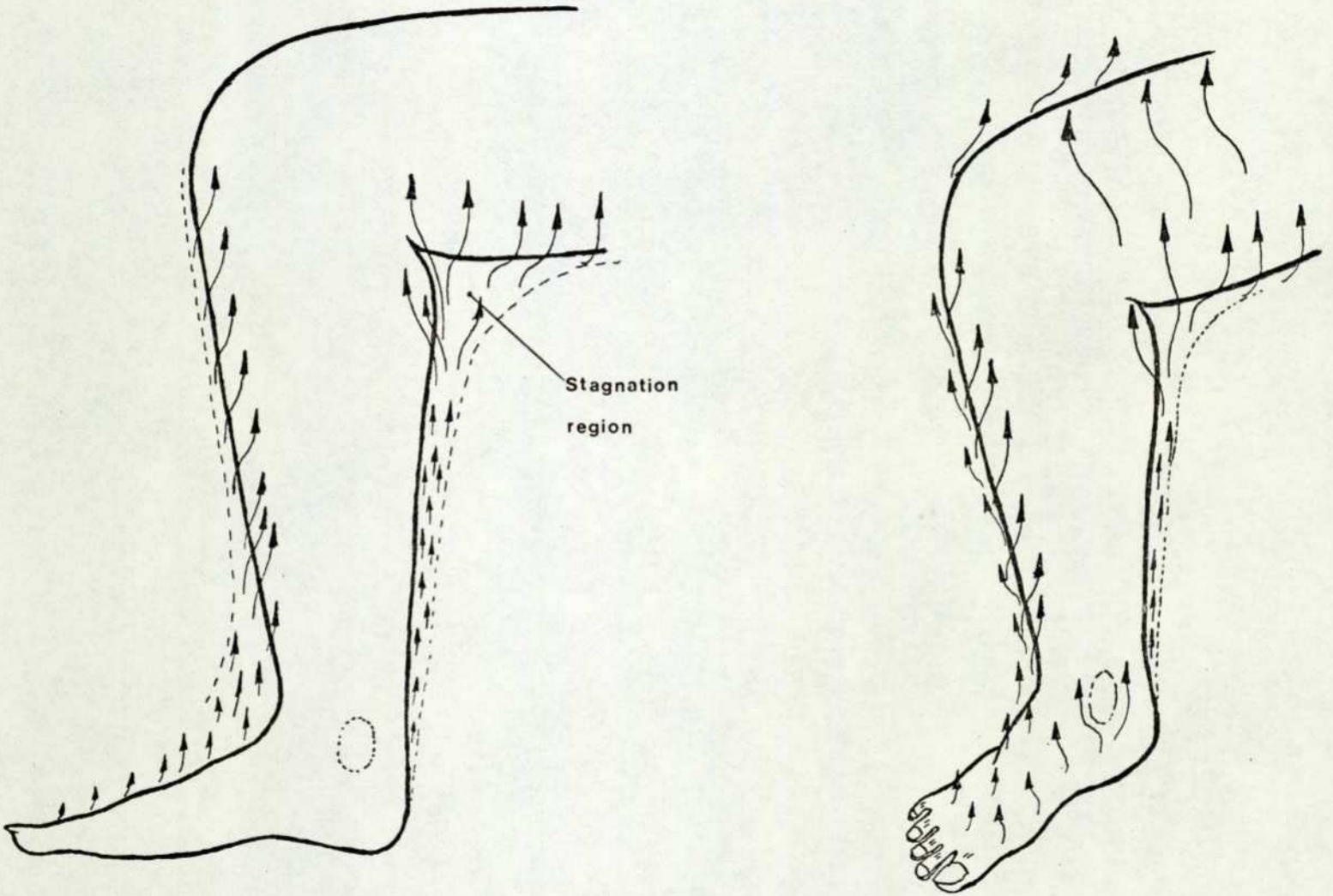


Fig. 28 Free convection flow along the right leg of a sitting subject

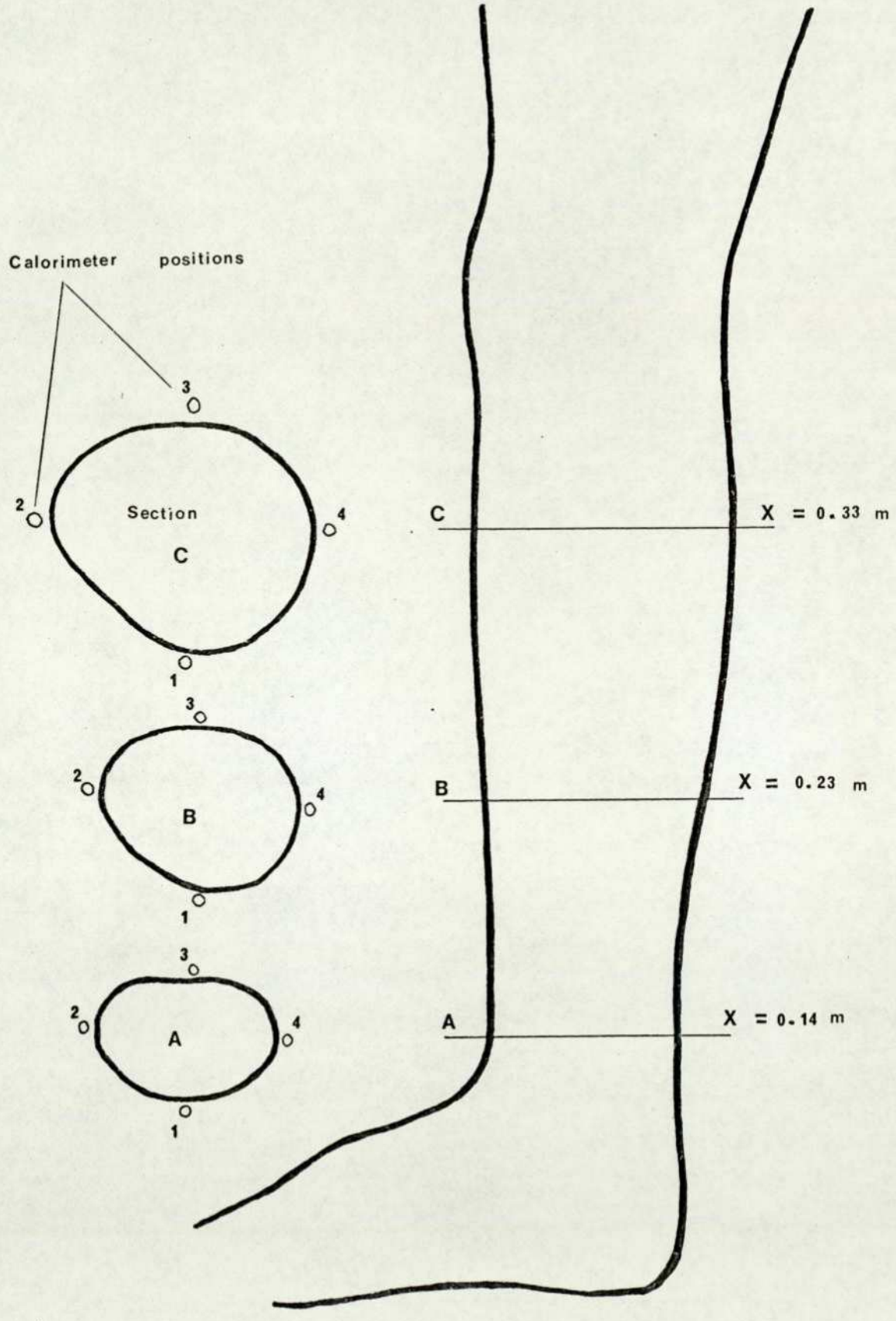


Fig. 29a Positions of 12 calorimeters around the leg of a subject.

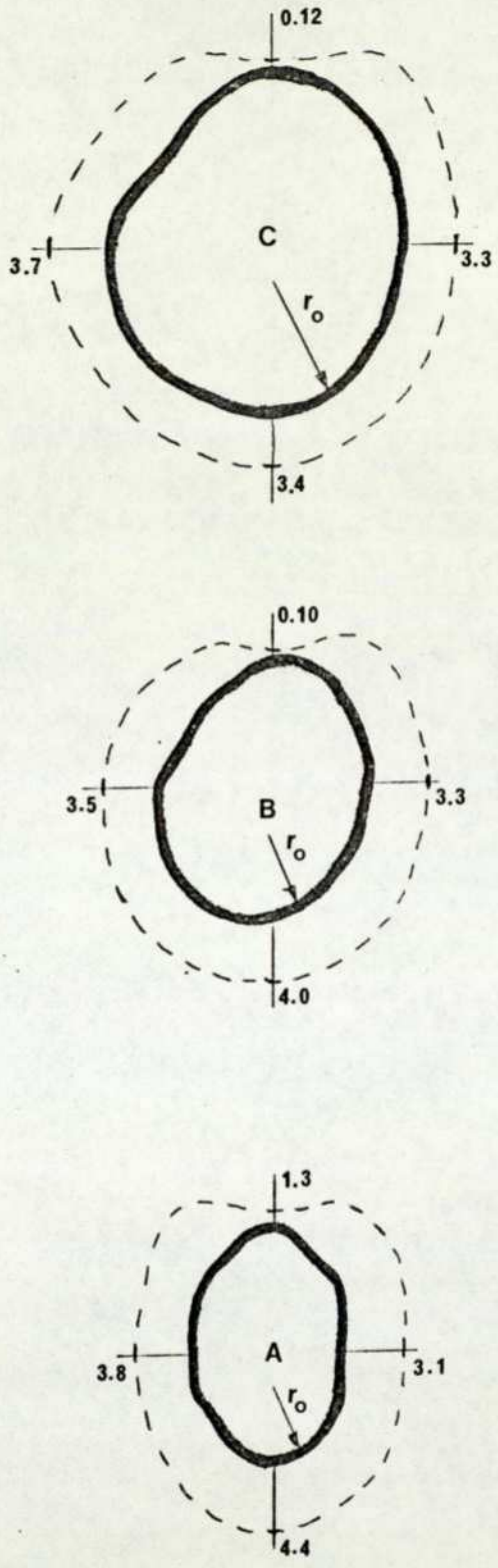


Fig. 29b Free convection heat transfer distribution (h_c W $m^{-2}K^{-1}$) around the horizontal leg of a subject.

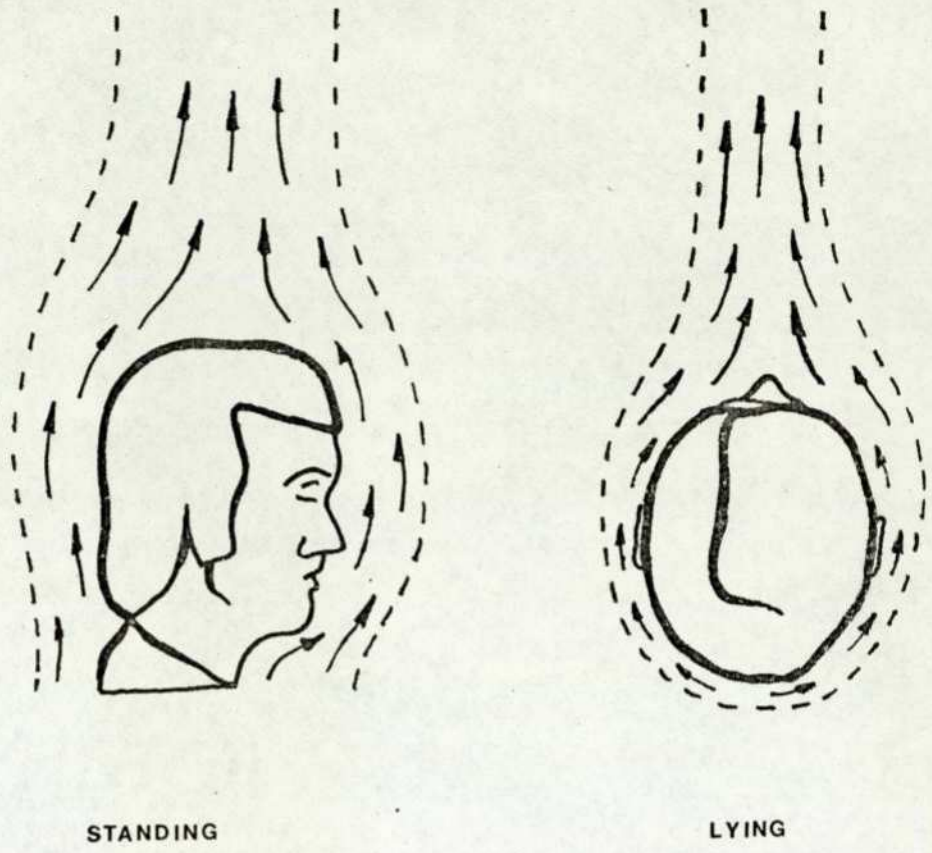


Fig. 30 The shape of the natural convective boundary layer over head of a subject for two postures.

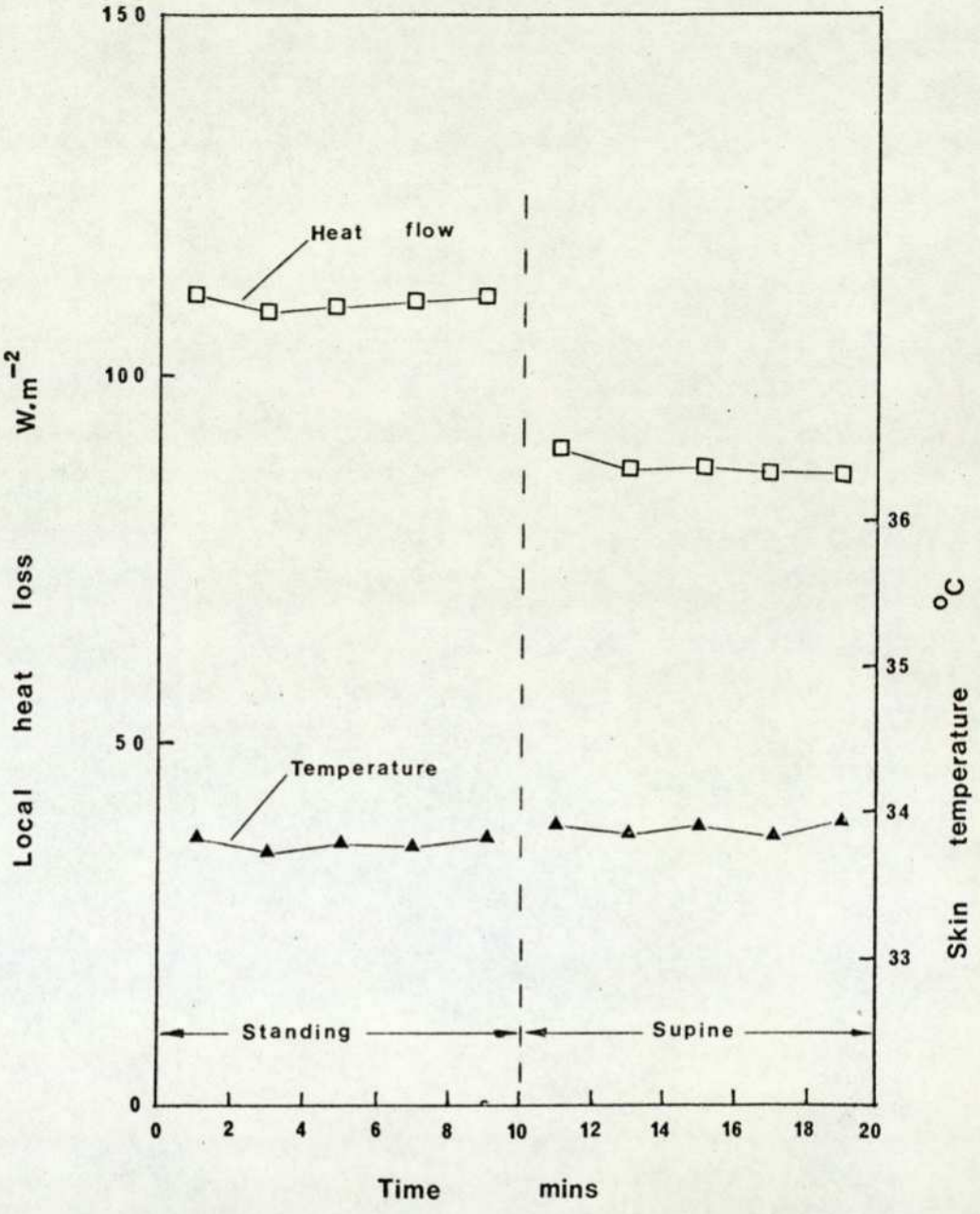


Fig. 31 Local convection and radiation heat loss and skin temperature from the centre of the forehead of a subject in two postures.

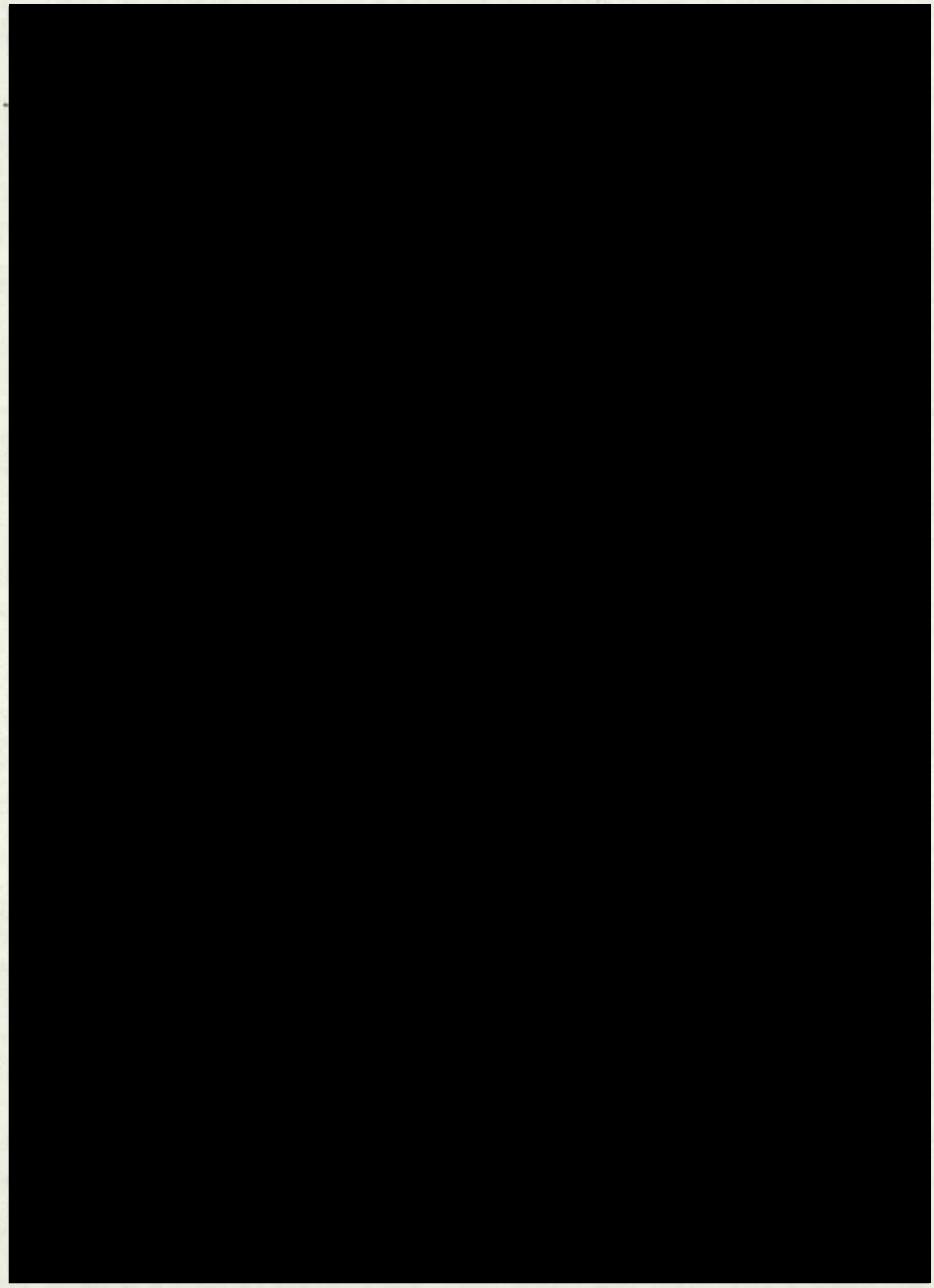


Fig. 32 Three surface plate calorimeters shown attached to the face of a subject (CB).



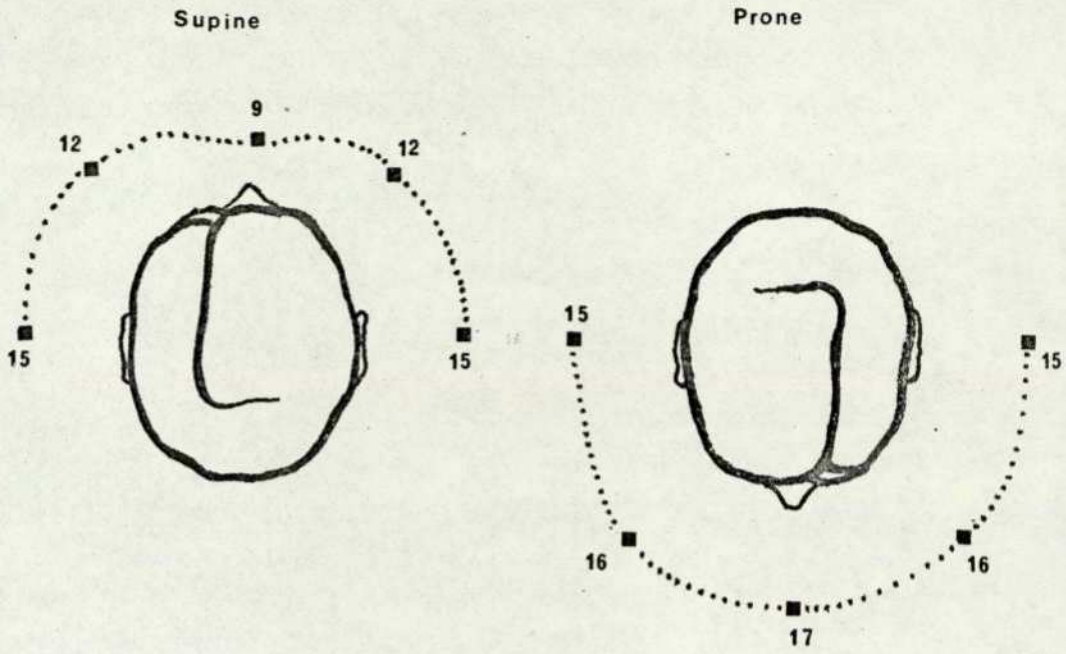


Fig. 33 Local convection and radiation heat loss ($W\ m^{-2}K^{-1}$) from the face of a supine and prone subject with a full head of hair. Skin temperature =33°C, ambient temperature= 23°C.

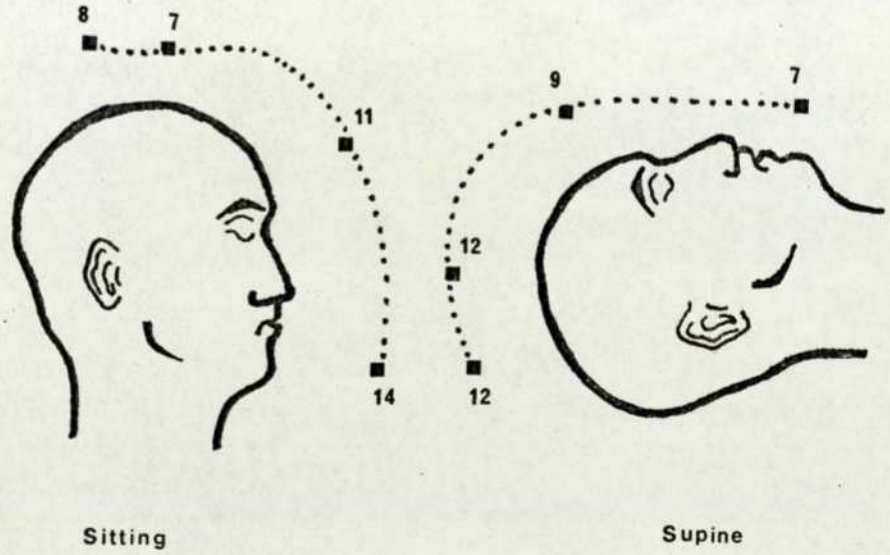


Fig. 34 Local convection and radiation heat loss ($W\ m^{-2}K^{-1}$) from the head of a balding subject in two postures.
Skin temperature = 34°C, ambient temperature = 22°C.

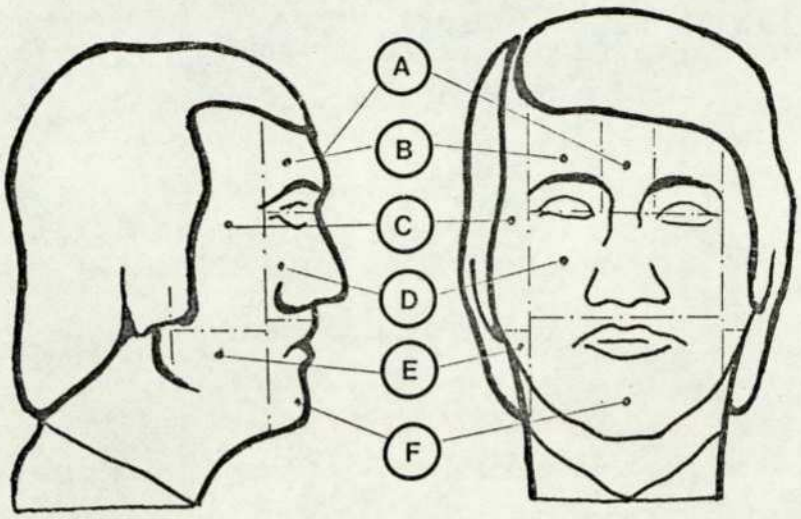


Fig. 35a Heat loss from the face of a standing subject.

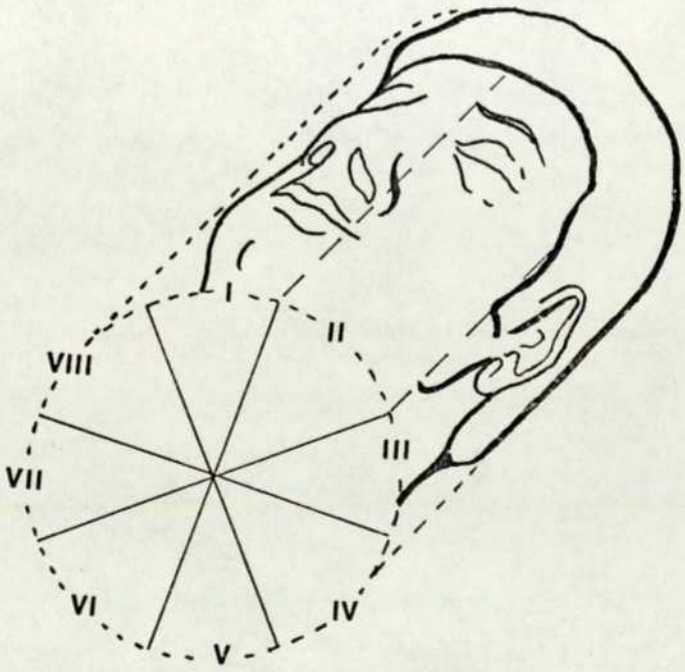


Fig. 35b Heat loss from the supine head.



Fig.36 A subject seated above the low speed wind tunnel with his right leg in the working section.



Fig. 37 A subject sitting inside the environmental wind tunnel at N.I.M.R. (Calorimeters are being attached to the head).





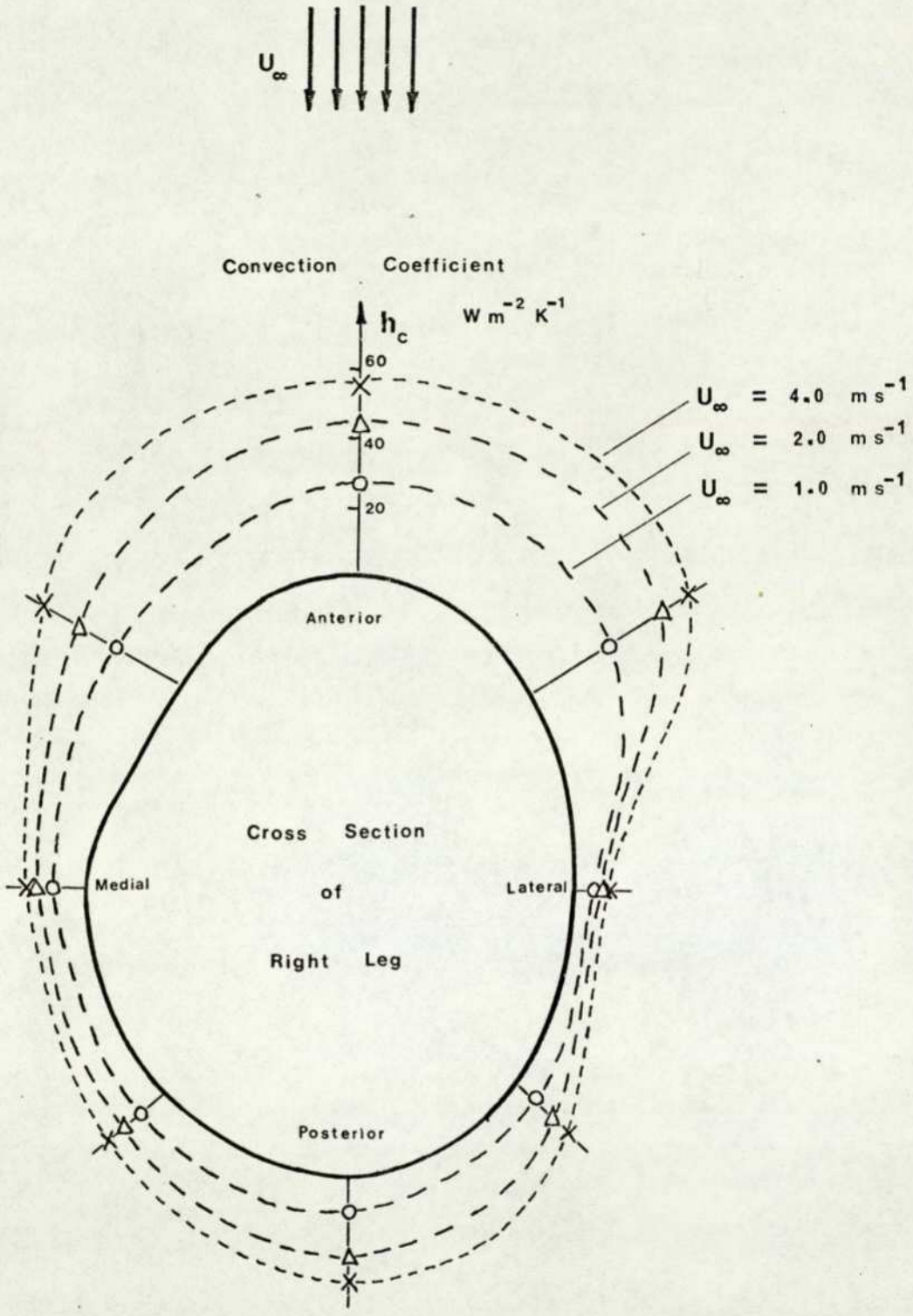


Fig. 38 Forced convection heat transfer distribution around the leg.

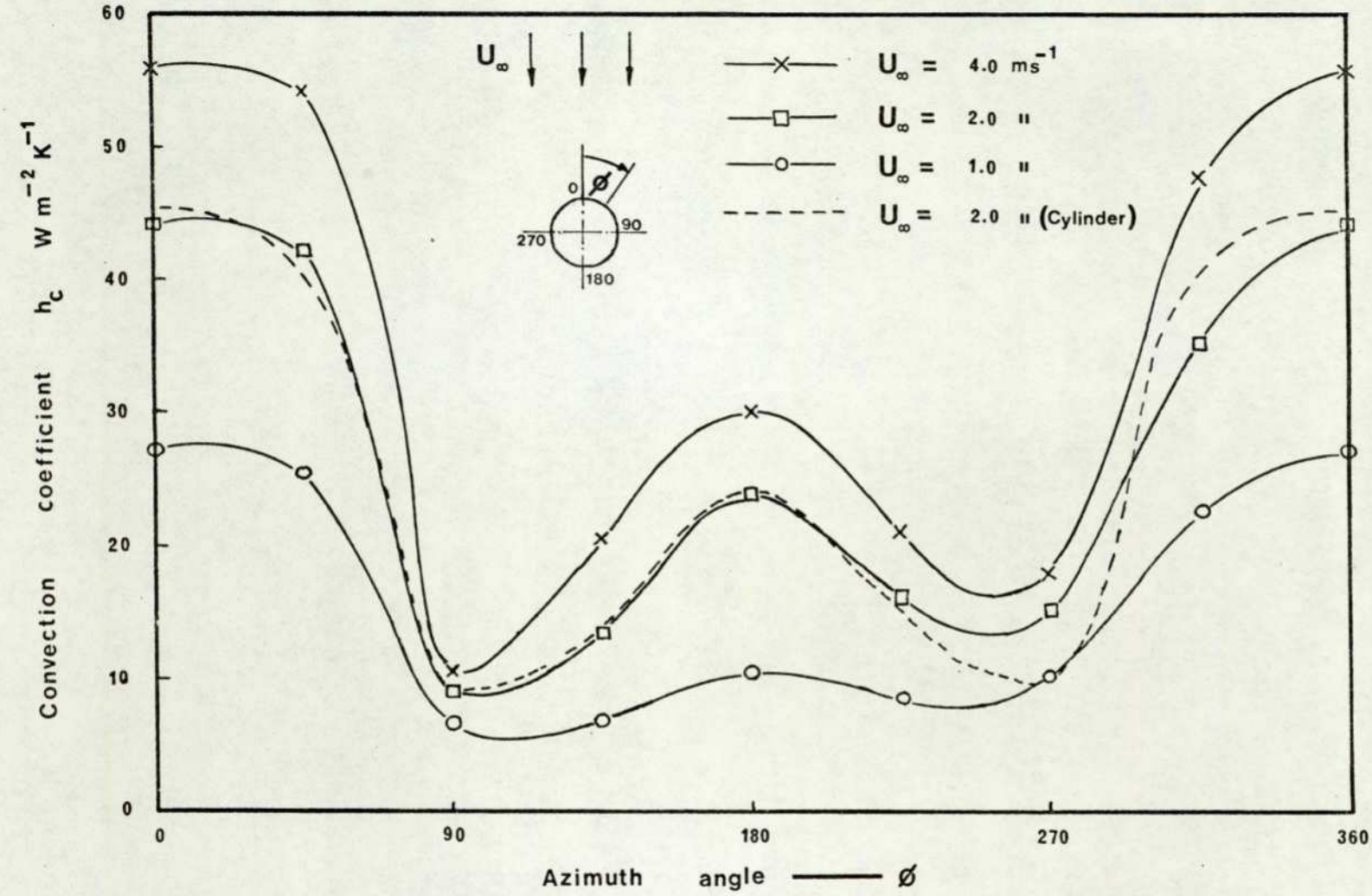


Fig. 39 Polar plot of the heat transfer distribution around the leg with that for a cylinder in a cross-flow of 2.0 ms^{-1}.

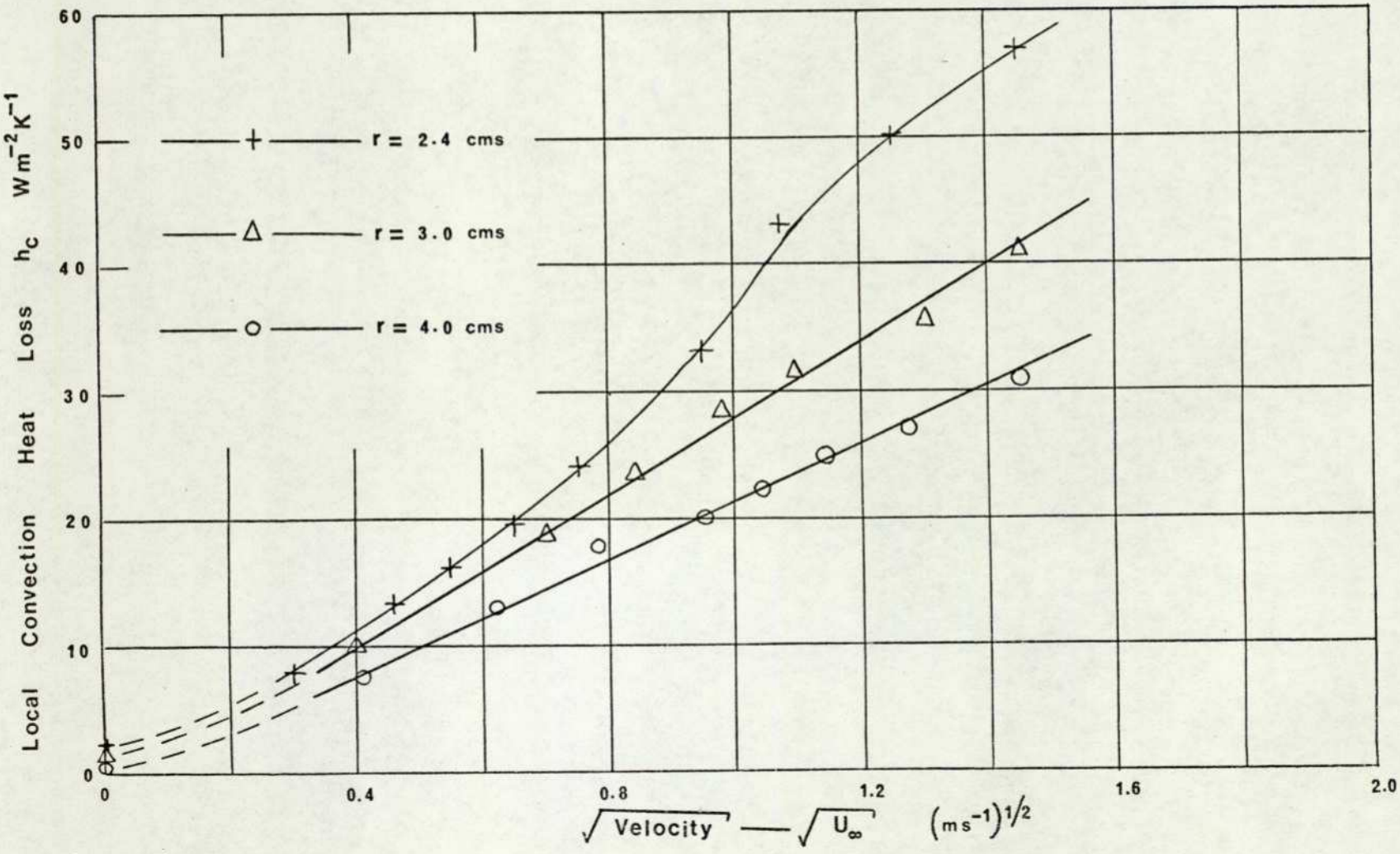


Fig. 40 Stagnation point heat transfer from the leg.

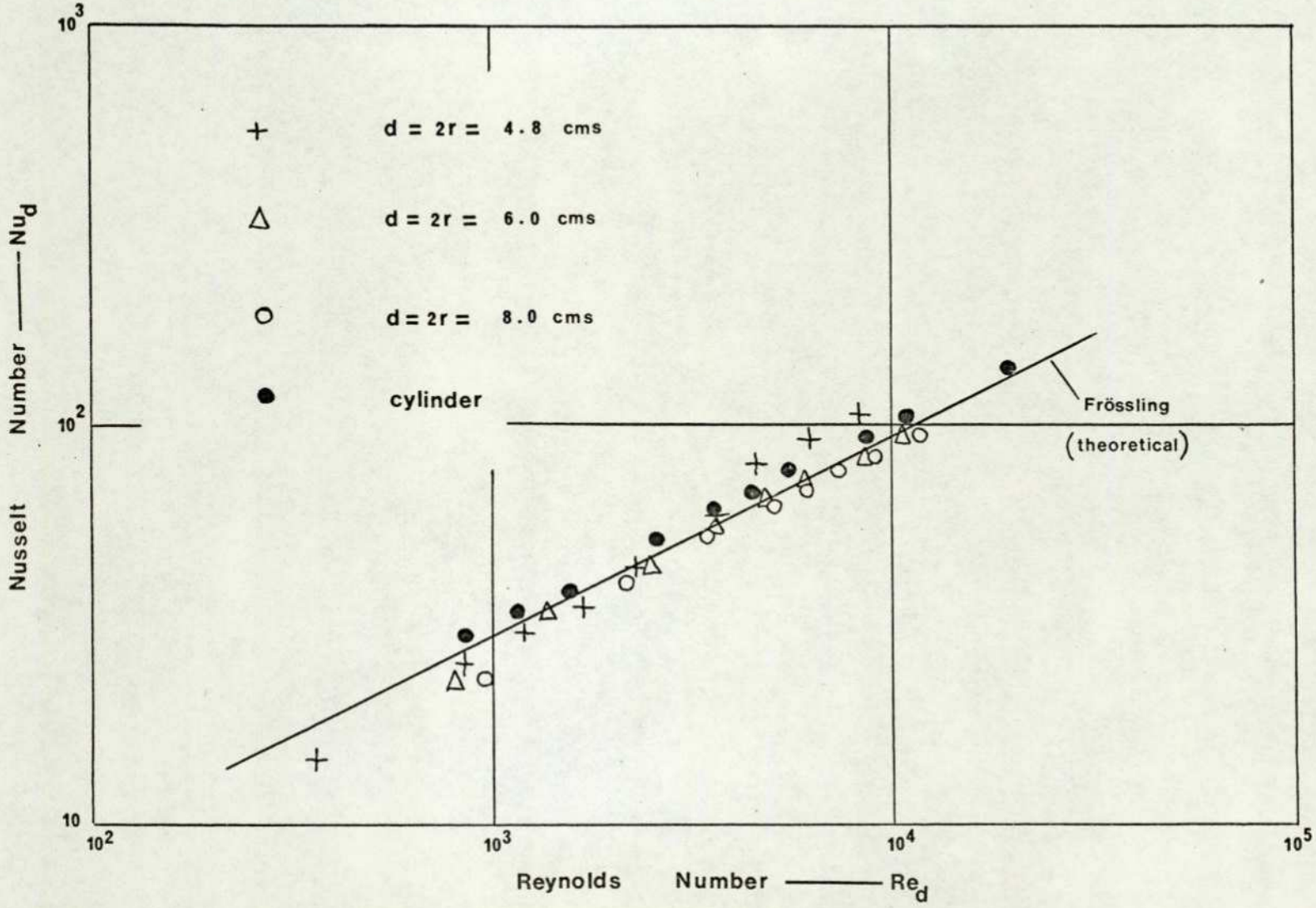


Fig. 41 Stagnation point heat transfer from a leg and a cylinder.

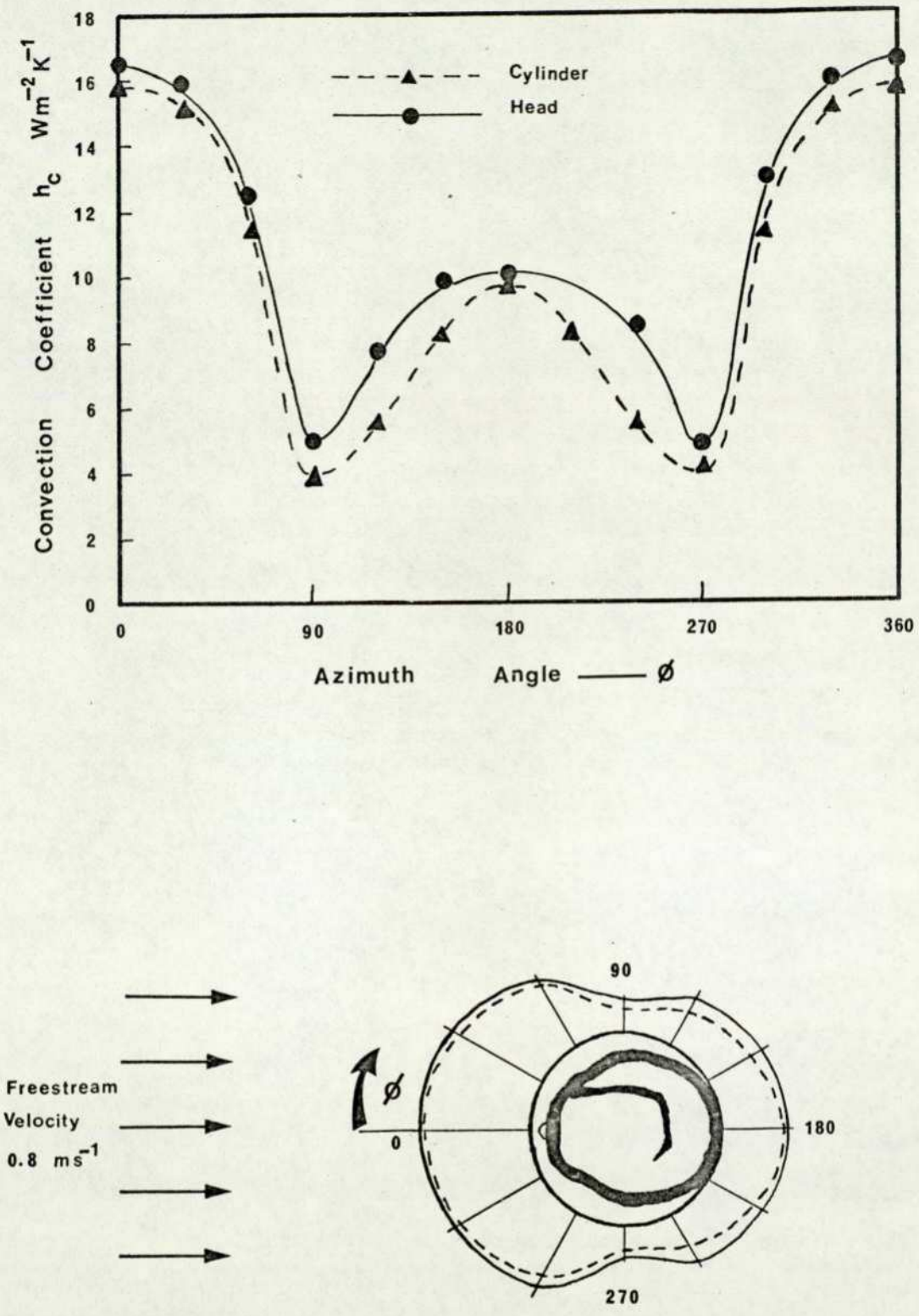


Fig. 42 Comparison of the heat transfer distribution around the head with that for a heated cylinder under the same flow conditions.

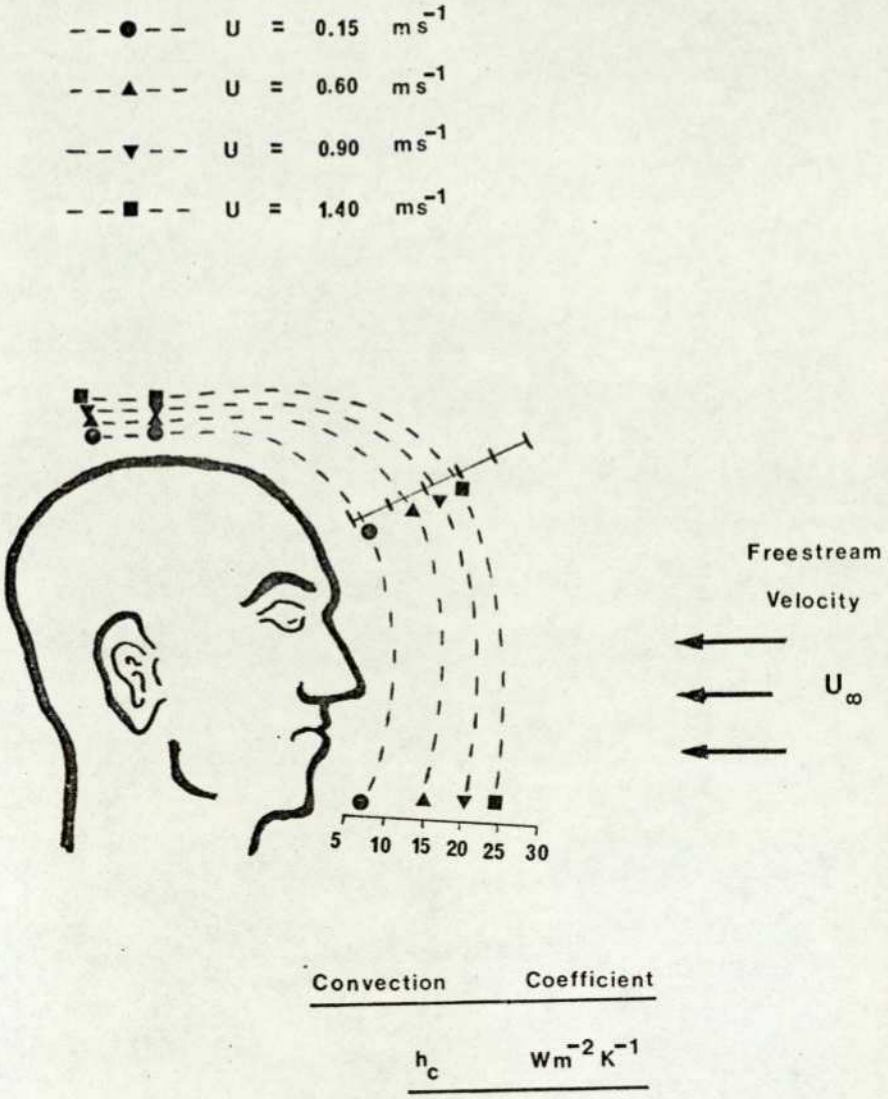
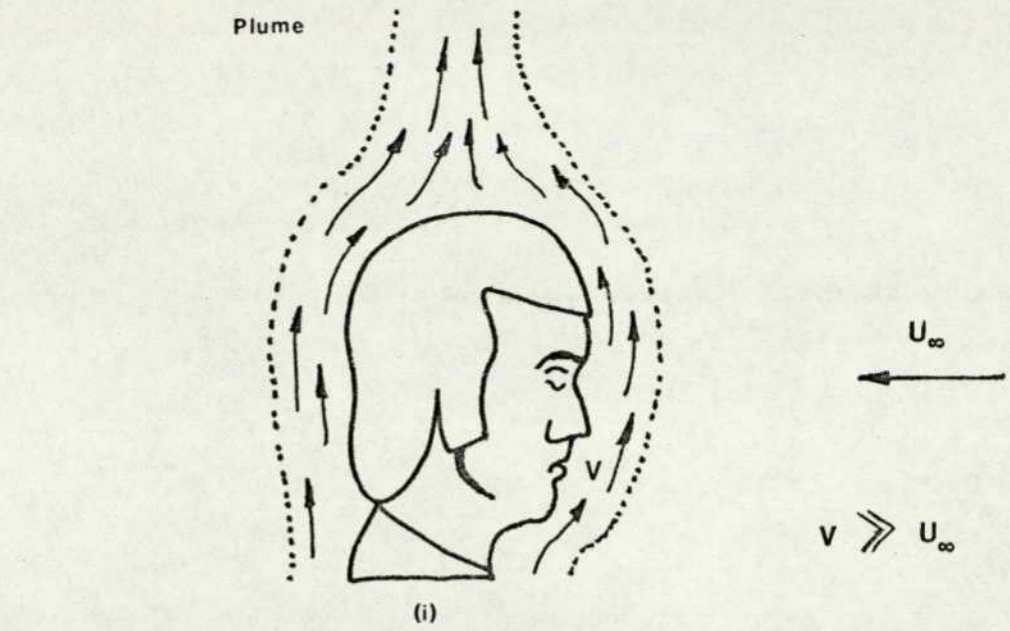
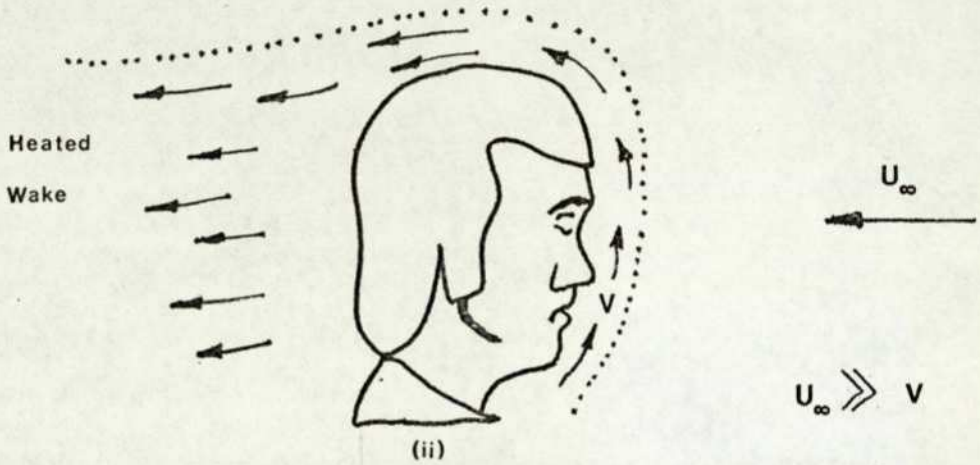


Fig. 43 Local convective heat loss coefficient (h_c) from the head in forced convection.



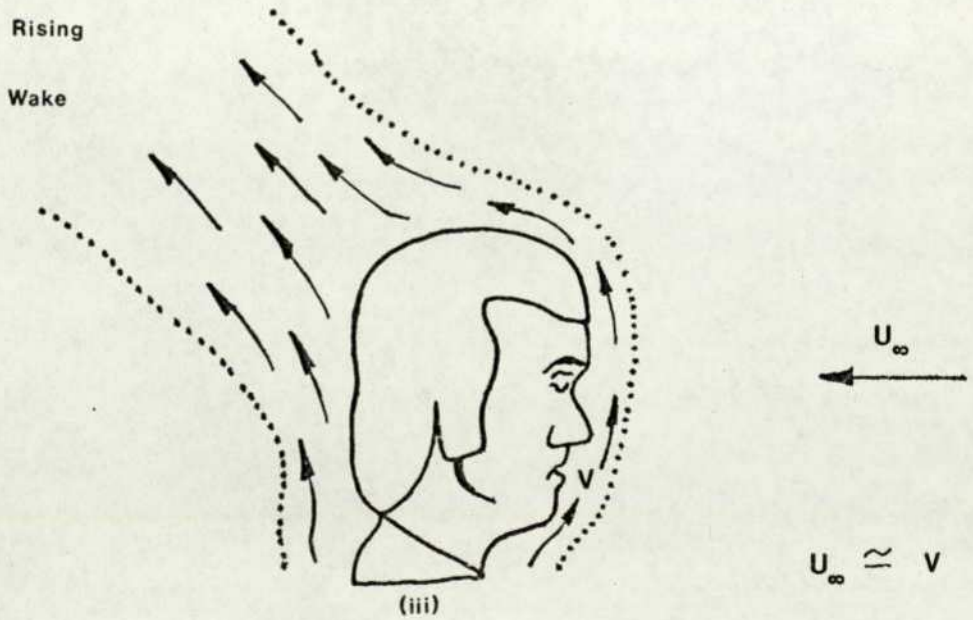
(i)

Free convection



(ii)

Forced convection



(iii)

Combined free and forced convection

Fig. 44 The shape of the convective boundary layer under different flow conditions.

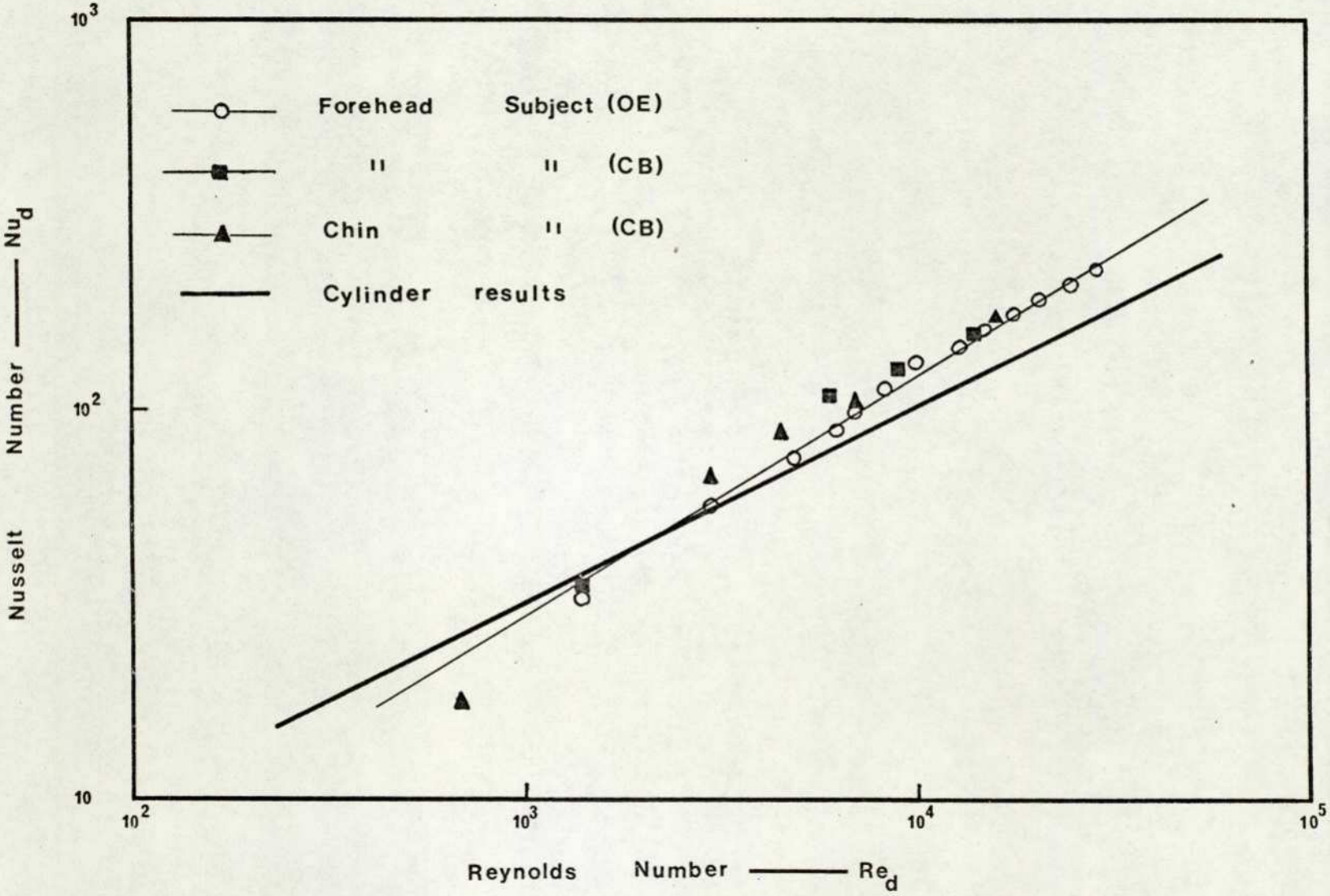


Fig. 45 Comparison of the forward stagnation point heat transfer from the face with that for a cylinder.

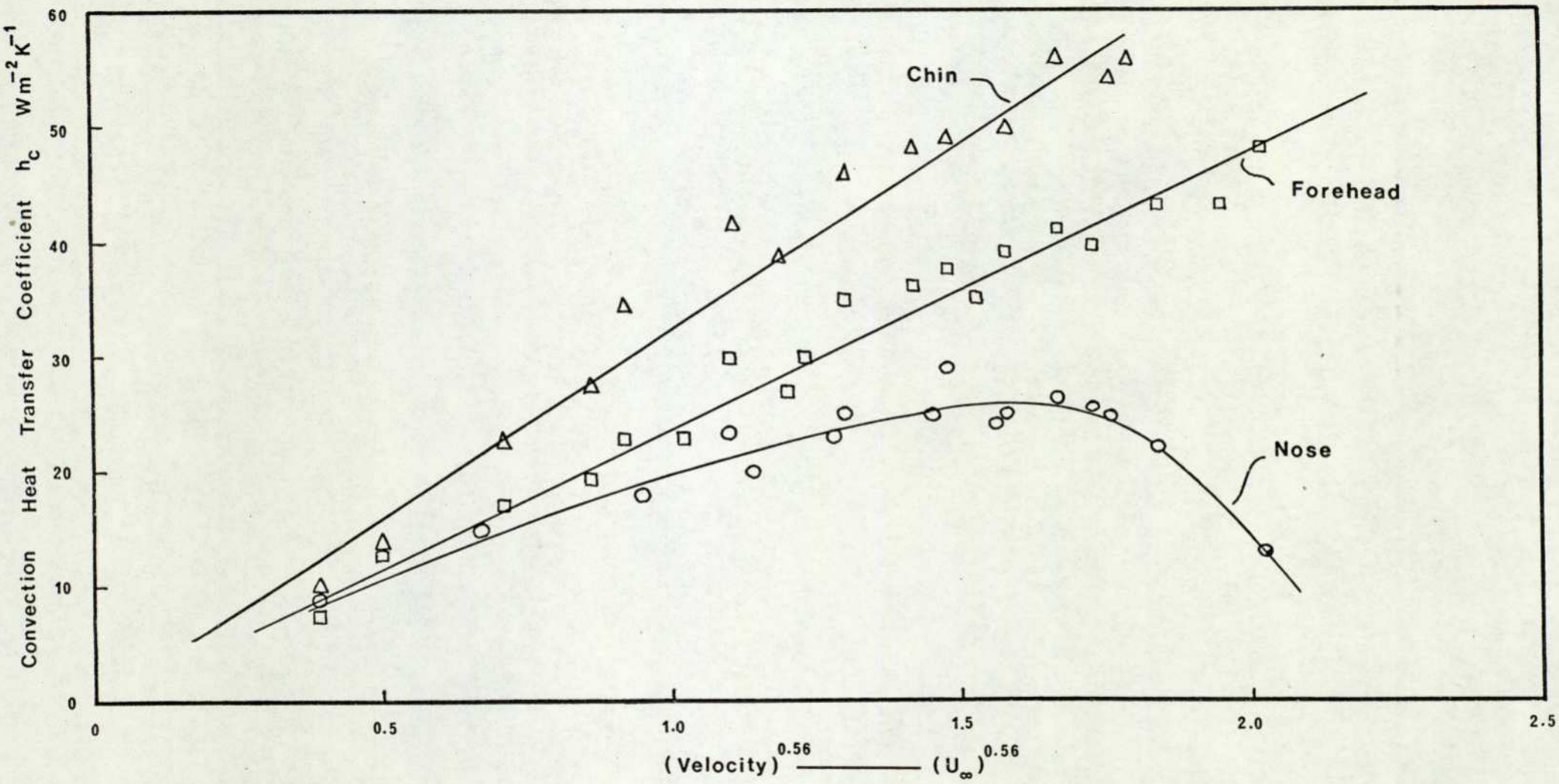


Fig. 46 Forced convection heat transfer from the Forehead, Nose and Chin.

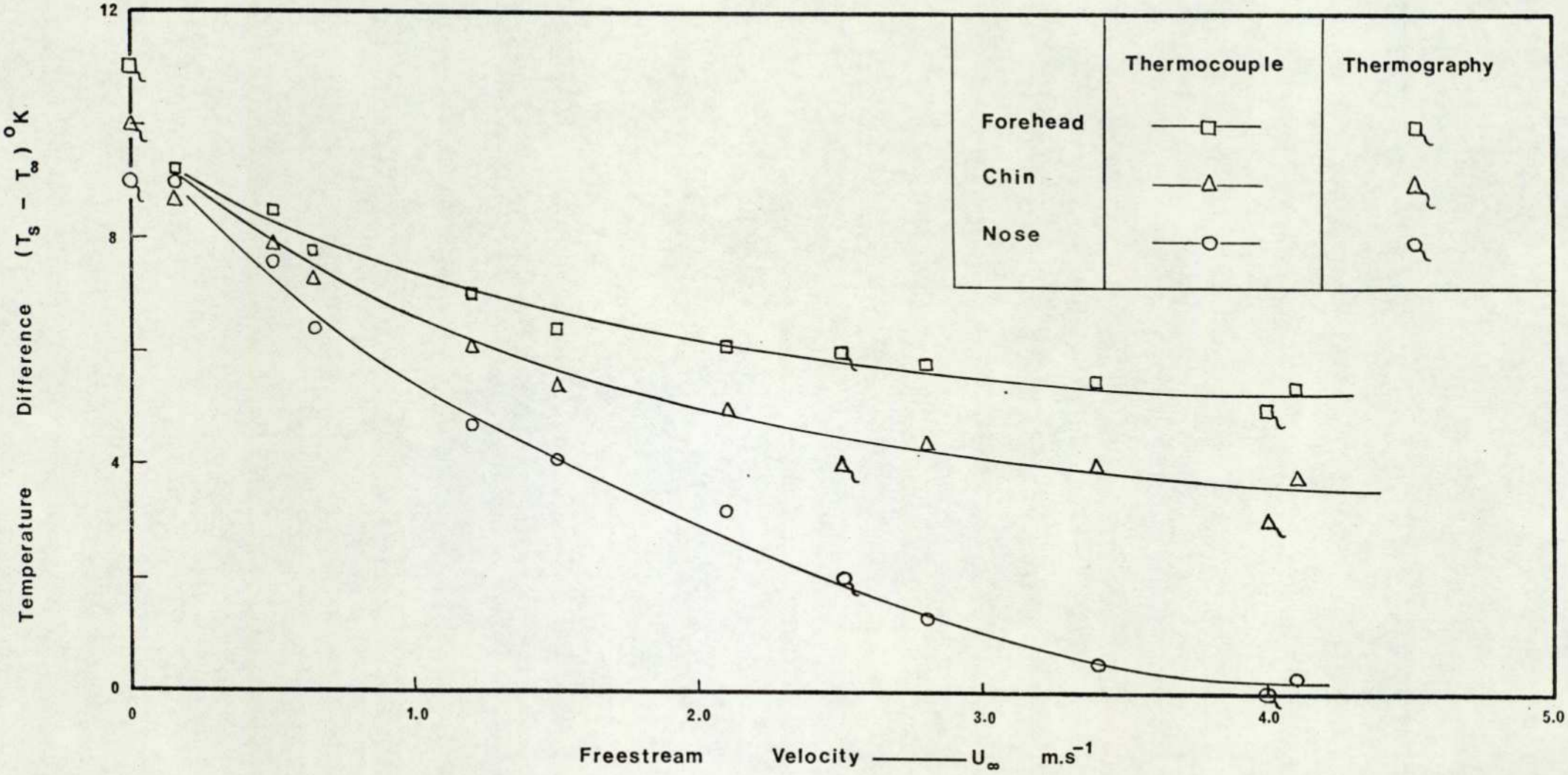


Fig. 47 Plot of the temperature difference $(T_s - T_\infty)$ for the Forehead, Nose and Chin in forced convection.

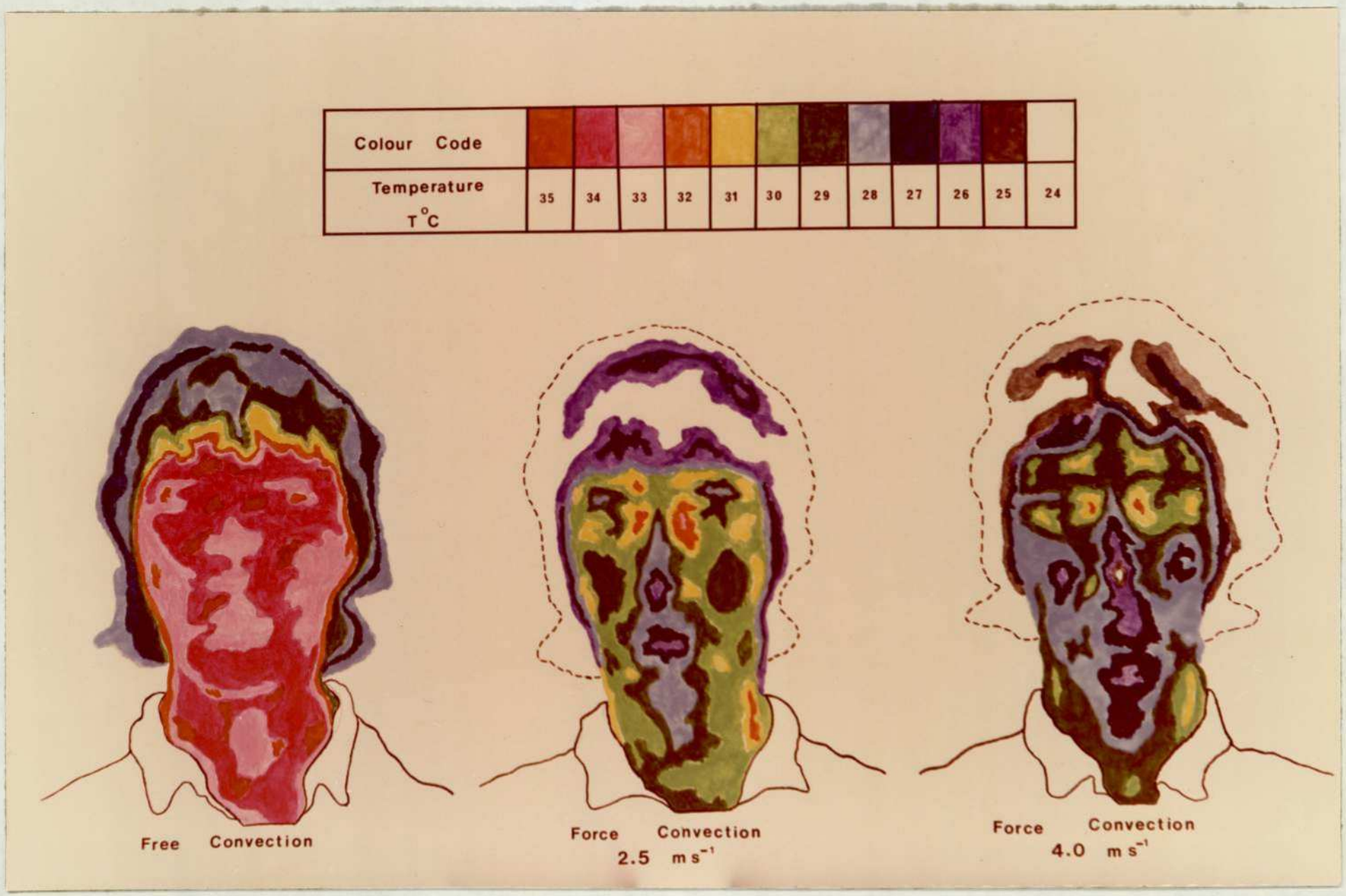


Fig. 48 Isothermal map of the face in free and forced convection. (From a series of photographs taken with an Infra-red radiation camera).

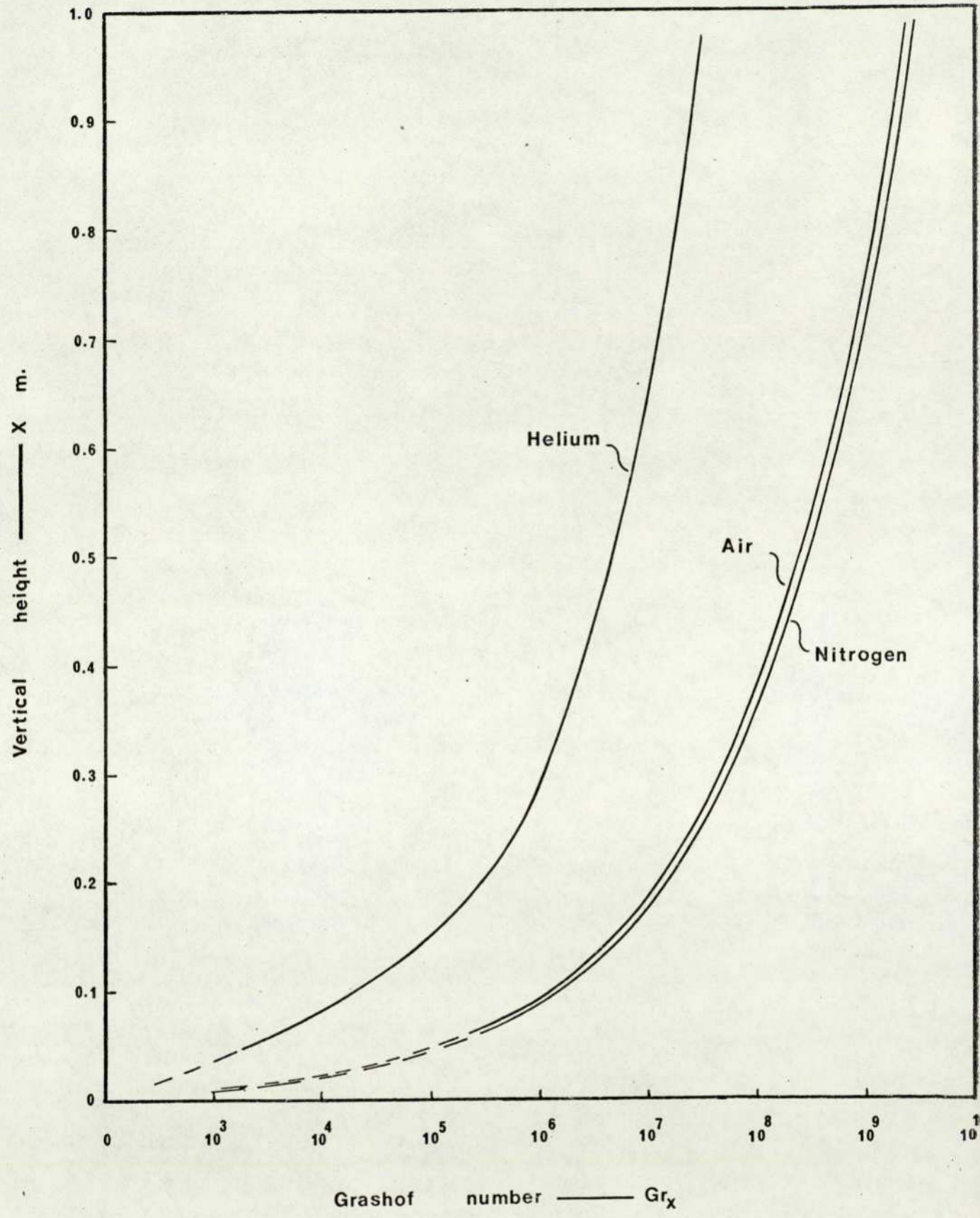


Fig. 49 Variation in the local Grashof number on a heated vertical flat plate immersed in different gases. $T_w = 33^oC$, $T_\infty = 20^oC$.

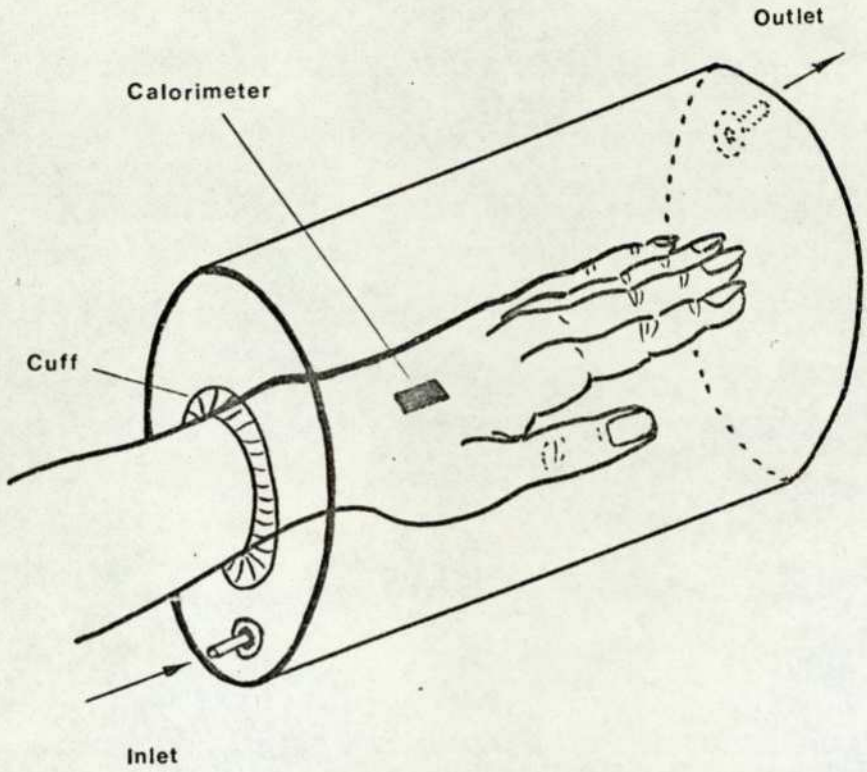


Fig. 50 Perspex cylinder used in the studies of the convective heat loss from the hand in different gas environments.

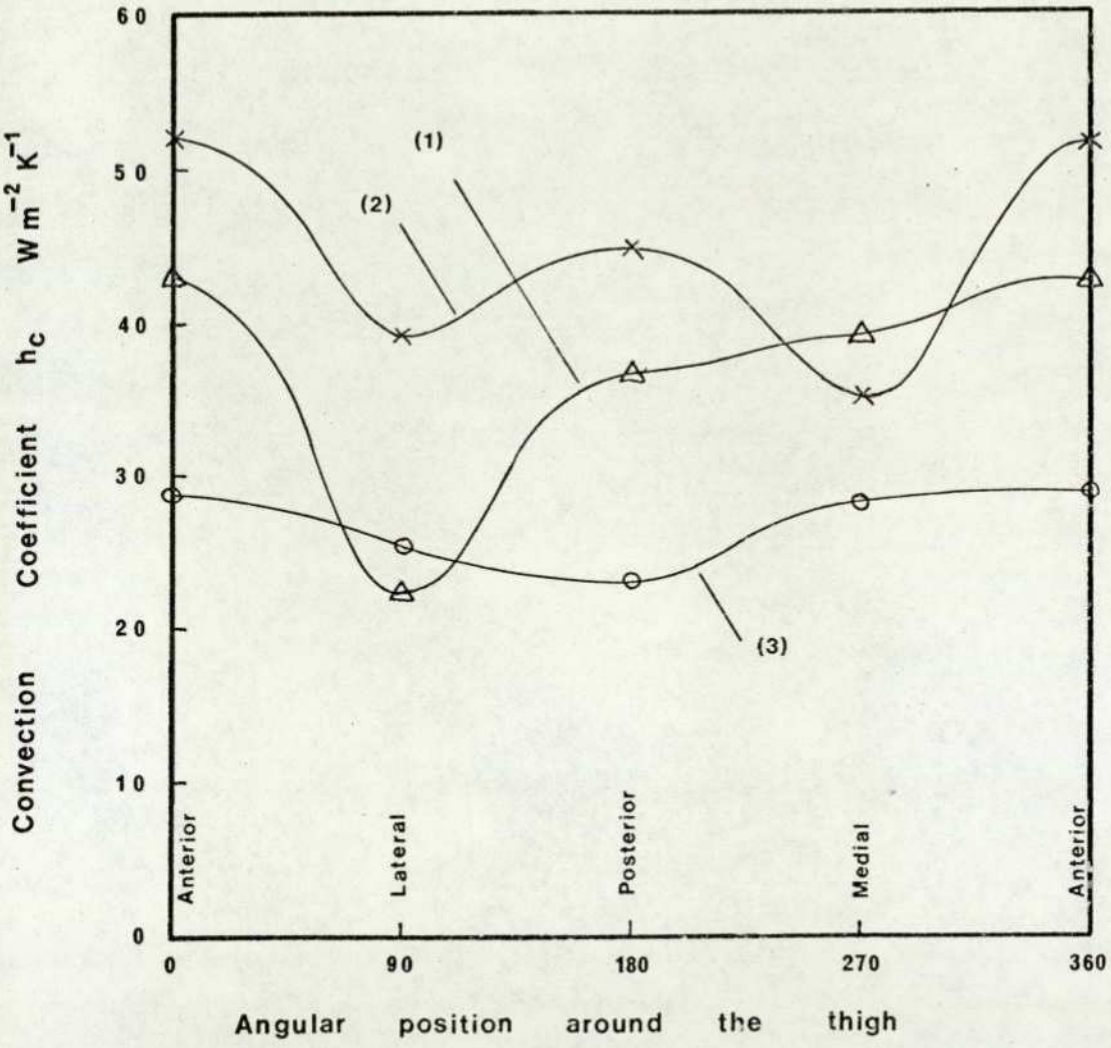


Fig. 51 Convective heat transfer distribution around the thigh of the right leg during running.
Curve 1, stationary subject in a 4.5 ms^{-1} wind,
Curve 2, subject running at 4.5 ms^{-1} in a 4.5 ms^{-1} wind,
Curve 3, subject running at 4.5 ms^{-1} with no wind.

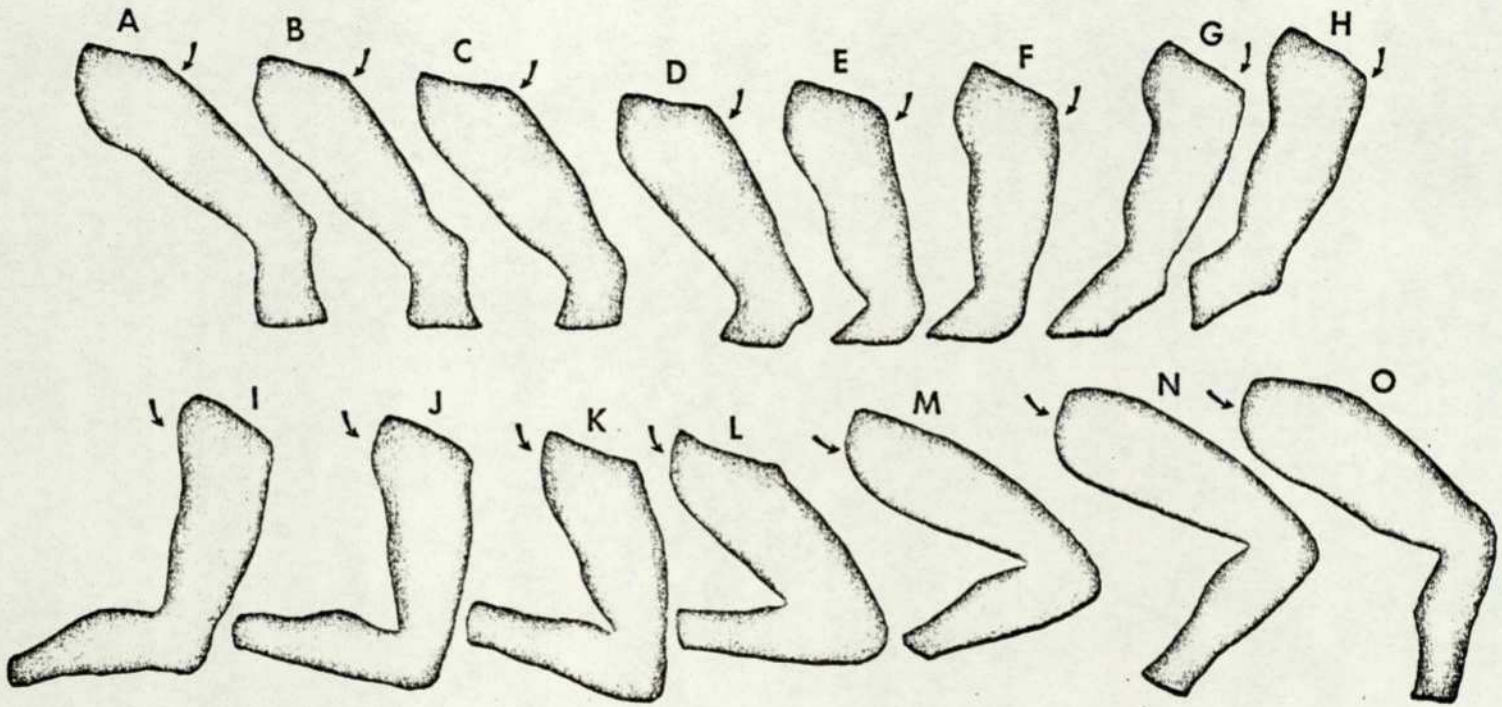


Fig. 52 (a) Sequential leg positions during running at 4.5 ms^{-1}.

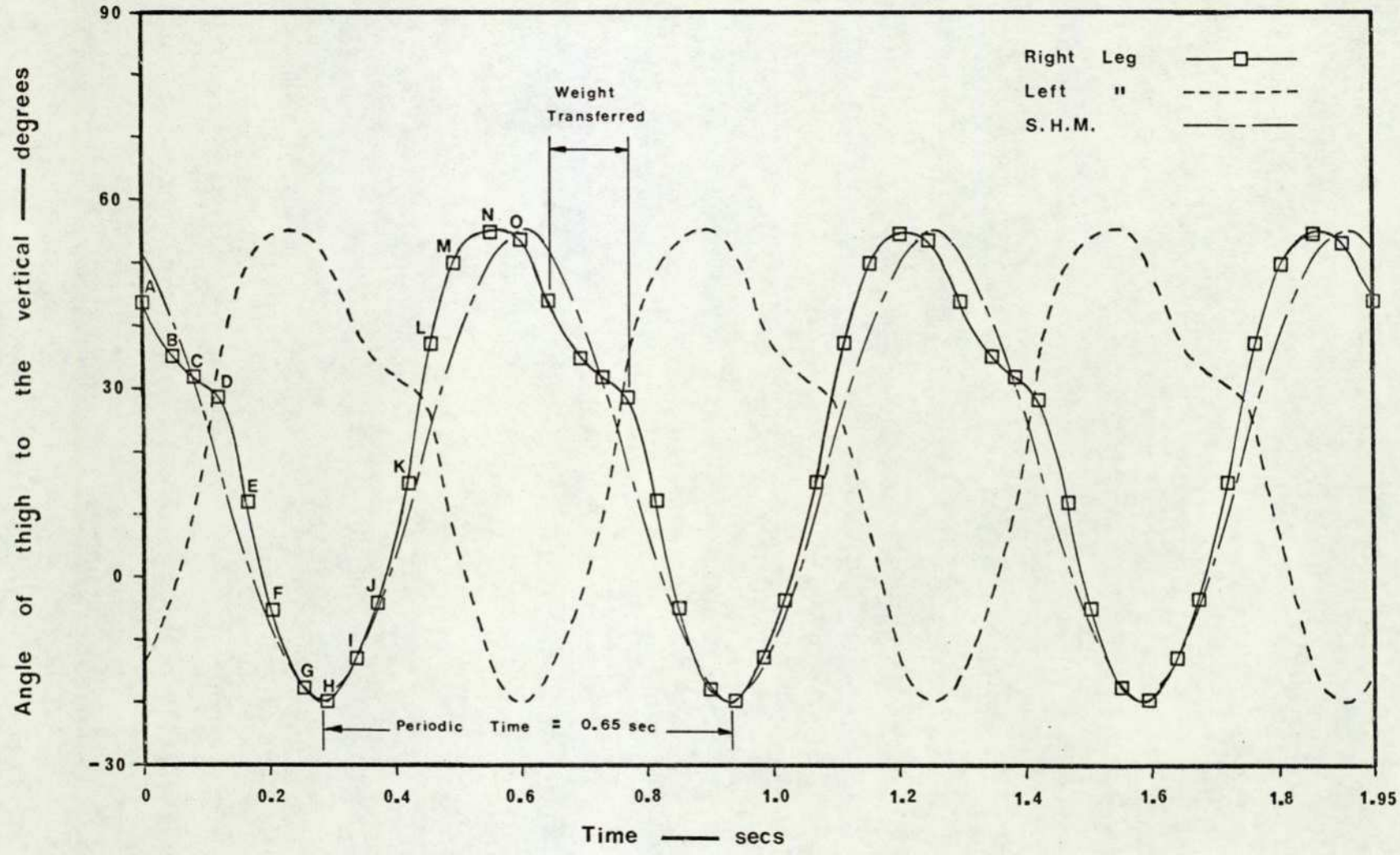


Fig. 52(b) Sequential leg positions during running at 4.5 ms^{-1}.

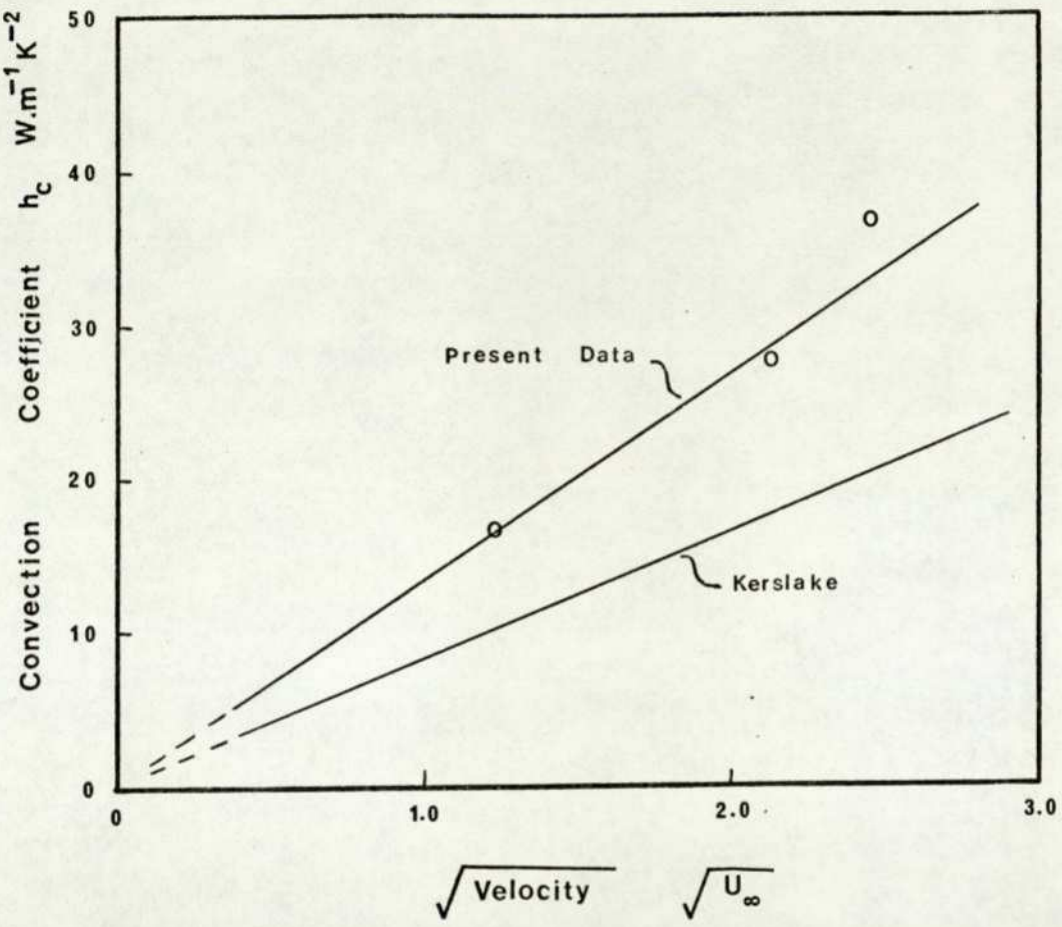


Fig. 53 The convective heat loss from the thigh of a runner compared with total body convective heat loss predicted by Kerslake.

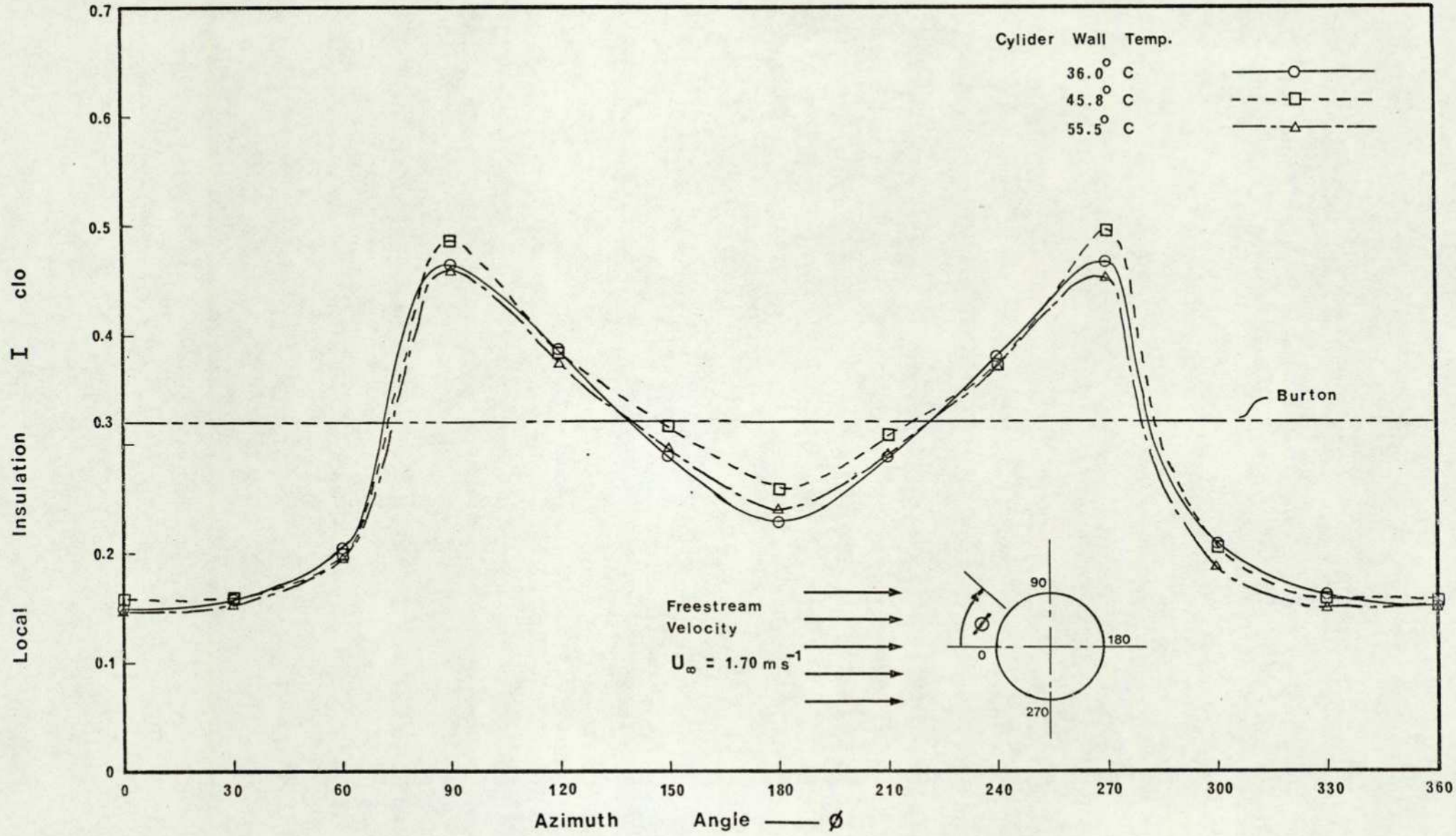


Fig. 54 Local insulation value of the air around a heated horizontal cylinder in forced convection.

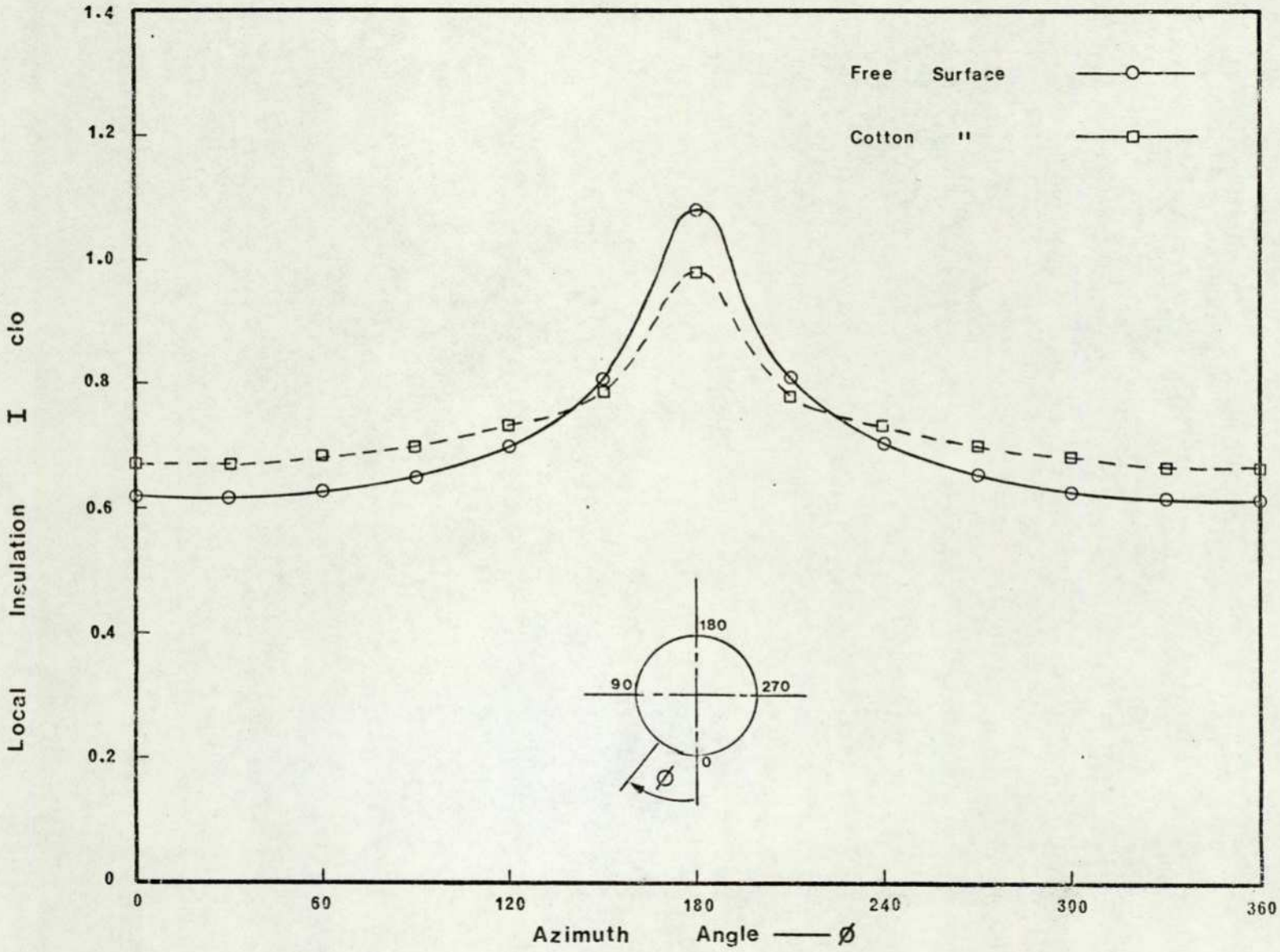


Fig. 55 Local insulation value of air and air+cotton combination around a heated horizontal cylinder in free convection.

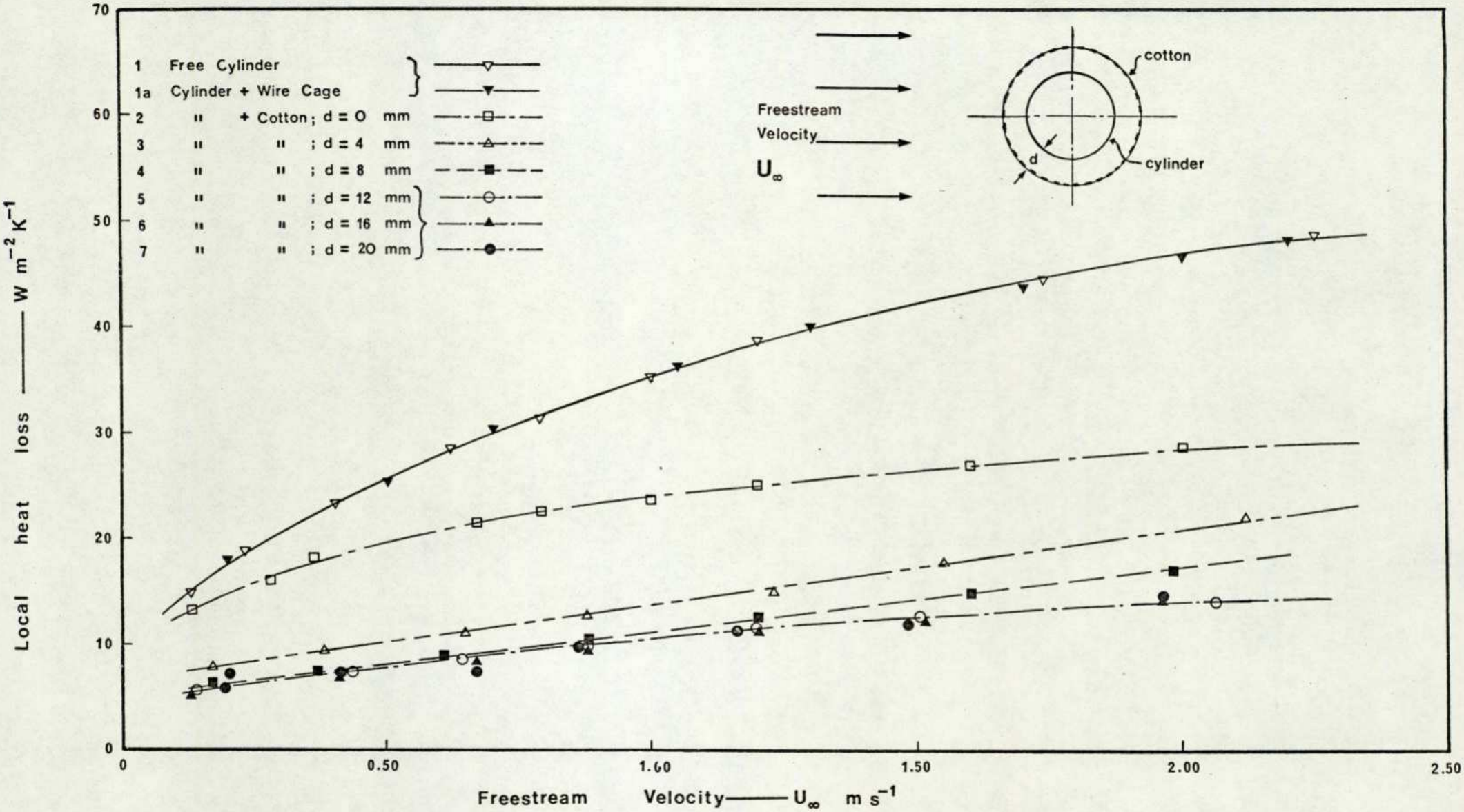


Fig. 56 Stagnation point heat transfer from a cotton covered cylinder in forced convection.

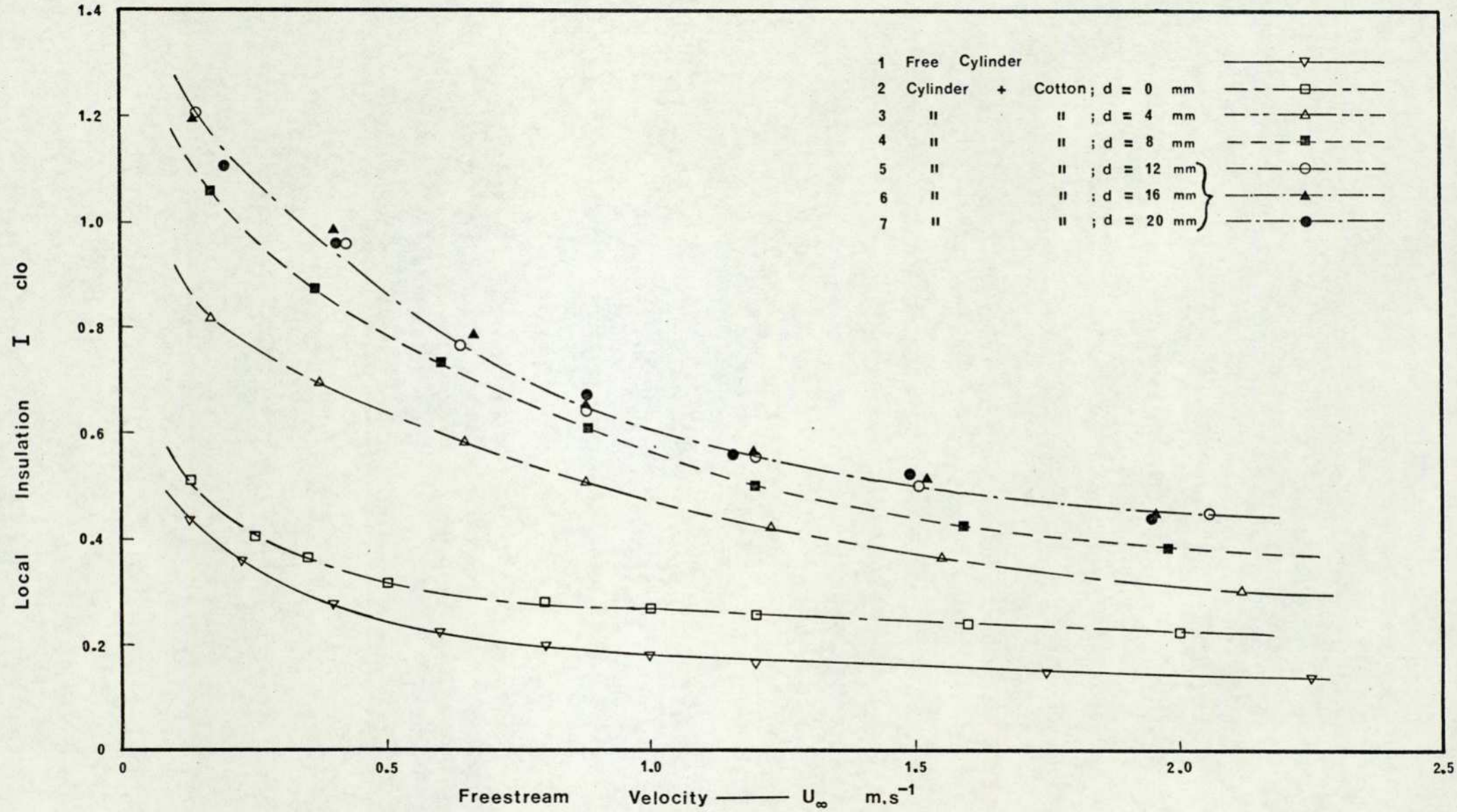


Fig. 57 Insulation provided by the cotton material covering the cylinder in forced convection.

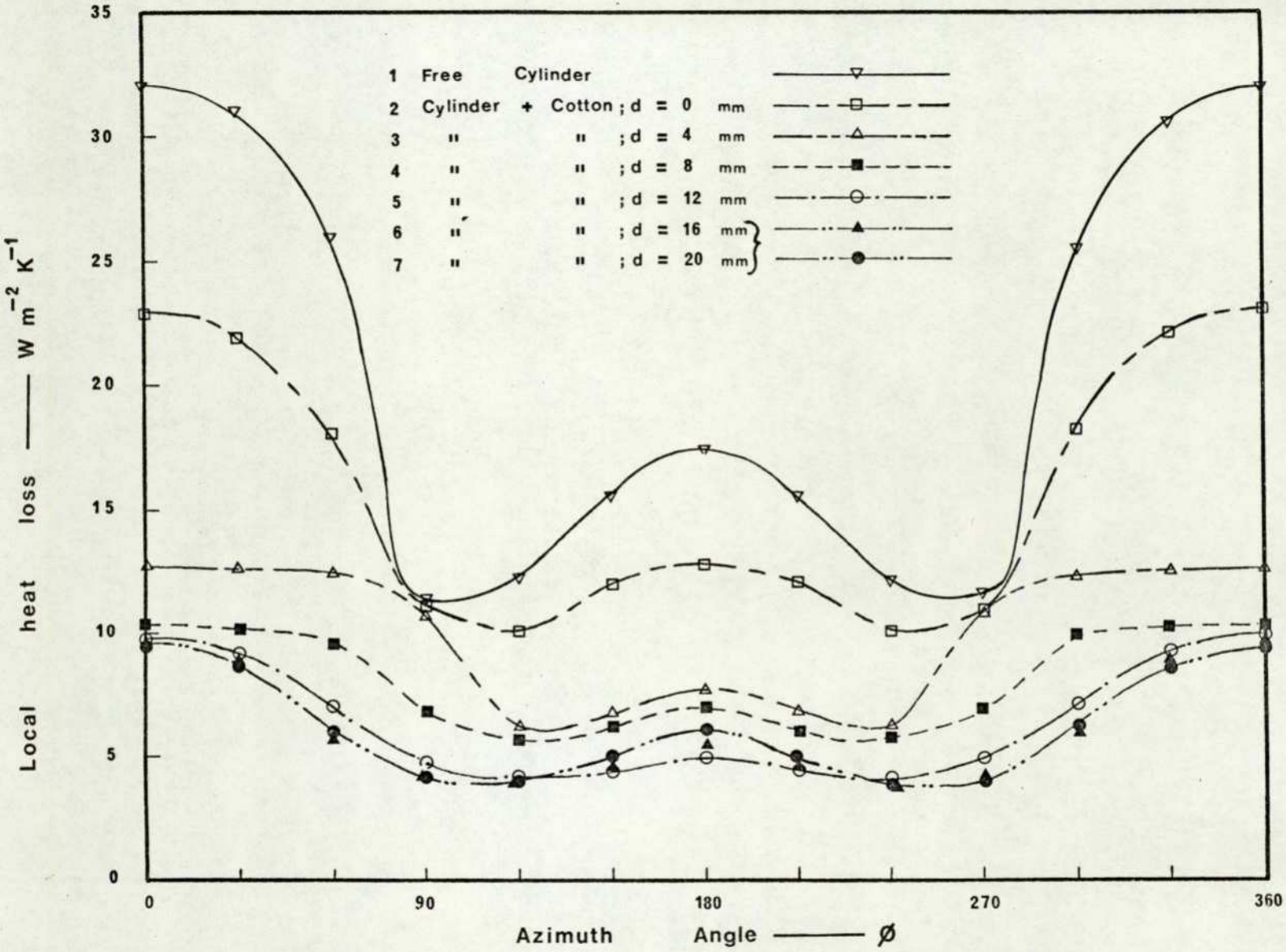


Fig. 58 Heat loss distribution around the cotton covered cylinder in a freestream velocity of 0.9 ms^{-1}

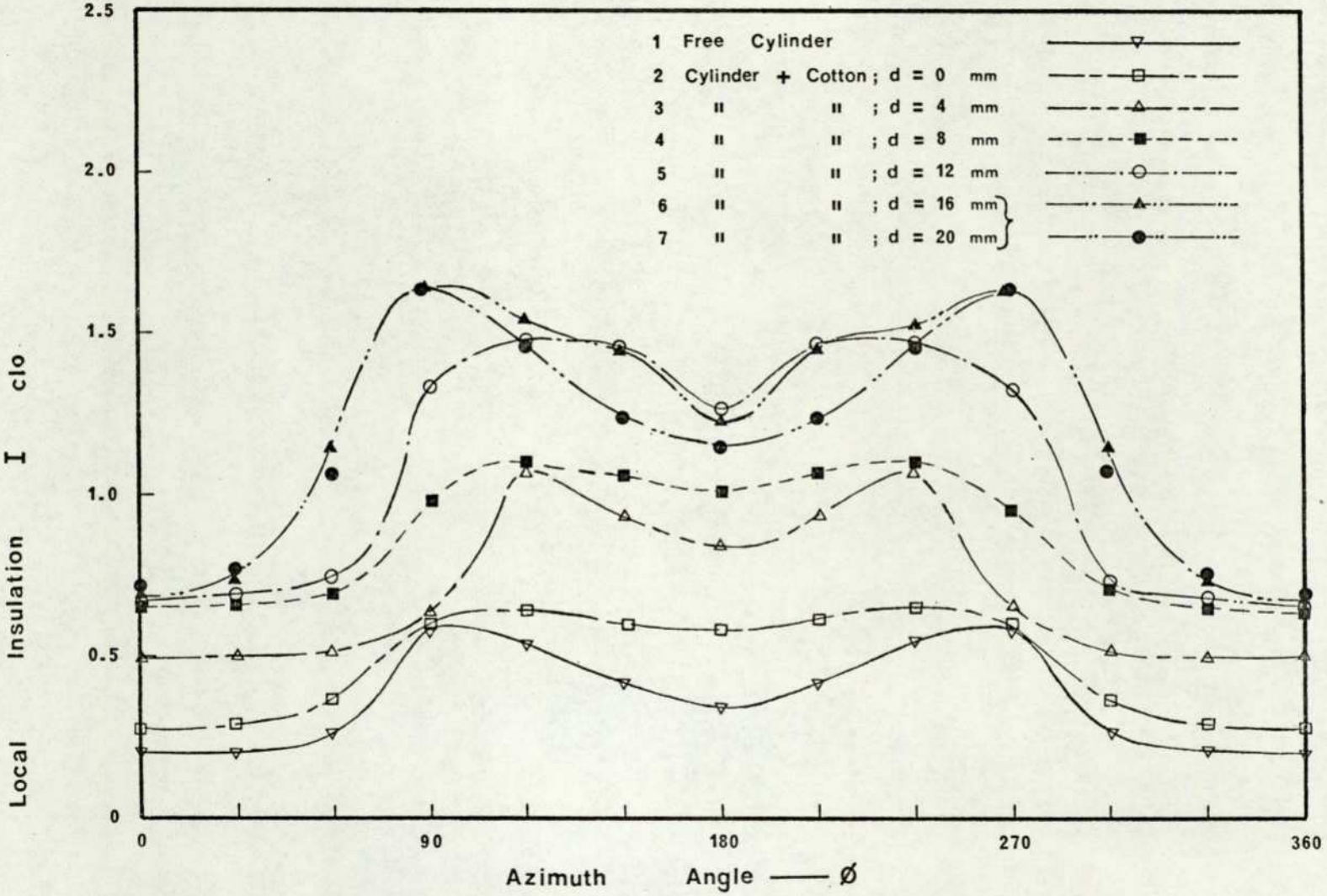
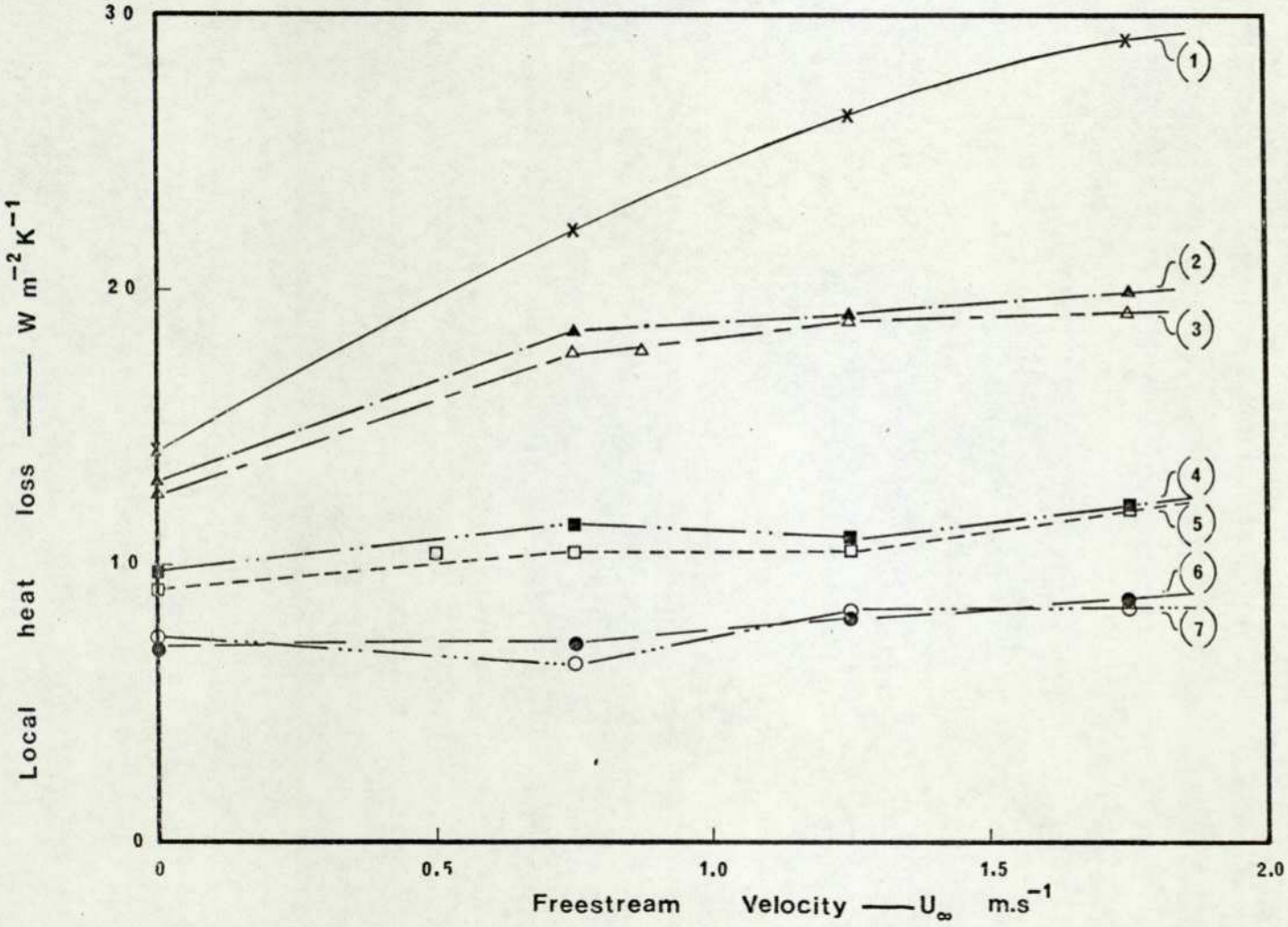


Fig. 59 Insulation around the cotton covered cylinder in afreestream velocity of 0.9 ms^{-1}.



	Code
1	Chest (unclothed)
2	Cotton singlet (cs)
3	String Vest (sv)
4	cs + Shirt
5	sv + "
6	cs + " + Overcoat
7	sv + " + "

Fig. 60 Local heat loss through different clothing assemblies in forced convection.

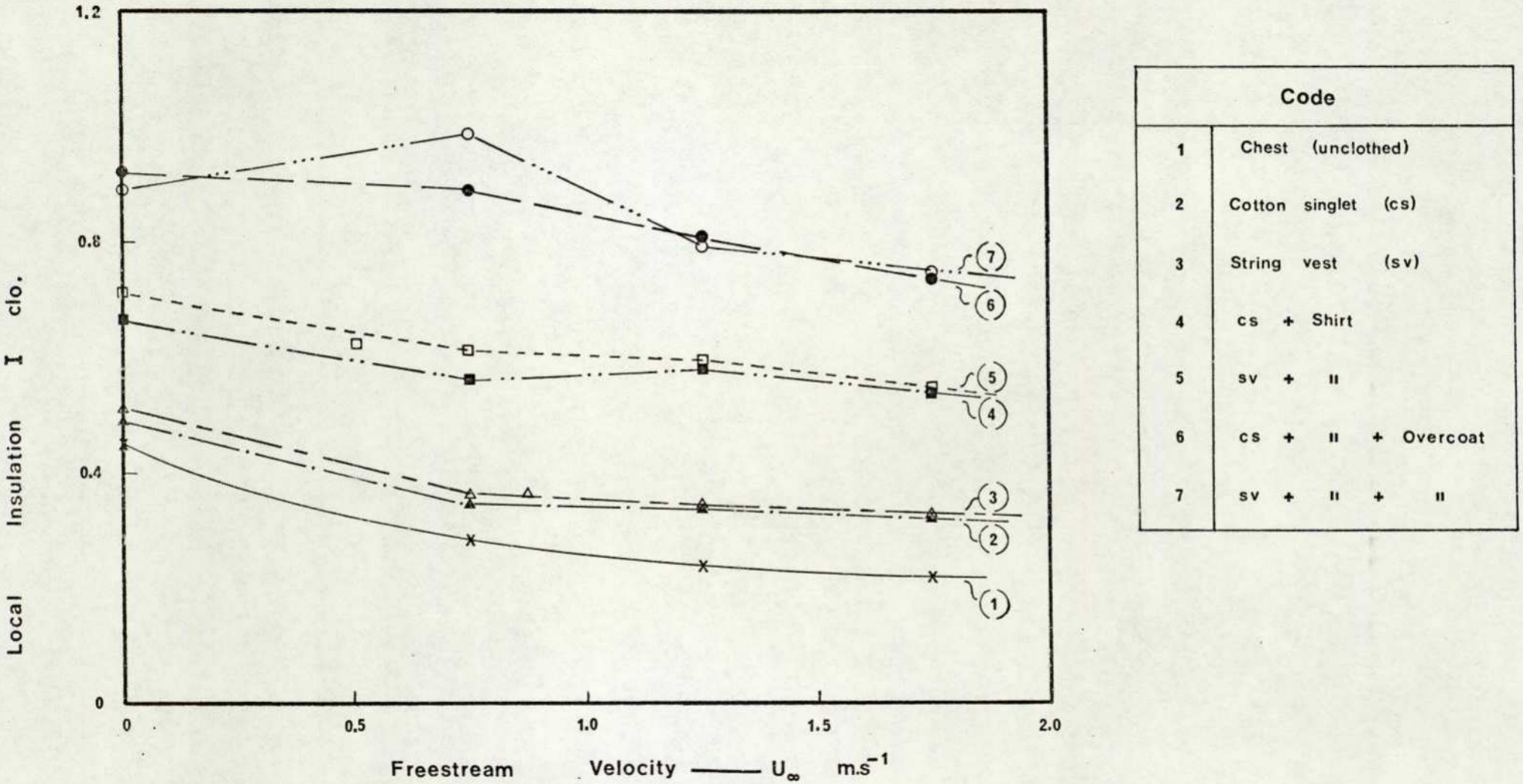
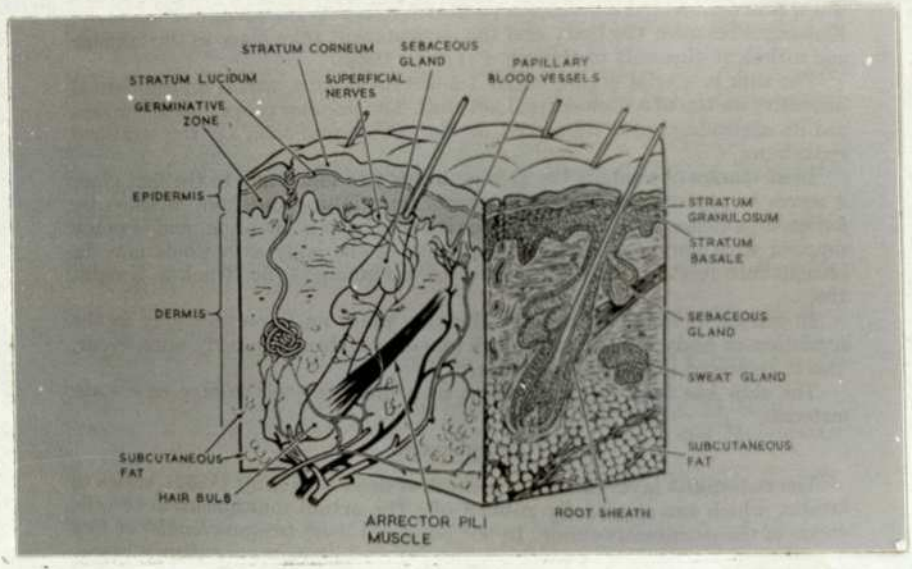
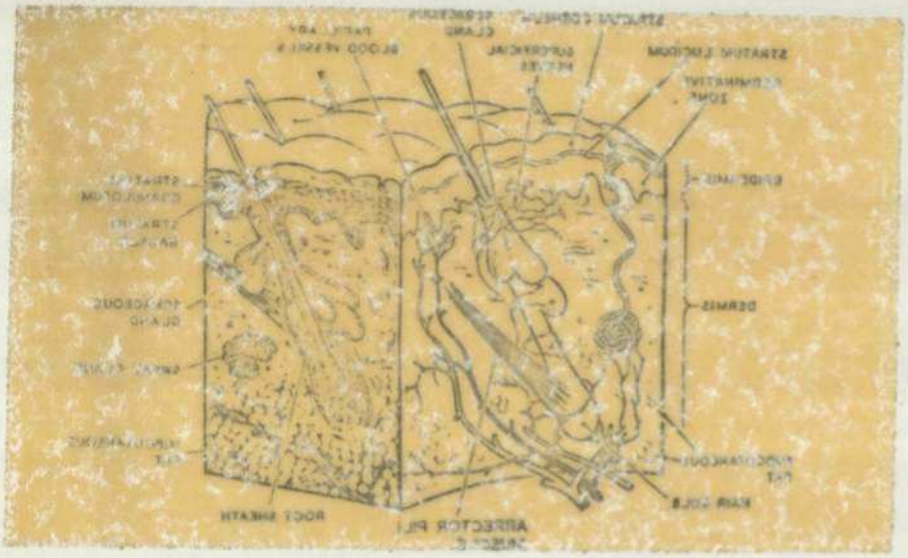
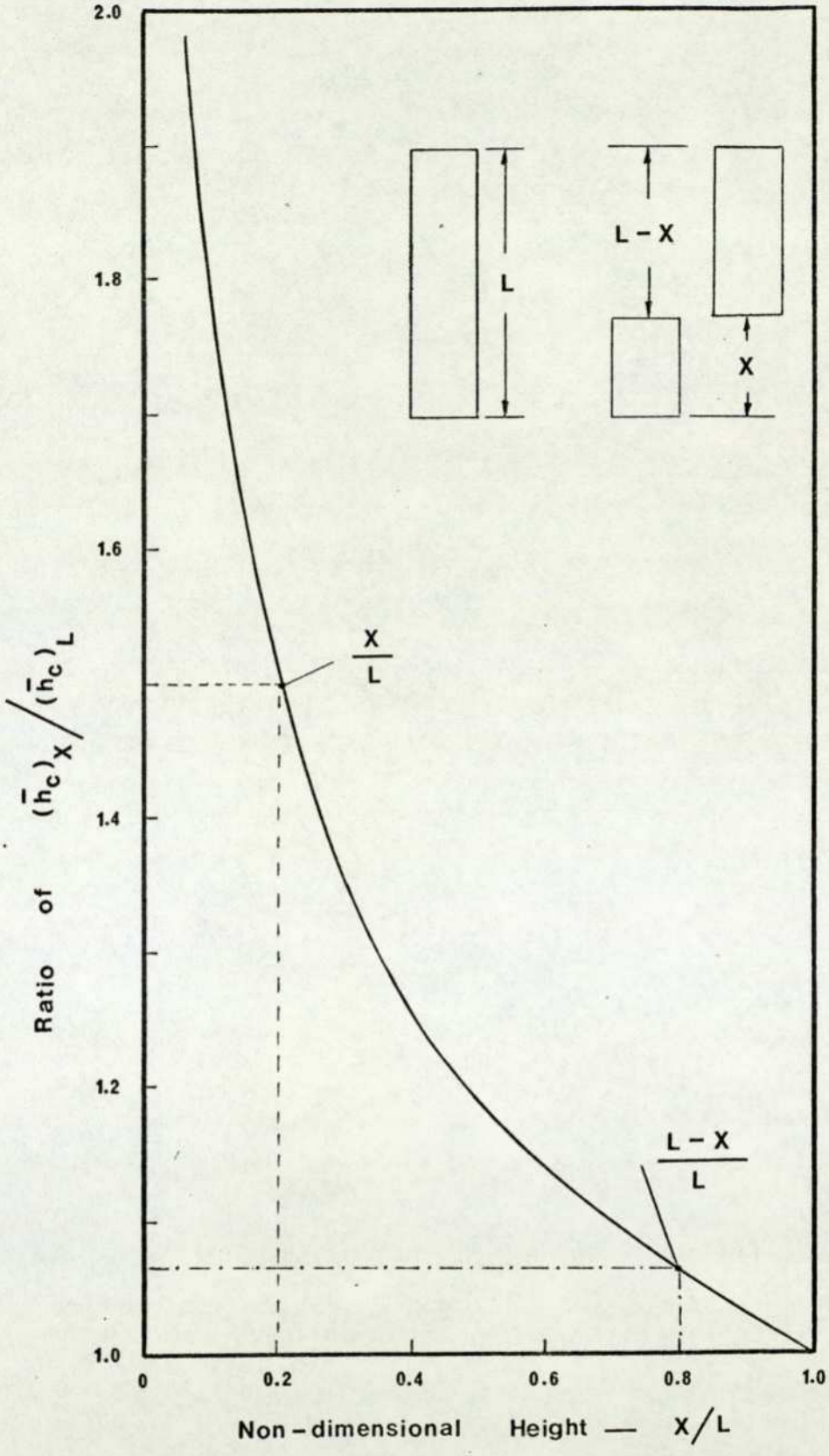


Fig. 61 Local insulation provided by different clothing assemblies in forced convection.

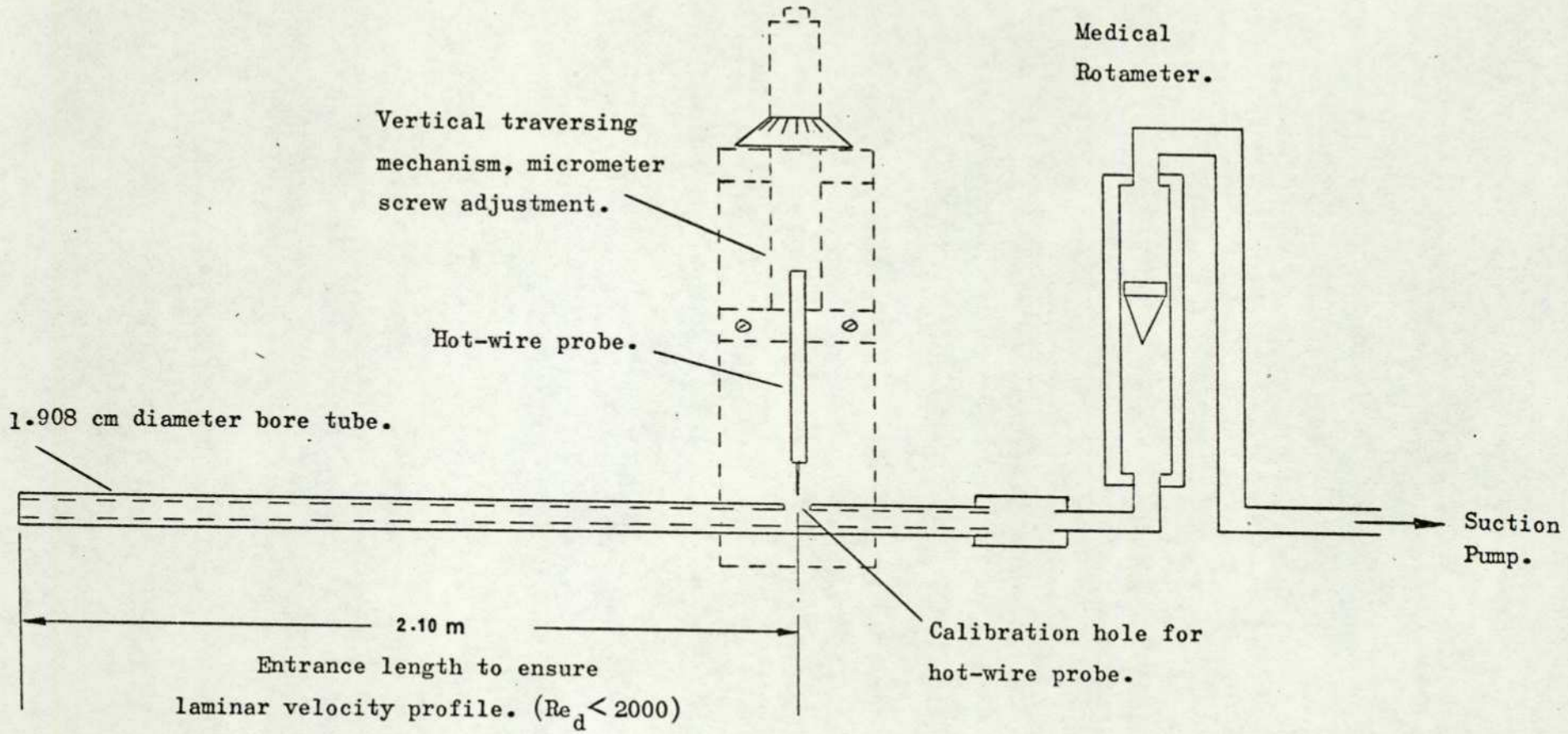


App. A —— Fig. 62 Diagram illustrating the structure of the Human Skin, (Lewis, ref. 88).

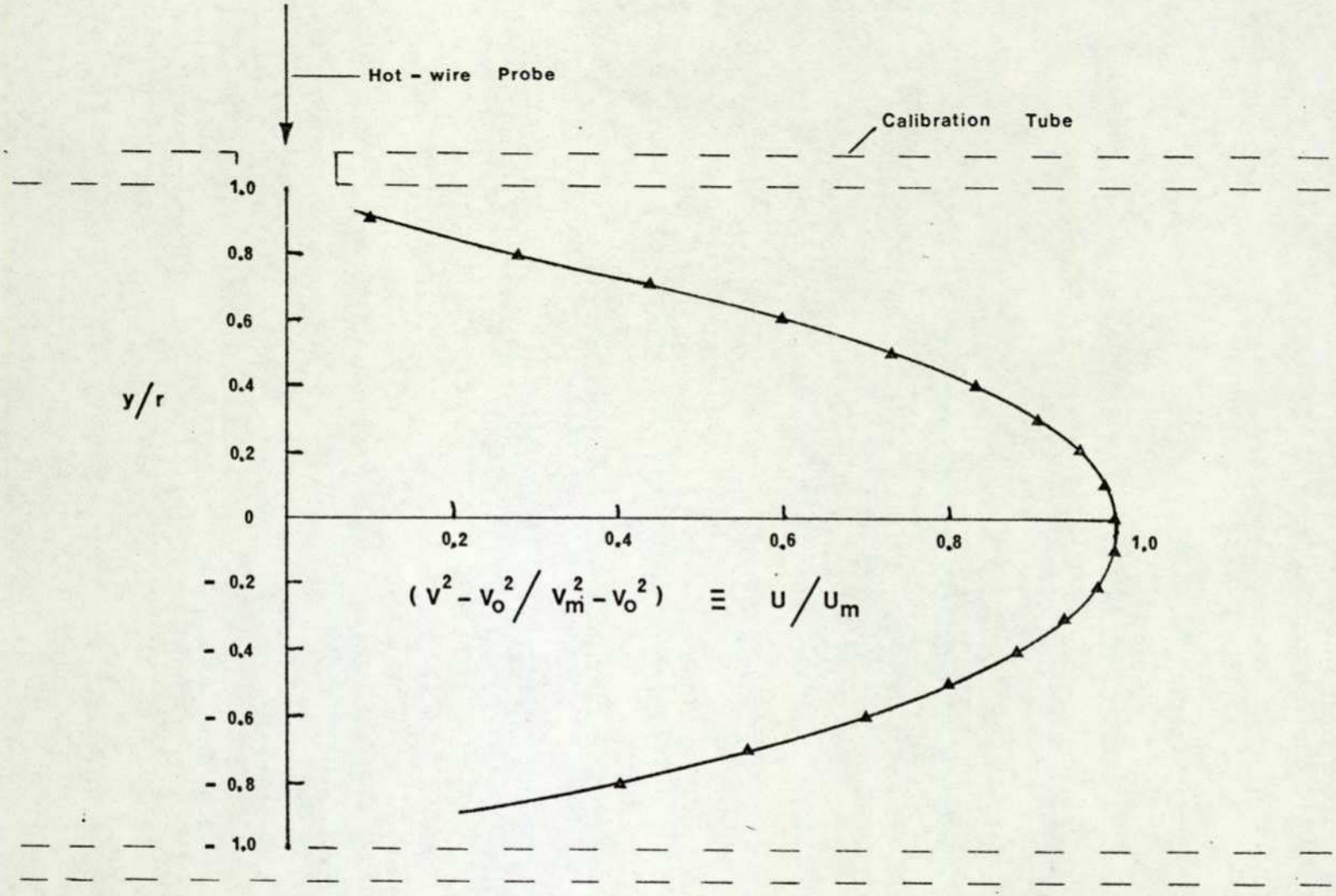




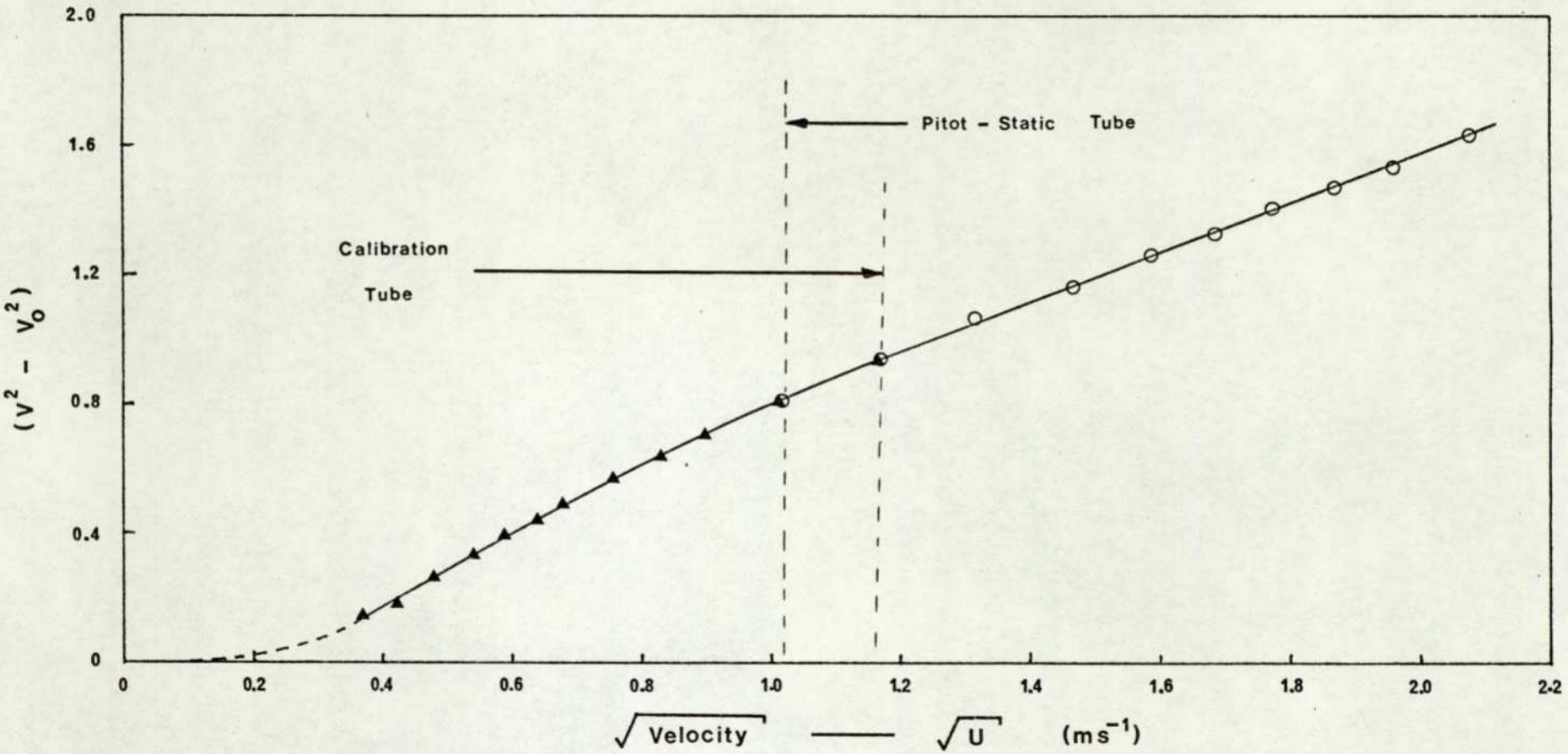
App. B — Fig. 63 The effect of cylinder height on the overall convective heat transfer coefficient $(\bar{h}_c)$.



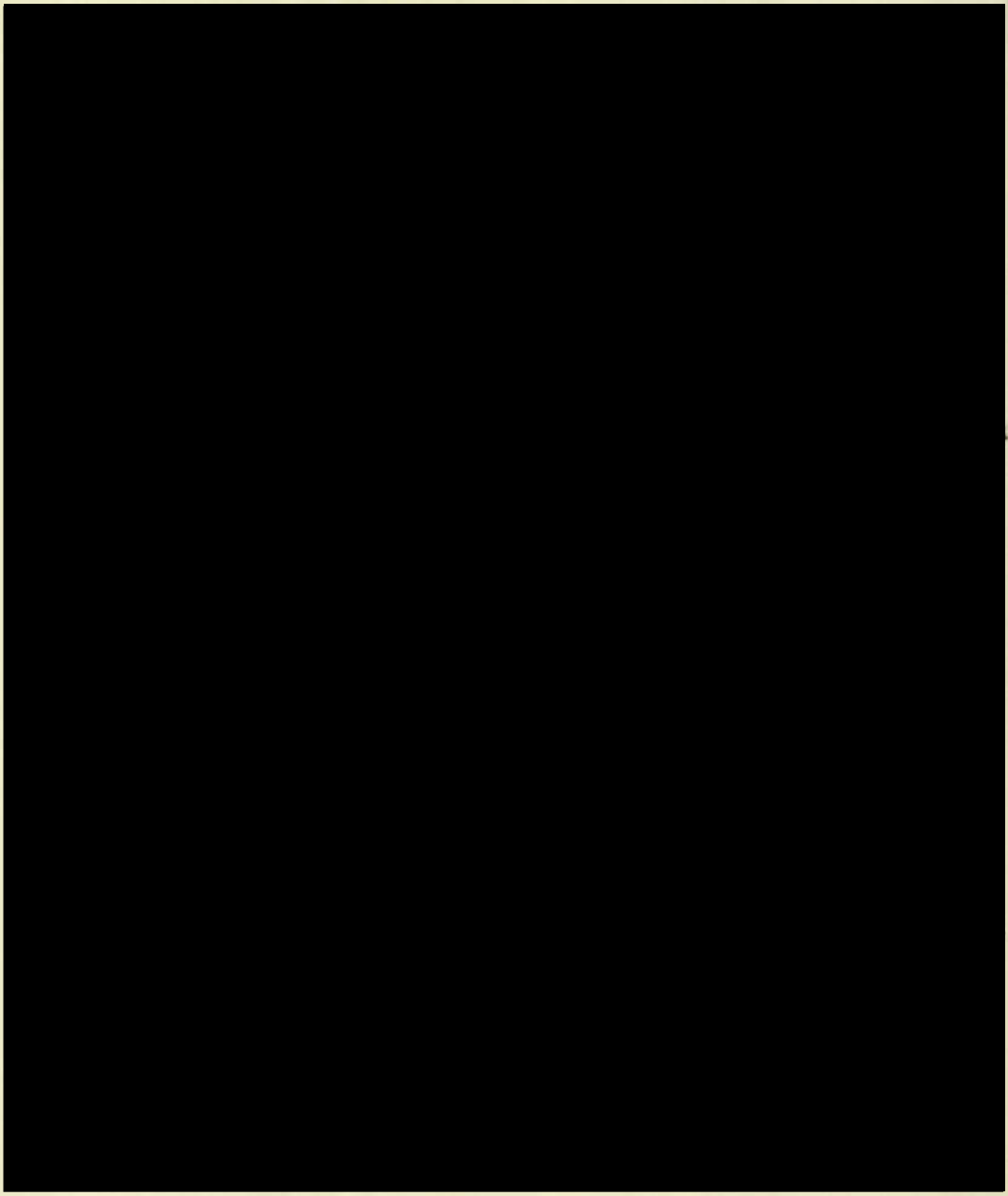
App. C — Fig. 64 Diagram of the hot-wire anemometer calibration apparatus for low velocities.

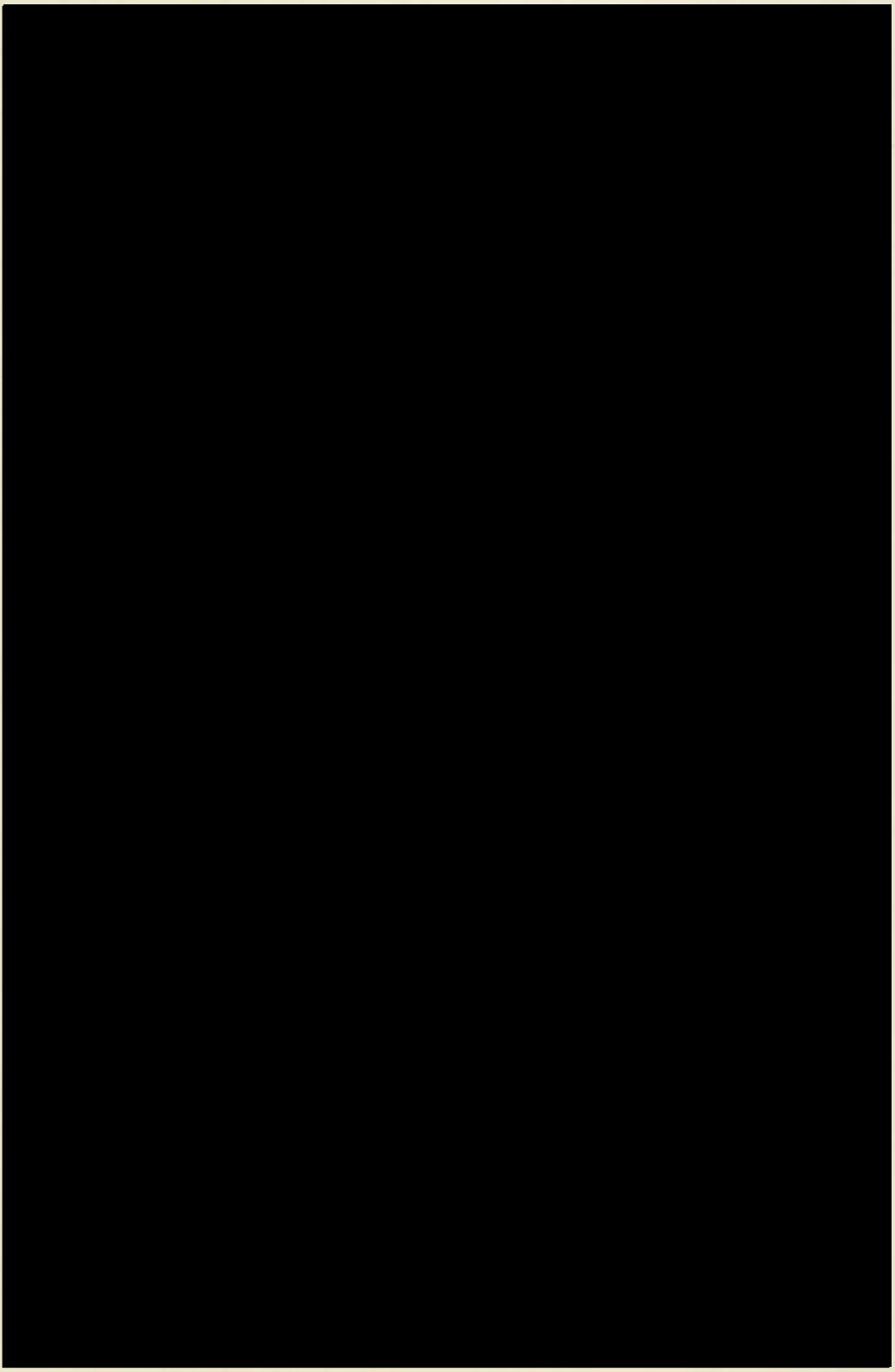


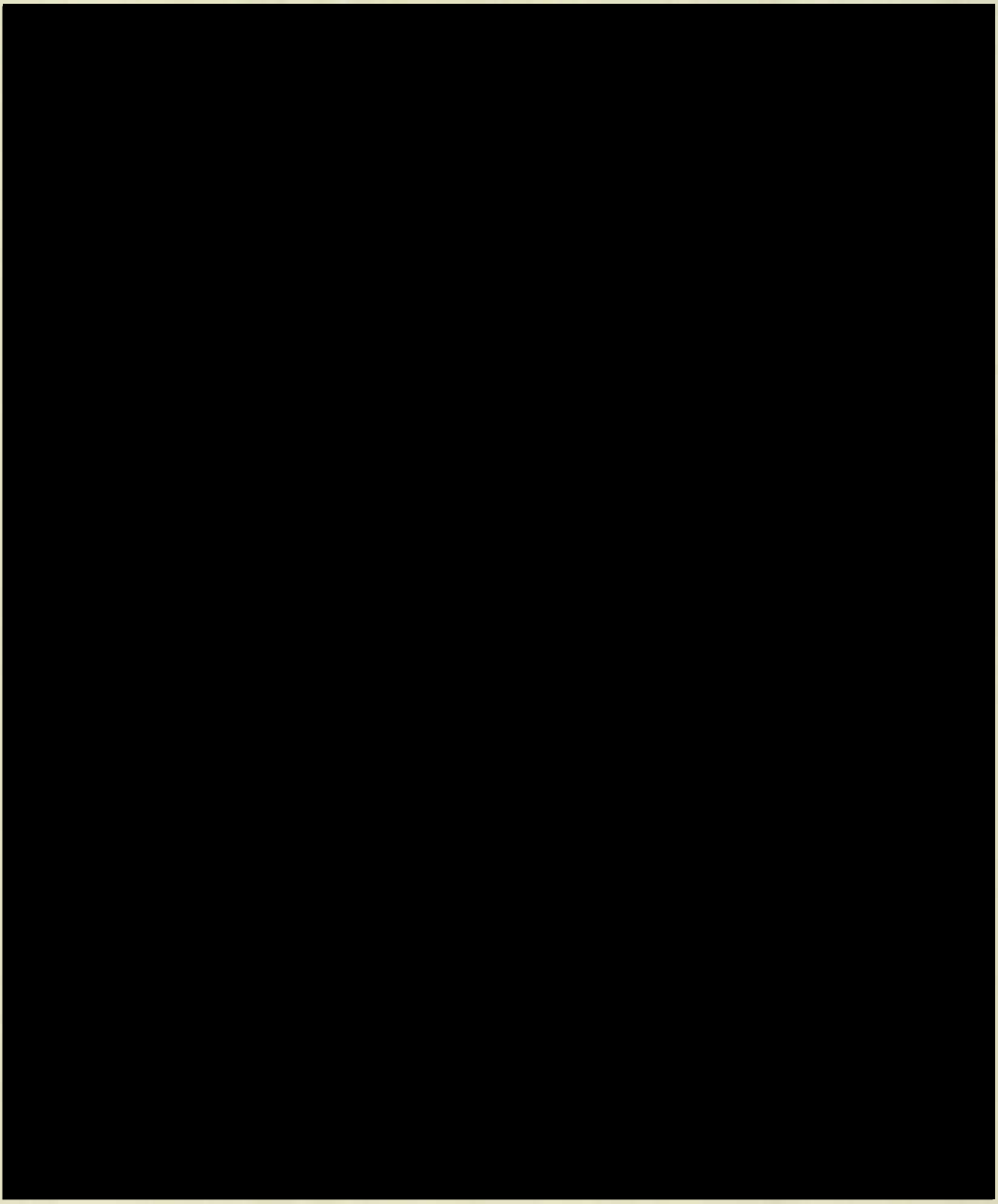
App. C — Fig. 65 Non-dimensional velocity profile in the calibration tube.



App. C—Fig. 66 Calibration curve for a hot-wire anemometer.







In the case of the standing man the boundary layer affords a degree of thermal protection since the flow has been increasing in thickness over the body. Consequently the temperature gradients over the head are shallow and the convective heat loss is limited.

If the subject is lying down the flow pattern over the head is substantially different. In this posture there is no flow over the head from below, there is only the boundary layer which has been generated over the head itself.

Because of these differences in flow fields it is to be expected that the local and total heat losses from the head may vary with changing body posture.

When the subject is lying down the convective flow pattern established around the head may be considered as being similar to that around a heated horizontal cylinder. For the standing subject the head may be represented by the same cylinder placed vertically on top of a second cylinder that generates a boundary layer to simulate the convective flow from the lower parts of the body.

This paper reports the results of experiments to measure these variations of heat loss from the human head with posture in free convection, and compares the results with calculated values for the cylindrical models.

METHODS

The convective flow patterns over the head of a subject in various postures were observed and photographed using a schlieren device, developed at this Institute (Lewis, 1967). From these observations diagrammatic illustrations were prepared to show the essential differences in the flow fields.

Small surface plate calorimeters which were a development of those previously described (Toy & Cox, 1973, 1974) were used to measure the local heat transfer from regions of the head. These calorimeters measured some 1·2 cm × 0·8 cm × 0·02 cm thick and were attached to the skin surface using double-sided adhesive tape with the insulation against the skin. This thickness of these calorimeters and their associated wiring was such as not to interfere with the convective flow patterns, as shown by the schlieren observations.

Electric power could be applied to the heating element until the temperatures registered by the two thermocouple junctions were equal. In this state there was no conductive heat flow across the calorimeter, and the power supplied to the heater was equivalent to the heat loss from the surface of the skin by radiation and convection. Before each series of tests the subject would remain in the posture to be tested for some time until a thermal equilibrium was attained as indicated by the steadiness of the calorimeter and thermocouple readings.

All of the experiments were performed in a climatic chamber at $22 \pm 1°$ C in 'still air' conditions (horizontal air movement less than 30 cm/sec). The walls, ceiling and floor were lined with similar material so that in all postures the radiation to these surfaces was substantially similar. Any changes in the measured heat output were therefore due to convective heat transfer differences.

Preliminary heat transfer measurements were made from a heated horizontal

cylinder (7 cm diameter and 60 cm long) and the results compared with established data (Schmidt, 1932). The convective flow pattern around the cylinder was also visualized in the schlieren system. Heat transfer measurements were taken from the forehead of a subject in the standing, sitting and lying positions, and their time dependency noted.

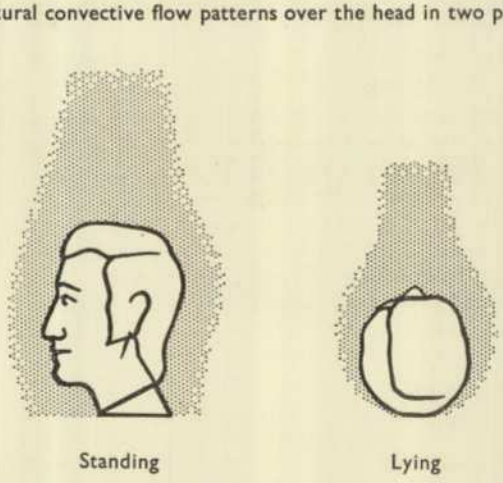
Two subjects were used in these experiments; one with a full head of hair and one who was nearly bald. Calorimeters were attached to the faces of both subjects and additionally, along the median line of the head of the bald subject.

In the experiments where the subject was supine or prone, the head was supported in a small sling so that the convective flow could develop all round the head; this was not possible if the subject lay on a board or bed. The total convective and radiative heat loss was determined from the local heat transfer rates measured at several positions over the head. The head was considered as being divided into small areas and the heat loss from each of these areas was determined from the local heat transfer measurements. Summation of the heat loss from each area gave the total heat output by convection and radiation from the head.

RESULTS

Local heat transfer measurements

Text-fig. 2 shows diagrammatically the differences in the convective flow over the head of a standing and lying subject as observed using the schlieren optical system.



Text-fig. 2. The dotted area indicates the extent and shape of the convective boundary layer for the two postures.

The flow over the head of a standing subject is some 15–20 cm thick and the velocities in the flow exceed 30 cm/sec.

By contrast the flow over the horizontal head reaches only some 5 cm/sec with a maximum thickness of about 1 cm on the side of the head. The hot air streams break away to form a gently moving plume leaving the head